LEVEL II

department of OCEANOGRAPHY

A&M UNIVERSITY

GEOCHEMISTRY OF DISSOLVED GASES IN THE HYPERSALINE ORCA BASIN

TECHNICAL REPORT
by
Denis A. Wiesenburg

Reference 80-14-T
December 1980

81 9 01 023

TEXAS A&M UNIVERSITY   COLLEGE OF GEOSCIENCES

MANDATORY DISTRIBUTION LIST

FOR UNCLASSIFIED TECHNICAL REPORTS, REPRINTS & FINAL REPORTS
PUBLISHED BY OCEANOGRAPHIC CONTRACTORS
OF THE OCEAN SCIENCE AND TECHNOLOGY DIVISIONS
OF THE OFFICE OF NAVAL RESEARCH
(REVISED NOV. 1978)

1   Deputy Under Secretary of Defense
     (Research and Advanced Technology)
     Military Assistant for Environmental Science
     Room 3D129
     Washington, DC 20301

     Office of Naval Research
     800 North Quincy Street
     Arlington, VA 22217
3 * ATTN: Code 483*
1   ATTN: Code 460
2   ATTN: 102B

1   ResRep (if any) - - - - - - - - - -Mr. Frank Lucas or Robert Prestridge
                                            ONR Resident Representative
     Commanding Officer   Room 582, Federal Building
     Naval Research Laboratory   300 E. 8th Street
     Washington, DC 20375   Austin, TX 78701
6   ATTN: Library, Code 2627

12** Defense Documentation Center
     Cameron Station
     Alexandria, VA 22314
     ATTN: DCA

     Commander
     Naval Oceanographic Office
     NSTL STation
     Bay St. Louis, MS 39522
1   Attn: Code 8100
1   Attn: Code 6000
1   Attn: Code 3300

1   NODC/NOAA
     Code D781
     Wisconsin Avenue, N.W.
     Washington, D.C. 20235

*   Add one separate copy of
     Form DD-1473

**   Send with these 12 copies two completed forms DDC-50
     one self addressed back to the contractor, then the
     other addressed to ONR, Code 480.

REPORT DOCUMENTATION PAGE		READ INSTRUCTIONS BEFORE COMPLETING FORM
1. REPORT NUMBER TAMU-REF-80-14-T	2. GOVT ACCESSION NO. AD--A103 536	3. RECIPIENT'S CATALOG NUMBER
4. TITLE (and Subtitle) GEOCHEMISTRY OF DISSOLVED GASES IN THE HYPERSALINE ORCA BASIN .		5. TYPE OF REPORT & PERIOD COVERED Technical Report.
		6. PERFORMING ORG. REPORT NUMBER 80-14-T
7. AUTHOR(s) DENIS A. WIESENBURG		8. CONTRACT OR GRANT NUMBER(s) N00014-75-C-0537 N00014-80-C-0113
9. PERFORMING ORGANIZATION NAME AND ADDRESS Department of Oceanography Texas A&M University College Station, Texas 77843		10. PROGRAM ELEMENT, PROJECT, TASK AREA & WORK UNIT NUMBERS 3200A-9 & 4200-9 NR 083-036
11. CONTROLLING OFFICE NAME AND ADDRESS Office of Naval Research Code 480 Arlington, Va. 22217		12. REPORT DATE December 1980
		13. NUMBER OF PAGES 282
14. MONITORING AGENCY NAME & ADDRESS(if different from Controlling Office) Texas A & M Research Foundation Faculty Exchange Box H Texas A&M University College Station, Texas 77843		15. SECURITY CLASS. (of this report) UNCLASSIFIED
		15a. DECLASSIFICATION/DOWNGRADING SCHEDULE

16. DISTRIBUTION STATEMENT (of this Report)

Approved for public release, distribution unlimited.

17. DISTRIBUTION STATEMENT (of the abstract entered in Block 20, if different from Report)

Approved for public release, distribution unlimited.

18. SUPPLEMENTARY NOTES

19. KEY WORDS (Continue on reverse side if necessary and identify by block number)

Orca Basin   Anaerobic decompositon
Brine pool
Dissolved gases

20. ABSTRACT (Continue on reverse side if necessary and identify by block number)

Hypersaline, anoxic waters significantly affect the biogeochemistry of dissolved gases in the Orca Basin (northern Gulf of Mexico). The high stability of the Orca brine pool makes it an ideal laboratory for studying production and consumption of dissolved gases during anaerobic decomposition. Depth distributions were determined for nitrogen, oxygen, argon, methane, ethane, propane, ammonia, hydrogen sulfide, and nitrous

(OVER)

DD FORM 1473 EDITION OF 1 NOV 65 IS OBSOLETE
1 JAN 73
S/N 0102-014-6601 |

20. ABSTRACT (cont.)

—oxide. *Physical stratification of the water column strongly
influences Orca Basin gas distributions. The high salinity
brine ($\sim 250\%_o$) is internally well mixed due to convective
overturning, but transfer across the brine-sea water interface
is controlled by molecular diffusion. With a molecular
diffusivity of $10^{-5}\ cm^2 \cdot sec^{-1}$, it will take 10^6 years for all
salts to diffuse from the basin. Heat diffuses faster than salt
and is lost from the basin at a rate of $0.5\ \mu cal \cdot cm^2 \cdot sec^{-1}$.
If geothermal heat input from the sediments is slightly higher,
this input could account for the higher temperature in the brine
($5.6°C$) compared to the deep Gulf waters ($4.2°C$).*

This study has shown the utility of dissolved gases in
examining water chemistry of unusual areas. Since sources of
dissolved gases are independent of the sources of major ions in
solution, calculations of gas distributions on a salt-free basis
are useful in examining production and consumption processes.
The high stability of the Orca brine pool makes it an ideal
natural laboratory for examining processes of anaerobic
decomposition.

Texas A&M University
Department of Oceanography
College Station, Texas

Research conducted through the
TEXAS A & M RESEARCH FOUNDATION

GEOCHEMISTRY OF DISSOLVED GASES IN THE

HYPERSALINE ORCA BASIN

by

Denis Alan Wiesenburg

REFERENCE 80-14-T

December 1980

Preface

This report was written by Denis Alan Wiesenburg as
partial fulfillment of the requirements for the degree of
Doctor of Philosophy in Oceanography at Texas A&M University.
Financial support was provided by the Office of Naval Research,
under Contracts N00014-75-C-0537 and N00014-80-C-00113.

ABSTRACT

Geochemistry of Dissolved Gases in the

Hypersaline Orca Basin (December 1980)

Denis Alan Wiesenburg, A.B., Duke University

M.S., Old Dominion University

Chairman of Advisory Committee: Dr. David R. Schink

Hypersaline, anoxic waters significantly affect the biogeochemistry of dissolved gases in the Orca Basin (northern Gulf of Mexico). The high stability of the Orca brine pool makes it an ideal laboratory for studying production and consumption of dissolved gases during anaerobic decomposition. Depth distributions were determined for nitrogen, oxygen, argon, methane, ethane, propane, ammonia, hydrogen sulfide, and nitrous oxide. Physical stratification of the water column strongly influences Orca Basin gas distributions. The high salinity brine ($\sim$ 250 $^\circ/_{\circ\circ}$) is internally well mixed due to convective overturning, but transfer across the brine-sea water interface is controlled by molecular diffusion. With a molecular diffusivity of $10^{-5} cm^2 \cdot sec^{-1}$, it will take 10^6 years for all salts to diffuse from the basin. Heat diffuses faster than salt and is lost from the basin at a rate of 0.5 $\mu cal \cdot cm^2 \cdot sec^{-1}$. If geothermal heat input from the sediments is slightly higher, this input could account for the higher temperature in the brine (5.6°C) compared to the deep Gulf waters (4.2°C).

The high stability of the brine (due to increased density) prevents either reactants or products of anaerobic decomposition from escaping by other than molecular processes. Concentrations

of biogenic methane and ethane are higher there than in any other anoxic marine basin. Oxygen, nitrate, and nitrous oxide are absent from the brine, while phosphate and ammonia levels are 60 and 500 $\mu mol \cdot liter^{-1}$, respectively. However, there is no hydrogen sulfide in the anoxic brine.

Rates of microbial activity are generally slower in the hypersaline Orca Basin. Organic matter is decomposed so slowly that fronds of Sargassum seaweed have been found buried at depths of 5 m in the sediment, the only sedimentary environment where this has been observed. The absence of free sulfide can be attributed to a slower rate of sulfate reduction. Not enough sulfide is being generated to complex the iron produced there. Iron has accumulated to levels of 30 $\mu mol \cdot liter^{-1}$ in the brine and only metastable iron sulfides, not pyrite, are found in the sediments.

Nitrogen and argon in the brine are supersaturated by 470 and 350 %, respectively, compared to atmospheric equilibrium solubilities. The N_2/Ar ratio, however, is 36.4, the estimated ratio from equilibrium of deep Gulf of Mexico waters with air. A comparison of brine and sea water nitrogen and argon concentrations on a salt-free basis showed that these brine gases are remnant gases from the original sea water that formed the Orca brine. This comparison also confirmed that the Orca brine formed by dissolution of a salt deposit at a temperature less than 5°C.

Production of nitrogen and light hydrocarbon gases (methane, ethane, and propane) was evident at the brine-sea water interface.

Methane maxima, similar to those observed in ocean surface waters, were found above the interface. Methane distribution at the interface was similar to the bacterial biomass profiles. Ethane at the interface exhibited a smaller maximum than methane, but the higher levels of ethane in the brine had the same distribution as methane, indicating bacterial production of both methane and ethane.

The carbonate system in the Orca brine closely resembles that of normal sea water. The lower Orca Basin pH (6.83) results mainly from the input of 2.2 mmol·liter^{-1} of biogenic carbon dioxide. The carbonate system dissociation constants were determined at 25°C to be 5.5 for pK_1' and 8.3 for pK_2'. At the pH of the Orca Basin brine, the $CO_3^=$ concentration of the brine is the same as normal sea water. Since the K_{sp}' of aragonite appears to be larger in the brine than in sea water, the increased calcium in the Orca brine must be responsible for the striking preservation of the aragonitic pteropod shells found in the basin sediments.

This study has shown the utility of dissolved gases in examining water chemistry of unusual areas. Since sources of dissolved gases are independent of the sources of major ions in solution, calculations of gas distributions on a salt-free basis are useful in examining production and consumption processes. The high stability of the Orca brine pool makes it an ideal natural laboratory for examining processes of anaerobic decomposition.

ACKNOWLEDGEMENTS

Without the encouragement, assistance, and tutorage of Norman L. Guinasso, Jr., this research would not have been possible. I thank him and Dr. David R. Schink, chairman of my advisory committee, for their valuable help in shaping my view of marine chemistry. I also thank the other members of my committee, Dr. W.M. Sackett, Dr. L.M. Jeffrey, Dr. M.W. Rowe, Dr. C.S. Giam, and Dr. J.W. Foster (Graduate Council Representative) for their contributions. Dr. Sackett was especially helpful in educating me in the fundamentals of stable isotope geochemistry.

Special thanks are due to my colleagues and fellow students at Texas A&M for allowing me to participate in their research cruises and to use their data along with my own. These include: J.M. Brooks, B.B. Bernard, B.J. Presley, J.H. Trefry, R.F. Pflaum, C.S. Schwab, B.P. Boudreau, P.J. Setser, and J.L. Bullister. John W. Johnson and Robert M. Key are gratefully acknowledged for their advice and comradery in the laboratory. Tonalee Carlson provided the pH data and showed me the importance of alkalinity titrations. L.A. Barnard took the excellent SEM pictures of the pteropods.

Special thanks go to my wife, Jean, for her understanding which remained intact long after her patience was exhausted.

TABLE OF CONTENTS

TABLE OF CONTENTS (continued)

TABLE OF CONTENTS (continued)

LIST OF TABLES

LIST OF TABLES (continued)

LIST OF FIGURES

LIST OF FIGURES (continued)

LIST OF FIGURES (continued)

LIST OF FIGURES (continued)

LIST OF FIGURES (continued)

LIST OF FIGURES (continued)

CHAPTER I

INTRODUCTION AND REVIEW

Every atmospheric gas is found dissolved in sea water. Oceanic gas concentrations are affected by the same equilibrium processes and transport mechanisms that control the overall geochemistry of the oceans. Unlike the major sea water components, however, the primary source for gases dissolved in sea water is not rivers, but the atmosphere. With a knowledge of the atmospheric input function and with an understanding of the rates and mechanisms of in situ production or consumption, dissolved gases provide a powerful tool for understanding physical and chemical processes in the ocean.

Much of the early work on dissolved gases in sea water has been reviewed by Richards (1957, 1965). Kester (1975) has summarized the more current studies. Historically, oxygen has been the most widely studied gas in the ocean. Oxygen is the only gas routinely measured by physical oceanographers (along with temperature and salinity) in evaluating water mass distributions. The value it has as a water mass tracer results from the relatively large variations in concentration which it experiences due to biological production or consumption. The fact that a precise, standardized technique (Winkler 1888) has existed for over 90 years has made oxygen measurements both routine and reliable, and thus widely accepted in the

---

The style and format of this dissertation follows that of the journal Limnology and Oceanography.

oceanographic community. The less variable, non-reactive gases have been intensely studied in sea water only in the last two decades. The application of gas chromatography and mass spectrometry has enabled oceanographers to study gases with small variations or in extremely low concentrations. As more information is obtained on dissolved oceanic gases other than oxygen, it has been realized that dissolved gases can be important geochemical tracers for examining both transport processes and reaction mechanisms.

While numerous studies of dissolved gas distributions have been made in fresh water and sea water of normal salinity (20-40 parts per thousand), little work has been done in hypersaline environments. Weiss (1969) measured argon, nitrogen and total carbon dioxide on two samples from the hot Red Sea brines. Using his data and calculated solubilities, he inferred that the source water for the Red Sea brines originated in the shallow coastal areas or near-surface waters of the southern portion of the Red Sea. Swinnerton and Linnenbom (1969) reported on the low-molecular-weight hydro-carbons in the same Red Sea samples and found the values to be much lower than in other anoxic environments. Brooks et al. (1979) described the hydrocarbon and major ion distributions in the East Flower Garden Brine in the Gulf of Mexico. Sackett et al. (1979) discussed the implications of methane and total carbon dioxide data from the Orca Basin waters and sediment. These few papers represent the total of previous work concerning dissolved gases in

hypersaline, oceanic waters. None of these studies have taken a systematic approach to determine the processes governing both the reactive and unreactive gases in hypersaline waters. It is my purpose in this dissertation to present a systematic study of the geochemistry of reactive and unreactive gases in the hypersaline Orca Basin and to show how these gas distributions can be used in interpreting other geochemical evidence of brine formation, reaction and interaction.

Basic Concepts

The Earth's atmosphere is a semi-homogenous mixture of water vapor, major gases (N_2, O_2, Ar and CO_2), unreactive minor gases (e.g., Ne, He, Kr, and Xe), and unstable minor gases (e.g., CH_4, CO, H_2, and N_2O). The concentrations of these gases in the standard atmosphere are presented in Table 1. The solubility of an atmospheric gas in sea water is described by Henry's Law which relates the concentration of an ideal gas in solution (C^*) to a constant times the partial pressure of the gas above the solution,

$$C^* = \beta \, P_G \qquad (1)$$

where β is the Bunsen solubility coefficient (a function of temperature and salinity) and P_G is the partial pressure of the specified gas in the atmosphere. The ideality assumption is reasonable for most gases since most non-ideal variations are less than 0.2%

(Table 1). P_G is related to the mole fraction of gas (f_G) in dry
air by the expression

$$P_G = \left[P_t - \frac{h}{100} P_{vp} \right] f_G \qquad (2)$$

where P_t is the total pressure (atm), h is the relative humidity
(percent), and P_{vp} is vapor pressure of the solution (atm). Com-
bining Eq. 1 and 2 gives an expression which can be used to calcu-
late solubilities,

$$C^* = \beta \left[P_t - \frac{h}{100} P_{vp} \right] f_G \qquad (3)$$

From Eq. 3, it becomes obvious that gas solubilities are a function
of the Bunsen solubility, atmospheric fraction, vapor pressure,
relative humidity, and total atmospheric pressure at the time the
water parcel in question equilibrated with the atmosphere. Bunsen
solubility coefficients have been accurately determined for most
major gases (Weiss 1970, 1974), noble gases (Weiss 1971), and
trace reactive gases (Yamamoto et al. 1976; Crozier and Yamamoto
1974; Gordon et al. 1977; Wiesenburg and Guinasso 1979). Atmos-
pheric gas concentrations are relatively constant. While water
vapor pressure can be calculated as a function of temperature and
salinity, the appropriate barometric pressure and relative humidity
when air and water equilibrate are not easy to obtain. Once a
water parcel is out of contact with the atmosphere, it is difficult
to determine the conditions under which it was equilibrated. It is,

Table 1. Abundance and properties of atmospheric gases.

Gas	Mole fraction in dry air* (f_G)	Molar volume at STP+ $(liter \cdot mol^{-1})$	Percent difference from 22.414
N_2	$0 \cdot 78080 \pm 0 \cdot 00004$	$22 \cdot 391$	0.10
O_2	$0.20952 \pm 0 \cdot 00002$	$22 \cdot 385$	0.13
Ar	$(9 \cdot 34 \pm 0 \cdot 01) \times 10^{-3}$	$22 \cdot 386$	0.12
CO_2	$(3 \cdot 3 \pm 0 \cdot 1) \times 10^{-4}$	$22 \cdot 296$	0.53
Ne	$(1 \cdot 818 \pm 0.004) \times 10^{-5}$	$22 \cdot 421$	0.03
He	$(5 \cdot 24 \pm 0 \cdot 004) \times 10^{-6}$	$22 \cdot 436$	0.10
CH_4	1.41×10^{-6}	$22 \cdot 356$	0.26
Kr	$(1 \cdot 14 \pm 0 \cdot 01) \times 10^{-6}$	$22 \cdot 350$	0.28
H_2	0.58×10^{-6}	$22 \cdot 430$	0.007
CO	0.11×10^{-6}	$22 \cdot 387$	0.12
N_2O	5×10^{-7}	$22 \cdot 228$	0.56
Xe	$(8 \cdot 7 \pm 0 \cdot 1) \times 10^{-8}$	$22 \cdot 277$	0.61

* From Glueckauf (1951), Valley (1965), and Schmidt (1978).
+ Based on van der Waals equation for gases using constants from Weast (1969).

therefore, reasonable to assume a standard pressure of one atmosphere and a relative humidity of 100%. With these simplifying assumptions, Eq. 3 reduces to:

$$c^* = \beta(1 - P_{vp}) \, f_G \qquad (4)$$

which is the equation most often used to express the atmospheric equilibrium solubility of a gas in solution.

Weiss (1970) has developed an equation to describe atmospheric equilibrium solubility from moist air as a function only of temperature and salinity. He expressed the temperature dependence of solubility at constant salinity by an integrated form of the van't Hoff equation and used the Setchénow relation to describe the salinity effect. Combining these two relationships and adding an additional term to account for the vapor pressure of water, he developed an atmospheric solubility equation of the form

$$\ln c^* = A_1 + A_2 \, (T/100) + A_3 \ln (T/100) + A_4 \, (T/100)$$
$$+ S\%_{\circ} \, [B_1 + B_2 \, (T/100) + B_3 \, (T/100)^2] \qquad (5)$$

where c^* is the equilibrium solubility in $nmol \cdot liter^{-1}$ (or other appropriate units), A_i and B_i are constants, T is the absolute temperature, $S\%_{\circ}$ is the salinity in per mil. Weiss (1970, 1971, 1974) and Weiss and Kyser (1978) have fitted solubilities for oxygen, nitrogen, argon, neon, helium, carbon dioxide and krypton to Eq. 5

to describe the atmospheric solubility of those gases relative to water saturated air at one atmosphere total pressure. Recently, Wiesenburg and Guinasso (1979) have rewritten Eq. 5 expanding the A_1 term to $f_g + A_1$, to include the atmospheric gas concentration as a variable. They have fitted solubility data for methane, hydrogen and carbon monoxide to the modified equation. All atmospheric solubility calculations in this work will be made using Eq. 5 or the modified version of Wiesenburg and Guinasso (1979).

The Study Site

The Orca Basin is located on the Louisiana continental slope in the Gulf of Mexico and is centered at 26°55'N, 91°20'W. In this region, salt tectonics have had an observable influence on the topography. Salt diapirs protrude almost to the surface from basement salt deposits in many areas near the Orca Basin. Salt flow and dissolution have created a relatively unstable sea-floor which has become pock - marked with intraslope basins (Fig. 1). The Orca Basin is but one of many of these types of basins which are situated within the growing margin of the Gulf Coast geosyncline.

The bathymetry of the Orca Basin is shown in Fig. 2. The basin itself encompasses an area of approximately 400 km^2 with an "L"-shaped trough along the eastern and southern portions. Enclosing slopes drop from an average depth of 1800 meters along the encircling continental slope to over 2400 meters within two separate
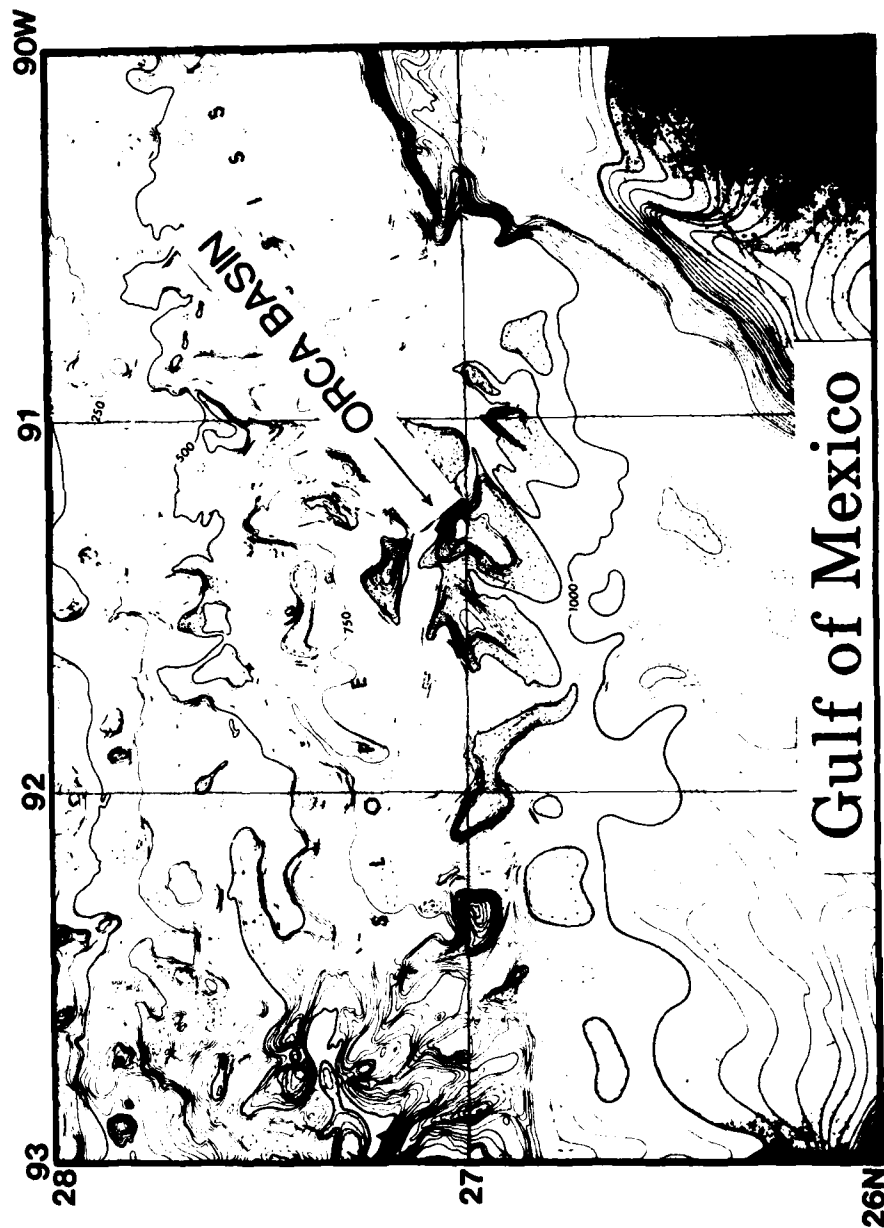
Fig. 1. Index map of the Texas-Louisiana continental slope showing several small basins which have resulted from salt flow and dissolution. Location of the Orca Basin is indicated. Depth contours are in fathoms.
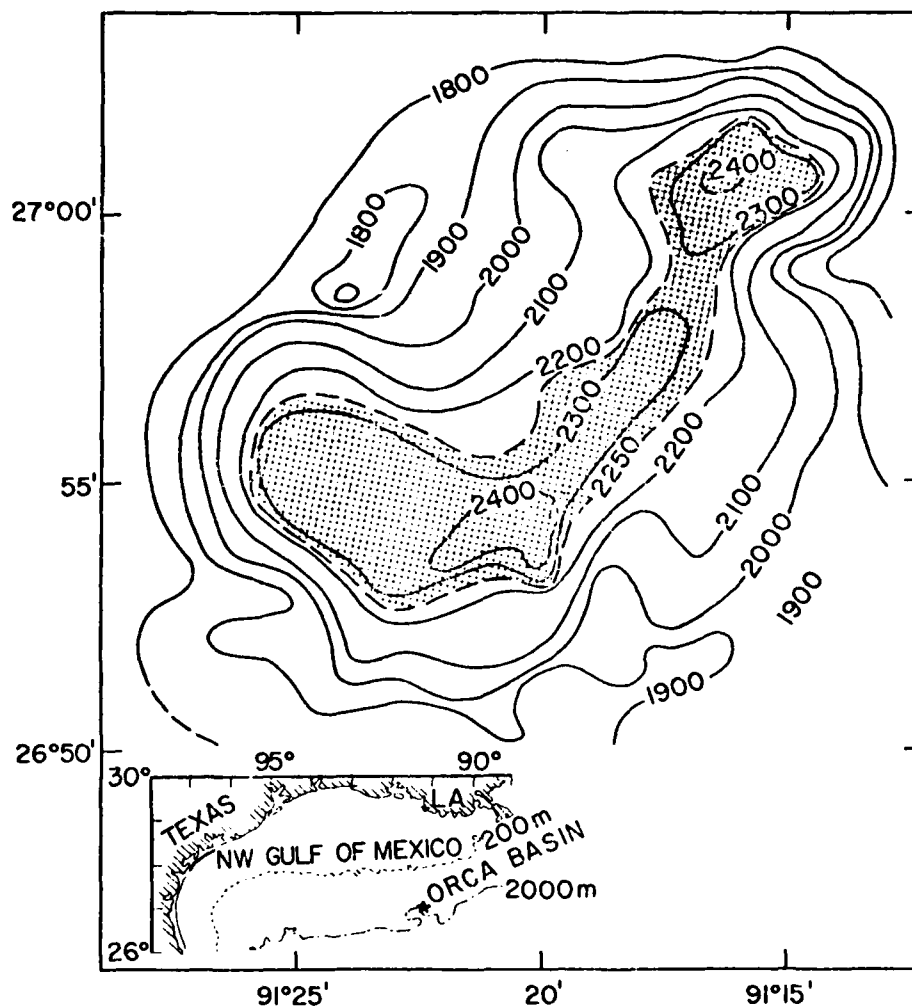
Fig. 2.   Bathymetric map of the Orca Basin based on the
seismic data taken on cruise 76-G-10 of the R/V Gyre (after
Shokes et al. 1977).   The stippled portion of the map repre-
sents the area covered by the high salinity brine.

areas. The bottom 200 meters of the Orca Basin is filled with water having an evaporative salinity of 250‰ and a temperature (5.6°C) more than 1.4°C higher than the overlying, freely circulating Gulf of Mexico water. The volume of brine in the Orca Basin is approximately 5 km^3, a volume several times larger than all of the Red Sea brines combined.

The temperature and salinity structure in the Orca Basin is shown in Fig. 3. Bottom water at 2000 meters in this area of the Gulf of Mexico has a characteristic temperature of 4.2°C and an average salinity of 34.976‰. Both the temperature and salinity begin to increase rapidly in the Orca Basin at a depth of approximately 2240 meters, with the salinity gradient being more dramatic than the temperature gradient. The sea water to brine transition zone from normal Gulf of Mexico deep water to maximum salinity brine is only about 50 to 60 meters and provides a very sharp density contrast. The density difference of the brine (1.185 kg/l) as compared to the deep Gulf water (1.025 kg/l) provides such a sharp interface that it can be seen using low-frequency acoustical sounding devices. Shokes et al. (1977) used a 700-joule minisparker to generate low frequency sound pulses in order to map the extent of the brine. Part of the record that they obtained in that study is shown in Fig. 4. The brine appears as a distinct layer due to the sound reflection from the interface. On cruise EN-32 of the R/V Endeavor, the brine interface could also be seen by
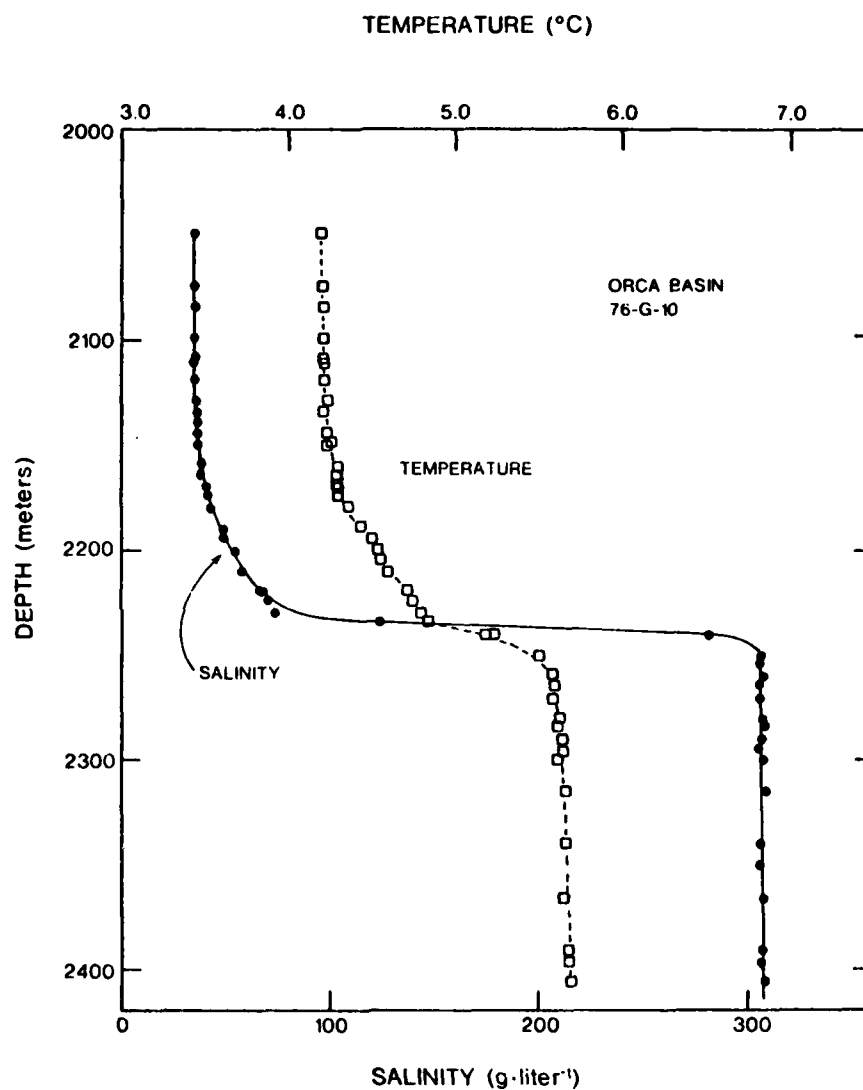
Fig. 3. Vertical temperature and salinity $(g \cdot liter^{-1})$ profiles extending from the deep Gulf of Mexico water into the hypersaline Orca Basin brine. Note the sharp transition between the Gulf water (ρ = 1.025) and the brine (ρ = 1.185 $kg \cdot liter^{-1}$).
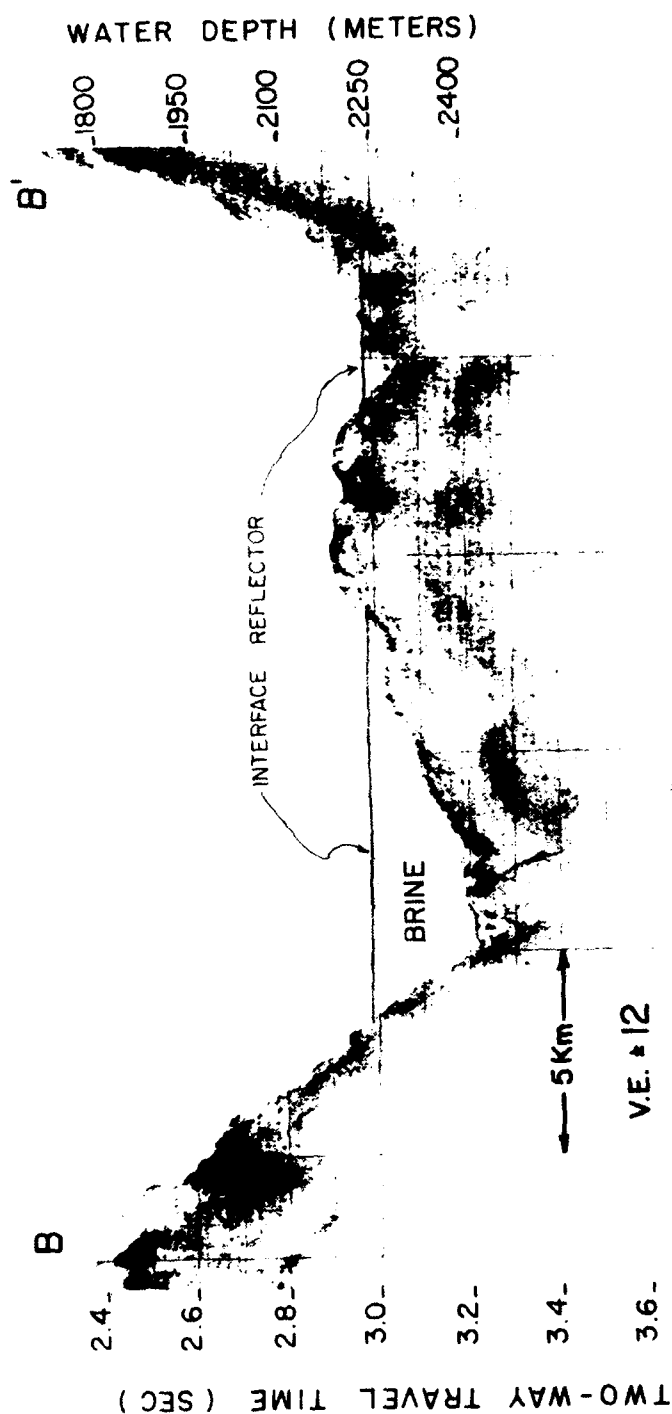
Fig. 4. One section of the minisparker record obtained by Shokes et al. (1977) during their mapping of the Orca Basin brine pool. The dark level line above the bottom is the result of sound reflections from the density interface.

using a 3.5 kHz bottom profiling system, which has a higher fre-
quency than the minisparker of Shokes et al. (1977). This device
was instrumental in positioning the ship above the brine for sam-
pling. The brine-sea water interface could not be seen with the
higher frequency 12 kHz bottom profiling system.

Previous Investigations

The Early Work

The geochemical investigation of the Gyre Basin in the north-
western Gulf of Mexico (Bouma et al. 1975) prompted researchers at
Texas A&M University to perform surveys of several other intraslope
basins on the Texas and Louisiana continental slopes. Most of the
other intraslope basins appear to be geochemically "normal" basins
similar to the Gyre Basin (C. R. Schwab, personal communication).
Only the Orca Basin was found to have water with above normal
salinities.

The Orca Basin was first sampled as part of the intraslope
basin study during cruise 75-G-16 of the R/V Gyre in November 1975.
During this cruise, a 185-190 cm gravity core was taken from the
shoaler northern end of the basin (Fig. 2). After the core was
sliced and the interstitial water removed by squeezing, the water
(brine) was placed in a freezer but it would not freeze completely!
Examination of the interstitial fluid from this core revealed that
the salinity was greater than 250‰ at a depth of 8 cm and

decreased slightly with depth in the core (McKee and Sidner 1976).
Although similar hypersaline conditions had been found in deep
borehole samples from the Gulf of Mexico (Manheim and Bischoff 1969),
this was the first observation of hypersaline fluids in any open
continental shelf or slope environment. With excitement running
high the brave men of the Gyre returned to the Orca Basin on cruise
76-G-2 in early 1976. A second gravity core was taken in the
deeper southern portion of the basin and water samples were taken
to characterize the water in the basin. They noted that the
basin had a local sill depth of 2000 m, with a 140 m thick bottom
layer of anoxic bottom water with a salinity of 270%$_{oo}$. The ob-
servations from these two cruises have been briefly summarized by
McKee and Sidner (1976). The first water column data (Table 2),
a description of the sediment features which result from the un-
usual environment was described. Since their observations are
relevant to all future studies, this author will briefly detail
them here:

1. The sediments are high in organic matter.
2. The presence of fine laminations reflect the lack of
    burrowing organisms.
3. Sediments from the basin are black due to the presence of
    metastable metal sulfides which rapidly oxidize to a red
    brown color upon exposure to air.

Table 2. First report of hydrographic data from the Orca Basin
(Tabulated from McKee and Sidner 1976).

Depth	Temperature ($°C$)	Salinity ($°/°°$)	Oxygen ($ml \cdot liter^{-1}$)
Sill	4.21	35.076	4.839
Sill + 100m	4.38	43	1.769
Sill + 200m (140m above bottom)	5.63	270	0.0

4. There was no noticeable hydrogen sulfide odor in the water
   or sediments.

5. The deeper water samples appeared gassy and the X-ray
   radiographs of the cores showed small gas bubbles which
   increased in concentration near the surface of the core.

6. The sediments show excellent organic preservation as
   evidenced by the presence of _Sargassum_ throughout the
   entire length of the gravity cores.

These observations (McKee and Sidner 1976) were preliminary and
there were no interpretations of results given.

The first study to make detailed observations of the water
column chemistry was done by Shokes et al. (1977), using data ob-
tained during R/V Gyre cruise 76-G-10 in October 1976. This work
led to the landmark paper which first showed the extent of the
Orca Basin and gave it its name. Shokes et al. (1977) did a com-
plete bathymetric survey of the basin using a low frequency mini-
sparker and estimated the brine volume to be 40 km^3. They made
the first extensive geochemical analysis of the anoxic brine in the
Orca Basin. In this analysis, detailed vertical measurements of
temperature, salinity, oxygen, and nutrients were made in
both ends of the basin (Fig. 5 and 6). The major ions in the
brine were also measured and these values were compared to the
Red Sea geothermal brines (Table 3). Shokes et al. (1977) con-
cluded that the brine must originate by solution (presumably by

Table 3. Moles per kilogram of ions in sea water and various brines.

	Na	K	Mg	Ca	Cl	SO4	HCO3
Sea water [*]	0.478	0.0102	0.0531	0.0102	0.547	0.0283	0.0022
Orca Basin brine [+]	3.980	0.0161	0.0432	0.0272	4.217	0.0381	0.0053
Dead Sea brine [‡]	1.596	0.163	1.559	0.493	5.684	0.0070	0.0034
Red Sea brine [§]	4.041	0.0552	0.0333	0.118	4.380	0.0078	0.0023
East Flower Garden [‖]	3.449	0.0093	0.0439	0.0403	3.695	0.0460	0.0024

[*] Average sea water
[+] Shokes et al. (1977)
[‡] Amit and Bentor (1971)
[§] Brewer et al. (1969)
[‖] Brooks et al. (1979)

18
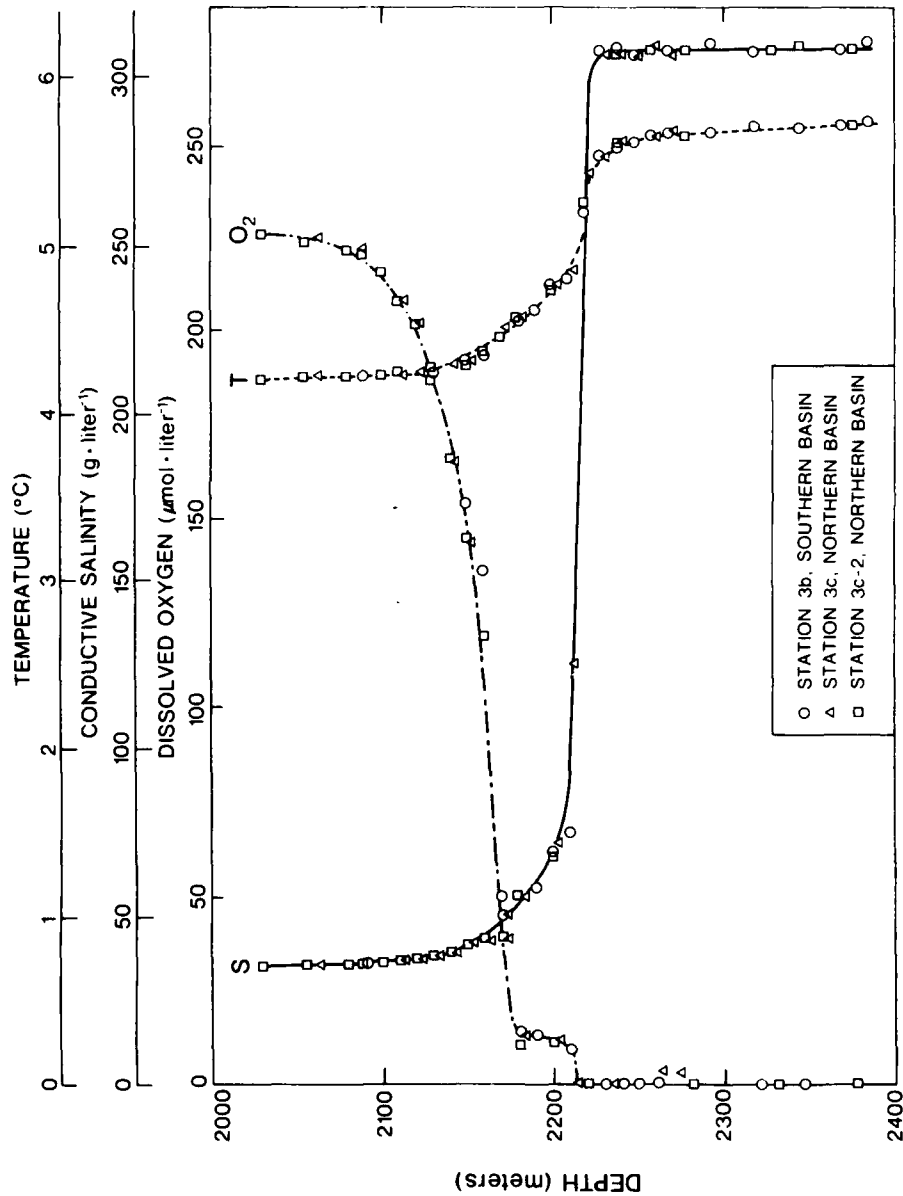
Fig. 5. Composite vertical profiles of temperature, shipboard conductive salinity and dissolved oxygen measured in both lobes or ends of the Orca Basin on R/V Gyre cruise 76-G-10 (after Shokes et al. 1977).
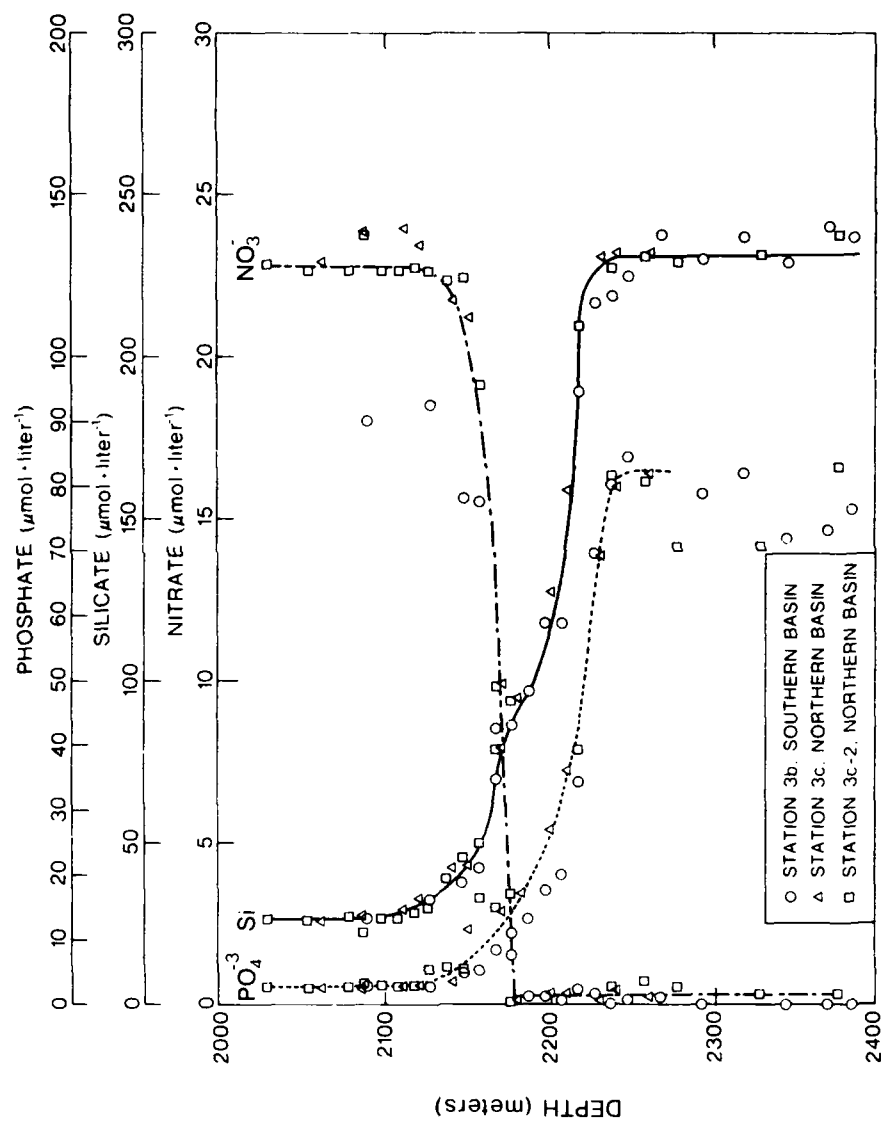
Fig. 6. Composite vertical profiles of dissolved orthophosphate, silicate and nitrate across the sea water-brine interface for three stations in the Orca Basin (after Shokes et al. 1977).

sea water) of a near-surface salt deposit (mainly NaCl). They reached this conclusion based on the absence of sulfate depletion in the brine and due to observations of minimal changes in temperature and ion compositions. Since there was a decreasing chloride gradient in the interstitial water of the basin sediment, it was suggested that the brine enters the basin laterally, rather than by diffusion upwards through the underlying sediments. Calculations of the heat input needed to raise the temperature of the 40 km^3 brine from the overlying Gulf temperature of 4.2°C to the present 5.6°C could be added in about 325 years, assuming an average oceanic geothermal heat flow (1 $\mu cal \cdot cm^{-2} \cdot sec^{-1}$). The only dissolved gas measured was oxygen, which decreased to zero within the brine.

In a follow-up paper, Trabant and Presley (1978) presented a more detailed geological description of the Orca Basin. The brine volume estimate was lowered to 5 km^3. The geological setting of the Orca Basin was compared to that of several other intraslope basins which have been defined and discussed on the basis of seismic reflection profiles (Antoine and Bryant 1969; Garrison and Martin 1973). It was concluded that geologically the Orca Basin represents a typical intraslope basin. However, it has water with uncommon chemical composition and associated sediment geochemistry because of the presence of regional salt massifs which have led to salt flow into the brine. Trabant and Presley

(1978) examined a three meter gravity core taken in the deeper end of the basin and came to the same conclusions as McKee and Sidner (1976), viz. the absence of laminae and apparent textural homogeneity indicated pelagic deposition and no burrowing by organisms. The presence of <u>Sargassum</u> throughout the core was also noted. A complete description of the core was produced and the following sediment properties were discussed:

1. The sediment was a silty clay with a clay size fraction of 60-75%, with little or no vertical change of clay mineralogy.

2. The acid-leachable iron content is similar to other Gulf sediments, but with a relatively high sulfur content (1%) compared to other Gulf of Mexico sediments.

3. Water content of the sediment ranged from 140% to 280% (dry weight method).

In discussing the brine geochemistry in the Orca Basin, Trabant and Presley (1978) make one significant new note. They measured the bromide level in the brine and found a value of 80 $mg \cdot kg^{-1}$. Due to the well-known partitioning effects associated with bromine as a salt solution evaporates, bromine can be useful in determining the origin of the brine (see later discussion on bromine). LouAnn Salt (a logical source for salt in the Orca Basin) was observed to have 34 to 51 ppm bromide (Holser 1966).

Dissolving 308 g of this salt in a liter of sea water would give a bromide concentration equivalent to that found in the Orca Basin. Thus, Trabant and Presley (1978) offered strong evidence that the Orca Basin brine forms from the dissolution of previously deposited salt.

In the same volume, a paper on basin and slope sediments by McKee et al. (1978) further emphasized this point, while comparing the sediment geochemistry of intraslope basins with the geochemistry of shelf and slope sediments. In this same study, they noted that the more rapid sediment accumulation rate in intraslope basins caused basin sediments to have a more anoxic character than typical slope sediments. Of the basins studied, only the Orca had brine in the bottom. However, one other basin — the Gyre Basin — exhibited a higher concentration of salt in one of the cores that were studied (up to 44.2 $g \cdot kg^{-1}$ of chloride compared to 19.4 $g \cdot kg^{-1}$ for average sea water). The salinity in this basin core increased with depth in the sediment indicating an upward diffusion of salt from some deeper formation.

Another significant feature of the study by McKee et al. (1978) was a comparison of sulfate profiles of the normal slope sediments, intraslope basin sediments, and the Orca Basin sediments. Even though the sedimentation rate in the Orca Basin is three times as great as found on the slope, the sulfate gradient from the upper 120 cm of two Orca Basin cores was not significantly greater

than gradients found in most slope sediments. In one other Orca

Basin core (9B), the slope of the sulfate profile indicated a dc/dx_o

of 0.27 $mmol \cdot liter^{-1} \cdot cm^{-1}$ which is higher than the value of 0.02

$mmol \cdot liter^{-1} \cdot cm^{-1}$ found outside the basin (but still lower than

some values found in the Gyre Basin which is not an anoxic basin).

The variability of sulfate gradients in the cores from the Gyre and

Orca Basins correlated with patterns of sediment redeposition within

the basins. More evidence of slumping was found in Gyre Basin

cores. However, those cores were more extensively studied than the

Orca Basin cores.

These initial studies on the Orca Basin were primarily con-

cerned with defining the origin of the brine. Two basic lines of

evidence were pursued: the decreasing chloride gradient in the

sediments and the bulk ion composition. The decreasing salt con-

centration with depth in the sediments is strong support for the

salt influx coming from other than the basin floor. However, the

ion composition is also an important piece of evidence in decipher-

ing this puzzle. The ionic composition of the Orca Basin brine as

reported by Shokes et al. (1977) is compared with standard sea

water and several other oceanic brines in Table 3. Unlike evap-

oration brines such as the Dead Sea brine, the Orca Basin brine

does not have tremendously increased concentrations of any

ions other than sodium and chloride. This fact, and more recent

evaluation of bromide data from the Orca Basin by McKee et al.

(1978), both support the contention that the Orca Basin formed as the result of the dissolution of a salt deposit. The bromide concept is important enough to describe in more detail.

Bromide does not form its own minerals when sea water evaporates. Some of it is lost from solution because it forms isomorphous admixture with chloride in the precipitates (Valyashko 1956; Braitsch and Herrman 1963). As sea water evaporates, the carbonates precipitate first, followed by the sulfates. During this stage of evaporation, little or no bromide precipitates, or if it does, it is occluded with the carbonates and sulfates (see Table 4).

Halite (NaCl) begins to precipitate when the chloride concentration reaches about 275,000 $mg \cdot liter^{-1}$ (cf. normal sea water, 19,000 $mg \cdot liter^{-1}$). Some small amount of bromide is entrained with chloride in the precipitate. However, as crystallization proceeds, more bromide is left in solution than is included in the precipitate. Sylvite (KCl) begins to precipitate when the chloride concentration has risen to about 360,000 $mg \cdot liter^{-1}$. Carnallite (Mg $Cl_2 \cdot KCl \cdot 6H_2O$) and bischoffite ($MgCl_2 \cdot 6H_2O$) precipitates follow. During evaporation the concentration of bromide in solution increases. Therefore, relative to chloride, the bromide concentration in a brine is a good indicator of the degree of sea water concentration. The above discussion assumes that appreciable quantities of biogenic bromide have not been introduced into the system. McKee et al. (1978) have discussed this idea and

Table 4. Concentration changes during evaporation of sea water and brine (after Collins 1969).

Element	Sea water	$CaSO_4$↓	NaCl↓	$MgSO_4$↓	KCl↓	$MgCl_2$↓
Lithium	0.2	2	11	12	27	34
Sodium	11,000	98,000	140,000	70,000	13,000	12,000
Potassium	350	3,600	23,000	37,000	26,000	1,200
Rubidium	0.1	1	6	8	14	10
Magnesium	1,300	13,000	74,000	80,000	130,000	153,000
Calcium	400	1,700	100	10	0	0
Strontium	7	60	10	1	0	0
Boron	5	40	300	310	750	850
Chloride	19,000	178,000	275,000	277,000	360,000	425,000
Bromide	65	600	4,000	4,300	8,600	10,000
Iodide	0.05	2	5	7	8	8
Total		295,000	517,000	469,000	538,000	602,000

illustrated it with a diagram (reproduced here as Fig. 7) that shows
bromide versus chlorinity for various pore waters including the
Orca Basin. As sea water evaporates, the chloride versus bromine
distribution is represented by the solid line which separates the
areas resulting from dissolving, evaporate-produced brine from
residual source-solution brines. The Orca Basin is higher in
chloride content without a significant increase in the bromide
concentration indicating a solution source. This data seems to
clearly establish the source of the Orca Basin as a dissolving
evaporite deposit rather than a brine formed by direct evaporation.

Subsequent Investigations

These papers caused a flurry of activity in the oceanographic
community. Besides cruises by Texas A&M University, expeditions
to the Orca Basin have been staged by the University of Miami, the
University of Texas and the University of Rhode Island. In the
Fall 1977 American Geophysical Union meeting, seven papers were
presented dealing with various geochemical aspects of the Orca
Basin (see, for example, Guinasso 1977).

Of the papers now published from the initial cruises to the
basin, I recognize two major categories: sediment geology and
organic-microbial interactions in the brine. The sediment papers
have been produced by geologists searching for the source of salt
or are attempting to describe the unusual effects that the high
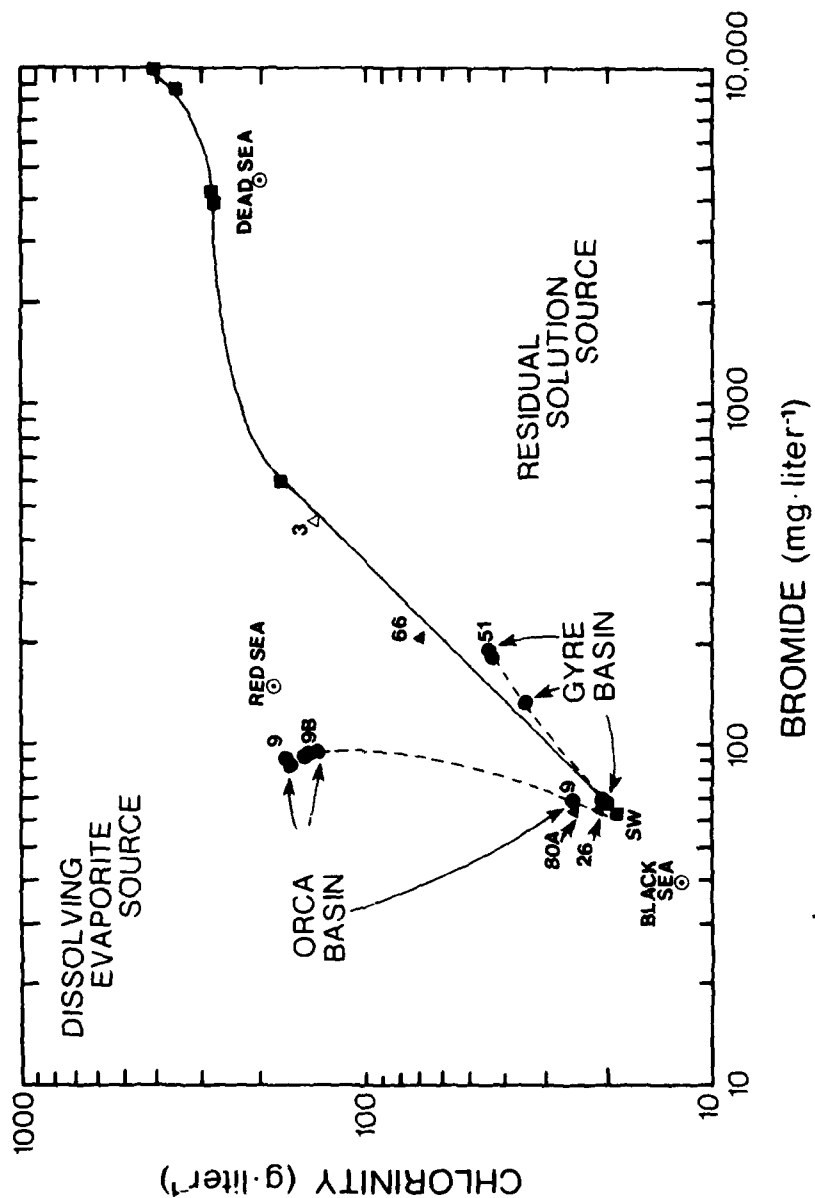
Fig. 7. Plot of bromine versus chlorinity for pore waters with chlorinity anomalies. The solid curve represents residual solution as sea water progressively evaporates, dividing two fields representing a dissolving evaporite source (above line) and a residual solution source (below line). Pore water data for the Orca Basin, Gyre Basin and Dead Sea are indicated.

salinity water has on various sediment properties (e.g., sedimentation rate, clay particle interaction, and preservation of carbonate and silicious materials). Kennett and Penrose (1978) used electron microscopy to examine the microfauna in the sediments. They noted that pteropod tests were extremely well preserved relative to other areas. Additionally, they noted the unusual occurrence of well preserved Sargassum particles deep in the core. While Sargassum has been found at the sediment surfaces as deep as 5300 m (Schoener and Row 1970), Kennett and Penrose (1978) noted that there are no previously documented cases of preserved seaweed in deep-sea sediments, especially with attached organisms as found in the Orca Basin.

Addy and Behrens (1980) also reported the presence of seaweed in their ten meter core from the knoll between two basins. They did a very complete study of the major ions in the interstitial water and for each 10 cm section of the core, determined grain size distributions. From radiocarbon dates, they determined that the bottom layer of the black mud in the sediments (which corresponds to the initial time of brine input to the basin) had an age of 7910 $\pm$ 170 years. This age was reported at a depth of 4.85 meters which gave an implied sedimentation rate of 61 cm·ka^{-1}. Measurements further down in the core in areas which were not deposited under anoxic (brine) conditions gave a sedimentation rate for that region of 43 cm·ka^{-1}. This difference implies an

increased sediment accumulation rate due to the anoxic conditions
existing in the brine. Carbonate percentages averaged four percent
higher in the black mud laid down under anoxic conditions than in
the gray mud that had an oxygenated origin. From this data, Addy
and Behrens (1980) concluded that the enhanced sediment accumula-
tion is due to increased preservation of carbonate test. The
higher sand fractions in the basin core were almost entirely skele-
tal carbonate.

Besides the color of the mud in the sediments, Addy and Beh-
rens (1980) used the presence of Sargassum fronds to ascertain the
conditions (anoxic or aerobic) under which the sediments were de-
posited. Aerobic conditions allow more degradation of organic
matter than in anoxic environments. The absence of recognizable
Sargassum in Orca Basin gray muds indicates deposition in an oxy-
genated environment; while the well preserved Sargassum fronds in
the black mud strongly suggest deposition in anoxic brine.

Addy and Behrens (1980) made several other measurements to
determine the conditions of deposition, including water content
(higher in the anoxic mud) and compaction (found to be less in the
black mud sediments). Deposition in a brine basin would account
for both of these observations.

The color of the black mud is due to very fine-grained, meta-
stable iron sulfides such as greigite (Fe_3S_4) and machinawite
(FeS), like those found in anoxic sediments of the Black Sea

(Berner 1974). Formation of metastable iron sulfides instead of pyrite (FeS_2) will result in the absence of significant H_2S (from SO_4 reduction) in the depositional environment. This observation has important implications for the work to be presented later.

Addy and Behrens (1980) approached the questions of brine origin by conducting seismic profiles of the slope area. If the Orca Basin brine is formed from dissolution of an exposed salt diapir, that feature should be found on the surrounding basin slope. In two multichannel subbottom profiles, Addy and Behrens (1980) noted several strong undulating reflectors with diapiric structures which they interpreted as salt surfaces. These salt surfaces become shallower to the north and possibly outcrop at the edge of the small basin east of the Orca Basin. A second salt structure similarly approaches the surface at the eastern margin north of the Orca Basin. A 3.5 kHz profile of the region showed hyperbolic reflections indicating a hummocky surface. Addy and Behrens noted that if salt were exposed, the dissolution would proceed along fractures and joints resulting in the uneven surfaces that were observed. Perhaps Addy and Behrens (1980) have located the source of the Orca Basin brine.

Another study dealing with sediment geology was that of Tompkins and Shephard (1979). They described possible depositional processes, geotechnical properties and clay mineralogy of two cores from the Orca Basin. One core was taken in the deepest

portion of the southern basin and gave sedimentation rates of over
100 $cm \cdot ka^{-1}$, based on microfaunal examinations. The conditions
within the core suggested that the sediment was originally depos-
ited under brine on the basin slope, and then slumped deeper
into the basin. Addy and Behrens (1980) had avoided problems re-
lated to slumping by sampling only on the knoll between the two
basins.

Tompkins and Shephard (1979) examined the clay mineralogy
and clay mineral variations in the basin sediments. They noted
an increase in smectite with increasing depth (and decreasing
salt) in the sediments. They attributed the highly open sediment
microstructure to the rapid sedimentation. Both the sediment micro-
structure and the levels of smectite seemed to control the diver-
sity in clay mineral abundances in the brine. Sediments that were
deposited outside the brine, then slumped into the basin, were
easily discernable by their properties which were similar to normal
continental slope sediments.

In a study which encompassed both water column and sediment
data, Sackett et al. (1979) developed a carbon budget for the Orca
Basin water column and sediments. Methane and carbon dioxide
increased with depth in the sediments and both were assumed to
result from the bacterial decomposition of organic matter. The
$\delta^{13}C$ values of carbon dioxide and methane in the sediments were
very negative (isotopically lighter) relative to water column

values. The value of $-105\%_{oo}$ that Sackett et al. (1979) observed

for the $\delta^{13}C$ of methane is the lightest (natural) methane isotope

ratio reported to date. The amounts of organic carbon found in the

sediments were somewhat higher than for normal shelf and slope

sediments. The $\delta^{13}C$ values of the particulate organic carbon in

the sediments ranged from $-22\%_{oo}$ (a normal value for open shelf

sediments) down to a $-26.7\%_{oo}$. They suggested that the lighter

samples may have resulted from slumped material originally depos-

ited in estuarine environments during the Pleistocene.

In the brine itself, Sackett et al. (1979) made concentration

and isotopic ($\delta^{13}C$) measurements of carbon dioxide, methane, and

organic carbon. Sackett et al. (1979) used a mass balance equation

of the following form:

$$[(mg\ C/L)(\delta^{13}C)]_{sea\ water} + [(mg\ C/L)(\delta^{13}C)]_{added\ carbon}$$

$$= [(mg\ C/L)(\delta^{13}C)]_{brine} \qquad (6)$$

to calculate the amount of isotopic composition of added carbon

that would be required (starting from sea water) to produce the

values for methane and carbon dioxide they observed in the brine

and sediments. These calculations revealed that the carbon added

to the Orca Basin had a concentration of 27.4 $mgC \cdot liter^{-1}$ with a

$\delta^{13}C$ of $-33\%_{oo}$. Sackett et al. (1979) were also able to partition

the 27.4 $mgC \cdot liter^{-1}$ between carbon dioxide added directly (via

fermentation) and carbon dioxide that had been cycled through an anaerobic methane consumption pathway ($CH_4 \rightarrow CO_2$). Their estimates from these contributions were 26.3 mgC·liter^{-1} from interstitial total carbon dioxide and 26.3 mgC·liter^{-1} of carbon dioxide from methane oxidation. They suggested that the observed isotopic ratios of carbon can be explained by some complex mixture of three bacterially catalyzed processes: carbon dioxide fermentation, acetate fermentation, and sulfide reduction (encompassing methane consumption).

Realizing the importance of bacteria in an anoxic environment such as the Orca Basin, LaRock et al. (1979) examined bacterial activity in the brine. Total biomass was measured in both the deep Gulf water and in the brine using direct counts of bacteria, ATP levels, and uridine uptake. ATP concentration and uridine uptake both decreased just below the interface and then increased with increasing depth. This pattern was similar to the ATP distribution in the Cariaco Trench (Karl et al. 1977). In the deepest sample from the brine an ATP value of 15.4 ng·liter^{-1} was found. This high level indicates that an active microbial population has developed within the brine of the Orca Basin.

The most interesting pattern shown by the microbial data was at the brine/sea water interface. Both ATP levels and uridine uptake values displayed similar patterns in the interface region. They increased in magnitude (relative to deep Gulf levels) above

the interface but decreased below the interface in the anoxic zone. This pattern, showing the existence of an interface population (or ATP subsurface maximum) at the brine/sea water interface, is consistent with the concept of particles resting on the density gradient. Bacteria and particles are closely associated in the deep ocean and conditions at the interface are well suited to the development of an autotrophic bacterial population. The anoxic zone provides a source of both nutrients and other energy yielding substrates (by diffusion upward from the brine) and could provide a rich medium for bacterial reproduction.

Ignoring the decomposition processes that had intrigued most other workers, Millero, et al. (1979) concentrated on the physical-chemical properties of the brine. They measured conductivity, density, and the speed of sound in the brine and in various brine dilutions. The speed of sound in the brine is 16% greater in the brine than in sea water with a salinity of 35°/₀₀ . This finding allows us to calculate the depth of the basin. The high sound velocity implies that the basin is deeper, and thus larger, than previously estimated by Shokes et al. (1977).

Millero et al. (1979) also found that salinity and density (under standard conditions) were consistent within the anoxic zone of the basin. These density and salinity measurements were done with exceptional care and corroborated the earlier data of Shokes et al. (1977). Millero et al. (1979) used the density measurements

to examine the physio-chemical nature of the brine. The ionic composition of the brine was used in additivity methods (of partial and molal volumes) to estimate the density of the brine. Measured values agreed with these estimates to within $\pm$ 280 x 10^{-6} g·cm^{-3}, from 15° to 35°C. Since this agreement was good, Millero et al. (1979) suggested that it seemed possible to make additional estimates of physio-chemical properties of brines using additivity methods.

Anaerobic Decomposition Processes

The salt that has flowed into the depths of the Orca Basin has created a large density gradient as was discussed earlier. Table 5 presents a list of various basins, both oxygen-bearing and anoxic, along with the stability of the water column in each basin. The hypersalinity in the Orca Basin has given the water in the basin water a stability that is nine orders of magnitude greater than the major anoxic basins in the ocean.

The stability of the Orca Basin has produced an isolated system removed from the general circulation of the oceans which provide renewal waters to other areas. With an absence of fresh, oxygenated water flowing into this geochemical system, oxygen becomes depleted and anaerobic decomposition processes begin. Little if any flushing can occur across its density gradient. The extreme stability of the Orca Basin thus makes it an ideal

Table 5.   Approximate stability across the sills of some basins and fjords (after Richards 1965).

BASIN	$\Delta\sigma_T/\Delta Z \quad x \quad 10^{-3} m^{-1}$
OXYGEN-BEARING BASINS	
Gulf of Mexico	2×10^{-6}
Catalina Basin	3.1×10^{-6}
Santa Barbara Basin	4.4×10^{-6}
Santa Monica Basin	8.8×10^{-6}
ANOXIC BASINS	
Kaoe Bay	2.4×10^{-5}
Cariaco Trench	3.2×10^{-5}
Gulf of Cariaco	3.5×10^{-5}
Saanich Inlet	1.5×10^{-5}
Black Sea	3.0×10^{-4}
Orca Basin[*]	$3.2 \times 10^{+3}$

[*] Calculated from data of Shokes et al. (1977).

laboratory for examining the mechanisms of anaerobic decomposition.

An understanding of anaerobic decomposition processes is important to marine geochemists. The sequence of oxygen depletion, followed by nitrate, nitrite, and sulfate reduction is an oft repeated pattern in anoxic marine basins and fjords (Richards 1965), evaporite basins (Borchert and Muir 1964), and during the early diagenesis of marine sediments (see, for example, Martens et al. 1978). Many marine sediments are anoxic, especially along continental margins where the sedimentation rate is high. Such sediments receive a large flux of organic matter, its origin being the fixation of organic carbon in the overlying photosynthetic zone. Organic-rich sediments undergo early diagenesis in which microorganisms consume the labile organic matter using first oxygen, then nitrate, nitrite, and sulfate as oxidizers until each is depleted and methanogenesis takes place. The products of this anaerobic decomposition diffuse out of the sediments into the overlying sea water.

Early diagenesis in sediments overlain by oxygenated waters cannot be interpreted by examining reduced species concentration in the overlying waters. Diagenetic products diffusing out of the sediment into oxygenated sea water are diluted or are consumed by oxidizing bacteria. The oxidation products in each case are compounds (e.g., CO_2) that are in large abundances or are rapidly diluted in aerobic sea water. It thus becomes difficult to assess

their input into the overlying water and consequently their geo-
chemical impact on the oceans. For sediments at the bottom of
anoxic basins or fjords, however, there is no free oxygen available
to act as an oxidant to alter the decomposition products.
Thus the terminal products of anaerobic decomposition accumulate in
the overlying anoxic waters.

Such anoxic basins and fjords provide scientists with natural
laboratories for examining the geochemistry and microbiology of
organic matter decomposition. The Black Sea, being the largest
anoxic basin in the world, has received the most attention. After
the results of the 1967 U.S. expedition had been reported (Degens
and Ross 1974), Laking (1974) compiled a bibliography with over
4,000 citations of research in the Black Sea. Since Richards (1955)
reported the discovery of anoxic sea water in the Cariaco Trench,
there have been over 120 papers published on this isolated Vene-
zuelan basin (for a review, see Richards 1975). Such intense
research activity is but another example of the scientific interest
in anoxic environments. This interest is well justified. The
chemical changes that led to the development of anoxic conditions
are of interest beyond the immediate confines of the stagnating
waters in basins and fjords where they are studied.

Examinations of regenerated nutrients and dissolved gases in
anoxic environments has led to various models which explain the
anaerobic decomposition of organic matter. During anaerobic

decomposition, organic material [represented here as $(CH_2O)_{106}$ $(NH_3)_{16}H_3PO_4$] is decomposed into the nutrient H_3PO_4, and the dissolved gases CO_2, CH_4, NH_3, N_2, and H_2S. To describe this process, simple stoichiometric reactions have been used with some success (Richards et al. 1965; Gaines and Pilson 1972; Adams 1973). An example is the reaction of Richards (1965) for phosphorus and nitrogen liberation during bacterial sulfate reduction.

$$(CH_2O)_{106}(NH_3)_{16}H_3PO_4 + 53SO_4^= \rightarrow$$

$$106CO_2 + 53S^= + 16NH_3 + H_3PO_4 + 106H_2O \qquad (7)$$
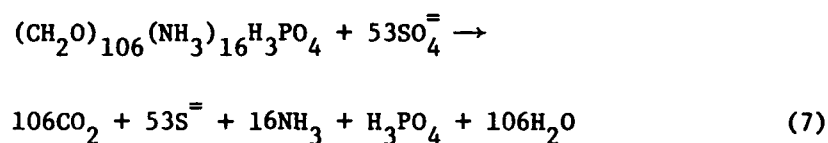
The C:N:P ratio of organic matter in this reaction is the average value of plankton of 106:16:1 given by Redfield (1934) and Fleming (1940).

Richards' model has been applied to the Cariaco Trench, Black Sea, Lake Nitinat, and Saanich Inlet. Most of these anoxic environments experience either periodic mass flushing or a slow continual input of oxygenated water into the anoxic waters. Unless the magnitude and time scale of the flushing can be accurately estimated for each area, it becomes difficult to apply the model. This is true since dissolved oxygen enters with renewal water. Input of oxygen can result in removal (oxidation) of reduced compounds and inhibition of anaerobic bacteria. With the discovery of the anoxic, hypersaline Orca Basin in the Gulf of Mexico (McKee

and Sidner 1976; Shokes et al. 1977) we have discovered a new
natural laboratory to study anaerobic decomposition processes. As
we shall see, this is a laboratory which does not experience the
mass periodic or even slow gradual flushings of other anoxic basins.

Research Objectives

The unusual circumstances involved in the formation and chem-
istry of the Orca Basin make it a desirable area for oceanographic
research. It is an unusual system when compared to the normal
distributions of major ions and gases in the ocean. However, it
probably is not unique when viewed in a geological perspective.
Basins similar in nature to the hypersaline Orca Basin must have
been common in the geological history of the Mediterranean Sea and
other regions where salt tectonics has played an important role
(N. L. Guinasso, personal communication). Remnants of basins
similar to Orca Basin (as evidenced by rapid sedimentation rate)
are found buried in the deeper sediments below the Mediterranean.
Understanding such basins may be important on a geological time
scale. Understanding decomposition processes is important on a
daily basis. Dissolved gases can be useful geochemical tracers
in such an environment. Inert gases can be used to elucidate
formation processes, while biogenic gases (major products of
anaerobic decomposition) yield information about current reactive
processes.

Most of the published work on the Orca Basin has ignored the dissolved gases in the basin. Shokes et al. (1977) noted that gases effervesced from the water (brine) when it was brought to the surface, but they made no measurements of the effluent gases. Only dissolved oxygen, which decreases to zero in the brine, was measured. In their carbon budget study, Sackett et al. (1979) measured both methane and carbon dioxide of the basin water and sediments. Their approach was to concentrate on the carbon compounds in the basin. Sackett et al. (1979) did not consider all the dissolved gases resulting from anaerobic decomposition.

In examining the hot, salty Red Sea brines, Craig (1969) pointed out that dissolved gas distributions could be a powerful tool in evaluating the mechanisms of brine formation. This is true since, unlike the major ions, initial gas concentrations are independent of both the ion ratios of the brine and the bulk ion composition of the salt from which the brine formed. Weiss (1969) used nitrogen, argon, and carbon dioxide values from the Red Sea brine to gain valuable information concerning its source of origin. He showed the utility of dissolved gas measurements in such unusual environments. With these ideas in mind, this author has undertaken a systematic study of the dissolved gases in the Orca Basin. The objective of this study has been to use dissolved gases to address some of the questions relevant to both the Orca Basin and to anaerobic decompositions in general.

These questions include:

1. What is the source of the Orca Basin brine and can dissolved gas data be used to confirm the source?

2. How is anaerobic decomposition of organic material affected by high salinity water?

3. What are the origin and significance of the isotopically light methane in the brine and sediments of the Orca Basin?

4. Why is there no hydrogen sulfide in the Orca Basin in spite of evidence of sulfate reduction in the sediments?

5. What role does the input of biogenic carbon dioxide gas play in the carbonate chemistry of the brine?

CHAPTER II

DENSITY EFFECTS AND PHYSICAL MIXING PROCESSES

Introduction

The dissolved gas distributions in the Orca Basin are directly
affected by the density gradient and interface mixing processes
which result from the presence of brine in the bottom of the basin.
Thus, a consideration of the physical characteristics of the Orca
Basin brine is important to this study. The Gulf of Mexico sea
water above the Orca Basin exhibits temperature and salinity depth
profiles (Fig. 8) which are typical of the expected distributions
in this area of the western Gulf (cf. Nowlin 1972). Below about
2000 m, however, the salinity concentrations begin to increase
slowly until an extremely rapid increase in temperature and salt
content are observed at about 2250 m (see Fig. 3). Salinity in-
creases from about 70%₀ to over 250%₀ over a depth interval of
only 17 m. This rapidly changing salinity has produced the dis-
tinct pycnocline at this level.

A true appreciation of the significance of the pycnocline in
the Orca Basin can be obtained by comparing the density gradient
in the Orca Basin with the pycnocline near the surface of the Gulf
of Mexico (Fig. 9). The surface pycnocline separates the homog-
enous mixed layer from the bulk of the oceans and it is this
pycnocline which is responsible for maintaining the nutrient and
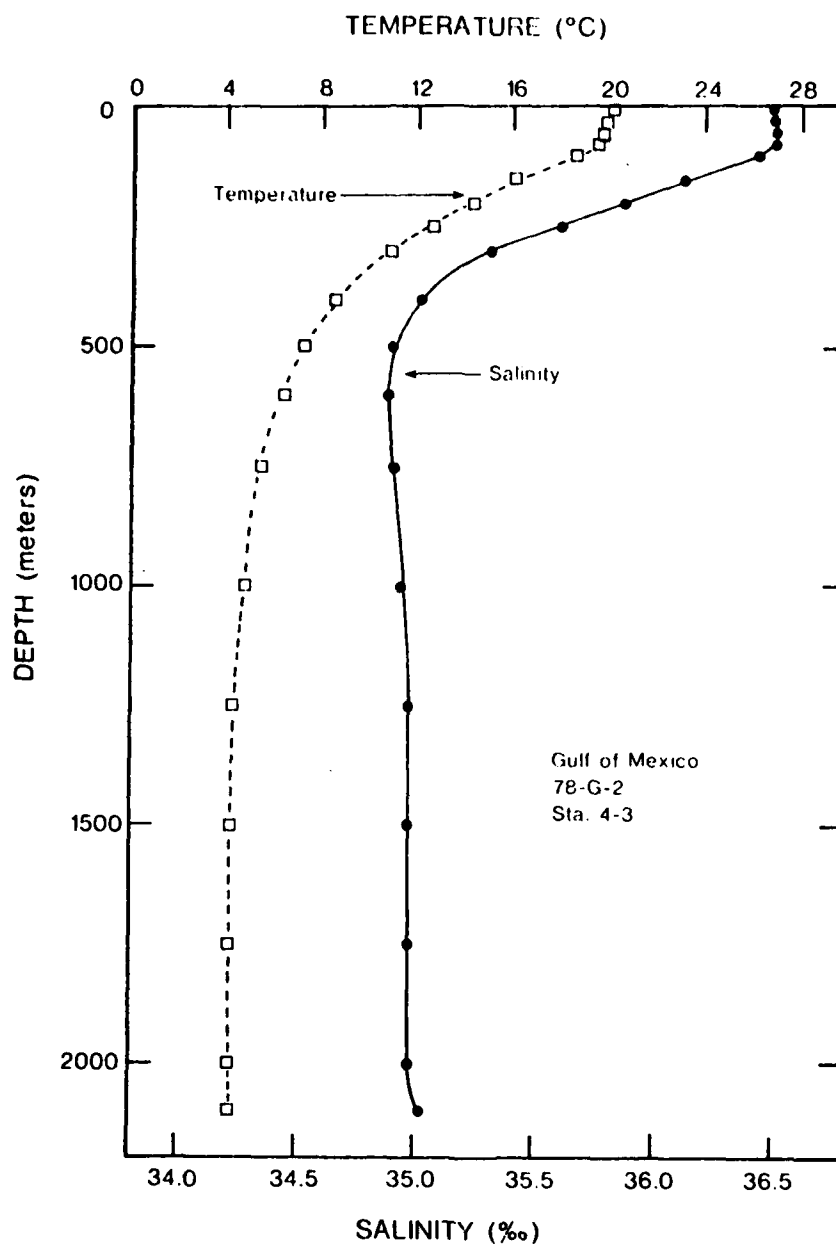
Fig. 8. Typical temperature and salinity depth profiles taken in the water column of the northwestern Gulf of Mexico above the Orca Basin.
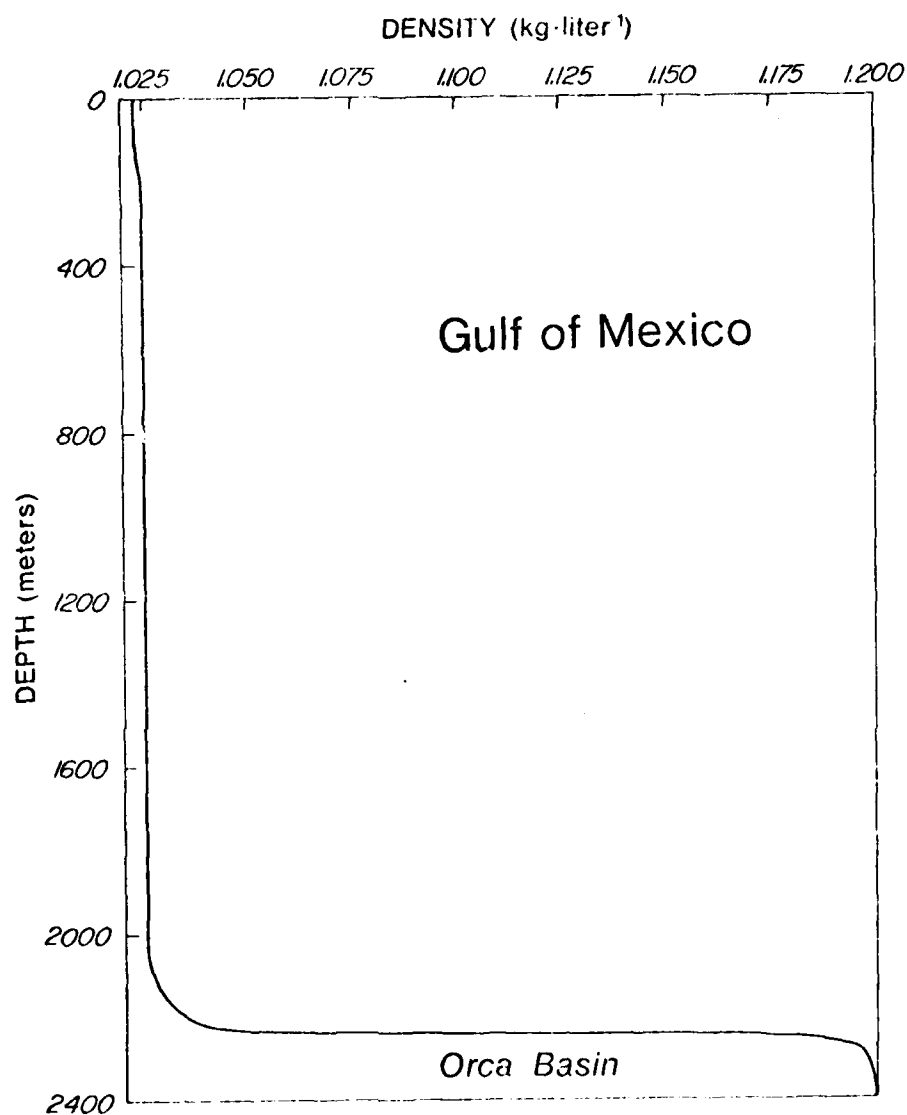
Fig. 9.   Density profile for the Gulf of Mexico, extend-
ing down through the Orca Basin brine.   Density at the brine
interface increases from 1.025 to 1.185 kg·liter^{-1} over a
depth interval of less than 50 meters.   This is one of the
most striking density gradients of an oceanic area (see
Table 5).

biological distributions in surface waters. That surface pycnocline is dwarfed by the density gradient at the surface of the Orca Basin brine layer. It is this gradient that reflects the low frequency sound waves that can be recorded even at a frequency as high as 3.5 kHz.

The Orca Basin pycnocline must act as a temporary trap for many of the particles which fall into the Basin. As particles settle through the water column, most have a density only slightly greater than the water through which they fall. Upon reaching the density gradient above the Orca Basin, their downward progress will be impeded. These particles probably stop at the density interface and begin to soak up salts (or dehydrate due to osmosis) until they reach isotonic balance with the brine. This may not be a continuous process. Particles may have to go through several layers or steps before their density will have increased suffi-ciently to allow them to proceed on their journey to the sediments. Even at the sediment interface, particles do not have a sufficient density, relative to the encompassing brine, to compact completely at first. As a result, the surface sediments are soupy, and they are difficult to sample since they tend to run out of the smallest hole in a box corer or other sampling device.

Support for the concept of an increased particle abundance at the brine-sea water interface comes from the bacterial biomass data of LaRock et al. (1979). They observed an increase in both

adenosine triphosphate levels and total bacterial cell counts in
samples taken from the Orca Basin interface, as opposed to samples
taken from the brine or from waters above the interface. Bacteria
in the deep ocean are usually attached to particles rather than
free-floating. Thus higher microbial biomass at the interface
would be indicative of an increased particle density at that level.
This increased microbial biomass was consistent with findings from
another stratified basin, the Cariaco Trench, where Karl et al.
(1977) observed a similar ATP distribution. The degree of strat-
ification in the Orca Basin can be discerned by a detailed exami-
nation of the temperature and salinity distributions through the
interface.

Temperature Distribution

Examination of a continuous temperature profile through the
interface to the bottom of the Orca Basin (Fig. 10) with a Plessy
Environmental Model 9040 STD shows that the Orca Basin brine is
not thermally homogenous. Temperature begins to increase at a
depth of around 2150 meters. The temperature depth profile goes
through several steps between 2150 and 2250 meters before a more
rapid increase begins. In the highest salinity brine (>250%oo),
there are at least two distinct layers having a temperature dif-
ference of about 0.05°C. This two-layer system within the brine
was not observed by Shokes et al. (1977), who used reversing
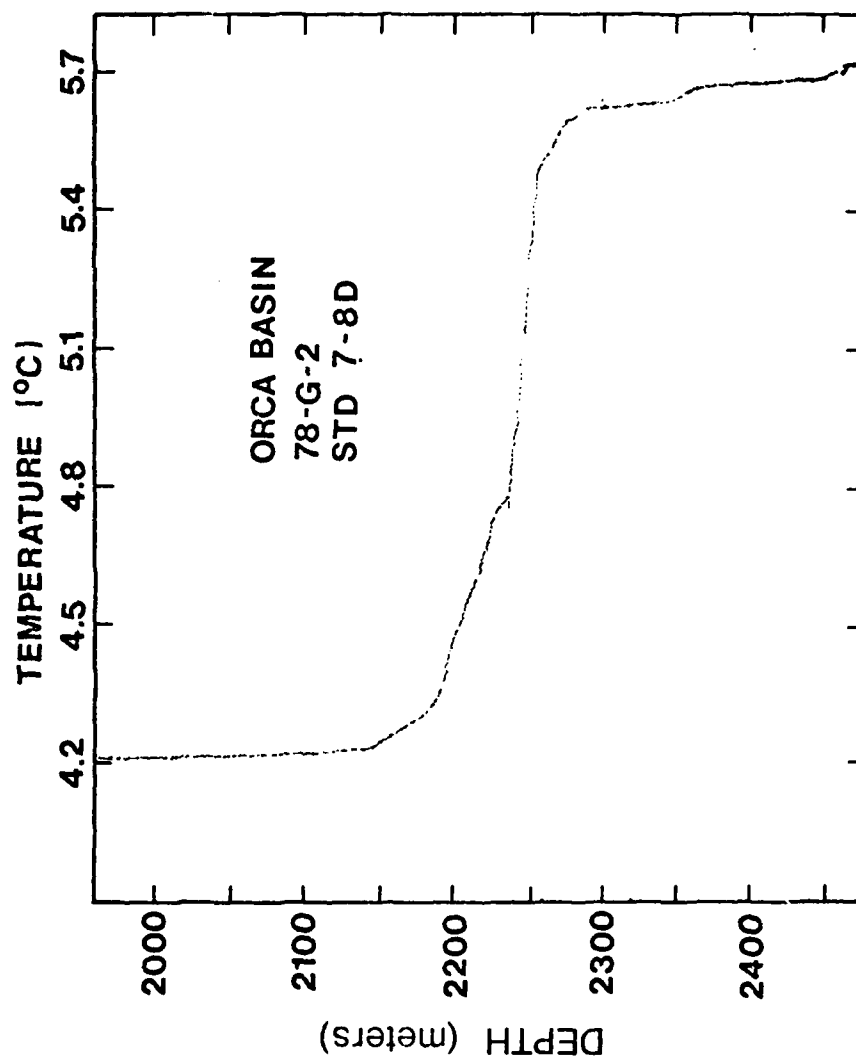
Fig. 10. Continuous temperature profile through the interface to the bottom of the Orca Basin made using a Plessey 9040 STD with the salinity probe disabled. Five thermal layers are observed above the high salinity brine, with at least two additional layers in the brine itself.

deep-sea thermometers to obtain their temperature profile.

Temperature of the Orca Basin sediment was measured (accidently) on cruise 77-G-3 of the R/V Gyre when the same STD used to make the profile in Fig. 10 was lowered into the mud. Due to the small density difference between brine and sediment particles falling into the basin, the top layer of sediment in the Orca Basin is very soft and unconsolidated, with about the same consistency as clam chowder (New England style). The surface sediments have a temperature of 5.77°C, a value 0.03°C higher than the bottom water temperature. This temperature differential between the brine and the sediment indicates that the brine is heated from below and would account for the heat flow required to raise the initial brine temperature from the original 4.2°C (Deep Gulf water) to the 5.6°C found today. Heat flow calculations and comparison with the estimates of Shokes et al. (1977) are given in a later section.

Salinity Distribution

The importance of the density gradient which results from brine in the bottom of the basin was discussed in Chapter One. This density gradient (Fig. 9) is dependent not on temperature, but salinity. The temperature of the high salinity (>35‰) water increases with depth (Fig. 10). A temperature increase would result in a corresponding density decrease without the effect of

salt on density. Since salt is the major factor influencing den-
sity, salinity can be equated with density for the following dis-
cussion.

The salinity depth distribution in the Orca Basin falls log-
ically into three zones. I have classified these zones (proceeding
from deep to shallow) as the high salinity brine, the interface
zone and the transition zone (Fig. 11). The high salinity brine is
a semihomogenous mixture (Millero et al. 1979) with a salinity
of 262°/$_{oo}$, relative to standard sea water. The brine, which
occupies the bottom 200 m of the Orca Basin, appears to have two
thermal layers (Fig. 10) with a slightly higher temperature in the
deeper region. This thermal gradient makes the lower layer slightly
unstable with respect to the upper layer of the brine and thus
could cause it to mix (see mixing discussion). The high salinity
brine is very stable, however, relative to the water above it.

The interface above the high salinity brine is the most marked
salinity gradient in the basin. Salinity increases from 70°/$_{oo}$ to
over 260°/$_{oo}$ with a depth decrease of only 17 m. This change
($dS/dz = 11.5°/_{oo} \cdot m^{-1}$) is an order of magnitude greater than the
zone either above or below it. It was very difficult to obtain
samples in this region. The points plotted on Fig. 11 were ob-
tained using the STD-rosette sampling system that was used to
produce Fig. 10. The data points that were plotted (Table 6) re-
veal the narrow range of depths involved. Data were taken from
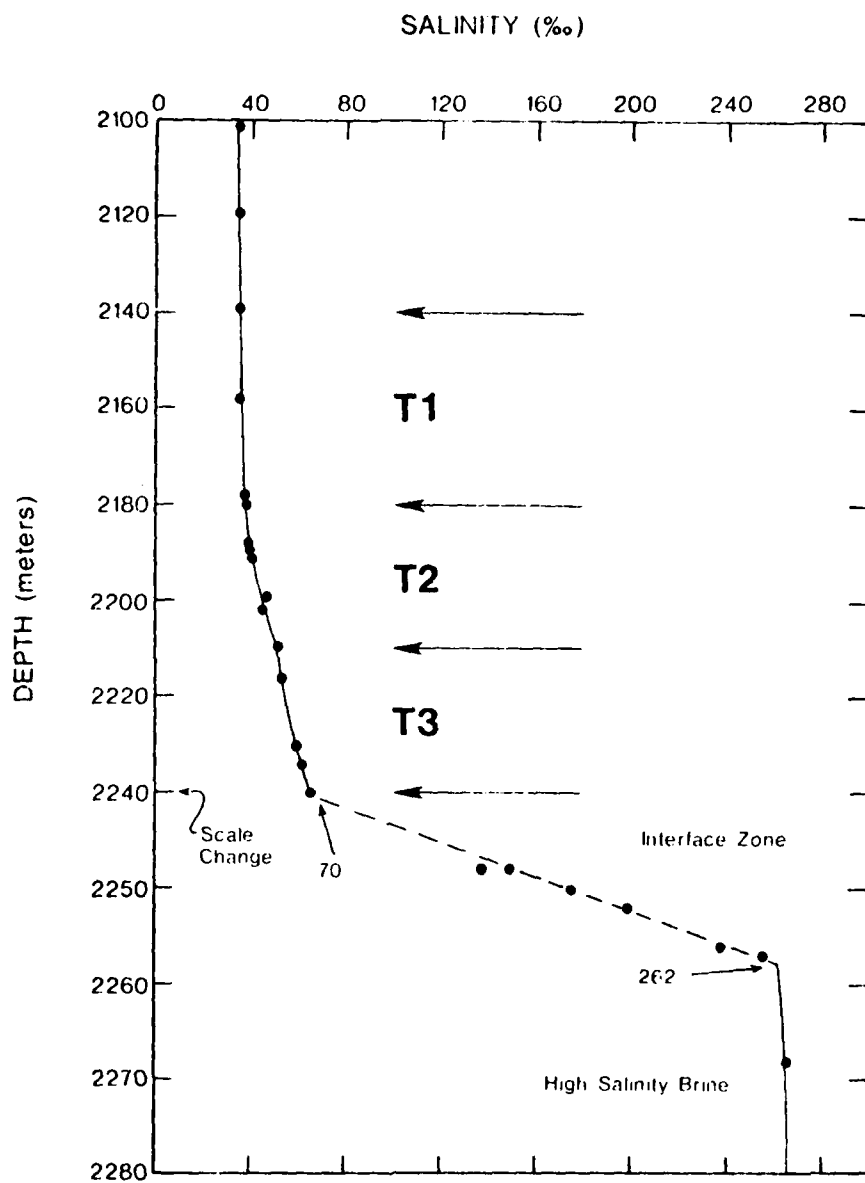
Fig. 11.   Detailed vertical profile of salinity through
the interface region of the Orca Basin.   Three zones are
identified: the transition zone from Gulf water, the true
interface zone where salinities increase from 70 to 262‰
and the high salinity brine with a constant salinity of
262‰.   The transition zone is subdivided into three
regions depending on the change in slope of salinity and
dissolved oxygen concentrations with depth (see Table 6).

Table 6.   Temperatures and salinities taken from two STD casts on cruise 77-G-13.   Note the large change in salinity over such a small depth.

Depth (meters)	Temp (°C)	Salinity* (‰)	Cast
2204	4.26	46	4
2230	4.54	60	4
2240	4.63	66	4
2248	4.77	138	4
2248	4.72	150	9
2250	4.81	176	9
2252	4.88	199	9
2256	4.96	238	4
2257	5.15	256	9
2268	5.38	266	9

* Salinity samples were volume diluted to a salinity near $35g \cdot kg^{-1}$ and analyzed using standard Copenhagen Water as a reference.   Volumes were converted to weights using a brine density of $1.185g \cdot kg^{-1}$.

two separate casts using the same system, yet samples from identical depths of 2248 m from each cast show a salinity difference of 12 $^\circ/_{oo}$ (138 cf. 150 $^\circ/_{oo}$, Table 6).

The interface zone probably results from a mixing of the high salinity brine below with the transition zone water above. The lower layer of the transition zone (T3) has a salinity at the bottom of 70 $^\circ/_{oo}$. A two point mixing curve for the interface zone would have 70 $^\circ/_{oo}$ and 262 $^\circ/_{oo}$ as the end points (Fig. 11). The two point mixing model seems to fit the salinity data in Fig. 11 reasonably well. Linear regression analysis of the data produces a straight line with a coefficient of variation of 0.991. Salinity changes by one part per thousand for each nine cm in this zone.

An STD system was the only reliable device capable of taking numerous samples in this narrow region on a single cast. The paucity of data from this region in other papers (e.g., LaRock et al. 1979) shows how difficult it is to obtain samples there. When closely spaced additional salinity samples are obtained, the two point mixing curve for this interface zone can be used to accurately calculate sample position relative to the high salinity brine.

The transition zone can be classified into three regions. The characteristics of each region are listed in Table 7. The upper region (T1) is the area where density first begins to increase from the constant values of the deep Gulf water. The

Table 7. Salinity zones in and above the Orca Basin.

Zone	Region	Salinity Range ($\%_{\circ\circ}$)	Depth Range (m)	$\dfrac{\partial S}{\partial Z}$ ($\%_{\circ\circ}m^{-1}$)	O_2 Range ($\mu mol \cdot L^{-1}$)	$\dfrac{\partial O_2}{\partial S}$ ($\mu mol \cdot L^{-1} \, \%_{\circ\circ}$)
Transition	T1	35.2	2130	0.031	225	30.5
		37.0	2178		170	
Transition	T2	37.0	2178	0.42	170	12.3
		50.0	2209		10	
Transition	T3	50.0	2209	0.62	10	0.5
		70.0	2241		0	
Interface	I	70.0	2241	11.53	0	–
		262.0	2258			
High Salinity Brine	B	262.0	2258	0	0	–
		±0.2	2430 (bottom)*			

* Exact bottom of Orca Basin varies.

salinity change is small, but the effects are apparent. The depth
of this region is about 50 meters. Transition region T2 spans a
depth interval of 31 m with a dS/dz of 0.42, an order or magnitude
greater than the region above. The salinity at the bottom of this
region is 50‰. The deepest transition region has a salinity of
between 50 and 70‰. Salinity in this region increases about 1.5
times as fast as in the region above. Region T3 abutts the
interface zone below. It is in this region (T3) that Shokes et al.
(1977) observed the step in the oxygen profile.

An examination of the temperature profile in the basin (Fig.
9) indicates that each salinity region is associated with a dif-
ferent slope in the temperature gradient. It is of interest to
note here, that the slope of zone T3 for temperature is not much
less than the thermal slope for the interface zone. Salinity
changes, on the other hand, represent an order of magnitude in-
crease in slope between region T3 and the interface zone.

The salinity distribution in the high salinity brine (Fig. 3)
shows no obvious differences with depth. These data were obtained
by volume dilutions of the brine before analysis by conductive
salinometry (Shokes et al. 1977). Millero et al. (1979) performed
precise weight dilutions on six samples from the brine and found
an average salinity of 262.84 ± 0.14‰. The bottom samples had
an average of 263.02‰ ($\sigma = 0.03$) and the four above then aver-
aged 262.75‰ ($\sigma = 0.02$). This slight difference gives an

indication of a two-layered salinity distribution. The difference
in the means of these two levels is significant at the 95% confi-
dence level, but only six samples were compared. More detailed
salinity sampling is necessary to precisely define the salinity
layering in the brine.

An attempt to obtain a detailed salinity profile was made on
Gyre cruise 78-G-2. The Plessey 9040 STD was modified to simul-
taneously measure temperature and salinity in the high salinity
brine. This STD has a normal salinity range of only 30-40 $^\circ/_{oo}$.
In more saline waters, the salinity output frequency overlaps into
the temperature frequency range, obscuring both the temperature and
salinity measurements. To measure salinity, a nylon plug was placed
in the center of the salinity-sensing induction toroid. Insertion
of this plug, with a 0.95 cm diameter hole drilled through its
center, reduced the effective cross-sectional area of the toroid.
The area was reduced sufficiently to make the measured inductance of
the high salinity water the same as the inductance of 37 $^\circ/_{oo}$ sea
water in an unmodified STD, while not interfering with the
temperature measurements.

The modified STD was lowered into the deepest portion of the
basin on March 28, 1978. The rough untreated data from this
attempt is shown in Fig. 12, along with an expansion of the tem-
perature trace in the high salinity brine. The salinity profile
shows a slight increase, with depth to the bottom, with two zones
having separate slopes. The observed change in slope of the

57

ORCA BASIN

Temperature

GY-78-02

LEG 1

STATION 007

CAST 4 D

(Salinity)

TEMPERATURE (DEG. C)

5.9 5.9 5.8 5.8 5.7 5.7 5.6 5.6 5.5 5.5

SALINITY (0/00)

2250 2275 2300 2325 2350 2375 2400 2425 2450 2475 2500
DEPTH (METERS)
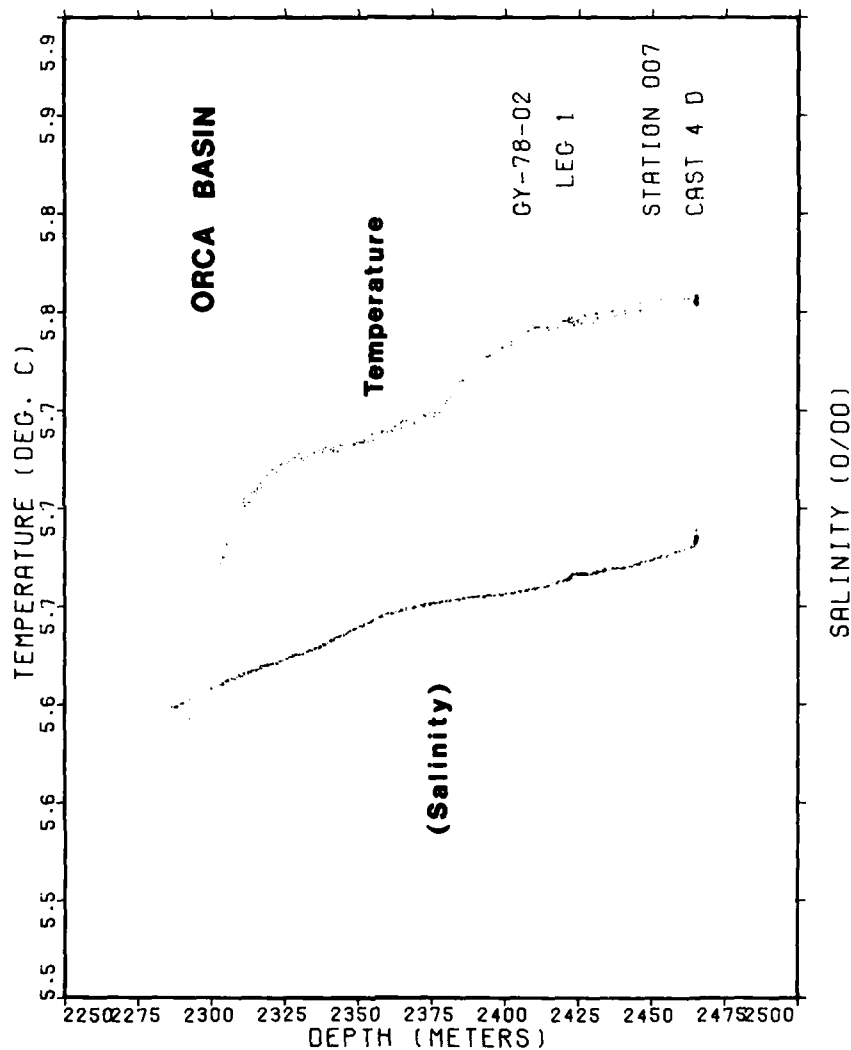
Fig. 12. Vertical profiles of temperature and arbitrary salinity in the high salinity water of the Orca Basin. The salinity data are presented to show trends in the salinity distribution. Gulf salinity is 35 °/oo and brine is about 263 °/oo.

salinity profile, however, does not occur where the temperature
profile shows an increase. Thus the continuous data do not indicate
that there are two separate layers with homogeneous temperature and
salinity. It must be remembered that the validity of this salinity
trace has to be questioned. The technique that was used to produce
the salinity profiles is rather unorthodox, and no calibrations
were made to determine the true salinities. The flushing volumes
of the smaller toroid also require investigation. The data does
indicate, however, that a detailed examination of the salinity
structure in the Orca Basin would be profitable in interpreting
water structures in the basin.

Mixing Processes in the Orca Basin

High Salinity Brine

In spite of the above discussion, the salinity distribution
in the high salinity brine is considered to be essentially uni-
form. This homogeneity is also true for several other parameters
that have been reported for the high salinity brine (see, for
example, Sackett et al. 1979). It follows that some mixing must
be taking place to create this homogeneous mixture in the brine.
There are several possible mechanisms for mixing. One mechanism
would be mixing due to input of new brine. Other possibilities
would be mixing resulting from thermal processes in the high
salinity waters or from seiching the brine.

New brine entering into the depths of the basin would mix until there was a re-establishment of the density structure in the brine. This mixing process would be rapid however, and would probably result in mixing of the brine such that both temperature and salinity were well mixed. As can be seen in Figs. 10 and 12, temperature is not thermally homogeneous in the brine. Thus, a slower mixing process must be invoked to account for the thermal layers, as well as the homogeneous salinity and other parameters.

Such a process might be convective mixing due to heating from below. This mechanism could only account for mixing in the high salinity brine where the salinity content is approximately constant at 262%o. The temperature differences in this high salinity brine are about 0.05°C between the two layers and could not support density imbalances with a significant salinity gradient. Thus the following discussion of possible convective overturn processes in the Orca Basin is applicable only to the high salinity brine. This is the 262%o brine in the bottom 140 m of the basin and not the lower salinity waters in the interface or transition zones that were described earlier.

It is quite possible that mixing in the basin deeps is driven by convective overturn resulting from the increasing temperature with depth in the high salinity brine. The bottom temperature measurement with the STD indicated that the Orca Basin is being heated from below. The bottom sediments are 0.03°C warmer than

the brine. The deep Gulf of Mexico water is 1.4°C cooler than the high salinity brine. The Orca Basin high salinity brine is similar to the classical thermal convection situation where there is heat-driven motion in a layer of fluid (the brine) contained between two horizontal planes, uniformly heated from below (the sediment) and cooled from above (Gulf water). In this type of system, deeper water becomes less dense than the water above it, due to increased heating from below, and can mix upward. Apparently, convective overturn is not uncommon in closed basins which are isolated from the more rapid advective mixing processes. For example, Newman (1976) examined the water structure in Lake Kivu and applied the same type of analysis to that system. Like the Orca Basin, he noted steps in the temperature profile in Lake Kivu and attributed the associated mixing in the lake to double-diffusive convective mixing. Turner (1968) also noted that there is increasing evidence that a step-like structure is characteristic of the ocean and some lakes. Instead of smooth gradients in temperature and salinity, well mixed layers separated by sharp interfaces are often observed. The layers would be the result of convective mixing of the waters due to heating from below. The same type of mixing may explain the homogeneity of salinity and other parameters in the high salinity brine of the Orca Basin.

The problem of convective overturn due to differential heating has been well studied in the realm of fluid mechanics. Benard

(1901) first showed that a thin layer of fluid becomes unstable
when the temperature (i.e., density) differences exceeds a minimum
value. Fluid motion takes place in a regular, steady pattern at
first, but can become turbulent with large temperature differences.
As described by Turner (1973), an unstable fluid layer of thickness
δ is driven upward (z direction) by buoyancy forces (density
differences) but retarded by viscosity, and neglecting inertial
effects there is a local imbalance. Unless the driving forces are
much greater than the dissipative forces, the system will remain
stable, in spite of the instability of a particular individual
layer. The mathematics of the instability was first formulated and
solved by Lord Rayleigh (Turner 1973). He showed that there is a
critical value of Ra, the non-dimensional Rayleigh number, below
which a fluid heated from below is stable to small disturbances.
The Rayleigh number, Ra, is given as

$$Ra = (g\alpha/\kappa\gamma)\ \Delta Th^3 \qquad\qquad (8)$$

where

    g is acceleration due to gravity

    α is the thermal coefficient of expansion

    κ is the thermal conductivity

    γ is the kinematic viscosity

    ΔT is the temperature difference across a layer

    h is the thickness of the layer

The Rayleigh number represents the balance between the driving
buoyancy forces and the diffusive processes which retard the
motion and tend to stabilize it. At a value of Ra_c of 10^3 to 10^4
cells which fill the gap between boundaries become unstable and
convective overturn can occur (Turner 1968, 1965).

Since fluid mechanicians usually deal with pure fluids (i.e.,
distilled water), the above description is normally applied to
systems that only have a temperature gradient to cause the density
imbalance. In the oceanic environment, however, there is usually
a salinity gradient to consider also in interpreting buoyancy
forces available to initiate convective overturn. The problem of
convective overturn in linearly stratified salt solutions has been
examined by Turner and Stommel (1964) and others. Turner and
Stommel (1964) gave a qualitative description of the motions that
result when a linearly stratified salt solution is heated uniformly
from below. That description was clearly summarized by Turner
(1968) and it could be used to describe the mixing regime in the
high salinity brine of the Orca Basin. Rather than attempt to
improve on his description, I simply quote:

> Convective stirring first produces a layer at the bottom
> of the containing vessel which is well mixed in both
> heat and salt, and which grows by incorporating fluid
> from above. This layer does not continue to deepen in-
> definitely, however: at some point a second layer forms
> on top of it, and this behaves in the same way. In time,
> many such layers can form, with sharp interfaces sepa-
> rating the turbulent convecting regions, and these inter-
> faces stay in nearly fixed positions until the bottom

one disappears as the lowest two layers merge. The
system can be maintained in this state because of the
very different molecular diffusivities of heat and
salt: heat can more easily escape from the top of a
layer to cause a convective overturning above, while
the salt mostly stays behind and preserves a net
stable density difference across the interface
(Turner 1968).

The question to be considered here is whether heat input from

the sediments into the Orca Basin brine is sufficient to create

the density imbalance required to exceed the critical Rayleigh

number, Ra_c. Unfortunately, various parameters such as the

viscosity and thermal conductivity have not been determined for the

Orca Basin brine. Thus in order to calculate Ra using Eq. 8, I

have chosen the values for the thermal coefficient of expansion,

thermal conductivity and kinematic viscosity that Newman (1976)

used for Lake Kivu. The values for sea water would be equally

applicable, since these terms are not the dominant terms in the

equation. Increases in salinity tend to cause both the viscosity

and the thermal coefficient of expansion to increase.

The two combined increases tend to cancel since the ratio

of the two is used in Eq. 8. Using Newman's (1976) data and the

Orca Basin values of 0.05°C difference between the two layers

with an interface distance of 25 m between the high salinity brine

layers, a Rayleigh number on the order of 10^{13} was calculated.

This value is several orders of magnitude larger than the critical

value of $Ra = 10^4$. Based on this calculation, it seems reasonable

to assume that the layering observed in the high salinity brine of the Orca Basin is due to double-diffusive convective mixing driven by geothermal heating from the basin sediments. Conclusive proof of this hypothesis requires a more sophisticated set of constants for the Rayleigh number calculation, as well as a better definition of the salinity and temperature microstructure in the high salinity brine.

Oxygen Step Region and General Mixing

One of the most striking features of the data presented by Shokes et al. (1977) was the anomaly (step) just above the high salinity brine in the oxygen depth profile. A comparison of the oxygen data (Fig. 5) and the temperature and salinity profiles (Figs. 10 and 11) indicates that the oxygen step is associated with one of the physical layers in the brine transition zone, region T3. There are many complex forces acting upon this interface region. Salinity increases from 50°/₀₀ to 70°/₀₀. Temperature increases from 4.25°C to 4.75°C. The brine interface may be oscillating with time. This region could be physically active. There are two plausible explanations for this step region. Either new, oxygenated brine is being put in at this level, or oxygenated water from above is mixing with water from the interface zone below to create this higher salinity,oxygenated water in region T3.

An examination of a temperature versus salinity plot for the
Orca Basin is helpful in understanding the processes acting on the
oxygen step region. Fig. 13 is a plot of the temperature and
salinity data from Fig. 3. The salinity data are given in units of
g·liter^{-1}, since the samples were volume diluted. Correcting
the data for density and replotting in salinity units of g·kg^{-1}
showed the same profiles, and would not alter the data interpre-
tations. Fig. 13a shows a plot of all the temperature and salinity
data taken from depths of 2050 m down to 2430 m, near the bottom of
the basin. The solid line drawn through the data follows the data
from a salinity of 35 °/oo to a salinity of 170 °/oo, and then the
second half of the curve (from 170 to 305 °/oo) is simply a mirror
image of the left hand portion of the solid curve. The curve was
drawn in this manner since this data set (after Shokes et al. 1977)
had only two data points in the high salinity region, other than in
the high salinity brine itself. Fig. 13b is an expansion of the
data between 35 and 70 °/oo from Fig. 13a, indicated by the area
between arrows on Fig. 13a. The T-S profile in this region is
almost a straight line, which is indicative of a two point mixing
condition. The two points representing the extremes of the straight
line drawn on Fig. 13b would be the temperatures and salinities of
the two water masses that are mixing.

Fig. 13c is an expansion of the data between 45 and 75 °/oo,
and also exhibits the same straight line structure indicative of
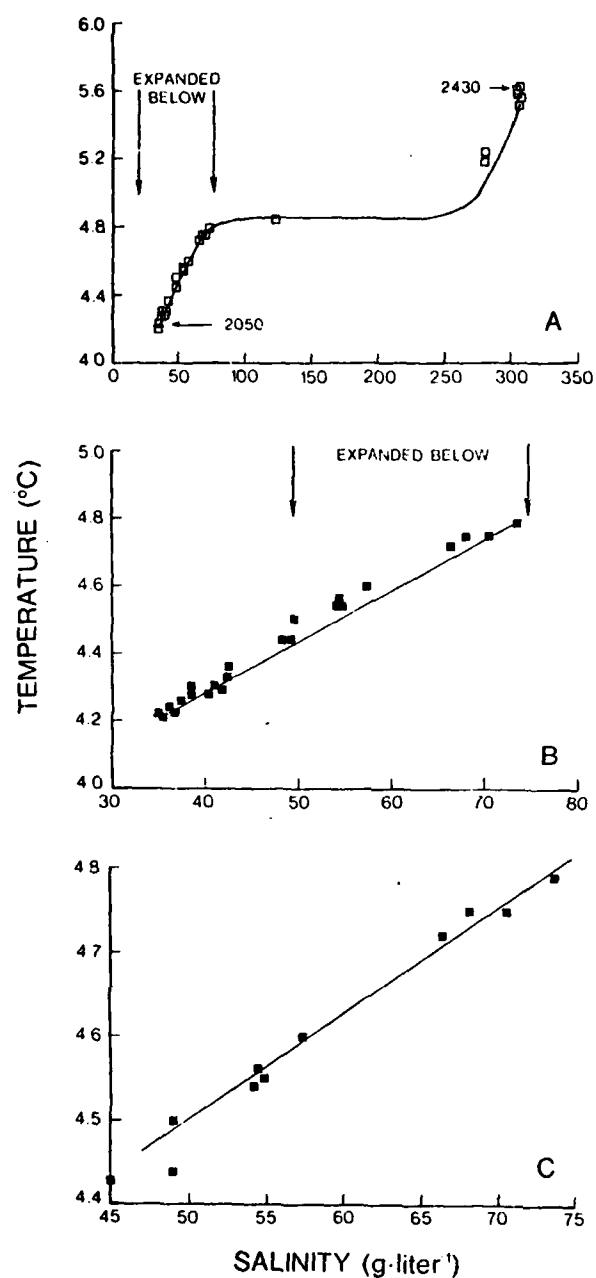
Fig. 13.   Salinity versus temperature
profile for the Orca Basin. Parts b and c
are expanded plots of the data presented in
part a. The data are taken from the same
data shown in Fig. 3.

a two-point mixing model. Most of the points on Fig. 13c are from the oxygen step region shown on Fig. 5.

If the water in the oxygen step region is the result of a two point mixing process, this could explain the oxygen concentrations found in that zone. The oxygen would be oxygen mixed downward from above. This mixing, however, is probably not due to convective overturn as was discussed in the previous section for the high salinity brine. Salinity increases from 50 $^o/_{oo}$ at the top of zone T3, to 70 $^o/_{oo}$ at the bottom, 32 m below. For this zone to turn over due to heating from below, the 70 $^o/_{oo}$ salinity water would have to reach a temperature of over 55°C. There is no evidence for such high temperatures at the Orca Basin interface. Yet, evidence for mixing of the oxygen step region(T3) is compelling.

The salinity-temperature plots presented in Fig. 13 might be explained by diffusive mixing processes alone, if one assumes that a double diffusive process is taking place. That is temperature and salinity are diffusing at different rates. For molecular diffusion, this is indeed the situation. Heat diffuses faster than salt (Munk 1966). Two questions to be considered in this discussion are what are the differences in the diffusion rates of these two parameters at the Orca Basin interface, and how does diffusivity change with distance from the interface.

If one assumes that the brine flowed without mixing into the depths of the Orca Basin at some initial time $t = 0$, then at that

time the brine was covered by Gulf of Mexico water with a sharp

boundary between the two. In fluid dynamics, this initial case is

described as one in which the distribution occupies a finite

region with an initial state defined by:

$$C = C_o, \quad Z < 0, \quad C = 0, \quad Z > 0, \quad \text{at } t = 0 \tag{9}$$

where C = concentration, Z = distance, t = time and $Z = 0$ at the

interface. This distribution is analogous to one in which a long

tube of clear water rests on a long column of solution, or when a

long water column of Gulf of Mexico water rests on top of the Orca

Basin brine. The case for the Orca Basin is shown diagramatically

in Fig. 14. At a time t_o, both the temperature and salinity pro-

files have only one value in the Gulf water (T_1, S_1) and a single

value in the brine (T_2, S_2). The profile at time t_1 is illustra-

ted by the solid line in Fig. 14.

After initial diffusive mixing, the Orca Basin interface must

reach steady-state to be maintained. This can be proved by performing

a simple calculation of how long the temperature profile would be

maintained at a constant thermal diffusivity of $10^{-3} \text{cm}^2 \cdot \text{sec}^{-1}$.

Using the simple relationship,

$$L^2 = Dt \tag{10}$$

where L is length, D is the thermal diffusivity, and t is time, one

can calculate the characteristic time for diffusion to spread an

initial temperature step function. The interface thickness is

1700 cm. With $D_T = 10^{-3}$, the time required for diffusivity to

spread an initial step function to the present thickness is
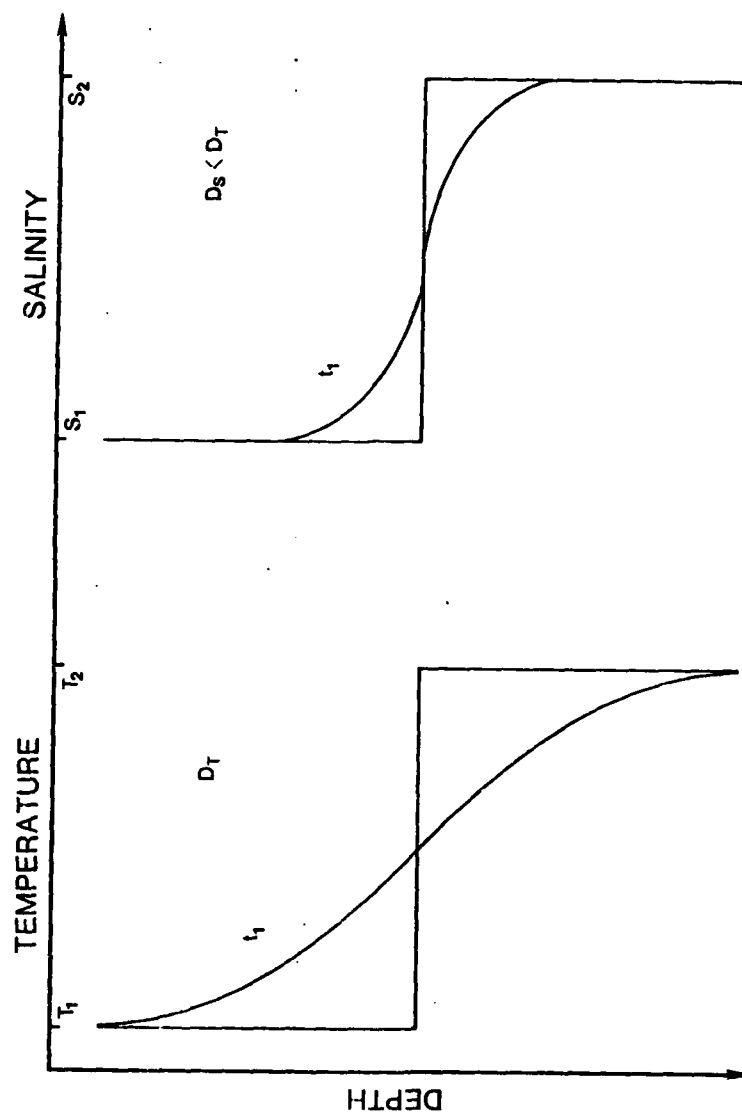
Fig. 14. Temperature and salinity profiles for the initial two-layer system in the Orca Basin if the brine entered the basin without mixing. The solid line indicates the degree of diffusion of each parameter at some characteristic time t_1. $D_T > D_S$.

2.9×10^9 sec, or about 90 years. Since the time of initial input of brine into the Orca Basin is $\sim$ 8000 years, time dependent processes would have removed the interface long ago. Similarly, time-dependent diffusion of salt ($D_s = 10^{-5}$) would spread the salinity interface in 3×10^{11} sec, or about 9000 years. The Orca Basin interface region would be unstable unless the system were steady-state.

A comparison of the STD temperature-depth profiles in the basin taken during three different years supports the steady-state concept. The first temperature-depth profile with an STD system was taken in 1977 by Guinasso (1977). The latest profile was taken in March, 1980, on Gyre cruise 80-G-4. The thermal layers throughout the basin (Fig. 15) are identical in both profiles, yet geothermal heat is entering the brine from below. This input would change the temperature interface without a balanced output. The Orca Basin diffusion must be in steady-state relative to heat.

Salt diffusion would not be steady-state without an input, but diffusion out would be very slow. Assuming a diffusion coefficient for salt of $10^{-5} cm^2 \cdot sec^{-1}$, one can calculate the time for all salt in the basin to diffuse out. A one cm^2 column in the deepest part of the basin would contain $2 \times 10^5 cm^3$ of brine, with each cm^3 containing 0.25 g of salt. With $D_s = 10^{-5}$, a salt flux of $1.25 \times 10^{-10} g \cdot cm^{-2} \cdot sec^{-1}$ is calculated. Dividing the mass of salt in the water column ($5 \times 10^4 g \cdot cm^{-2}$) by the flux gives 4×10^{13} sec, or about 1,300,000 years, as the time for all the salt to diffuse out of the basin. In the 8000 years since the brine entered the
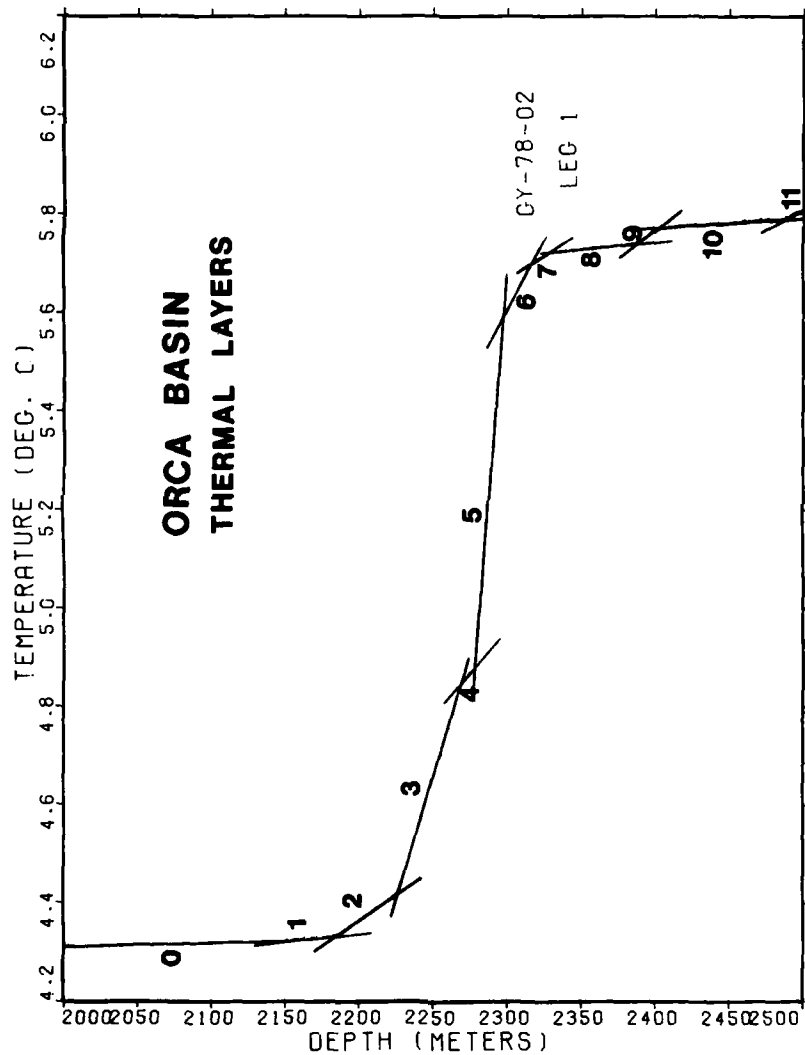
Fig. 15. Modified temperature depth profile showing the linear thermal layers through the interface into the high salinity brine. Each layer has a different thermal diffusivity. Depths have not been corrected.

basin, only 0.6% of the salt could have diffused out. The same
would be true for other solutes produced there. Transport of
solutes from the brine to the overlying Gulf waters would be very slow.

The slope of the twelve thermal layers in Fig. 15 can be used
to calculate changes in thermal diffusivity. Through the interface
(layer 5) diffusion must be entirely molecular. With such a large
temperature and salinity increase over the short distance (17 m)
of this zone, processes more rapid than molecular would rapidly
distort the interface. With only molecular diffusion, the trans-
port of heat through the interface is due only to the thermal
conductivity of the brine. The average salinity in layer 5 is 167 $^{\circ}/_{\circ\circ}$.
A 17% NaCl solution would have a thermal conductivity of 1.345 x
$10^{-3} cal \cdot cm^{-1} \cdot sec^{-1} \cdot {^{\circ}}C^{-1}$ (Weast 1969). The temperature change
across the 1700 cm interface is 0.65°C, giving a slope, dT/dz, of
3.76 x $10^{-4} \cdot {^{\circ}}C \cdot cm^{-1}$. Heat flux through the interface (layer 5)
can be calculated by the formula:

$$\text{Heat Flux} = \frac{dT}{dz} \cdot \kappa \tag{11}$$

where κ is the thermal conductivity. Heat flux through the inter-
face was calculated as 0.5 $\mu cal \cdot cm^{-2} \cdot sec^{-1}$. This flux is half of
the world average geothermal heat flow used by Shokes et al. (1977)
to calculate the time to heat the brine to 5.6°C. Since the Orca
Basin brine is in approximate geothermal balance, their estimate
is probably too high for this area.

If heat transport in the Orca Basin is steady-state, the heat
flux through any layer in Fig. 15 will be the same. The heat flux
through layer 5 has been calculated. Thus, using the slope of each

layer (dT/dz) and Eq. 11, the thermal conductivity can be calcu-
lated for each layer. The thermal diffusivity (D_T) is related to
the thermal conductivity (κ) by

$$D_T = \frac{\kappa}{C_p \rho} \qquad (12)$$

where C_p is the heat capacity and ρ is density. Using an average
density for each layer and assuming C_p was unity, thermal diffu-
sivities were calculated for each of the twelve layers in Fig. 15.
Thermal diffusion constants are plotted against depth in Fig. 16.
The lowest diffusivity (molecular) is in layer 5, and the
diffusivities increase in both directions away from the interface.
The changes are regular and predictable above the interface
(except layer 4), but very irregular in the high salinity brine.
Where thermal diffusivity is greater than molecular, salt should
diffuse at the same rate giving the linear temperature-salinity
distributions that were observed.

The above discussion has shown that in addition to molecular
processes, eddy diffusion is operative in the transition zone.
This would require the input of energy into the basin to produce
this type of mixing. One possibility for this input of energy
into the basin would be a seiching of the brine in the basin. If
the interface were oscillating, there would be sufficient energy
input to cause turbulent mixing.

Evidence for seiching in the basin comes from the minisparker
profiles obtained by Shokes et al. (1977). The dark line
representing the brine interface appears to be elevated on the
right side of the profile in Fig. 17. This profile could have been
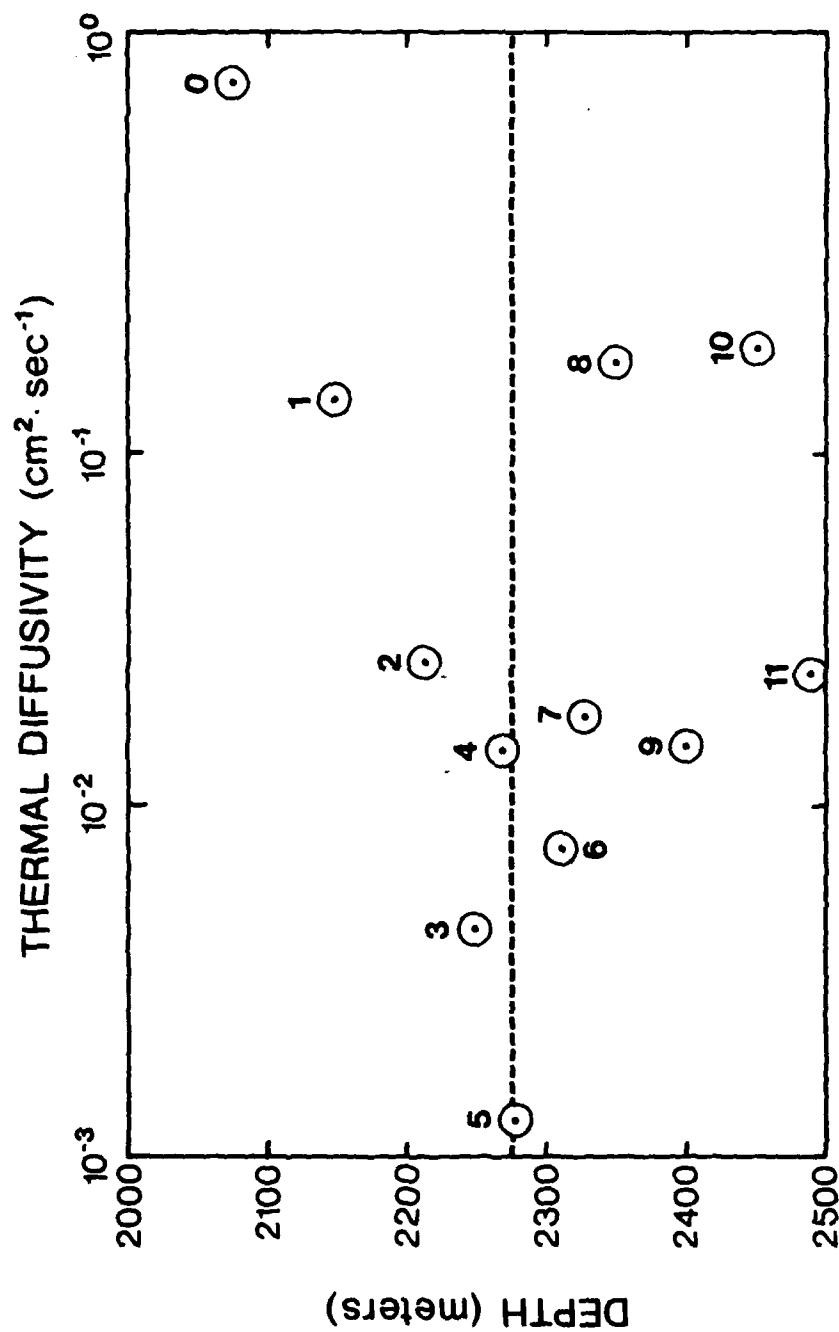
Fig. 16. Plot of diffusion coefficients for temperature (D_T) with increasing distance from the Orca Basin interface zone (layer 5). Layer numbers (given by each point) refer to thermal layers in Fig. 15.
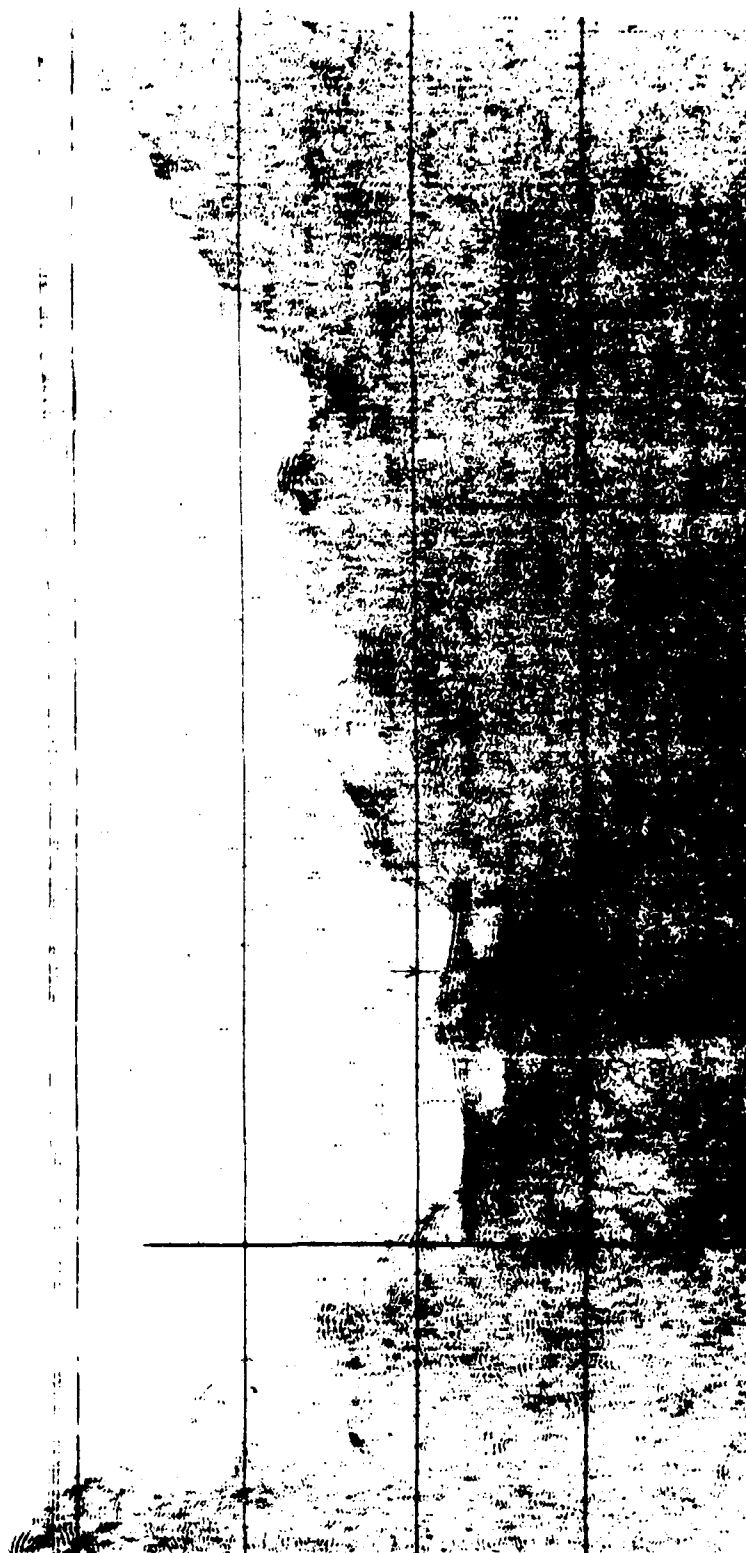
Fig. 17. One section of the minisparker profile taken on Gyre cruise 76-G-10. The profile crosses the longest section of the southern lobe of the basin. The right side of the profile is 3% higher than the left hand side.

taken when the interface was tilted due to seiching. Examination
of several other of the minisparker records from cruise 76-G-10
showed that several transects exhibited a tilt in the interface.
One of the profiles examined is shown in Fig. 17. The right
hand side of this profile, which was taken along the longest
section of the big basin is slightly higher than the left hand
side of the profile. Energy to induce seiching could result from
internal waves or even storms passing over with a reduction in
barometric pressure. Merrell (1971) has calculated that
energy from passing storms can influence bottom currents several
thousand meters below.

When seiching occurs in the basin, turbulent mixing will
occur on both sides of the brine sea water interface (layer 5).
This is identical to the case in fluid mechanics of oscillations of
the common boundary of two superimposed liquids. The motion will
be damped more quickly than seiches in lakes since the low density
contrast has the effect of diminishing the velocity of propa-
gation of waves of any given length in the ratio $[(1-s)/(1+s)]^{1/2}$,
where s is the ratio of the density of the Gulf water to that of the
brine (0.88).

In oscillations of a water mass with two layers, there will be
a discontinuity of motion at the interface. Fig. 18 shows mixing
processes as a result of seiching in a two layer system with arrow
vectors indicating the magnitude and direction of the water
movements. The normal velocities are continuous, but the tangential
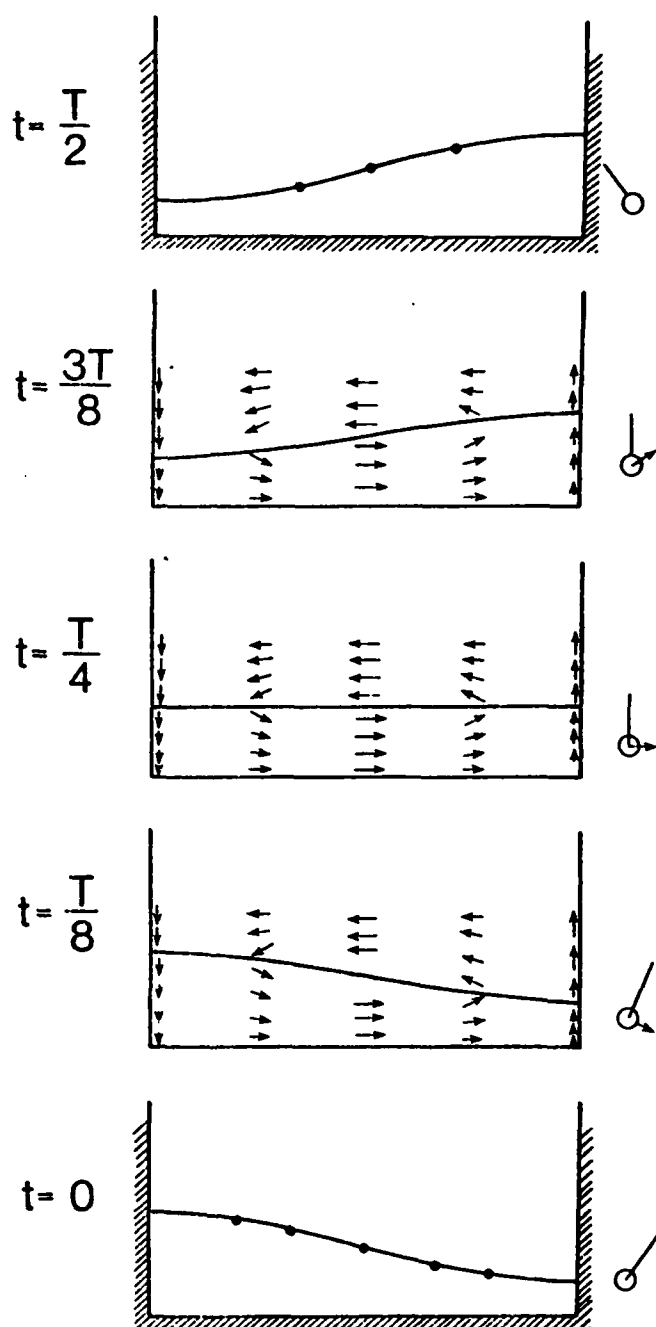
Fig. 18. Oscillations of a seiche in steps of one-eighth of a cycle for one-half of a complete oscillation. The depth is exaggerated (after Neumann and Pierson 1966, with modifications to show the two-layered system).

velocity changes direction as the interface is crossed (Lamb 1945).
With the mixing at the interface, it is possible that the
oxygenated water from above would mix with the brine from below and
produce the oxygen step region that was observed. The diffusivities
above the brine (Fig. 16) should be high enough to allow mixing of
oxygen downward into this region.

CHAPTER III

MAJOR ATMOSPHERIC GASES IN THE
ORCA BASIN BRINE

Of the twelve atmospheric gases listed in Table 1, only nitrogen, oxygen and argon have concentrations of about one percent (Ar) or larger (N_2, O_2). These major, atmospheric gases have been measured in many oceanic environments. Their high atmospheric concentration results in dissolved levels in sea water which are great enough to be measured by simple gas chromatographic techniques. Oxygen is by far the most important gas in the ocean. It is required by all marine animals for survival and is produced during primary production by the phytoplankton in the surface oceans. In deeper waters, oxygen is consumed more rapidly than it is produced. The term apparent oxygen utilization (A.O.U.) has been defined (Redfield 1934) as the amount of oxygen removed due to respiration processes.

Argon and nitrogen are generally regarded as nonreactive in ocean waters. Some qualification of this assumption may be necessary for nitrogen, since it has been shown to be produced in the anoxic waters of the Cariaco Trench (Richards and Benson 1961; Linnenbom and Swinnerton 1969) and in some anoxic sediments (Wilson 1978). The oceanic distribution of argon and nitrogen is determined by physical mixing processes and by the effects of temperature and salinity on their solubility. In contrast, the

distribution of oxygen is influenced by biological as well as
physical properties. Thus measurements of unreactive gases, along
with oxygen, are useful in obtaining a quantitative separation
of the effects of physical and biological processes on the distri-
bution of oxygen in the ocean.

As was discussed in detail in Chapter I, the atmospheric
equilibrium of dissolved gases in sea water is a function of both
the temperature and salinity. The atmospheric equilibrium solu-
bilities of oxygen, nitrogen and argon in sea water at 35°/oo
salinity are given in Table 8. These values were calculated from
Eq. 5, using the constants determined by Weiss (1970). A plot
of temperature versus solubility for argon and nitrogen (Fig. 19)
shows that the relationship is not a linear one. This concept is
important in interpreting the gas solubility data from a particular
area, since the mixing of two water masses with the same salinity
and different temperatures would produce an apparent supersatura-
tion. For example, if two waters of 35°/oo salinity, one having a
temperature of 0°C and the other at 30°C, the apparent supersatur-
ation would range from 7.8% for nitrogen to 8.6% for argon (Fig.
19).

In studying the major atmospheric gases in the Orca Basin, I
have examined both the concentrations and the solubilities of the
gases in the brine. A major purpose of these measurements is to
determine whether or not there has been dissolved nitrogen

Table 8.   Solubilities of N_2, O_2, Ar in sea water at 35%.
salinity based on Eq. 5 and coefficients from Weiss (1970).

t°C	Solubilities ($\mu mol \cdot kg^{-1}$)		
	N_2	O_2	Ar
0	616.3	349.5	16.98
5	549.6	309.1	15.01
10	495.6	274.8	13.42
15	451.3	247.7	12.11
20	414.4	225.2	11.03
25	383.4	206.3	10.11
30	356.8	190.3	9.33
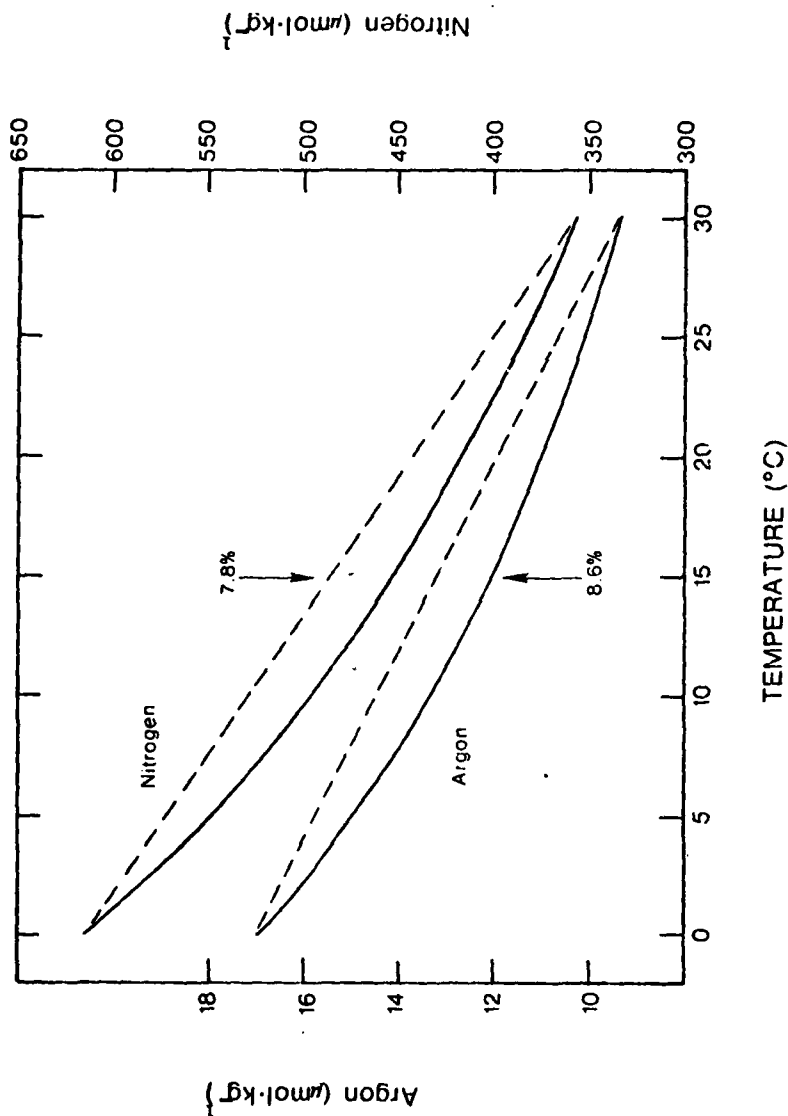
Fig. 19. Plot of temperature versus atmospheric solubility for argon and nitrogen, indicating that the relationship is not a linear one. Thus, if two water masses of equal salinity but different temperatures are mixed, an apparent dissolved gas supersaturation will be observed without the addition of any gas. Examples are shown for mixing of water at 0°C with water at 30°C (dashed line).

production in the brine. It will be observed that both nitrogen and argon are supersaturated in the brine relative to the brine temperature and salinity at one atmosphere total pressure. This chapter addresses the question of the origin of nitrogen and argon in the brine and what one can learn from these unreactive gases concerning the origin and geochemistry of the Orca Basin.

Methods

Gas Solubilities

Since gas solubilities had not been previously measured in hypersaline waters, there was a need to determine whether or not actual measured solubilities deviated significantly from the extrapolated data obtained using the equations of Weiss (1970). To equilibrate the brine with gases, a glass, thermally-regulated equilibration chamber was constructed using a design similar to one used by Schmidt (1979) for measuring atmospheric solubilities of hydrogen and carbon monoxide (Fig. 20). Into this chamber, approximately 400 ml of brine (or sea water for comparison) was introduced and gas was bubbled through at a rate of 40 ml$\cdot$min^{-1} for 30 min. The time required to saturate the brine with the equilibration gas should follow a simple first order exponential decay curve, assuming that equilibrium is reached between the bubbles in the equilibration gas and the bubbles in the stripper.

GAS VENT

PLATINUM
RESISTANCE
THERMOMETER

COOLANT
OUT

PURGING
CYLINDER

STOPCOCK

COOLANT IN

STANDARD
GAS INLET
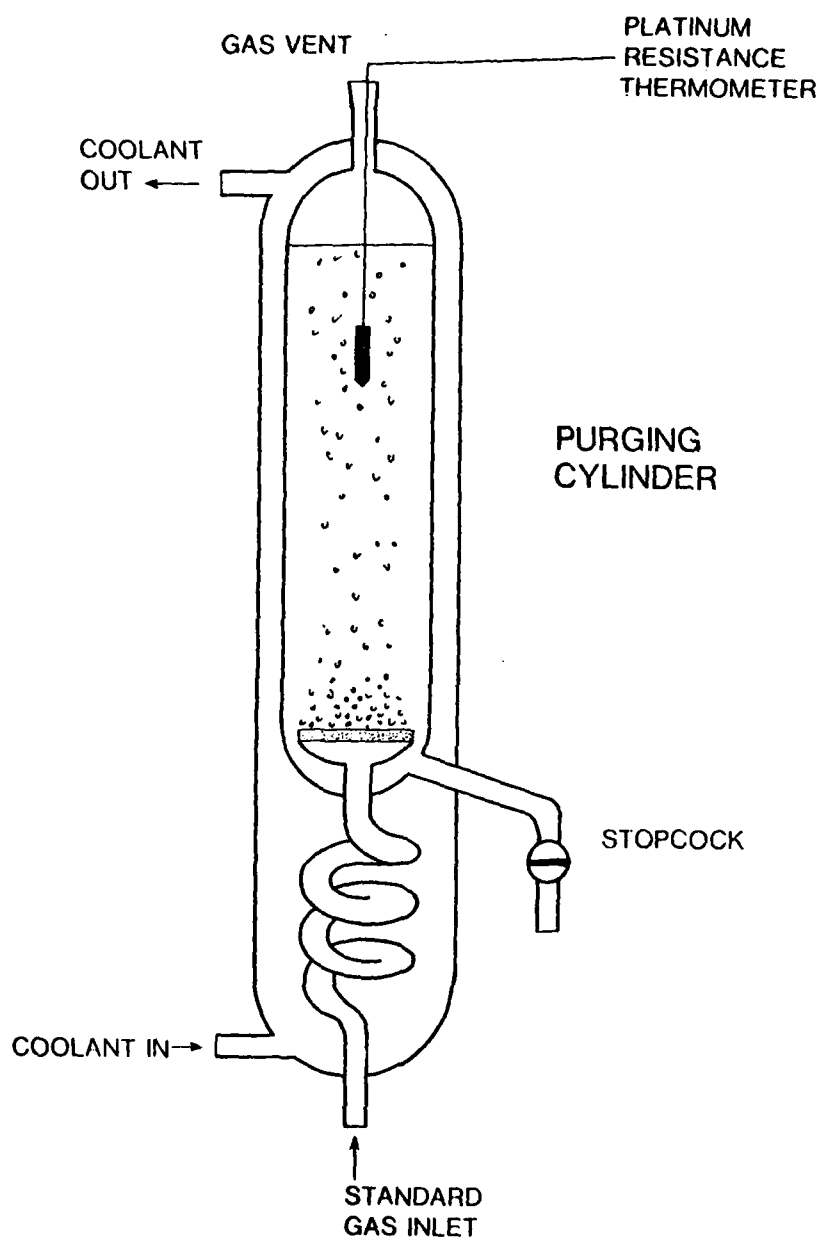
Fig. 20. Schematic diagram of thermal jacketed
purge cylinder used to equilibrate the brine with
dissolved gases.

The characteristic time required to increase the concentration of the gas i in solution by a factor of 1/e is given by

$$t_i = \frac{B_i V_1 P}{F^+} \qquad (13)$$

where B_i is the Bunsen solubility coefficient of the gas i at the temperature of the liquid, V_1 is the volume of the liquid, F^+ is the volume rate of flow of i in the equilibration gas at STP, and P is the partial pressure of i inside the equilibration chamber, in atmospheres (1 atm = 101.325 kPa). To make this calculation, Bunsen coefficients were calculated for each gas, and other values (e.g. flow rate) were measured. At 0°C the characteristic time required to equilibrate sea water at 20°C was 15 sec for oxygen, 17 sec for argon and 8 sec for nitrogen. For each of the brine and sea water measurements, the equilibration gas was allowed to flow for a period of 30 min to assure that complete equilibration was reached. Air was used for the nitrogen source gas yielding atmospheric equilibrated values. Pure (>99.995%) argon and methane were used to measure Bunsen coefficients for those gases.

Since the bubbling of a gas through a liquid may tend to supersaturate the liquid with the gas used, one further precaution was taken during these measurements. After the 30 min equilibration period, the equilibration gas was shut off and the system sealed with one atmosphere of gas above the sample for two min before the brine was sampled. Analysis of the dissolved gas was

accomplished using the same gas chromatographic techniques as were used for Orca Basin samples (see below). As an additional check on possible supersaturation, sea water samples of a known salinity were analyzed using the same procedures as for the brine. Since the equilibrium solubilities of dissolved gases in sea water of normal salinity are known very precisely as a function of temperature and salinity, these measurements served as external standards for the equilibrium process.

The temperature of the brine in the equilibrator was monitored using a thin film platinum resistance electrode which was epoxy coated and immersed in the brine during the equilibration process. This probe was calibrated against the high precision platinum electrode (Leeds and Northrup, S/N 1762254) used to calibrate the Texas A&M University reversing deep-sea thermometers. The high precision probe is calibrated periodically against NBS temperature standards. The temperature measurements in this equilibration study are accurate to $\pm$ 0.02°C.

Dissolved Oxygen

Dissolved oxygen was measured on the sea water samples we collected from the Orca Basin by the microWinkler method of Carpenter (1965). No oxygen was found in the high salinity brine so no problems due to effervescing of the brine were observed here. Nor was the degassing effect noted in samples taken from the

interface where small amounts of oxygen had been previously mea-
sured (Shokes et al. 1977). As discussed previously, Shokes et al.
(1977) had found an unusual step-like feature in the oxygen profile
just above the brine interface, with values constant at about 0.1
ml·liter^{-1}. After Wiesenburg et al. (1977) reported finding high
nitrite concentrations in the interface area of the Basin, the
standard Winkler technique was modified by adding one gram of
sodium azide to the NaOH-NaI reagent. Any nitrite in a Winkler
oxygen sample will reduce iodide to iodine just as oxygen does,
thus erroneously causing a larger value to be reported. Adding
sodium azide to the alkaline iodide reagent will prevent this
nitrite interference (Broenkow and Cline 1969).

Argon and Nitrogen Sampling

Samples obtained from the Orca Basin brine for argon and ni-
trogen are supersaturated with these gases when sampled at one
atmosphere total pressure. Since these gases will bubble out of
the water during sampling, special precautions had to be taken to
avoid both atmospheric contamination and loss of gas due to effer-
vescence of the samples. A system was devised to capture the
water sample before degassing took place.

A major problem with brine degassing was related to the type
of sample bottles used. All plastic Niskin sampling bottles are
the preferred water sampling device for marine geochemists. They

provide large volumes of water, are relatively inert and are trace

metal free. These bottles, however, have a closing device comprised

of a rubber band between two end caps. The pressure on the seal

is minimal at best, and could not keep the Orca Basin gases from

effervescing in the sample bottle, before they could be transferred

to some suitable sample container. Sampling with teflon-coated,

brass, 1.2 liter Nansen bottles proved more fruitful. These bottles

have a metal, ball-valve type sealing system which closes off both

ends of the bottle with a metal-to-metal seal when the bottle is

tripped. The seal produced by these bottles was tight enough to

prevent gas effervescence before transfer from the Nansen bottle.

However, using Nansen bottles, there was more variability between

samples in the brine than can be accounted for by analytical error

(assuming the brine is a homogenous mixture) so some of the Nansen

bottles probably worked more effectively than others.

To test the ability of the Nansen bottles to capture reproduc-

ible samples, samples were taken with gas tight "piggyback" bottles

designed from the information given by Weiss (1968). These sam-

plers consisted of a 0.95 cm O.D. (3/8 in) copper refrigeration

tube placed between two high pressure ball valves (Hoke No.1874392).

The ball valves of the piggyback sampler are attached to the ball

valves on the Nansen bottles. This is accomplished by attaching a

flange to the Nansen bottle to replace the nut which normally

holds the Nansen ball valve together. The piggyback sampler is

attached to this flange. When the Nansen bottle is tripped, the ball valves on the piggyback sampler are closed simultaneously with the valves of the Nansen bottle. When the high pressure ball valves are closed, they trap a water sample at in situ pressure in the copper tube. With a tubing length between the valves of 56 cm and an 0.64 cm I.D., a sample of approximately 23 ml is collected. The sample is returned to the surface in the tubing at the in situ pressure. At the surface, a segment of the sample is sealed off in the copper tubing by placing refrigeration pinch off clamps (Imperial Eastman Corp., 105-FF pinch off tools) at either end of the tubing between the ball valves. The tubing and clamps can then be removed from the ball valves with a sealed off sample available for analysis in the laboratory.

Since the high pressure ball valves and the copper tubing have only a 0.63 cm (1/4 in) internal diameter, flow through the tubing can be impeded. Restriction of flow would require a larger flushing distance (volume) to assure a representative water sample. To insure proper flushing when lowering, a funnel is attached to each of the ball valves. These funnels have a maximum diameter of 5 cm, a size selected to give the greatest flushing with the minimum drag through the water. Weiss (1968) used smaller size funnels and tested the flushing efficiency of the samplers using fluorescein dye. The dye was placed in a 1.8 m curved copper tubing attached to the ball valves and lowered to various depths. After

tripping the sampler and retrieving the water, the remaining fluorescein dye was measured with a fluorometer. Casts to various depths were carried out. Extrapolations from the larger volume, curved tube to the normal 56 cm tube used in this study indicated that a normal piggyback sampler should flush 50% in approximately 2 m of lowering. To assure complete flushing in the samples from the Orca Basin brine, all bottles were placed at least 10 m apart, and they remained opened at depth for at least 15 min before they were closed (while the thermometers equilibrated). Comparison of samples in the narrow interface region indicated that sample flushing was essentially complete when these funnels and this sampling procedure were used.

The amount of water sampled by the piggyback sampler can be measured in either of two ways. The volume of water can be collected after analysis and measured volumetrically. This is the preferred method if the sample is to be analyzed aboard ship. If the sample is measured in the laboratory, the weight of the tubing, clamps and sample can be measured before analysis. After the water sample is removed from the tubing, the tubing and clamps can then be reweighed to determine the weight of the sample. Since the temperature and salinity of the water are usually available from the water sample taken in the companion Nansen bottle, a density can be calculated for the sample. With the mass and density, the volume of water that was analyzed can be determined. This second

procedure described here was used in obtaining sample volume during this work, since all piggyback samples were analyzed in the shore-based laboratory at Texas A&M University.

To obtain companion water samples for dissolved gas analysis from the Nansen bottles (both with and without piggybacks), several all-glass sampling chambers were constructed (Fig. 21). These devices were calibrated gravimetrically to a volume of 0.01 ml. Samples were taken from Nansen bottles by attaching a short piece of Tygon tubing between the spigot of the bottle and the lower port of the sample holder. Each end of the sample holder was equipped with a three port stopcock which was used both to seal the samples and to transfer them into a stripping chamber for gas analysis. The water from the Nansen bottle was allowed to flow into the glass water sampler through the lower port and to overflow a volume equal to two or three volumes of the sampler through the upper port. When the sampler had been flushed, the bottom and then the top stopcocks were closed, sealing the water sample in the container. This sample could then be attached to the gas chromatographic gas stream and analyzed as described in the next section.

Chromatographic Analysis of Argon and Nitrogen

The gas stripping and chromatographic system for the analysis of argon and nitrogen is shown in Fig. 22. The gas system is

2 cm × 0.64 cm O.D.

1.3 cm I.D.

BRINE
SAMPLING
DEVICE

12 cm

3 mm
T-bore
Stopcock
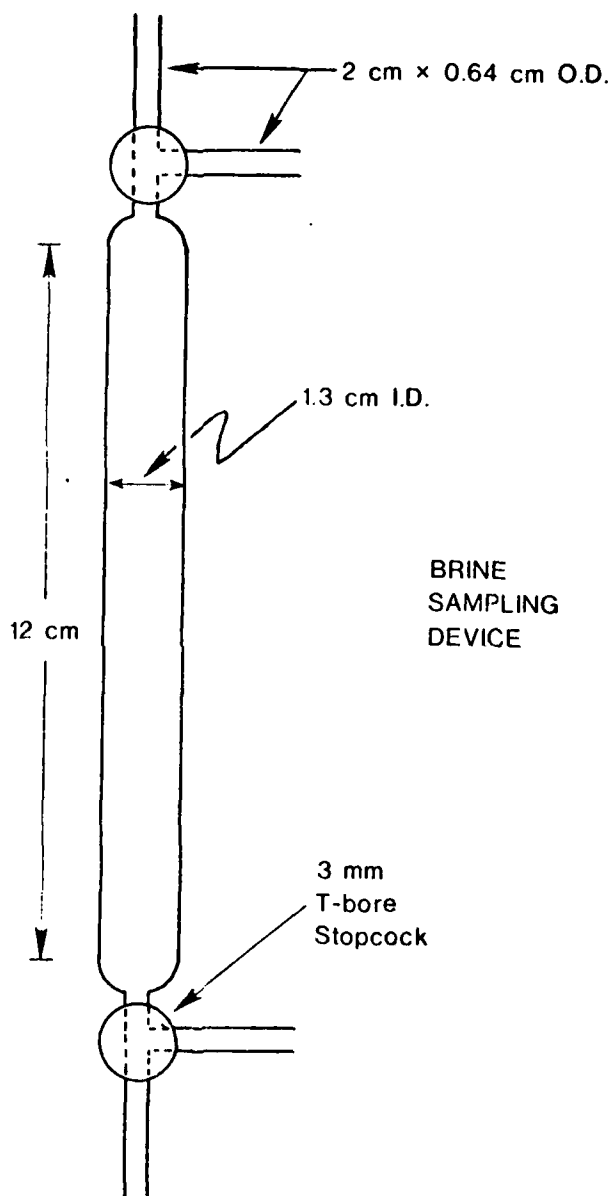
Fig. 21. All-glass sample chambers constructed
to take uncontaminated water samples from Nansen
bottles for dissolved gas analysis.
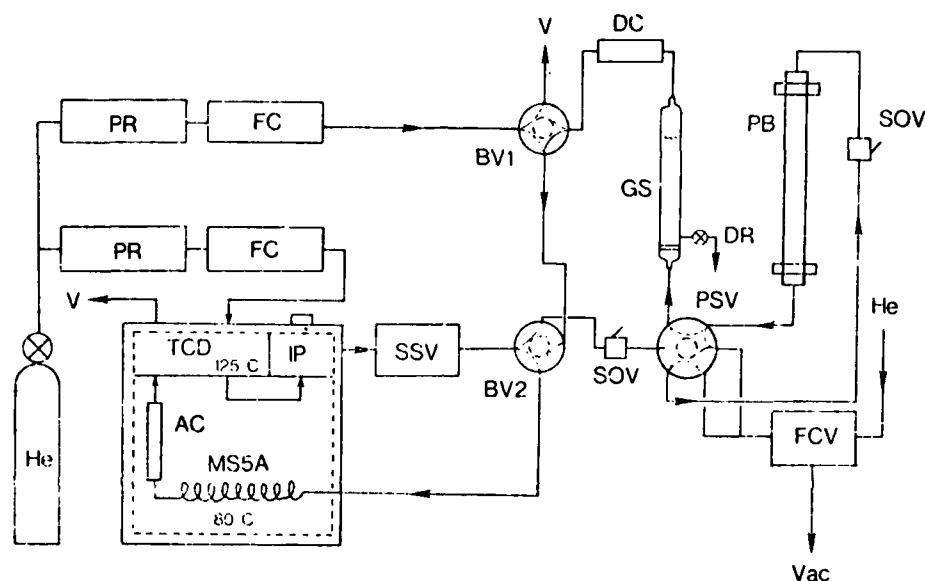
Fig. 22. Dissolved gas extraction and analysis system.
The piggyback water sample (PB) is attached to the system
using valve PSV. Any trapped air is removed from the gas
lines by alternately evacuating the system and purging it
with helium using valve FCV. With valve FCV and shut-off
valve SOV closed, the piggyback clamps are removed and the
water sample is transferred to the gas stripper (GS) using
valve PSB (after reopening valve SOV). Gas dissolved
in the water is extracted by the helium flow, dried on a
drying column (DC), separated on a 5A molecular sieve column
(MS5A), and analyzed using a thermal conductivity detector
(TCD). An activated charcoal column (AC) is used before the
detector to remove oxygen from the sample. Standard gas
samples are introduced through a standard sample valve (SSV)
with a 0.5 ml sample loop. Standards can be bypassed directly
to the gas chromatograph using bypass valve two (BV2) or it
can be passed through the stripper and drying columns before
analysis. Bypass valve one (BV1) is used to provide helium
to the thermal conductivity detector when the gas stripper is
being drained and purged after sample analysis.

designed so that the piggyback sampler can be attached to the gas lines and all contaminant air can be removed before the pressurized brine sample is released to the gas stream. For this purpose, the piggyback sampler (PB) is attached to the gas lines using the same 3/8 in (0.95 cm) Swagelok fittings with which it was attached to the high pressure ball valves. When the sampler is connected at both ends, it is isolated from the stripping gas stream by a 6-port delrin plastic sampling valve (PSV). With a 3-port brass flow control valve (FCV), the gas stream connected to the isolated PB sampler can be alternately purged with helium and evacuated. The backpressure valve (SOV) is open during this air removal process. The gas lines were evacuated and purged with helium ten times to insure complete removal of atmospheric gases. Analysis of gas remaining in the lines after ten purgings and evacuations indicated no detectable argon or nitrogen. After the tenth purging, helium was left in the gas line and the system was isolated by moving valve FCV to the neutral position. Valve SOV was then closed and a positive helium pressure of 240 kPa was maintained in the system.

With valves FCV and SOV closed, the clamps are removed from the PB sampler and used to re-round the 3/8 in (0.95 cm) O.D. tubing, thus releasing the sample to the gas line. Immediately after the tube is opened, valve SOV is opened and the 6-port rotary valve (PSV) is turned clockwise transferring the brine into a 35 cm by 1.5 cm O.D. glass stripper chamber (GS) which has a

10 mm coarse glass frit at the bottom. Helium from the gas chro-
matographic stream pushes the brine downward from the PB sampler
through the 6-port valve (PSV) and into the stripper. When all
the brine has been pushed through the frit, the carrier gas begins
to bubble through the sample thereby stripping the dissolved gases
out of solution. Weiss and Craig (1973) have given a complete
description of stripping characteristics and efficiencies of this
type of gas extractor.

The effluent carrier gas and extracted gases exit at the top
port of the stripper and pass through a 20 mesh indicating drierite
($CaSO_4$) column to remove water vapor. After the drying process,
the extracted gases pass through two bypass valves (BV1 and BV2)
and are subsequently separated and detected using gas chromato-
graphic methods. A Hewlett-Packard 5830A gas chromatograph with a
thermal conductivity detector was used for separation and analysis.
The sample gas is separated on a 30/60 mesh activated 5A molecular
sieve column (2.0 m in length and 3.6 mm internal diameter) which
retards N_2 relative to the combined O_2 + Ar peak. At the 80°C
operating temperature, this column also absorbs any evolved CO_2.

Argon and oxygen cannot be resolved with the column and temp-
erature settings used here. In past studies, various techniques
have been used to separate the argon and oxygen components. With-
out reacting the gases, they can be separated using either columns
which are extremely long or which must be operated at very low

temperatures. Weiss and Craig (1973) used a hydrogen carrier gas
and a palladium catalyst to convert oxygen to water, enabling the
analysis of oxygen in the form of a water peak. Since there is no
oxygen in the Orca brine and Winkler oxygen measurements of O_2
were available in the overlying water, this author has chosen to
use a simpler analytical technique. Oxygen is simply removed
from the gas chromatographic stream, thus enabling the argon con-
centration to be measured without interference.

The removal of oxygen from the gas chromatographic stream was
accomplished by placing a stainless steel column (0.5 m in length
by 3.6 mm internal diameter) containing "superactivated charcoal"
(Cooke 1973) between the MS5A column exit and the thermal conduc-
tivity detector. When activated charcoal is heated to temperatures
greater than 800°C and then cooled to 80°C, it will quantitatively
absorb oxygen passed over it. This method was found to be supe-
rior to removing O_2 by reaction with a solution of chromous sulfate
(Lingane and Pecsok 1948) that has been used by other investigators
(Reeburgh 1969, 1976). Typical chromatograms for room air analyzed
with (B) and without (A) the oxygen removal column are shown in
Fig. 23.

Gas analysis after separation is performed using a thermal
conductivity detector operating at 125°C. Flow rate through the
detector was 40 ml·min^{-1}. Detector response is monitored using
the thermal printer-plotter associated with the chromatograph.

97
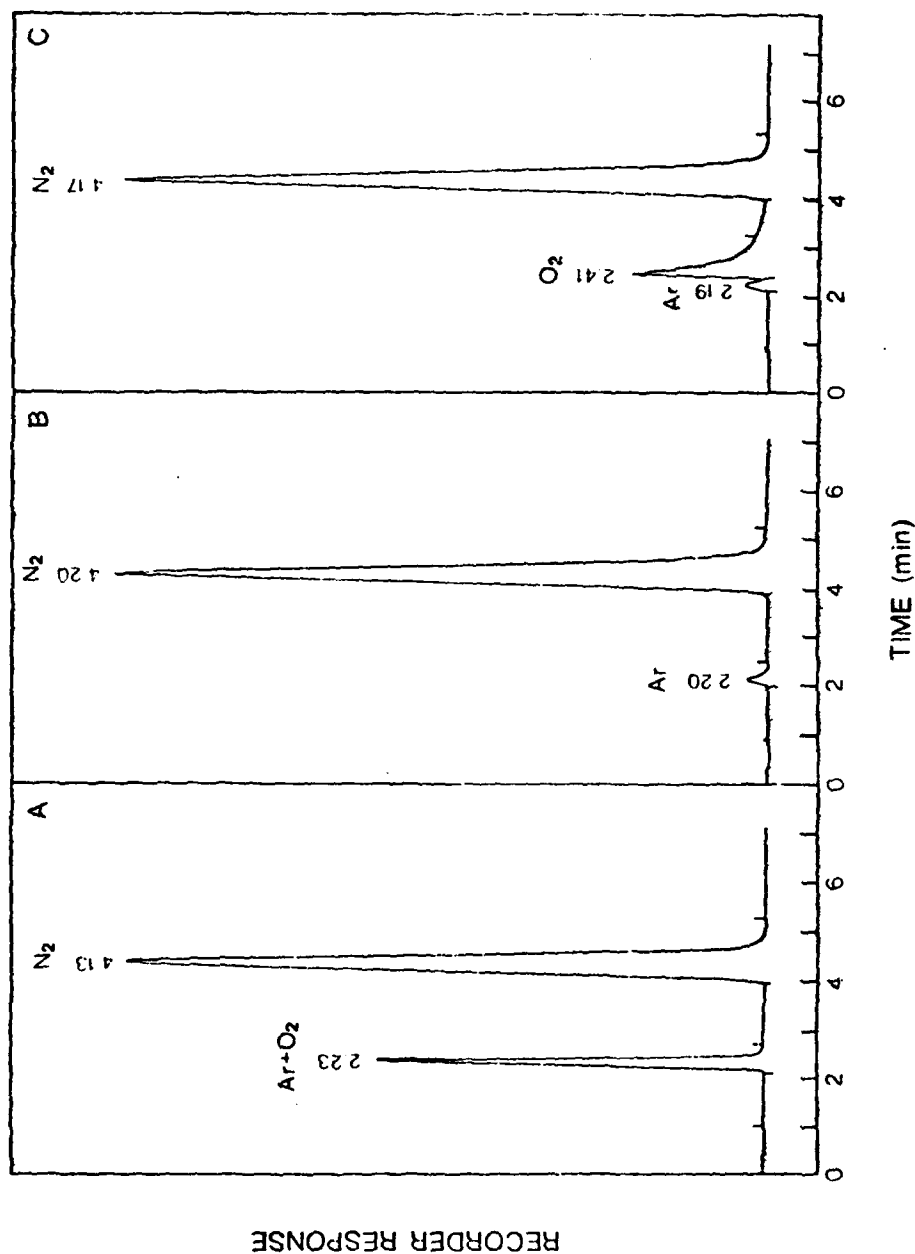
Fig. 23. Typical chromatograms showing the analysis of major dissolved gases in oxygenated sea water with (B) and without (A) the activated charcoal trap in the gas flow line. Deactivation of the trapping column can be easily recognized (C) when encroaching oxygen peaks begin to appear as tailing peaks after the argon peak.

Peak areas are automatically integrated and retention times recorded
by the microprocessor system of the 5830A gas chromatograph and
are automatically reported along with the peak area percentages.
A typical chromatogram for Orca Basin brine is shown in Fig. 24.

The chromatographic system was standardized for argon and
nitrogen analysis by injecting standard volumes of dry air into
the column using a calibrated sampling loop (0.493 ml) and an auto-
mated sampling valve (SSV). The gas concentration in the sample
in units of ml (STP)/ml is given by

$$C_x = \frac{A_x}{A_s} \cdot \frac{V_g}{V_1} \cdot \frac{T_o}{T_s} \cdot \frac{P_s}{P_o} \cdot C_s \tag{14}$$

where A_x and A_s are the peak area for the particular gas in the un-
known sample and the calibration mixture, respectively; C_s is the
standard gas concentration (v/v); V_g is the sample loop volume and
V_1 is the liquid volume. P_s and T_s are the pressure and absolute
temperature in the sample loop; and P_o and T_o are the standard
conditions of temperature (273.15°k) and pressure (1 atm) for
gases. Corrections for nonideality are not necessary for argon,
nitrogen or methane under these conditions (see Table 1).

The glass container water samples taken from the Nansen
bottles were analyzed using the same chromatographic system used
from the piggyback (PB) samples. The gas stripping system de-
scribed above was also used, but it was modified slightly to
account for the varying requirements of the glass samplers. The
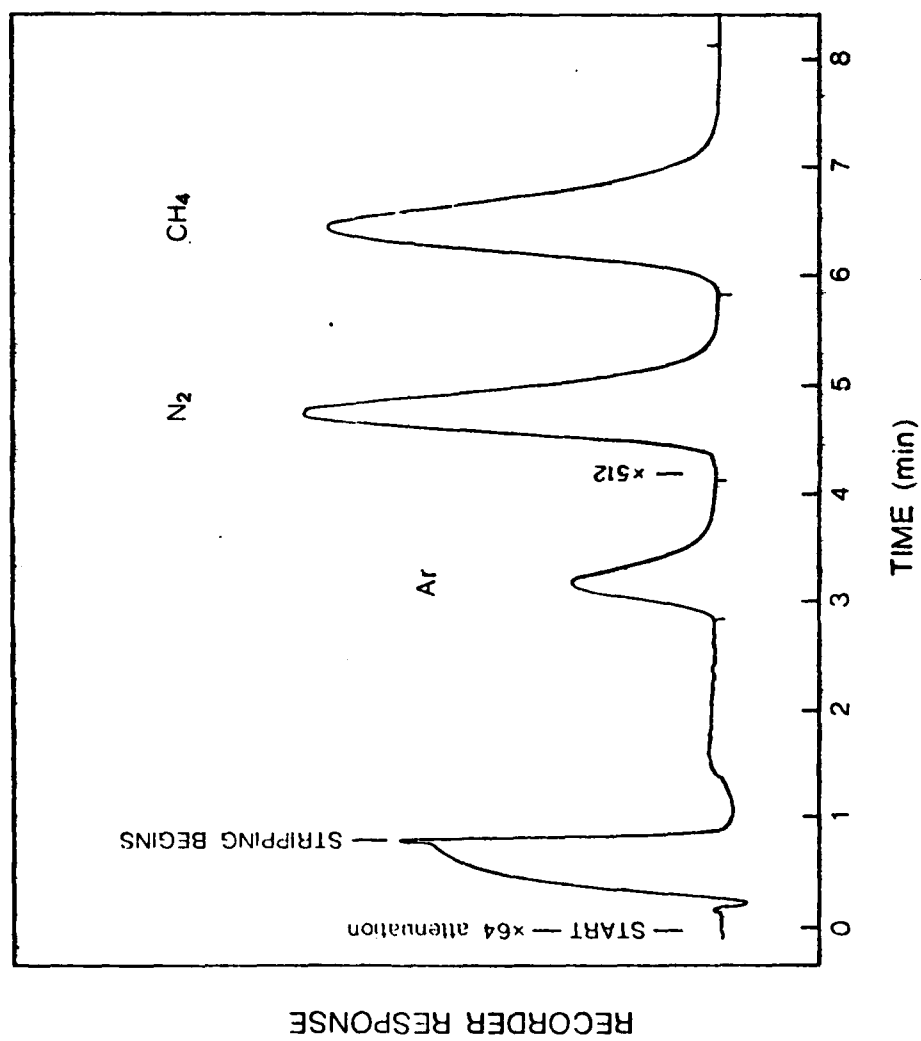
Fig. 24. Typical gas chromatograph for the anoxic water of the Orca Basin derived from the analytical techniques described in Fig. 15.

samplers (shown in Fig. 21) were attached to the gas stream between the PB sample valve (PSV) and the gas stripper (GS). The gas bypass valve (BV1) was turned clockwise passing clean helium to the TCD while the sampler gas lines were being purged. In purging the lines, the water sampler stopcocks are turned so the carrier gas passes around the sample, through the stripper and drying column and exits the vent port of bypass valve BV1 (see Fig. 22). After five minutes of purging, the lines are free of any contaminating atmospheric gases and valve BV1 is returned to its normal position (counter-clockwise). The carrier gas now flows again to the GC column and detector. After the detector baseline was restabilized from flow switching, the two three-way stopcocks of the glass samplers were turned to allow the helium carrier to push the brine into the stripper for analysis as described above.

Results

Solubility Comparisons

The solubility measurements made on the brine and corresponding sea water samples are given in Table 9. Only a few measurements were made, since the purpose here was not to establish a complete data set of brine solubility data. A high precision solubility data set would require microgasometric equipment (Douglas 1964) which was not available. The object of these measurements was simply to determine whether or not the equations defined

Table 9. Measured gas solubilities of Orca Basin brine and sea water. All values are atmospheric equilibrium solubilities except those marked with an asterisk.

Solution	Gas	Temp. (°C)	Sal. (°/$_{oo}$)	Predicted Solubility (μmol·liter^{-1})	Measured Solubility (μmol·liter^{-1})	% Difference
	N_2	4.26	34.635	575.2	579.4	+0.7
	N_2	11.17	34.635	498.3	515.5	+3.5
Sea Water	N_2	20.49	33.970	423.7	431.2	+1.8
	Ar	4.26	34.635	15.70	16.28	+3.7
	Ar	11.17	34.635	13.47	14.14	+5.0
	N_2	4.21	250.0	121.9	100.7	−17.4
	N_2	10.89	250.0	114.7	99.8	−13.0
	N_2	10.94	250.0	114.7	101.1	−11.8
Brine	N_2	21.01	250.0	106.5	92.4	−13.3
	N_2	21.01	250.0	106.5	90.9	−14.7
	Ar	4.21	250.0	3.75	3.48	−7.1
	CH_4*	25.06	250.0	306.6	269.9	−12%
	CH_4*	22.86	250.0	313.2	288.1	−8%
	Ar*	4.21	250.0	402.0	314.1	−21%

* Pure gas.

by Weiss (1970) could be extrapolated from sea water salinities
to the higher salinity of the brine. This extrapolation was be-
lieved to be feasible since the major factor governing gas solu-
bility in saline solution is the temperature. Salinity has a
smaller effect. Yet, since the constants for salinity in Eq. 5
are small relative to the temperature coefficients, they can cause
a large error to be propagated in any extrapolation process. The
measured solubility data from this work is compared with the pre-
dicted solubility values in Table 9. Percentage differences be-
tween measured and calculated values are indicated.

Due to low solubility of argon in brine, it was difficult to
measure precisely the argon concentration which resulted from
equilibrating the brine with air in the equilibration chamber.
One successful argon measurement of the atmospheric equilibrium
solubility of argon was made at 4.21°C. At higher temperatures,
however, the digital integrator would not sense the small argon
peaks with enough regularity to integrate them accurately. Thus,
pure argon was used to measure the Bunsen coefficient of argon.
Also, the concentration of methane in the standard atmosphere (1.41 ppm;
Prabhakara et al. 1974) does introduce enough methane into the
equilibrated brine to measure with a thermal conductivity detector.
Pure methane was used to determine the Bunsen coefficient of that gas
as well.

The solubility data for the brine for all three gases

indicated that the equation of Weiss (1970) predicts a gas concentration in the brine that is over ten percent higher than the measured values. This agreement is not bad, considering the difficulties in extrapolating the equation to salinities an order of magnitude higher than was intended. Also, the Orca brine is not just a higher concentration of sea water. It is a sodium chloride saturated solution, with a mixture of other components. For example, total carbon dioxide of the brine is twice normal sea water values (Sackett et al. 1979). These other compounds also contribute to the fact that lower values were observed than were predicted.

The equilibrated normal sea water samples analyzed by this procedure show a slight supersaturation, in the range of one to five percent. This supersaturation was expected as has been discussed previously. These results indicate that it was not a complication of the analytical technique which caused the lower levels of argon, nitrogen, and methane solubility, relative to the calculated values. The true values are probably lower than predicted ones, due to the differences in salt content between sea water and the brine, and due to difficulties in extrapolating empirical equations beyond their working range. This information implies that either the equation does not follow the chemistry at the higher salt concentrations or that the nature of the interactions change under hypersaline conditions. From data on the

changes in ionic activity as a function of increased ionic strength
(Harned and Owen 1950), there is some indication that the latter
is the case. However, that problem is not germane to this dis-
cussion.

The solubilities of argon, nitrogen, and methane are low in the
brine, yet the measured values are relatively close to the
predicted values. These low solubilities and the gas levels in the
brine explain the effervescence which occurs when the brine is
brought to the surface. Effervescing gas bubbles were captured on
four samples taken directly from Nansen bottles on cruise EN-32 of
the R/V Endeavor. One ml of this gas was analyzed by direct in-
jection into the gas chromatograph. The gas collected was found
to contain 1.1% argon, 63.7% nitrogen, 34.6% methane and 0.6% car-
bon dioxide (average of four samples). Although the methane levels
are higher in the brine than nitrogen (see next Chapter), there is
more nitrogen in the effervescing gas, since nitrogen is less sol-
uble in the brine than is methane (Table 9).

Dissolved Oxygen

Dissolved oxygen has been measured on every Texas A&M cruise
to the Orca Basin. The original data of McKee and Sidner (1976)
and the plot of Shokes et al. (1977) were presented in Chapter I.
I shall not give all of the newer data. The data from four
cruises (77-G-2, 77-G-13-I, 77-G-13-III, and 78-G-2) are presented

in Fig. 25. These four oxygen and sigma-t profiles were taken

over the span of one year. The oxygen profiles from each cruise

show oxygen values at the top of the basin (2000 m) which are

fairly typical of deep Gulf oxygen concentrations in this area,

approximately 225 μmol·liter^{-1}. As density begins to increase

(along with salinity) from the deep Gulf levels, oxygen concentra-

tions begin to decrease gradually from about 200 μmol·liter^{-1} at a

depth of 2175 m, to near zero but not exactly zero at about 2215 m.

This same pattern can be seen in all the profiles. Below this

gradual oxygen gradient there is a region of approximately 20 to 30

m where the oxygen concentration is very low, but measureable. The

oxygen   levels   are   between 2 and 10 μmol·liter^{-1} in this nar-

row zone, and absent or less than the Winkler detection limit below.

The anomalously low dissolved oxygen values are paralleled by

a change in the slope of the temperature profile (see Fig. 10).

The change in temperature is not as obvious as the oxygen change

(step) when viewed from temperature data taken only from deep-sea

reversing thermometers. However, examination of the trace taken

from the STD (Fig. 10) clearly shows the discontinuity in temper-

ature that is associated with this step in the oxygen profile.

The temperature gradient in this region is different from the

gradient either above or below. This oxygen step-like feature is

in the region where the salinity is increasing from 50 to 70°/₀₀

(Fig. 11). The feature is a persistent one and is not an artifact

DISSOLVED OXYGEN (µmol·liter⁻¹)
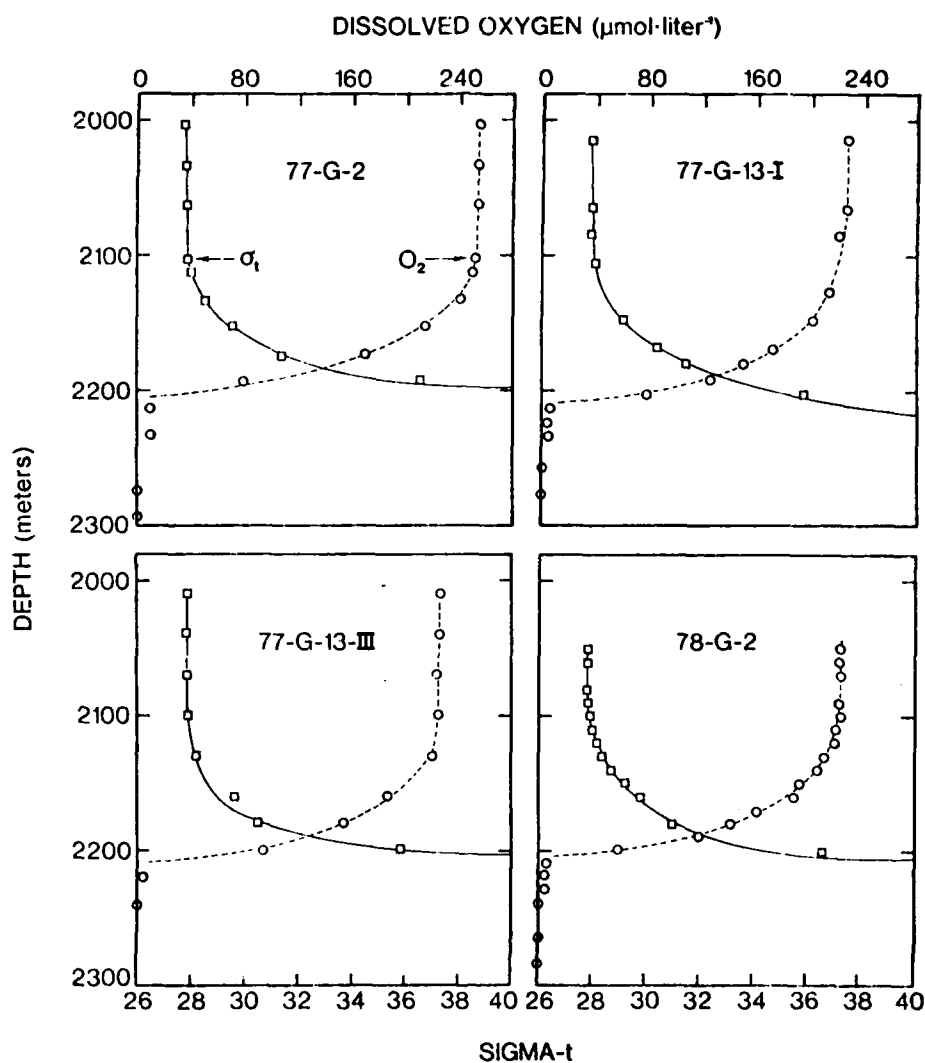
Fig. 25. Dissolved oxygen profiles measured by the micro-Winkler technique (Carpenter 1965) for four different Texas A&M cruises during 1977 and 1978. Note the persistent step in the oxygen profiles. There appears to be a systematic error in the 77-G-2 oxygen data. However, the shape of this profile is consistent with the other cruises.

of the Winkler dissolved oxygen technique.

Argon and Nitrogen

Attempts to sample and analyze the Orca Basin brine for argon
and nitrogen were made on four cruises during 1977 and 1978. The
early efforts yielded only limited success. Plastic syringes used
on the first cruise allowed gas to diffuse out of the sample before
analysis. The sampling systems described in the previous section
were used on the last three cruises (77-G-13, 78-G-2 and EN-32).
Even using these more sophisticated techniques, some samples were
contaminated with atmospheric gases or depleted due to degassing of
the brine. Criteria for determining the reliability of the data
were established. One evaluative method was examining the methane
concentration of each sample. Since methane is relatively constant
in the brine (Sackett et al. 1979), extremely low methane concentra-
tions in the brine samples would indicate gas loss before sample
analysis. Nitrogen/argon ratios were also used in sample evalua-
tion. Samples which had both an unusually high nitrogen/argon
ratio high argon concentrations and very low methane levels were
obviously contaminated with air (N_2/A in air = 83.6) and these data
were discarded.

In the highest salinity brine (S = 262%$_{oo}$), 25 measurements
of nitrogen were reliable and 9 argon values were believed correct.
The number of argon values is lower since this gas is found in very
low concentrations in the brine and the gas chromatographic

peaks for this gas were not always integrated properly. Also, the standard for this gas was air and could only be determined when the activated charcoal column was in place in the analysis system (AC, Fig. 22). Since the column was not always used in the analysis system, fewer total determinations of the argon were made in the brine.

Nitrogen values from the brine averaged 568 $\mu mol \cdot liter^{-1}$ (σ = 70) while the argon measurements averaged 15.6 $\mu mol \cdot liter^{-1}$ (σ = 1.2). Measured atmospheric solubilities of these gases in the brine at 4.21°C (Table 9) were 100.7 $\mu mol \cdot liter^{-1}$ for nitrogen and 3.5 $\mu mol \cdot liter^{-1}$ for argon. These values represent a supersaturation in the brine of 560% and 450% for nitrogen and argon, respectively. The reliable measurements of argon and nitrogen are plotted in Fig. 26. Data in this figure are a composite of gas data taken with the pressurized piggyback samplers (open symbols) and Nansen samples collected in glass containers (closed symbols). Methane data analyzed at the same time (discussed in the next chapter) are presented in Fig. 26 as a reliability comparison and to indicate the demarkation line between Gulf water (no CH_4) and the brine (average CH_4 = 714 $\mu mol \cdot liter^{-1}$).

One nitrogen point is not plotted, although it could be significant to the following discussion. The nitrogen gas concentration at 2234 meters on cruise 77-G-13 was measured at 1061 $\mu mol \cdot liter^{-1}$ using a piggyback sampler. The argon concentration was 9.86 $\mu mol \cdot$
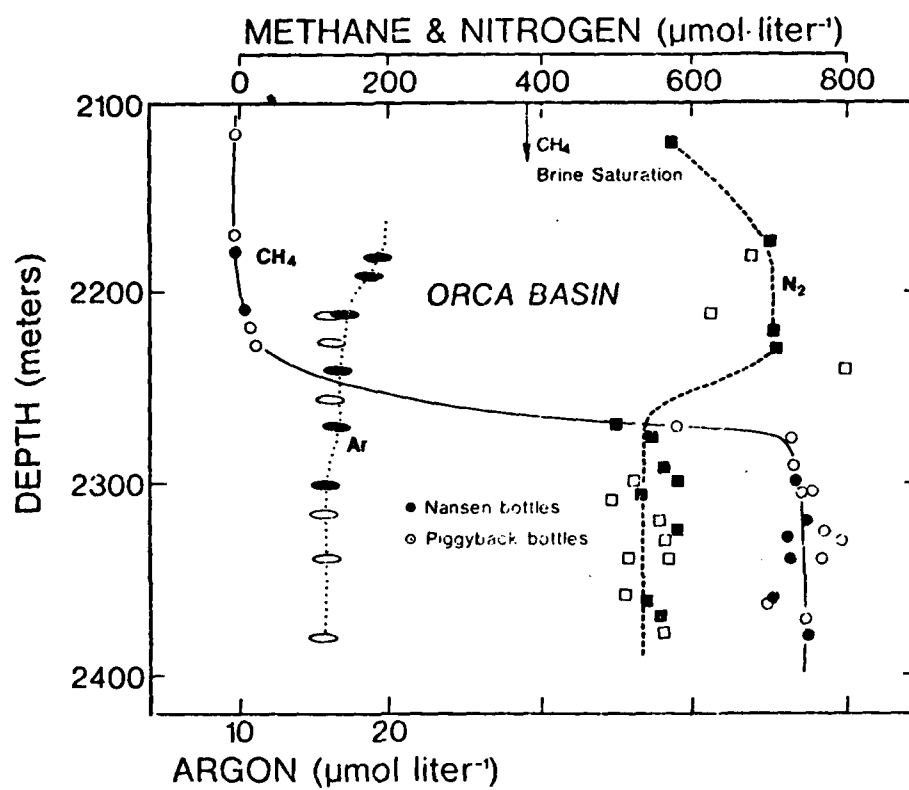
Fig. 26. Vertical profiles of dissolved argon, nitrogen, and methane through the Orca Basin interface region into the high salinity brine. The N_2/Ar ratio in the brine is 36.4.

liter^{-1} and the salinity of the water at this depth was 64.65°/$_{oo}$.

This sample is found in the oxygen step region where O_2 levels

ranged from 4-20 μmol·liter^{-1} (Fig. 18). Several other nitrogen

measurements just above the high salinity brine also reflect levels

higher than would be predicted from atmospheric equilibrium solu-

bility. The bulge in the N_2 distribution between 2185 m and 2250 m

(Fig. 26) also shows supersaturation, while the value at 2169 m

(N_2 = 567 μmol·liter^{-1}) is within 1.5% of the predicted sea water

solubility value. The one very high nitrogen value in the oxygen

step region may be questionable, since the associated Ar measurement

is so low. The N_2/Ar ratio (108) cannot, however, be accounted for

by atmospheric contamination. The other N_2 and Ar data in this

region are considered reliable for the following discussion.

Discussion

Dissolved Oxygen

The dissolved oxygen profiles in the Orca Basin (Fig. 25) show

a general decrease through salinity transition zones T1 and T2. A

constant but low oxygen level was observed in transition zone T3.

Oxygen was absent in the interface region and high salinity brine.

Oxygen is the first oxidizing agent consumed in the organic matter

decomposition process (Richards 1965). The equation used to

describe oxygen consumption is

$$(CH_2O)_{106} \ (NH_3)_{16} \ (H_3PO_4) + 138 \ O_2 \longrightarrow 106CO_2 + 16HNO_3 \quad (15)$$
$$+ H_3 \ PO_4 + 122 \ H_2O$$
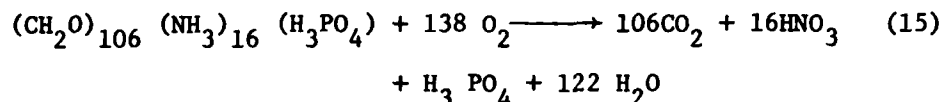
In this decomposition reaction, 138 μmol of oxygen are consumed for every 106 μmol of carbon dioxide that are produced. If the brine was originally Gulf sea water (T = 4.2, S = 35°/$_{oo}$), it would have had an original oxygen concentration of 322 $\mu mol \cdot liter^{-1}$ (Weiss 1970). Removal of this amount of oxygen via Eq. 14 would produce 247 μmol of carbon dioxide. The amount of carbon dioxide that has been added to the Orca brine due to decomposition has been calculated as 2290 $\mu mol \cdot liter^{-1}$ (Sackett et al. 1979). Thus, the CO_2 input from oxygen consumption would account for only 11% of the total CO_2 input. The major input of carbon dioxide must result from other, anaerobic decomposition processes which will be discussed in the next chapter.

The decrease in oxygen in the transition zone must be due to oxygen consumption as described in Eq. 14. The convex downward slope of the profiles in regions T1 and T2 are indicative of consumption in that region. The increase in excess total carbon dioxide through this region is about 470 $\mu mol \cdot liter^{-1}$ (Sackett et al. 1977), while oxygen decreases from 225 to 10 $\mu mol \cdot liter^{-1}$. This oxygen decrease via Eq. 14 would result in the production of 165 $\mu mol \cdot liter^{-1}$ of carbon dioxide. That value represents 35% of the amount supposedly produced in this region. If oxygen is

consumed in producing this carbon dioxide, one can assume that 65%
of the excess CO_2 in this region comes from anaerobic decomposition
or from diffusion of CO_2 from the zone below.

The oxygen step zone has a low but measurable amount of oxygen.
Water in this zone has a characteristic salinity between 50 and
70%oo. All samples in this salinity range have measurable oxygen
less than 15 μmol·liter^{-1}. No exceptions have been found. The
microWinkler oxygen technique (Carpenter 1965) is not very precise
in this area due to interferences at low concentrations. However,
even with care to eliminate the possible effect of nitrite on the
samples (Broenkow and Cline 1969), oxygen showed some variability
in the step region, i.e., transition region T3. Although it is
impossible to be certain, the oxygen levels in this region seem to
be relatively constant. They decrease to zero within a very small
depth region where salinity increases above 70%oo, i.e., in the
interface region.

This step-like feature in the oxygen profile is an unusual
occurrence. Like other variables in the ocean, this feature must
represent a balance between transport processes and removal mech-
anisms. Oxygen can be transported into this region by diffusive
mixing from above, and by possible advection of new water/brine
from the side. The change of oxygen with salinity in this zone
(Table 7) is much lower than in either of the regions above. This
may result from the low oxygen concentration, if the rate of

consumption is first order with respect to concentration. However, this is improbable. In other environments with low oxygen values, oxygen profiles decrease smoothly to zero without going through a step (see, for example, Richards 1975).

Nor does this step-like feature appear to be the result of input of new brine into the basin. The density of the high salinity brine is greater than the density of the water in the step region and would not remain on top of the interface as this feature does. A biological mechanism may explain the oxygen levels found there. In this region, the salinity increases from 50 to 70%. Just above this region (based on oxygen data), LaRock et al. (1979) observed a large increase in ATP and uridine uptake, with lower values below. It is possible that the microbial population which mediates consumption of oxygen in the ocean is inhibited by salinities greater than 50‰. If the microbes cannot metabolize oxygen effectively, the oxygen input due to diffusive mixing from above (see Chapter II) would be very slowly consumed and might remain in balance with oxygen consumption causing the observed feature.

Inhibition of bacterial activity in hypersaline waters exists in the Red Sea brines. However, most of this work has been done on the anaerobic bacteria. Trüper (1969) found that bacterial sulfate reduction is inhibited at high salinities, with significant decreases in microbial activity at 60‰ and greater. The

Orca Basin brine is not sterile (LaRock et al. 1979) like the hot

metalliferous Red Sea brine (Watson and Waterbury 1969). A slowing

of bacterial activity, however, combined with slow or periodic

oxygen mixed into this region could produce the feature that was

observed.

Argon and Nitrogen

The argon and nitrogen distributions in the Orca Basin can be

divided into two zones of interest: the transition zone and the

high salinity brine. In both of these zones, nitrogen gas concen-

trations are higher than would be predicted on the basis of solu-

bilities. The nitrogen data in the high salinity brine show some

random variability, with a relative standard deviation (RSD) of 12%.

However, within the precision of the sampling and analytical tech-

niques both nitrogen and argon levels (RSD = 8%) are considered

constant in the high salinity brine (Fig. 26). On the other hand,

there is an obvious trend in the nitrogen distribution in the

transition zone.

Transition Zone. Nitrogen values were higher in the transi-

tion zone than in either the brine, or the freely circulating

Gulf water above. This increase in the nitrogen levels was found

in the area where nitrate is being reduced to essentially zero. While

the nitrate may not be the main source of excess nitrogen in the

transition zone, denitrification processes must be the cause of

the excess nitrogen. The added nitrogen is calculated to be 140 $\mu mol \cdot liter^{-1}$, which represents a supersaturation of 25%.

Denitrification is the biological reduction of nitrate or nitrite to nitrous oxide or free nitrogen. Denitrification can be carried on by a wide variety of faculative anaerobic bacteria (Brisou and Vargues 1961). The source for hydrogen in the reaction may come from either organic or inorganic substrates (e.g., $H_2 \cdot H_2S$). Several feasible reactions at 25°C are given by Vaccaro (1965).

$$2NO_3^- + 2H + \longrightarrow N_2O + 2O_2 + H_2O \qquad (16)$$
$$\Delta G° = + 21 \text{ kcal.}$$

$$4NO_3^- + 3CH_4 \longrightarrow 2N_2 + 3CO_2 + 6H_2O \qquad (17)$$
$$\Delta G° = -475 \text{ kcal.}$$
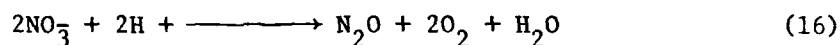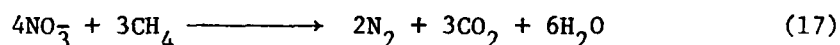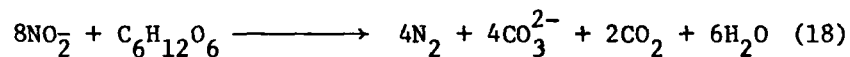
$$8NO_2^- + C_6H_{12}O_6 \longrightarrow 4N_2 + 4CO_3^{2-} + 2CO_2 + 6H_2O \quad (18)$$
$$\Delta G° = -728 \text{ kcal.}$$

When an organic substrate supplies the hydrogen, the reactions are energetically feasible in aerobic waters. If the hydrogen comes from an inorganic source (Eq. 16), reaction is feasible only in the absence of oxygen.

The nitrate levels in the deep Gulf average 23 $\mu mol \cdot liter^{-1}$. Reduction of 23 μmol of nitrate would produce only 11.5 μmol of

molecular nitrogen. Thus nitrate reduction alone cannot account
for the nitrogen increase of 140 μmol$\cdot$liter^{-1} that was observed in
the transition zone. Another source of nitrogen substrate is
needed to provide the starting material for nitrogen gas production.
Two possible sources are ammonia produced from organic material
decomposition at the brine interface or ammonia diffusing up from
the brine. Ammonia levels in the brine (see Chapter IV) are about
500 μmol$\cdot$liter^{-1}, but diffusion from the brine would be very small.
Possible mechanisms of nitrogen gas formation are shown in Fig. 27.

Ammonia diffusing out of the brine or produced in the oxygen
step region could be oxidized to nitrate and/or nitrite. These
nutrients could be subsequently converted to nitrogen in this low
oxygen environment. The biological oxidation of ammonia to nitrite
then nitrate in sea water has been described in the clas-ic laboratory
experiments of von Brand and his co-workers (cited in Vaccaro 1965).
The oxidation process is mediated by various nitrifying bacteria
including Nitrosomonas and Nitrobacter (Zobell 1946) and Nitro-
socystis (Murray and Watson 1963). These processes are well
documented in the literature.

There is no evidence, however, for the direct conversion of
ammonia to molecular nitrogen. While ammonia oxidation during
denitrification is thermodynamically possible (Cline and Richards
1972), there is little, if any, experimental evidence for the
direct biological oxidation of ammonia to free nitrogen. In the
low oxygen waters of the eastern tropical Pacific, Goering (1968)
detected no oxidation of ammonia during studies of natural
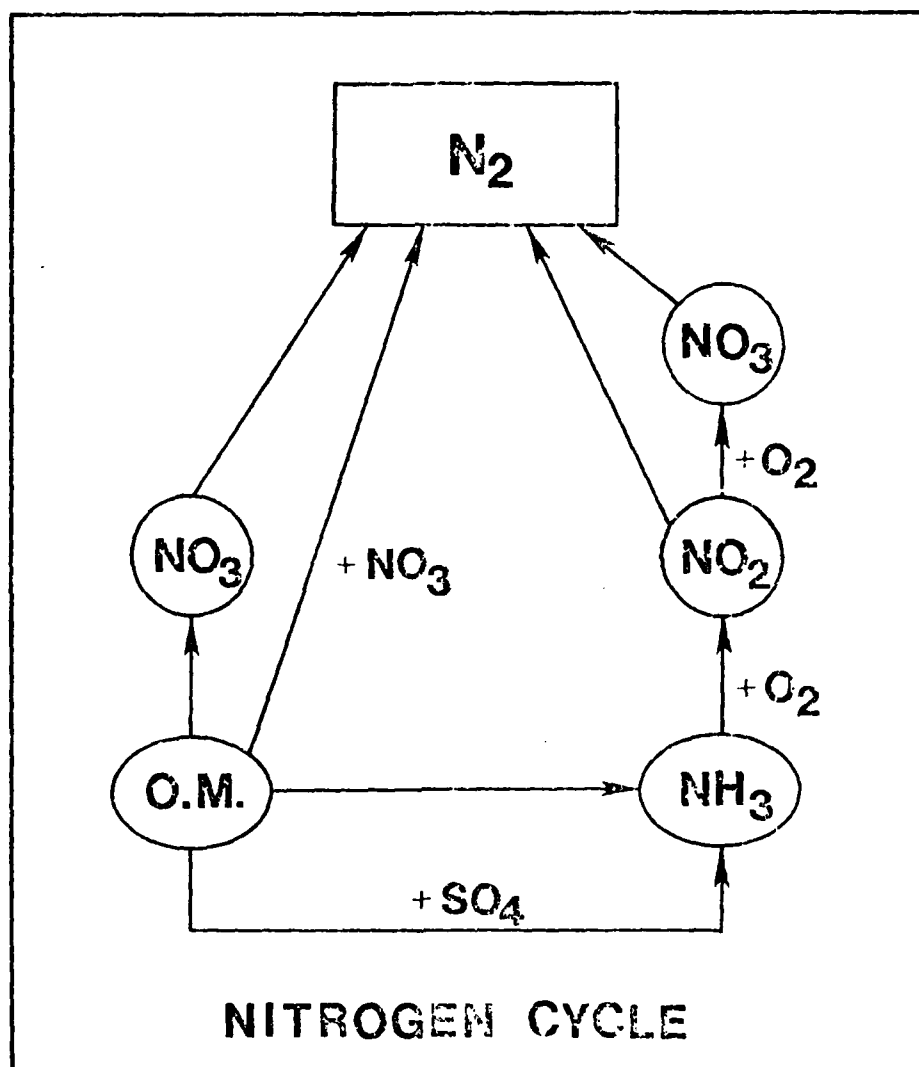
Fig. 27.   A schematic representation of the possible pathways
through which organic nitrogen or ammonia may be converted to
molecular nitrogen. All of these pathways are thermodynamically
possible, but not all under the same conditions.

microbial populations. Cline and Richards (1972) also reported no apparent oxidation of ammonia in their study of nitrate reduction in the same region. The low ammonia concentrations observed in the Pacific were attributed to removal of ammonia during bacterial assimilation, not nitrification to molecular N_2.

For production of molecular nitrogen from ammonia, a two-step process must exist:

$$NH_4 \xrightarrow{\;1\;} (NO_2 \text{ or } NO_3) \xrightarrow{\;2\;} N_2 \qquad\qquad (19)$$
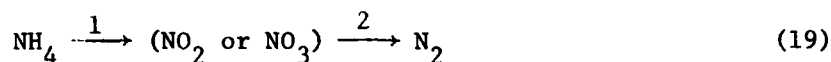
Oxygen concentration in the oxygen-step region of the Orca Basin (zone T3) averages 10 $\mu mol \cdot liter^{-1}$. Carlucci and McNally (1969) have demonstrated that oxidation of ammonia to nitrite can occur under conditions of low oxygen tension, down to 2 $\mu mol \cdot liter^{-1}$. Such conditions prevail in the Orca Basin interface region. In the eastern tropical Pacific, Cline and Richards (1972) observed the simultaneous occurrence of nitrite, along with the apparent loss of nitrate and suggested that nitrite is an intermediate in the reduction of nitrate to free nitrogen. Since nitrite does not accumulate in the Orca Basin from ammonia oxidation, it appears that the reduction of nitrate to nitrite and of nitrite to free nitrogen occur simultaneously (i.e., as coupled reactions (Eq. 19) which may be carried on by the same or different organisms).

Nitrate or nitrite may be the major intermediate in the production of nitrogen. Wiesenburg et al. (1977) noted the presence of high nitrite concentrations (up to 15 $\mu mol \cdot liter^{-1}$) in the

interface region (transition zone) of the Orca Basin. Their data
(Fig. 28) indicated that the nitrite maximum was found well above
the region of lowest oxygen values. The nitrite maximum may have
resulted from nitrate reduction. A nitrite maximum above the
brine was not observed on subsequent cruises, however. This max-
imum may have been a transient feature, with the nitrite being
subsequently converted to molecular nitrogen as in Eq. 18.

A continuing supply of dissolved oxygen could be provided by
mixing from above. This oxygen could be used in the oxidation
of ammonia. The nitrate or nitrite so produced would in turn be
reduced to N_2 as in Eqs. 16-18. These conclusions are valid for
the Orca Basin brine-sea water interface. They are also the same
conclusion Barnes et al. (1975) suggested for the Santa Barbara
Basin sediments. Barnes et al. (1975) examined nitrification and
denitrification in suboxic sediments of the Santa Barbara Basin.
Increases in both dissolved molecular nitrogen and the N_2/Ar
ratio were observed in the sediment pore waters. Nitrogen in-
creases (up to 17% above bottom water values) could not be
accounted for by nitrite (or nitrate) reduction alone. It was
concluded that ammonia, derived from organic matter containing
nitrogen, was converted to molecular N_2 through a nitrite inter-
mediate under conditions of low oxygen tension. Since methane is
also present in the sediments of this basin (Emery and Hogan 1958),
the sediment-sea water interface geochemistry in the Santa Barbara

120
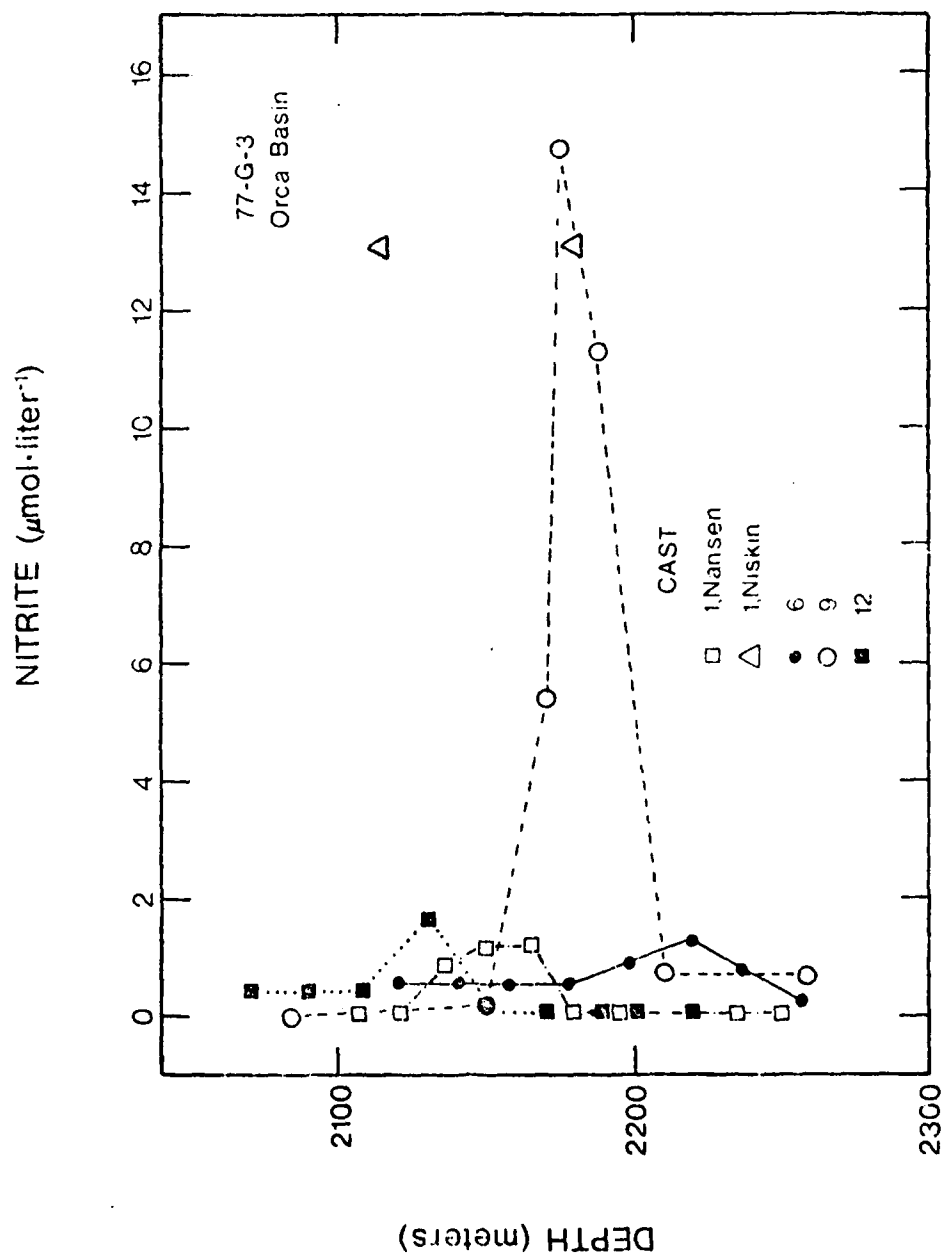
Fig. 28. Nitrite profiles above the Orca Basin obtained during R/V GYRE cruise 77-G-3 and reported by Wiesenburg et al. (1977). The 15.86 $\mu mol \cdot liter^{-1}$ value for nitrite is one of the highest values known and the depth of the nitrite maximum (~2200 m) would make it the deepest reported to date.

Basin may be similar to the brine-sea water interface geochemistry in the Orca Basin. In both areas, ammonia is being converted to molecular nitrogen via a nitrate or nitrite intermediate.

High Salinity Brine. Both argon and nitrogen are supersaturated in the high salinity Orca brine. The excess gas, relative to atmospheric solubilities (Table 9), must arrive with the entry brine into the basin, or be produced in the brine after deposition. Argon has no known biological source. Production of argon by radioactive decay of ^{40}K, however, does occur. Craig (1969) attributed the 10% excess argon in the Discovery Brine of the Red Sea (relative to the Atlantis II brine) to excess radiogenic ^{40}Ar. This concept is consistent with a model of the Discovery Brine as a stagnant overflow from the Atlantis Deep, as discussed by Weiss (1969). In the Orca Basin brine, however, radiogenic ^{40}Ar is probably not an important constituent of the total argon observed. It can be calculated (Table 10) that radiogenic argon production would only be 9×10^{-7} $\mu mol \cdot kg^{-1}$ during the 7900 year age of the brine in the Orca Basin. Even if the excess argon came from the Jurassic LouAnn salt (an unlikely case) an increase of only 2 $\mu mol \cdot kg^{-1}$ would be predicted. The observed excess argon is over 10 $\mu mol \cdot kg^{-1}$ (Fig. 26). Unlike the Red Sea brines, argon production is not important in the Orca Basin.

Molecular nitrogen in the Orca Basin remains relatively constant, below the zone where oxygen is present. There is abundant

Table 10. Calculated theoretical production of dissolved argon
in the high salinity Orca Basin brine.

Assume the brine potassium content has been constant over time
at the present concentration (0.63 g.kg^{-1}) and that A is pro-
duced by radioactive decay of 40K.

K content of brine:

$= 0.63$ gK $=$ kg^{-1} $= 16.1$ mmol$\cdot$K $=$ kg^{-1} brine

$= 9.7$ x 10^{21} atoms K$\cdot$kg^{-1} brine

Atoms ^{40}K: (Atomic abundance $= 0.0118\%$)

$= 1.1$ x 10^{18} atoms K$\cdot$kg^{-1} brine

Atoms ^{40}K decaying to Ar: (Branching ratio $= 0.11$)

$= 1.3$ x 10^{14} atoms$\cdot$kg^{-1} brine

Growth of Ar: (t $= 7900$y, decay const $= \lambda = 5.4$ x 10^{-10} y^{-1})

Ar $= {}^{40}$K $(1-e^{-\lambda t}) = 5.4$ x 10^{11} atoms Ar$\cdot$kg^{-1} brine

$= 9.0$ x 10^{-7} μmol Ar$\cdot$kg^{-1} brine

ammonia in the high salinity brine (see next Chapter), but there
is no apparent nitrogen gas production in this zone. Even though
N_2 is the thermodynamically stable species in sulfate reducing
environments, a biochemical pathway for the direct conversion of
ammonia to dissolved molecular nitrogen must not exist. Barnes
et al. (1975) also came to this conclusion for the anoxic zone of
the Santa Barbara Basin sediments. They observed near-uniform N_2
distribution in the anoxic zone and noted that N_2 production would
increase the N_2/Ar ratio. In the Orca Basin, the N_2/Ar ratio
in the brine was 36.4 (average of 25 points) while the predicted
solubility values for N_2 and Ar at 250°/oo salinity and 5.65°C
gave a N_2/A ratio of 36.5. There was no N_2/Ar increase.

Neither nitrogen or argon is being produced in the high
salinity bottom water of the Orca Basin, yet elevated concentra-
tions (relative to solubility) of both gases are observed. One
can show that the observed nitrogen was present when the brine
formed. The sea water which dissolved the salt exposure to form
the brine must be deep Gulf water like that at the basin sill
(T = 4.2°C, S = 35°/oo). This deep Gulf water probably originates
from the Upper North Atlantic Deep Water (UNADW), with a very
small component of Mediterranean Sea water (J. Cochrane, personal
communication). Assuming (the extreme) that the UNADW (2°C) is
the initial component in the mixture which produces the Orca Basin
sill water, it would have to be mixed equally with water at 6.4°C

(and 35°/$_\circ$ salinity) to reach the values observed. Since mixing

two waters of different temperatures can cause an apparent super-

saturation (Fig. 19), this mixing effect was investigated as a

possible cause of the supersaturation of N_2 and Ar. Such a mixture,

however, would only cause a supersaturation anomaly of 0.1% for

Ar and 0.2% for N_2, far below the observed excesses. Having dis-

counted all other possibilities, we are able to conclude

that the Orca Basin brine is simply salt-saturated, deep-Gulf sea

water with the N_2 and Ar gases intact. This conclusion is sub-

stantiated by the following discussion.

Argon concentration is plotted against nitrogen concentration

in Fig. 29. All concentrations in the plot are expressed as µmol

per 1000 g H_2O, and are thus not affected by the dissolving or

precipitation of salt. The observed concentrations for the Orca

Basin were converted to these units by converting from $\mu mol \cdot liter^{-1}$

to $\mu mol \cdot kg^{-1}$ using the density equations of Millero et al. (1979),

and to µmol per 1000g water using the value of 741.9 grams of H_2O

per kg of brine. The Red Sea brine data, given for comparison,

are from Weiss (1969).

Solubility values for fresh water and 35°/$_\circ$ sea water (Orca

Basin sill water, OBSW), in equilibrium with air at one atmosphere

total pressure (including vapor pressure) are also plotted in

Fig. 29. These curves (in units of $\mu mol \cdot kg^{-1}$) were calculated

using Eq. 5 and the coefficients given by Weiss (1970), and were
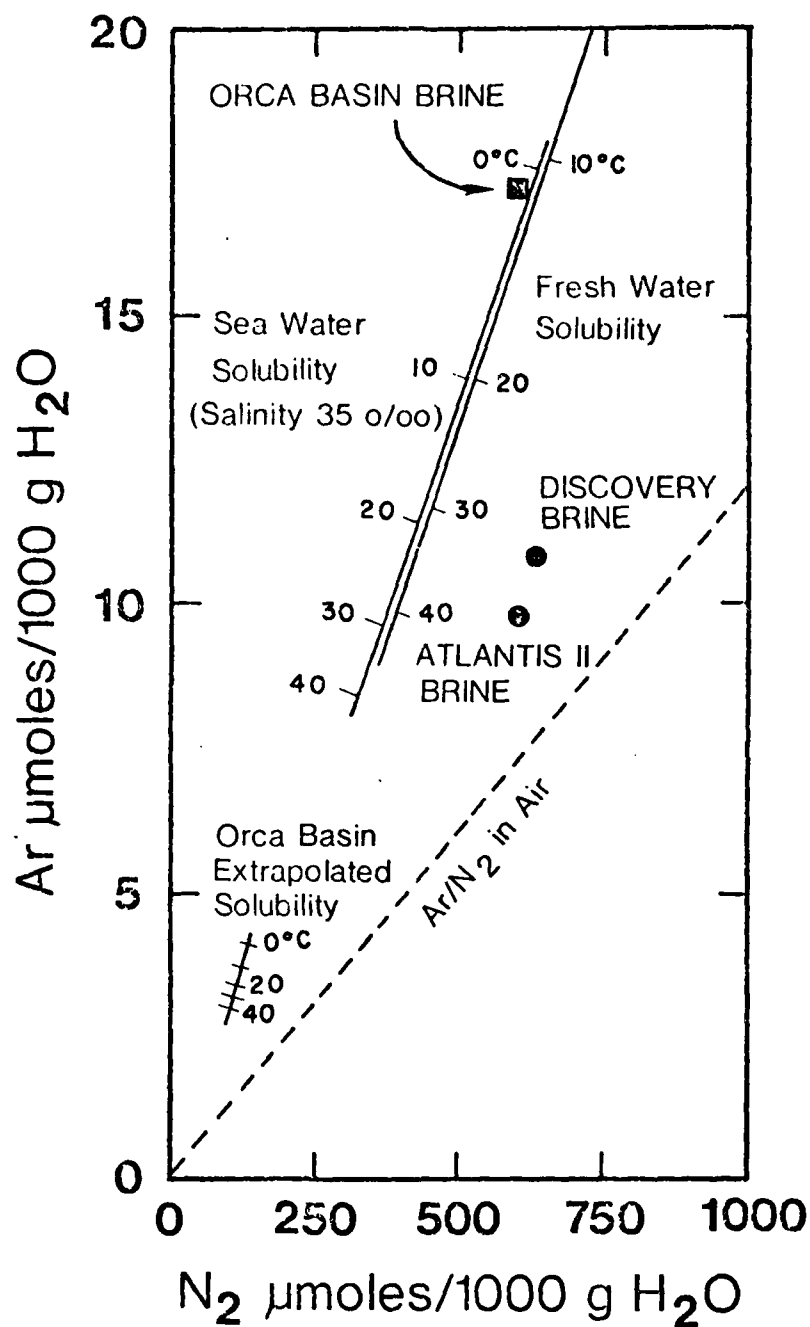
Fig. 29.   Argon versus nitrogen in the Orca Basin
brine and solubility values for fresh water, 35‰
sea water and Orca Basin brine in equilibrium with
the atmosphere.   Data for argon and nitrogen (Weiss
1969) from the Red Sea brines are given for compar-
ison.

corrected using a value of 965.0 g water per 1000 grams of sea water. Using Eq. 5, N_2 and Ar solubilities were extrapolated to the salinity of the Orca Basin brine. As was previously discussed, these extrapolated values are a few percent higher than the observed atmospheric solubilities in the brine (Table 7), but are close enough for the comparisons presented here. The Ar/N_2 ratio in air is also plotted in Fig. 29.

Fig. 29 indicates that the observed N_2 and Ar concentrations in the Orca Basin are supersaturated approximately 250% with respect to brine in equilibrium with air at 5.6°C. Although this difference could be produced by addition of radiogenic argon and large amounts of air, the existence of such a natural process is extremely improbable. Contamination can also be excluded. Bulk sample loss would move the brine N_2/Ar value in Fig. 29 along a straight line toward the origin, while air addition would move the point away from the origin along a line with a slope equal to the Ar/N_2 ratio in air. Neither case is observed here.

The large saturation anomalies in Ar and N_2 can be best explained, not by gas production, but rather by the simple addition of salt to deep Gulf water - the mechanisms proposed by Shokes et al. (1972) for Orca brine formation. Comparison data for the Orca Basin - Gulf water and Red Sea brine - Red Sea water systems are given in Table 11. Weiss (1969) and Craig (1969) explained the N_2 and Ar saturation anomalies in the Red Sea brine on N_2

Table 11. Dissolved gases in Red Sea water, Red Sea brines, Gulf of Mexico Deep Water and Orca Basin brine. Gas concentrations are expressed as μmol (STP)/kg of 38.2°/oo salinity (Red Sea) or 35.0°/oo (Gulf of Mexico) calculated from data of Weiss (1969). Δ values are excess concentrations relative to sea water, δ values are relative to the PDB standard. $\delta^{13}C$ (ΔCO_2) is the calculated $\delta^{13}C$ of carbon dioxide that would have to be added to sea water to yield the observed $\delta^{13}C$ of ΣCO_2 in the brines.

	Red Sea Water $S = 38.2\,°/oo$ $T = 28°C$	Atlantis II Brine	Discovery Brine	Gulf of Mexico Sea Water $S = 35.0\,°/oo$ $T = 4.2°C$	Orca Basin Brine
N_2 μmol Kg^{-1}	359	584	602	558	632
ΔN_2	–	225	243	–	74
Ar	9.41	9.41	10.35	15.3	17.7
ΔAr	–	0.000	0.936	–	2.4
ΣCO_2 mmol/L^{-1}	(2.84)	4.20	0.90	2.28	4.57
ΔCO_2	–	1.36	-1.94	–	2.28
$\delta^{13}C$ (°/oo)	(-1)	-5.6	-16.8	0.3	-16.4
$\delta^{13}C$ (ΔCO_2) (°/oo)	–	-15.2	+6.3	–	-32.2

production from organic matter in both brines and radiogenic Ar

production for the Discovery Brine only. Considering the above

discussion, these mechanisms are not operative in the Orca Basin

brine. Both average N_2 and Ar values are slightly higher than the

predicted values (Table 10), but the uniform differences (13%) in

each indicate a physical rather than a biochemical or radiogenic

effect. This difference may be due to some of the assumptions

(e.g. initial equilibrium) made in calculating the theoretical

values. If error limits for N_2 and Ar are taken as twice the

standard deviation of the determinations, then the uncertainty

envelope for the Orca Basin, Ar/N_2 point on Fig. 29 encompasses

4.2°C and 35‰ on the sea water solubility curve. Thus, all

the Ar and N_2 in the Orca Basin high salinity brine can be account-

ed for by the addition of salt to deep Gulf water.

Shokes et al. (1977) surmised that the brine in the bottom

140 meters of the Orca Basin resulted from the underwater disso-

lution of a surface or near-surface salt deposit on the basin

slope. This exposed diapir must be dissolving due to contact with

deep Gulf water and the resultant brine flows down the slope into

the bottom of the basin. The previous evidence for this mechanism

of formation of the Orca Basin brine has been:

1.   The decreasing salinity gradient in the sediments.

2.   The relative ion abundances of potassium and calcium

relative to sodium, which are unlike the Red Sea
brines and indicate a low temperature halite disso-
lution.

3. The bromine content of the Orca Basin water, which indi-
cates that the brine is formed by the dissolution of an
evaporite deposit rather than by an exaporative process.

4. The seismic data of Addy and Behrens (1980) which indi-
cate that exposed salt diapirs do exist in the vicinity
of the Orca Basin and support the earlier contentions
of Shokes et al. (1977) concerning the location of the
source salt.

The other piece of information which now emphasizes the
origin of the brine is the nitrogen-argon relationships determined
as part of this study. Dissolved argon and nitrogen data provide
independent evidence that the Orca brine did form due to low
temperature dissolution of a salt deposit by sea water. Since the
gas data is not based on the major ions, which have been used in
the other evaluation techniques, the conclusions based on these
data are independent of the ionic balance percentages in the salt
that was dissolved. The only assumption that was made, in using
the gas data to make this evaluation, was that the sea water that
participated in the dissolution of the salt diapir had an original
salinity of 35%$_{oo}$. The temperature at which the salt water was

saturated with brine is estimated from Fig. 29 to be between 0 and 5°C and further supports the low temperature dissolution assumption of Shokes et al. (1977).

CHAPTER IV

DISSOLVED REDUCED GASES

Organic matter is thermodynamically unstable in sea water and

eventually decomposes into various small molecules in the $C-N-S-H_2O$

system. Decomposition of organic material in anoxic basins and

sediments has been extensively studied (see for example, Richards

1965). These studies are important to an understanding of marine

geochemistry since such environments enable us to determine the

mechanisms by which organic material is recycled from the sediments

back into the water column.

The most widely accepted model of organic matter decomposition

is related to the free energy of the oxidant involved in the dia-

genesis process. Organic matter [assumed to have an idealized

composition of $(CH_2O)_{106}(NH_3)_{16}(H_3PO_4)_1$ (Fleming 1940; Redfield

1958)] is oxidized by the oxidant having the greatest free energy

yield per mole of organic carbon oxidized (McKinney and Conway

1957; Richards 1965; Claypool and Kaplan 1974). When an oxidant

is depleted, the oxidant with the next highest energy yield is

consumed until every oxidant is removed, or until all organic car-

bon has been depleted. Table 12 (Froelich et al. 1979) summarizes

the predicted sequences of reactions. In anoxic marine environ-

ments, the decomposition reactions are mediated by denitrifying,

iron oxide reducing, sulfate reducing and methanogenic bacteria

Table 12.   Oxidation reactions of sedimentary organic matter.[*]

1. $(CH_2O)_{106}(NH_3)_{16}(H_3PO_4) + 138 \ O_2 \longrightarrow 106 \ CO_2 + 16 \ HNO_3 + H_3PO_4 + 122 \ H_2O$

$\Delta G°' = -3190$ kJ/mole of Glucose

2. $(CH_2O)_{106}(NH_3)_{16}(H_3PO_4) + 236 \ MnO_2 + 472 \ H^+ \longrightarrow 236 \ Mn^{2+} + 106 \ CO_2$

$+ 8 \ N_2 + H_3PO_4 + 366 \ H_2O$

$\Delta G°' = -3090$ kJ/mole (BIRNESSITE)
-3050 kJ/mole (NSUTITE)
-2920 kJ/mole (PYROLUSITE)

3a. $(CH_2O)_{106}(NH_3)_{16}(H_3PO_4) + 94.4 \ HNO_3 \longrightarrow 106 \ CO_2 + 55.2 \ N_2 + H_3PO_4$

$+ 177.2 \ H_2O$

$\Delta G°' = -3030$ kJ/mole

3b. $(CH_2O)_{106}(NH_3)_{16}(H_3PO_4) + 84.8 \ HNO_3 \longrightarrow 106 \ CO_2 + 42.4 \ N_2 + 16 \ NH_3$

$+ H_3PO_4 + 148.4 \ H_2O$

$\Delta G°' = -2740$ kJ/mole

4. $(CH_2O)_{106}(NH_3)_{16}(H_3PO_4) + 212 \ Fe_2O_3 \ (or \ 424 \ FeOOH) + 848 \ H^+ \longrightarrow$

$424 \ Fe^{2+} + 106 \ CO_2 + 16 \ NH_3 + H_3PO_4 + 530 \ H_2O \ (or \ 742 \ H_2))$

$\Delta G°' = -1410$ kJ/mole (HEMATITE, Fe_2O_3)

$- 1330$ kJ/mole (LIMONITIC GOETHITE, FeOOH)

5. $(CH_2O)_{106}(NH_3)_{16}(H_3PO_4) + 53 \ SO_4^{2-} \longrightarrow 106 \ CO_2 + 16NH_3 + 53 \ S^{2-} + H_3PO_4$

$+ 106 \ H_2O$

$\Delta G°' = -380$ kJ/mole

6. $(CH_2O)_{106}(NH_3)_{16}(H_3PO_4) \longrightarrow 53 \ CO_2 + 53 \ CH_4 + 16 \ NH_3 + H_3PO_4$

$\Delta G°' = -350$ kJ/mole

[*] See Froelich et al. (1979) for an explanation of how free energies were calculated.

(Reactions 3-6), resulting in the production of N_2, NH_3, HS^-, CO_2, HCO_3^-, CH_4, and other related compounds. Interstitial waters from the upper meter of anoxic marine sediments often represent the early stages of the diagenetic process (Thorstenson and MacKenzie 1974; Froelich et al. 1979), while deeper sediments usually exhibit complete sulfate reduction and large increases in methane and carbon dioxide (Hammond 1974).

Anoxic waters overlying reduced sediments have chemical distributions which reflect the oxic and suboxic processes (Reactions 1-4, Table 12) taking place at their oxic-anoxic sea water boundary, as well as the sulfate-reduction-catalyzed reactions taking place in the water and sediments. The combined influence of these decomposition processes in anoxic marine waters has been described for the various nutrients (Richards 1965; Richards et al. 1965; Fanning and Pilson 1972). Only a few studies, however, (Atkinson and Richards 1967; Linnenbom and Swinnerton 1969; Reeburgh 1976; Cohen 1978) have considered the role of various reduced gases in anoxic waters.

In many anoxic areas (e.g., Cariaco Trench) the stability of the water column is relatively low (see Table 5), and periodic inputs of oxygenated water replace some of the anoxic waters. In these other basins, the oxygenated, renewal water both dilutes and oxidizes the reduced products (nutrients and gases) of anaerobic decomposition (see Table 12). In the Orca Basin,

however, the great stability of the hypersaline water ($\sim$250 $^\circ/_{oo}$)
precludes input of any significant amount of renewal water. With
no input of renewal water, and with little (other than diffusive)
loss of decomposition products from the brine, the Orca Basin is
an ideal location for studying the processes on anaerobic
decomposition.

Shokes et al. (1977) have described nutrient distributions
resulting from the anoxic conditions in the basin. Phosphate
levels increased from 2.5 μmol$\cdot$liter^{-1} above the brine to between
60 and 80 μmol$\cdot$liter^{-1} near the bottom, with no obvious trends in
the depth profile within the brine. Silicate likewise increased
from 25 μmol$\cdot$liter^{-1} to over 235 μmol$\cdot$liter^{-1}, while nitrate de-
creased from 23 μmol$\cdot$liter^{-1} above the brine to zero level through-
out the brine. This chapter presents a detailed description of
the geochemistry of reduced gases (CH_4, C_2H_6, C_3H_6, N_2O, NH_3 and
H_2S) in the waters of the Orca Basin, and describes the distri-
butions which have resulted from the anoxic, hypersaline conditions.

Methods

Sampling

Observations of reduced gases were made on five cruises
aboard the R/V Gyre during October 1976 (76-G-10, April 1977 (77-
G-2 and 77-G-3), November 1977 (77-G-13), and one aboard the R/V

Endeavor in February 1979. Stations were taken in both the northern and southern lobes of the Orca Basin and samples were collected both above and in the brine between 2000 m and 2500 m. Most water samples for reduced gas analysis were taken with standard 1.2-liter teflon-coated Nansen bottles. As was previously discussed, sampling with 5-liter Niskin bottles proved ineffective since gases in the Orca Basin brine are supersaturated at atmospheric pressure and degas as hydrostatic pressure is reduced. Since Nansen bottles have a ball valve-type closing apparatus these bottles seemed to inhibit degassing and gave representative results for most gas measurements in the brine.

Sampling from the Nansen bottles was performed initially by transferring the brine to glass bottles (cruise 76-G-10) for later analysis of the reduced gases. This technique gave low values, due to the effervescence which occurred during gravity transfer of brine from the Nansen bottles. During subsequent cruises, brine samples were drawn directly from the Nansen bottles into helium purged glass syringes which were used either to inject samples directly into an all-glass stripping chamber (Swinnerton et al. 1962) or to equilibrate the water with helium (McAuliffe 1971). Samples for methane analysis were collected in piggyback samplers on cruises 77-G-13 and 78-G-2, to compare the Nansen samples with the pressurized samples. On cruises EN-32, samples for methane analysis were also collected in the all glass sampling containers shown in Fig. 21.

Analytical Techniques

The data for this chapter on reduced gases in the Orca Basin brine include measurements of oxygen, nitrous oxide, hydrogen sulfide, ammonia, methane, ethane, and propane as well as determinations of temperature, salinity, iron, sulfate, nitrate, and phosphate. A complete set of these values was needed to make a comprehensive evaluation of anaerobic decomposition processes outlined in Table 12, but it was impossible for one researcher to make all of these measurements simultaneously on every cruise to the Orca Basin. Table 13 gives a description of the various parameters measured on each of the six cruises as well as the analyst who was responsible for providing the data for this comprehensive interpretation. A list of analytical techniques that were used is given in Table 14.

Briefly, temperature was measured using standard reversing thermometers attached to Nansen bottles. As previously mentioned, salinity was obtained by performing either weight or volume dilutions (density corrected) to near $35\%_{\circ}$, followed by analysis using a Plessey Environmental Systems 6230N inductive salimometer which was standardized against standard sea water. Salinities measured by this method are only relative since the Orca Basin brine is not just a concentrated sea water with ion ratios equivalent to those of normal sea water.

Dissolved oxygen was measured by a modification (Broenkow and

Table 13. Analyses of Orca Basin water performed by various chemists on samples from different cruises aboard the R/V Gyre and aboard cruise EN32 of the R/V Endeavor. A dash indicates that measurements were not made on that cruise.

Cruise	Temp.	Salinity	O_2	PO_4	NO_3	NH_3	H_2S	Fe	SO_4	N_2O	CH_4	C_2H_6	C_3H_8
76-G-10	T*	T	T	T	T	-	-	-	-	-	B	B	B
77-G-2	T	T	T	T	T	B	-	P	P	-	B	B	B
77-G-3	T	T	T	T	T	W	W	-	-	-	W	-	-
77-G-13	T	T	T	T	T	B	W	-	-	B	W	-	-
78-G-2	T	T	T	T	T	-	-	-	-	-	W	-	-
EN-32	W	W	-	-	-	-	W	-	-	-	W	-	-

* Key for analysts is as follows: Texas A&M Technical Operations (T), James M. Brooks and Bernie B. Bernard (B), Ronald Pflaum (P), Denis A. Wiesenburg (W) all of Texas A&M University.

Table 14. Method of analysis used for Orca Basin samples.

Component	Method Used	Reference
Salinity	Conductive salinometer	
Sulfate	Gravimetric as BaSO4	Vogel (1968)
Dissolved Oxygen	MicroWinkler titration	Carpenter (1965)
Hydrogen Sulfide	Mixed diamine method	Cline (1969)
Iron	Ferrozine colorometric complexation	Stookey (1970)
Phosphate	Photometric as molybdenum blue	Murphy & Riley (1962)
Nitrate	Reduction to nitrite, photometric	Amstrong et al. (1967)
Nitrite	Diazo complexation, photometric	
Ammonia -1	Phenol hypochlorite method	Solorzano (1969)
-2	Phenate colorometric	Weatherburn (1967)
-3	Electrode referenced to NH_4Cl	
Nitrous Oxide	Trapping and electron capture GC	Cohen (1978)
Methane	Gas stripping and thermal conductivity GC	Swinnerton et al. (1962)
Hydrocarbons	Trapping and flame ionization gas chromatography	Brooks et al. (1980)

Cline 1969) of the microWinkler method of Carpenter (1965) as was
described in the previous chapter. Nutrients were measured coloro-
metrically by AutoAnalyzer using dilutions to bring the concen-
tration of salts down to a level where they did not inhibit the
relative responses to the nutrients alone. Dilution was also
necessary due to the high nutrient concentrations observed. Inor-
ganic phosphate was determined by the ascorbic acid-potassium anti-
monyl tartrate method of Murphy and Riley (1962) as modified for
use on the AutoAnalyzer by Atlas et al. (1971). Nitrate ions
were determined by the cadmium reduction method of Armstrong et al.
(1967).

Ammonia was measured by three different techniques. On cruise
77-G-2, ammonia was measured using an Orion Research Model 95-10
specific ion electrode standardized against NH_4Cl-ammonia solu-
tions. This probe had been used previously for studies of inter-
stitial waters and had proven to be very effective for samples
of high concentration. There seemed to be very little, if any,
salt effect associated with this probe at the high NH_3 levels
found in the Orca brine. On cruise 77-G-3, ammonia was determined
manually using the phenol hypochlorite method of Solorzano (1969).
Samples for ammonia were taken in syringes or pipettes filled di-
rectly from the Nansen bottles and introduced into 50 ml serum
vials below the surface of the complexing reagents. Ammonia
samples collected in this way seem to be little affected by the

degassing which caused inaccuracies with other reduced gas measure-
ments. On cruise 77-G-13, ammonia was determined by AutoAnalyzer
using the phenate method of Weatherburn (1967) modified for use on
the AutoAnalyzer II. Samples for AutoAnalyzer analysis were
transferred into sample cups before analysis. There was a pos-
sibility of degassing in these samples since they remain open to
the air while they await analysis. However, no apparent loss of
ammonia was observed after sample collection, as evidenced by the
consistency of the three methods.

Hydrogen sulfide was determined using the mixed diamine
reagent method of Cline (1969). Samples were drawn from Nansen
bottles directly into pipettes and the brine sample was introduced
into the acidified reagent under the liquid surface, thus avoiding
any contact with air which would rapidly oxidize free sulfide.
Sulfate was measured gravimetrically using a standard barium pre-
cipitate method described by Vogel (1968). Dissolved iron in the
water column was also measured using the ferrozine method of
Stookey (1970).

Nitrous oxide was determined on cruise 77-G-13 by a technique
similar to the one described by Cohen (1978) with modifications:
an Ascarite column was placed after the magnesium perchlorate
column to remove CO_2. An electron capture ([63]Ni) detector oper-
ated at 300°C, was used in conjunction with a Hewlett-Packard
5830A gas chromatograph for sample analysis, after separation on

a Porpak Q column. Calibration was accomplished by comparing the measured values against a standard calibration mixture.

Methane in the brine was determined by gas chromatography using both thermal conductivity and flame ionization detectors. During cruise 76-G-10, samples were collected in 300 ml sample bottles and returned to the lab for analysis by the method of Brooks et al. (1980). Some gas was lost from these samples due to degassing, bubble formation and escape during transfer to the sample bottle. To prevent degassing on samples taken on cruise 77-G-2, the brine was drawn directly into 50 ml equilibration syringes as previously described. Gaseous hydrocarbons were determined using the techniques of McAuliffe (1971). Methane on samples taken on cruises 77-G-3 and 77-G-13 was analyzed in water transferred from the Nansen bottle directly via nylon tubing into 12 ml syringes. The water in these syringes was injected through a septum into a 20 ml stripping chamber. Methane was stripped by the carrier-gas helium flow, and swept directly onto a 5A molecular sieve column, for separation from dissolved atmospheric gases. Methane was measured with a Hewlett-Packard 5710A gas chromatograph using a thermal conductivity detector. Sample transfer and chromatographic analysis techniques for methane from the piggyback and glass-container samplers used on cruises 78-G-2 and EN-32 were the same as were used for N_2 and Ar on those cruises (see Chapter III).

Gaseous hydrocarbons, ethane, and propane were determined on

samples from cruises 76-G-10 and 77-G-2 using the technique described for methane (Brooks et al. (1980). The $^{13}C/^{12}C$ isotopic ratio of the methane was determined by B. B. Bernard by degassing the brine, removing CO_2 and combusting methane to carbon dioxide at 800°C. $\delta^{13}C$ was determined using a Nuclide mass spectrometer and referenced to the PDB standard (Sackett et al. 1970).

$$\delta^{13}C = \left[\frac{(^{13}C/^{12}C)\ \text{sample}}{(^{13}C/^{12}C)\ \text{standard}} - 1 \right] \times 1000 \qquad (20)$$

Results

Gaseous Hydrocarbons

Fig. 30 shows salinity, temperature, dissolved oxygen, methane, ethane, propane, and $\delta^{13}CH_4$ profiles from three stations in the Orca Basin for cruise 76-G-10. Results are plotted as distance above the bottom. The bottom depth for the stations plotted here was 2436 m. These data were taken from the same hydrocasts that Shokes et al. (1977) used to characterize the Orca Basin brine. Methane in the brine from cruise 77-G-3 is also plotted (closed circles). Samples which were collected in the brine exhibited effervescence during gravity transferal from the Nansen bottles. Thus, these values of approximately 580 $\mu mol \cdot liter^{-1}$ of methane in the brine are lower than the 750 $\mu mol \cdot liter^{-1}$ levels measured on cruise 77-G-2 (Table 15), when samples were drawn directly from
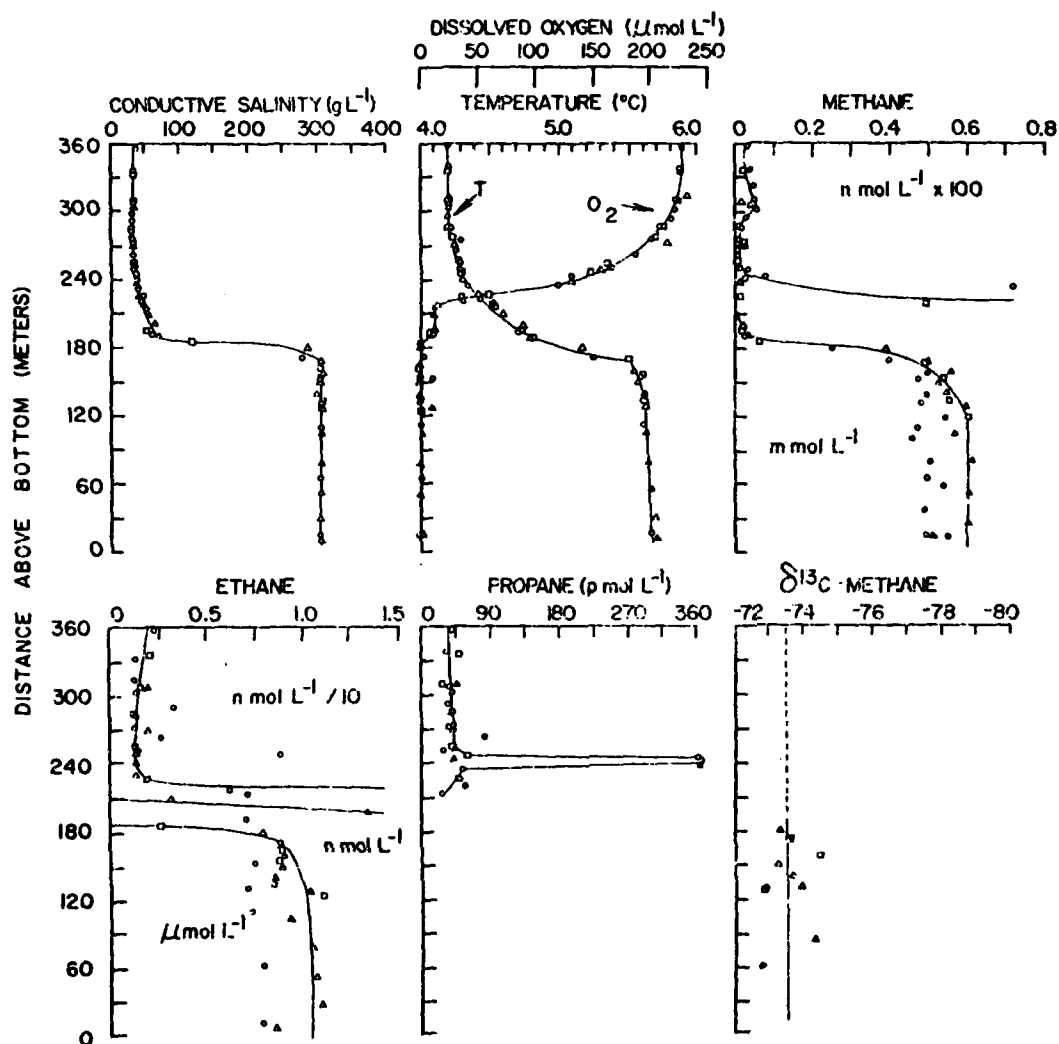
Fig. 30. Vertical distributions of temperature, salinity, dis-
solved oxygen, methane, ethane, propane and $\delta^{13}CH_4$ in the Orca Basin.
Data are plotted as distance above the bottom. Bottom depth = 2436 m.
Gas measurements were made on stored samples from cruise 76-G-10, thus
methane levels are slightly lower than true value, due to degassing
of the supersaturated brine. The closed circles for methane are from
cruise 77-G-3.

Table 15. Low-molecular-weight hydrocarbons in the Orca Basin during cruise 77-G-2. A dash indicates sample was lost.

Depth (m)	Salinity (‰)	Temp. (°C)	Oxygen (μmol·liter⁻¹)	Methane (μmol·liter⁻¹)	Ethane (nmol·liter⁻¹)	Propane (nmol·liter⁻¹)	$\frac{C_1}{C_2 + C_3}$
2023	34.98	4.20	255	0.0040	0.020	0.022	97
2033	34.99	4.21	254	0.0024	0.017	0.038	42
2063	35.02	4.20	254	0.0040	0.017	0.030	84
2103	35.10	4.20	252	0.0047	0.041	0.030	66
2113	35.24	4.21	259	0.0054	0.019	0.029	112
2133	35.92	4.20	240	0.0007	0.010	0.016	27
2153	37.16	4.22	214	0.0023	0.010	0.015	95
2173	39.48	4.27	169	–	0.007	0.007	–
2193	45.98	4.38	77.6	0.0011	0.013	0.019	35
2213	55.98	4.56	8.9	–	1.49	0.113	–
2233	68.88	4.75	9.8	–	0.97	0.430	–
2273	259.7 *	5.57	0	784	1320	<0.9	648
2293	258.5 *	5.62	0	711	1130	<0.9	684
2313	258.3 *	5.62	0	899	1320	<0.9	742
2363	258.4 *	5.65	0	674	1130	<0.9	649
2393	257.9 *	5.66	0	715	1249	<0.9	624
2403	258.2 *	5.65	0	645	1254	<0.9	562
2408	257.8 *	5.66	0	776	1204	<0.9	703
2413	257.8 *	5.66	0	830	1053	<0.9	859

* These salinity data are from volume dilutions corrected for the density of the brine, $\ell = 1.185$ at 22.5°C.

the Nansen bottles into equilibration syringes. Some small loss of methane may have occurred when the hydrostatic pressure was reduced on the bottles during their ascent from depth. However, the 750 $\mu mol \cdot liter^{-1}$ average of methane (Table 15) is believed to be actual methane concentration in the brine. The methane data from the pressurized samples taken on cruise 78-G-2 and EN-32 substantiate this conclusion. The 78-G-2 and EN-32 methane data are given in Fig. 31. The problems with sampling in the brine preclude observations of any trends in the data in the high salinity brine.

Some structure in the light hydrocarbon distributions was observed in the pycnocline above the brine. In the profiles from cruise 77-G-2 (shown in Fig. 32), a methane maximum was observed above the interface, just above the oxygen depletion zone, at a depth of 2120 m. Methane values from several cruises are given in Fig. 33. Methane concentrations begin to increase above deep ocean concentrations about 50 m above the brine interface. Less distinct ethane and propane maxima also appear above the brine in this region of oxygen depletion (Fig. 32).

The carbon isotopic ratios of methane are shown in Fig. 30. They range from -73 to -74%₀ (relative to PDB) and relatively high $C_1/(C_2 + C_3)$ ratios (average = 684) indicate that the methane is principally of biogenic origin.

METHANE (umol·liter⁻¹)
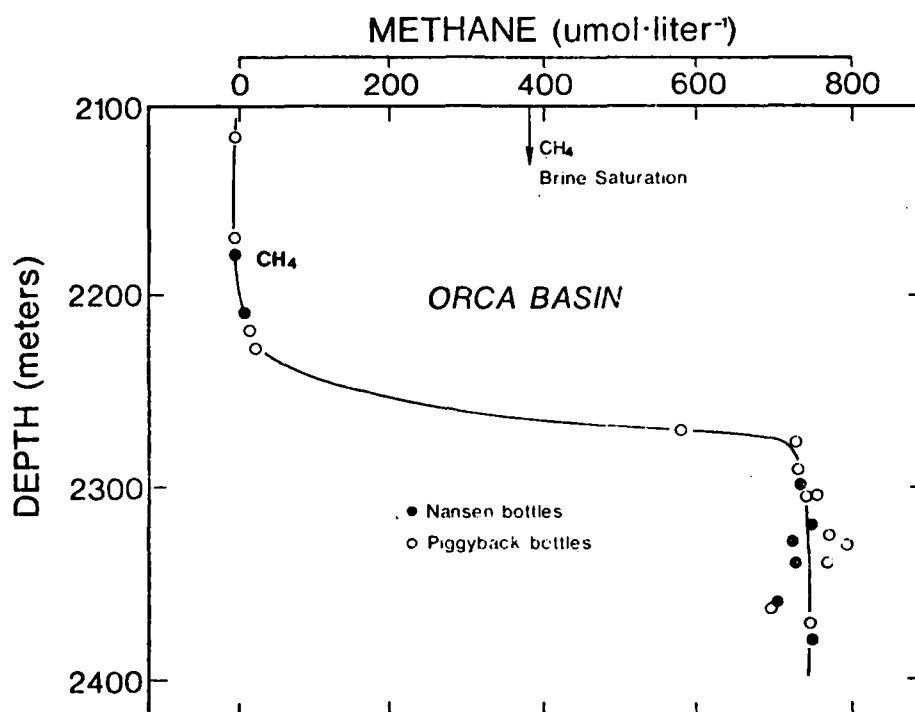
Fig. 31. Dissolved methane depth distributions in the Orca
Basin taken from gas-tight piggyback samplers and standard
Nansen bottles. Data are from cruises 77-G-13 and EN-32.
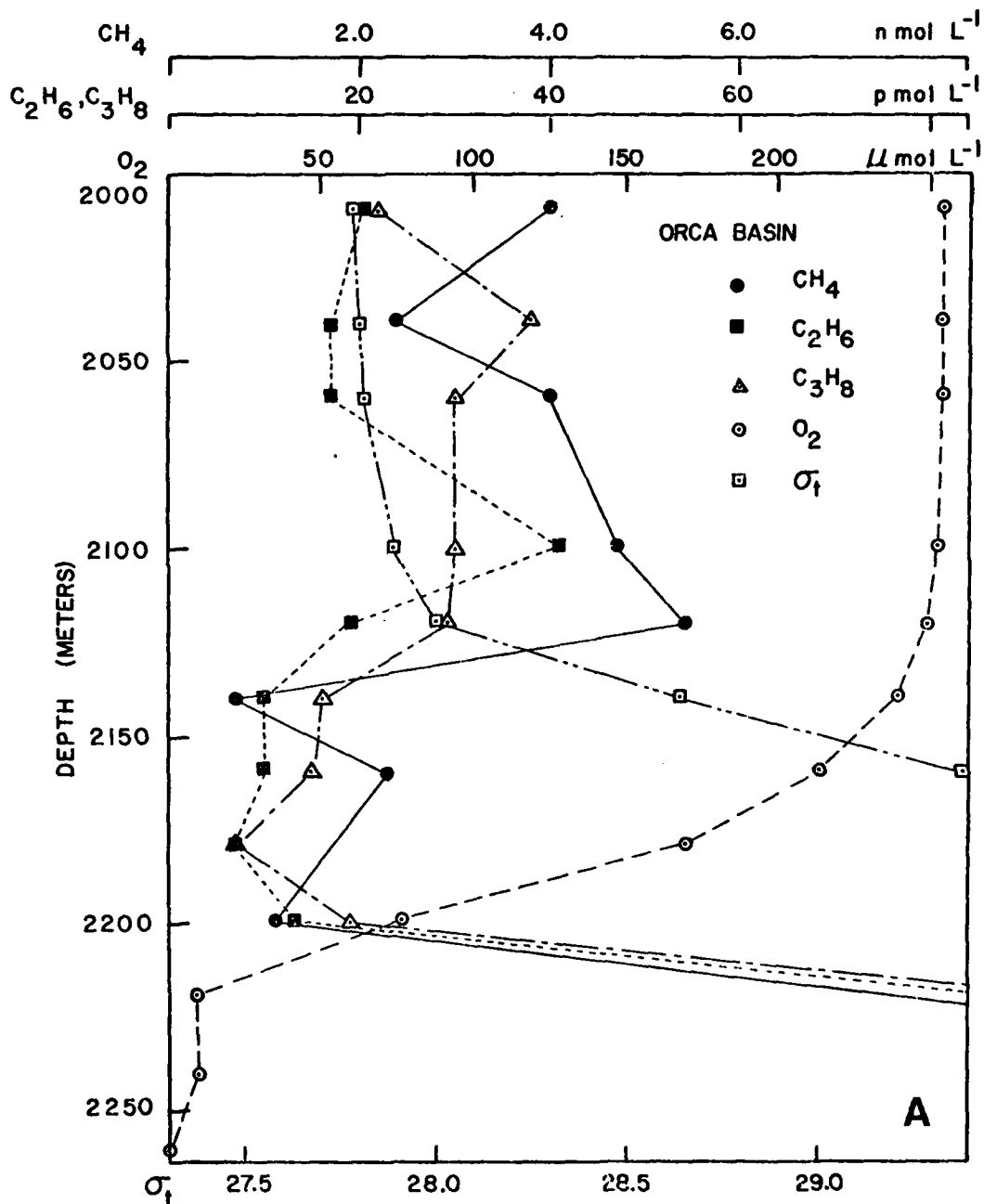
Fig. 32.   Hydrocarbon, oxygen and σ_t data from the basin pycnocline
(cruise 77-G-2 data).   Note the maxima in the methane and ethane pro-
files at the level where density begins to increase rapidly.
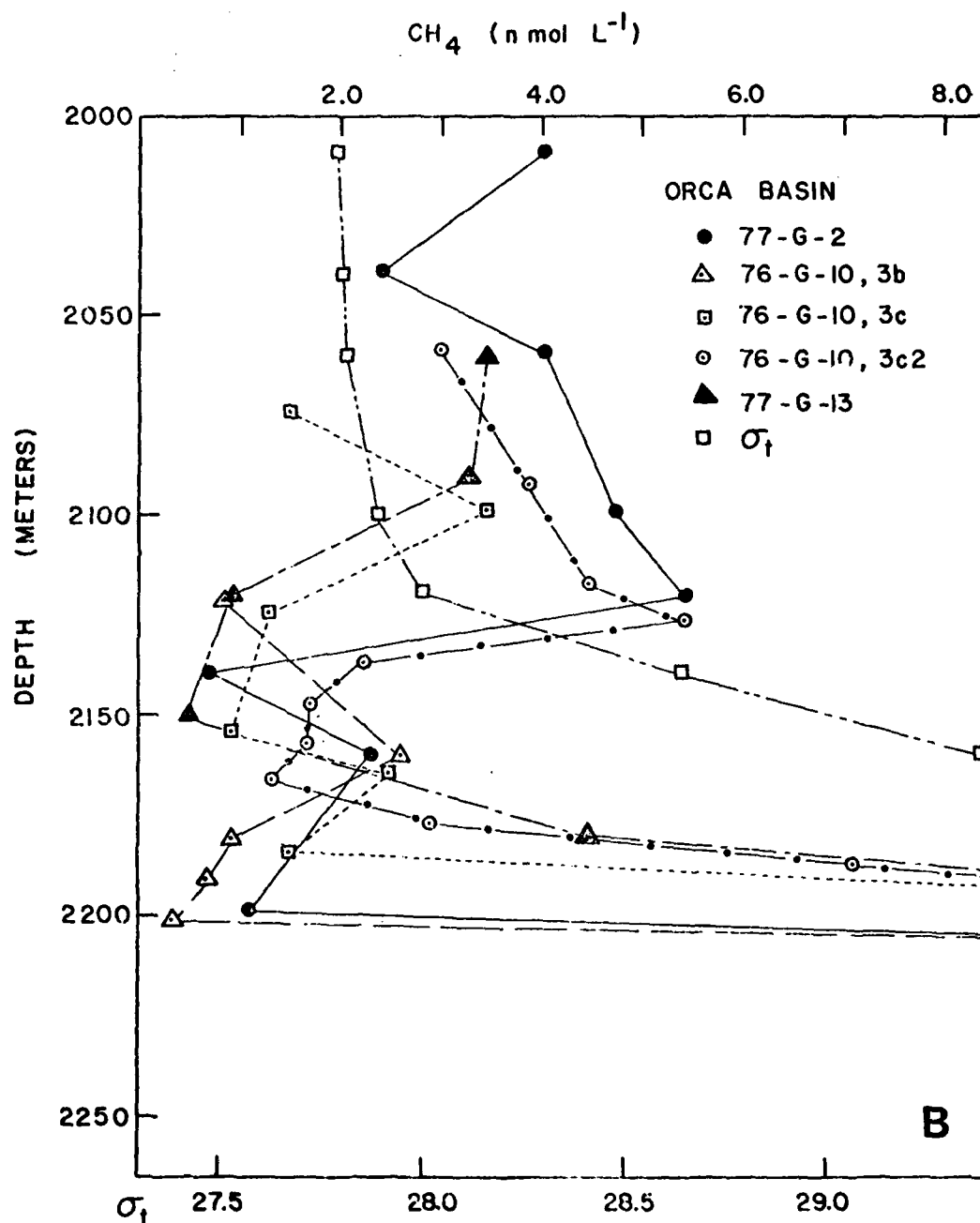
Fig. 33.   Methane depth distributions in the pycnocline from different hydrocasts on two separate cruises.

Nitrous Oxide and Ammonia

The nitrous oxide data collected during cruise 77-G-13 are plotted in Fig. 34, along with dissolved oxygen, nitrate and ammonia measurements from the same cast. Nitrous oxide concentrations above the brine average 15.3 $nmol \cdot liter^{-1}$. This value is near the atmospheric solubility level that would be predicted (12 $nmol \cdot liter^{-1}$) from the constants of Weiss and Price (1980), Eq. 5 and a value of 290 ppbv as the atmospheric concentration of N_2O. N_2O decreases rapidly near the interface and reaches a near constant level of 0.28 $nmol \cdot liter^{-1}$ within the brine. The N_2O level in the brine may be real, although possible contamination during sample transfer cannot be totally eliminated. Ammonia levels (Fig. 34) increase from essentially zero above the brine to over 500 $\mu mol \cdot liter^{-1}$ within the brine itself. Ammonia values measured by the three different methods on different cruises (Fig. 35) are consistent, and indicate little structure in the brine itself. While ammonia increases in the brine interface region, nitrate decreases from a mean value in deep Gulf water of 22.6 $\mu mol \cdot liter^{-1}$ to zero within the brine (Fig. 34). This is direct evidence of the denitrification occurring at the brine interface.

Hydrogen Sulfide

Hydrogen sulfide, which was also measured on three separate cruises, was not present in the Orca Basin as free H_2S. Measure-
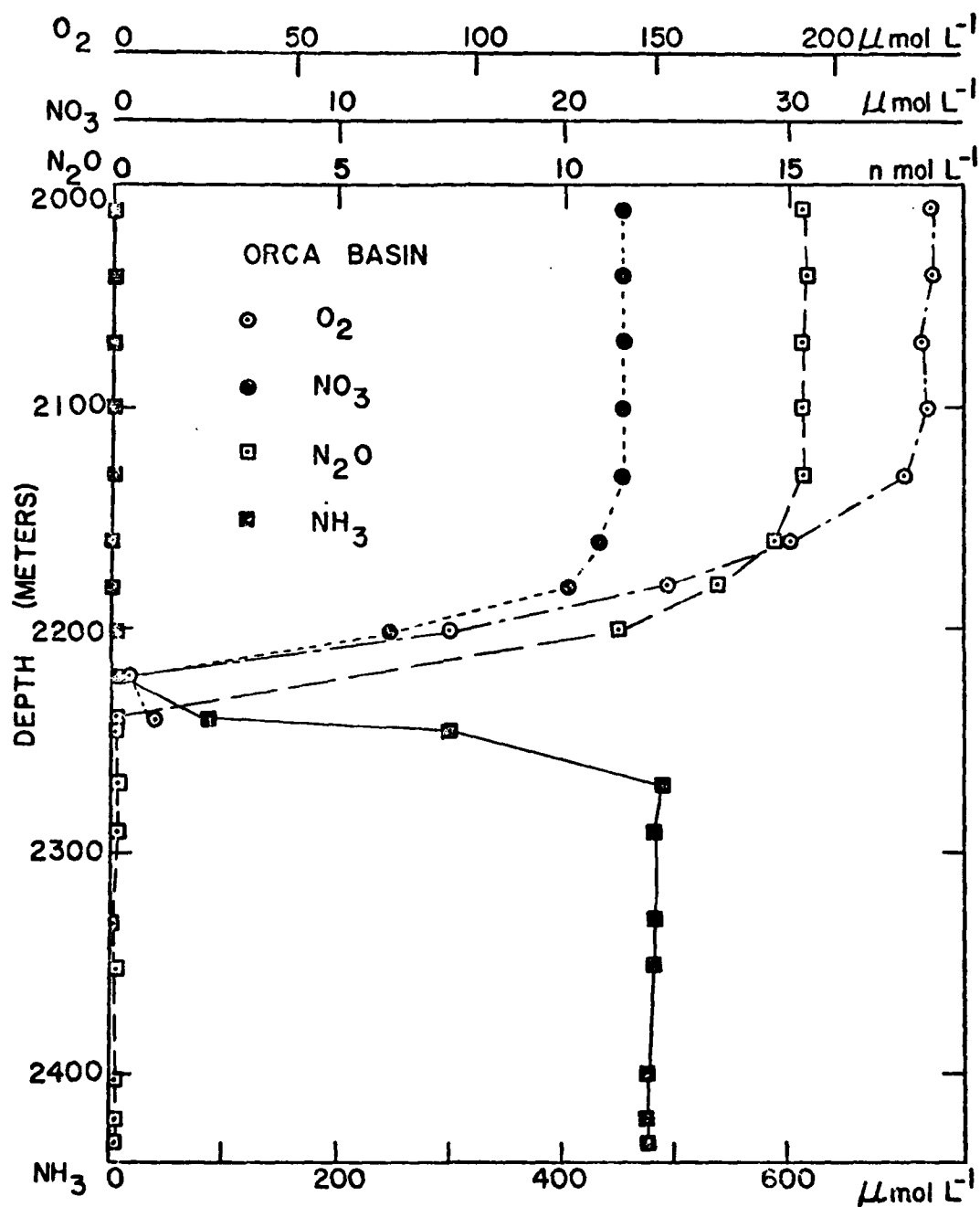
Fig. 34. Vertical distribution of dissolved oxygen, nitrate, N_2O and ammonia in the Orca Basin. N_2O is consumed in the anoxic brine along with nitrate while ammonia increases to about 500 μmol$\cdot$liter^{-1}.
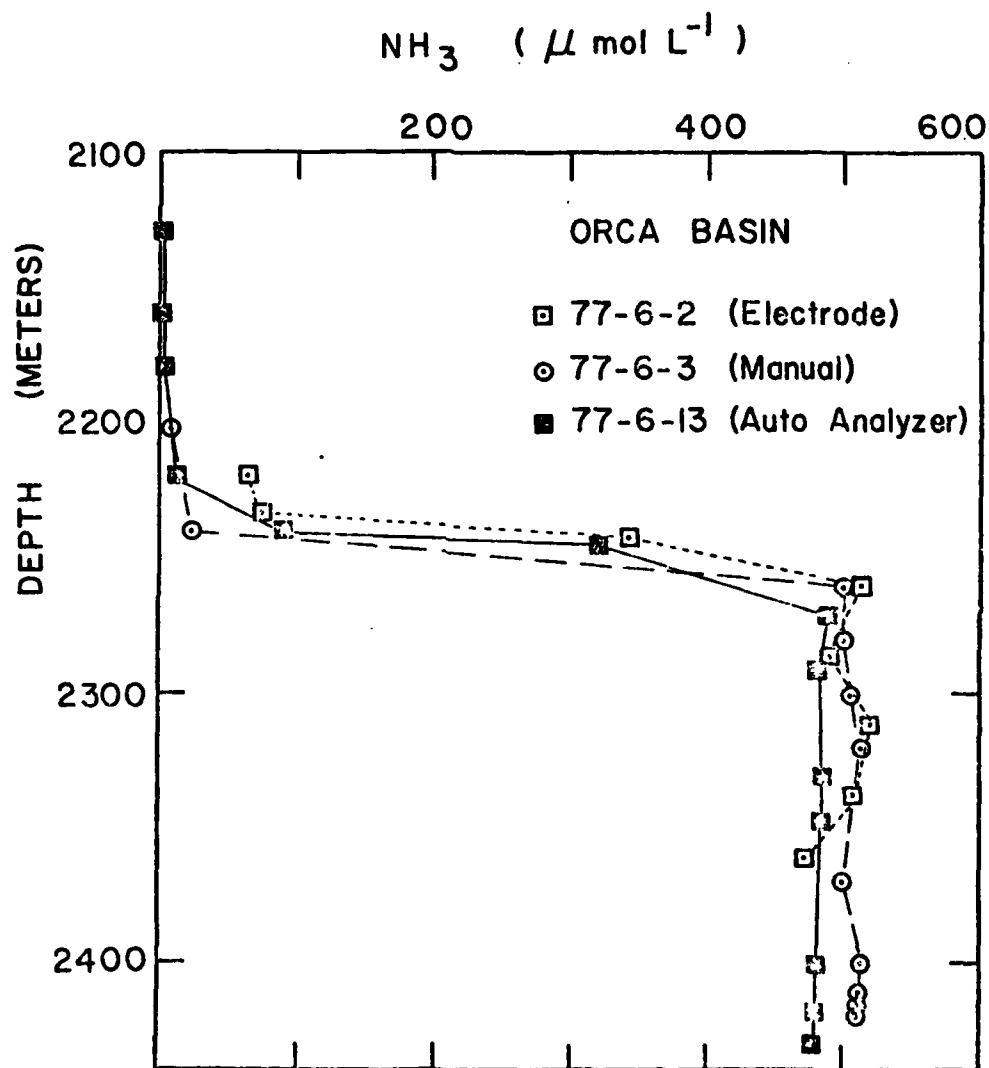
Fig. 35.   Vertical profiles of ammonia measured by three
separate methods (see text) on three different cruises. No obvious
structures appear in the ammonia profile within the brine.

ments in the 3-1000 $\mu mol \cdot liter^{-1}$ range indicated that there was no
sulfide in the Orca Basin, although some sulfate reduction must be
taking place to produce the biogenic iron sulfide found in the
Orca Basin sediments (Addy and Behrens 1980). Attempts to measure
H_2S in the 1-3 $\mu mol \cdot liter^{-1}$ range showed no sulfide, except just
below the interface where the highest concentration measured was
2.8 $\mu mol \cdot liter^{-1}$ (Fig. 36). Water that was filtered from the
interface region contained black particles of iron sulfide. Thus
it is plausible that the H_2S values that were measured at the
interface were not free H_2S. The Cline (1969) method of H_2S
analysis requires the analysis to be performed in an acid solution.
Any particulate iron sulfides present in the brine would be con-
verted to free sulfide and appear as H_2S in the measurement.
Hydrogen sulfide, if present in Orca brine, may be lower than the
sensitivity of the methodology.

Fig. 36 shows the distribution of H_2S sulfate and iron in
the Orca Basin. The sulfate levels (33.5 $\mu mol \cdot liter^{-1}$ average)
are about 18% higher than the sulfate concentrations in deep Gulf
of Mexico water above the brine. Iron concentrations increase
from trace amounts above the brine to over 30 $\mu mol \cdot liter^{-1}$
in the anoxic brine.

Discussion

The Orca Basin is a giant, flow-through chemical reactor which
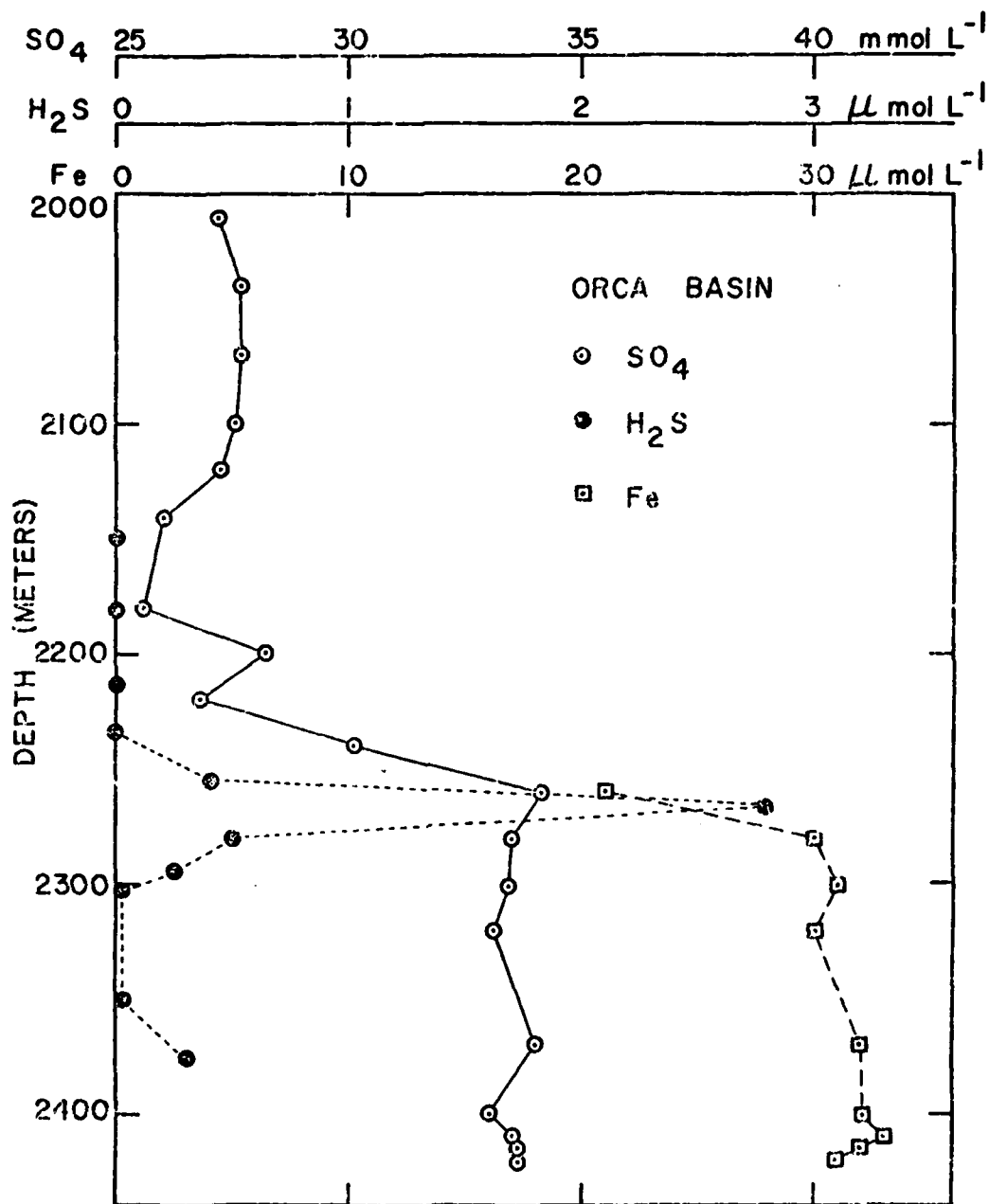
Fig. 36. Depth distributions of sulfate, sulfide and iron in
the Orca Basin. Free H_2S is probably absent from the brine with
iron sulfides causing the apparent H_2S distribution observed. Iron
has accumulated in the Orca Basin, unlike other anoxic marine
waters, due to the lack of available sulfide to precipitate the iron.

is only unusual in that a very small percentage of the reaction products escape. In any chemical reactor, processes that modify the concentration of a dissolved component can be classified as: external processes, which are active only at the boundaries and internal processes, which are active everywhere in the system. The external processes are of importance in determining the concentration at the boundaries, while the internal processes, together with the boundary concentrations, determine the distribution throughout.

The general equation for the rate of change of the concentration of a dissolved component at any point in a water column may be written as:

$$\frac{\partial c}{\partial t} = \frac{\partial}{\partial x}\left(A_x\,\frac{\partial c}{\partial x}\right) + \frac{\partial}{\partial y}\left(A_y\,\frac{\partial c}{\partial y}\right) + \frac{\partial}{\partial z}\left(A_z\,\frac{\partial c}{\partial z}\right) \qquad (21)$$

$$- u\,\frac{\partial c}{\partial x} - v\,\frac{\partial c}{\partial y} - w\,\frac{\partial c}{\partial z} + R$$

where

A_x, A_y are horizontal eddy diffusion coefficients,

A_z is the vertical eddy diffusion coefficient,

u, v   are horizontal advection velocities,

w   is the vertical advection velocity with z positive downward, and

R   is the net rate of production or consumption of a component which is not conservative.

This equation describes the effects of diffusion and advection on

the local time rate of change, $\frac{\partial}{\partial t}$, of a nonconservative solute whose concentration, c, is changed chemically or biologically at rate R.

In the chemical reactor that is the Orca Basin, organic material raining down from the surface provides the fuel for the diagenetic reactions given in Table 12. The processes of decomposition in the Orca Basin are no different than in other anoxic basins, but the high salt content of the water can have a great influence on reaction rates and mechanisms. Eq. 22 also applies to the Orca Basin, but rates of advection, diffusion and reaction may be slower in this dense, hypersaline environment than in other anoxic environments.

It will be argued in this discussion that the processes of decomposition in the Orca Basin are no different than in other anoxic environments, only slower. Briefly summarized the evidence for reduced microbial activity in the Orca Basin is

(1) The presence of fronds of Sargassum seaweed in deep cores. Kennett and Penrose (1978) have noted that this type of preservation has never been observed before in the deep ocean.

(2) A comparison of the initial sulfate gradients between the Orca Basin and the basin next to it indicates that sulfate is not as rapidly reduced in the Orca Basin sediments.

(3) The isotopic composition of carbon dioxide and methane is

unusually light (relative to PDB standard) in the Orca

Basin. Sackett et al. (1979) suggested that the isotop-

ically light methane was the result of an unknown lighter

source material. However, slower rates of methanogenesis

would produce greater fractionation and could account for

the observed $\delta^{13}C$ values starting from the organic ma-

terial found in the brine.

(4) No pyrite is found in the Orca Basin sediments. If there

is only a slow production of sulfide in the Orca Basin,

the high iron levels would rapidly remove the sulfide

from solution and inhibit the continued reaction of

metastable iron sulfides to pyrite. Metastable iron

sulfides are found in the Orca Basin sediments, pyrite

has not been found.

Overall Effects of Decomposition

Organic matter in the marine environment has an ideal C:N:P

ratio of 106:16:1 by atom which is close to the statistical aver-

age of planktonic material, the primary source of organic carbon

to the marine ecosphere. Anaerobic decomposition of this organic

matter can be expressed by the reactions in Table 12. The most

important reaction is sulfate reduction, given by the equation:

$$(CH_2O)_{106}(NH_3)_{16}H_3PO_4 + 53 \ SO_4^= \longrightarrow \tag{22}$$

$$106 \ CO_2 + 53 \ S^= + 16 \ NH_3 + 106 \ H_2O + H_3 \ PO_4$$
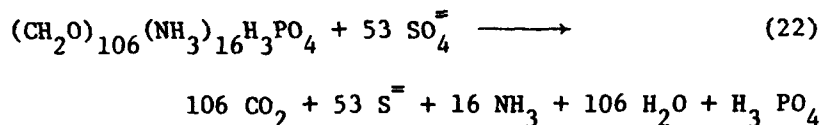
This reaction yields mole ratios for $CO_2:S^=:NH_3:H_3PO_4$ of 106:53:16:1.
Methane production during anaerobic decomposition will alter the
ratios predicted by this model by either liberating or consuming
carbon dioxide. Richards et al. (1965) proposed that one repre-
sentation of methanogenesis might be

$$(CH_2O)_{106}(NH_3)_{16}H_3PO_4 \longrightarrow \tag{23}$$

$$53 \ CH_4 + 53 \ CO_2 + 16 \ NH_3 + H_3 \ PO_4$$
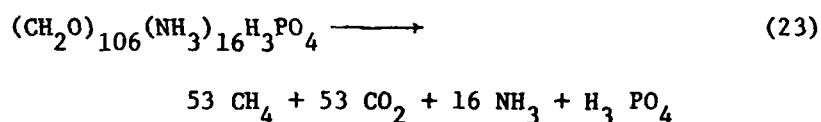
yielding mole ratios for $CO_2:CH_4:NH_3:H_3PO_4$ of 53:53:16:1 for the
products. This reaction would alter the ratios predicted by Eq.
7 by an amount dependent upon the quantity of methane produced.
In the anoxic waters of the Orca Basin, the average concentrations
observed for excess decomposition products are 2.28 mmol·liter^{-1}
for CO_2, 0.7 mmol·liter^{-1} for CH_4 (Sackett et al. 1979), less than
1 µmol·liter^{-1} for $S^=$, 500 µmol·liter^{-1} for NH_3 and 60 µmol·liter^{-1}
for PO_4^{-3} (this study). These values result in $\Delta CO_2:CH_4:NH_3:H_3PO_4$
mole ratios of 38:12:8.3:1, far different than predicted by
Richard's (1965) model.

How can these differences be explained? It is doubtful that
these differences can be accounted for by compositional differen-
ces between Gulf plankton, and the world average planktonic ratios.

Plankton falling through the water column decomposes into particulate organic matter (POM). The POM in the deep water should have the same characteristics as the plankton debris which reach the bottom. Particulate organic carbon (POC) and particulate organic nitrogen (PON) have been reported by Fredericks (1972), in both surface waters of the Gulf and at depth. The average values he measured for POC and PON at the surface, and at 200 to 2200 m, are shown in Table 16. When converted to a mole carbon and mole nitrogen ratio, the C/N ratio in surface waters was 3.62 and increased to a deep water C/N ratio of 7.78. The average of C/N ratio for the model of Richards (1965) is 6.6, while the ratio of excess carbon $(CO_2 + CH_4)$ to nitrogen (NH_3) in the Orca Basin is 6.0. Considering variations in Fredericks' (1970) data with depth all of these ratios are approximately the same.

Since the excess carbon to nitrogen ratio in the Orca Basin approximates the theoretical ratio, there must be excess phosphate in the brine (brine $PO_4 = 60$ $\mu mol \cdot liter^{-1}$). Phosphate could be added to the brine from organic matter decomposition or by input of phosphate associated with the brine coming from the LouAnn salt, from which the Orca brine originated. Unfortunately, a detailed study of phosphorus content in natural solution brines has not been made. Of the few brines that have been analyzed, most have contained less than 1 $mg \cdot liter^{-1}$ (Collins 1975). For phosphorus, 1 $mg \cdot liter^{-1}$ is equal to 32 $mmol \cdot liter^{-1}$.

Page 159

Table 16. Average concentrations of POC and PON in deep Gulf samples along with mole ratios (after Fredericks 1972).

| | Gulf Surface | | Deep Gulf | | Orca Basin |
	µg·liter⁻¹	µmol·liter⁻¹	µg·liter⁻¹	µmol·liter⁻¹	
PON	6.5	0.46	1.5	0.11	
POC	20	1.66	10	0.83	
C/N		3.62		7.78	6.03

The excess C/N ratio in the brine can be used to calculate the predicted phosphate from anaerobic decomposition alone. Using the brine C/N value of 6.0, the decomposition-produced phosphate would be 27.8 μmol$\cdot$liter^{-1}. This value would give a C:N:P ratio of 106:18:1, which is very near the predicted values from Richard's model. This calculation suggests that there is an excess 32 μmol$\cdot$liter^{-1} of phosphate in Orca Basin. Considering the high phosphorus content of natural brine, the excess could be from the original brine that entered the basin before any decomposition of organic matter had occurred.

Microbial Activity in the Orca Basin

Distributions of the reduced species in the brine are controlled either by in situ processes within the brine and sediment and/or by the evaporite dissolution and migration of the brine into the basin. Since the brine originates from solution by sea water of a near-surface salt deposit within the basin, the reduced gases should be controlled primarily by in situ processes within the brine, after migration into the basin. The inflowing brine should have initial reduced gas concentrations similar to overlying sea water, as was shown for argon and nitrogen. Thus biological action by anaerobic bacteria in the Orca Basin brine must produce the concentrations of reduced species that were observed.

LaRock et al. (1979) have reported that ATP concentrations and uridine uptake show an increase in magnitude above the brine interface, followed by a decrease below the interface into the anoxic zone. Substantial ATP increases were found further down in the anoxic zone. As in other anoxic environments, the bacterial populations required to mediate the decomposition of organic matter are present in the hypersaline waters of the Orca Basin. One might expect the high salt content of the Orca Basin to inhibit microbial activity. However, the observed ATP levels (3-15 ng ATP·liter^{-1}) indicate a larger bacterial population than in the overlying deep Gulf waters, where values from 1-3 ng ATP·liter^{-1} were observed (LaRock et al. 1979). This large bacterial population is probably associated with the high concentration of dissolved organic carbon (3.5 mg C·liter^{-1}) and particulate organic carbon (70 µg C·liter^{-1}) observed in the brine (Sackett et al. 1979). Although the total bacterial biomass is larger in the brine than in the deep Gulf, one must consider the inhibitory effects of salt on the reaction rates during bacterial decomposition.

Unfortunately, bacteria activity at high sodium chloride concentrations has received limited attention in the literature. Larsen (1967) and Kushner (1968) have reviewed the literature on halophilic bacteria and noted that they do not exclude salts, but have an internal environment as high in ionic strength as their external environment. Many bacteria are faculative halophiles,

and the sulfate reducers, methanogens, and other anaerobes have probably accomodated themselves to the Orca Basin brine well enough to produce or consume the reduced gases observed. Like increasing pressure or decreasing temperature, the increasing salt content of a solution will reduce the rate at which microbes perform their metabolic activities (Kushner 1978). Most bacteria in hypersaline waters grow slowly, with mean generation times of 7-15 hours at 37°C (Kushner 1968), compared with generation times of less than an hour for bacteria at sea water salt concentrations and 37°C. The large concentrations of biogenic methane in the Orca Basin (750 $\mu mol \cdot liter^{-1}$, $\delta^{13}C_{CH_4}$ = -74°/$_{oo}$), relative to other anoxic basins, and the evidence of sulfate reduction in the sediments suggests that anaerobic bacteria are able to tolerate the hypersaline conditions and actively reduce organic material even at 5.6°C, a temperature much lower than the 30-40°C preferred by most halophilic bacteria. Their slower rate of metabolism in the Orca Basin, however, has a profound influence on the compositions of the decomposition products found there.

Another bacterially-mediated decomposition reaction must be considered in addition to those presented in Table 12. That is the process of anaerobic methane consumption during sulfate reduction. Although the process of methane oxidation under aerobic conditions is well documented (Vary and Johnson 1967; Wertlieb and Vishniac 1967; Quale 1972; Rudd, Hamilton and Campbell 1974)

and bacteria are known to anaerobically utilize hydrocarbons higher than methane (Novelli and Zobell 1947; Rosenfeld 1947; McKenna and Kalio 1965), the actual consumption of methane by bacteria under anoxic conditions is not well understood. Davis and Yarbrough (1966) have suggested that methane could be an additional carbon source for sulfate-reducing bacteria, and Fuhs (1961) has shown several reactions for anaerobic methane consumption that are energy-yielding. Generally, the longer the carbon chain, the more energy the bacteria can obtain.

Although bacteria prefer to use the energy source with the highest potential, it appears that methane consumption can occur during sulfate reduction. In studies of the anaerobic oxidation of ^{14}C-labeled methane by the sulfate-reducing bacteria, _Desulfovibrio_ _desulfuricans_, Davis and Yarbrough (1966) noted that these bacteria can consume methane, although at a slow rate. The following reaction was proposed by Fuhs (1961)

$$CH_4 + SO_4^= \longrightarrow HS^- + HCO_3^- + 2H_2O \qquad (24)$$
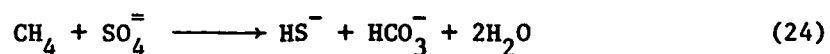
with the reaction having a free energy of -4.5 kcal$\cdot$mole^{-1}. The consequences of anaerobic methane consumption would be decreased methane levels in the immediate vicinity of consumption, and an increase in the $\delta^{13}C$ of the methane. Isotopically lighter methane would be preferentially consumed.

Methane and Hydrogen Sulfide in the Brine

The concentration of methane in the Orca Basin is extremely
high when compared to other anoxic areas (Table 17). The methane
levels are over 100 times higher than the concentrations found in
any other anoxic sea water, except for the oil-related East Flower
Garden brine in the Gulf of Mexico (Brooks et al. 1979). The only
natural water with higher methane content is Lake Kivu, an east
African rift lake where Deuser et al. (1973) reported finding a
methane concentration of 22 mmol·liter^{-1}. The high methane levels
in the Orca Basin probably result from the inability of methane
produced there to easily escape from the brine.

The methane distribution across the brine-sea water interface
is extremely sharp, with almost a six order of magnitude increase
in methane concentration as the depth increases only 50 m. Such
a sharp gradient is indicative of very slow mixing processes. Thus
methane can probably be removed from the basin only by molecular
diffusion, a very slow process. The gas that bubbles out of the
brine at the surface has a large component of methane. Methane is
supersaturated by several hundred percent (at one atm). This
supersaturation is the result of methane production with little
removal. The methane is produced in the sediments and perhaps at
the brine-sea water interface.

It is the density structure of the Orca Basin (Fig. 9) which
effectively inhibits removal of methane from the basin. Due to

Table 17. Molecular and isotopic composition of methane and other gaseous hydrocarbons in anoxic waters.

Location	Depth (meters)	Methane (μmol·liter^{-1})	Ethane (nmol·liter^{-1})	Propane (nmol·liter^{-1})	C_1/C_2+C_3 (by mole)	$\delta^{13}C$ (‰)	Reference
Lake Kivu	425	22000	16000[†]		1000[†]	-44	1
Black Sea	1900	5.5	13.7	0.15	400		2
Black Sea	2000	7.6	17.4	0.11	430		3
Cariaco Trench	1250	6.7	1.8	0.24	3200		4
Cariaco Trench	1200	10					5
Cariaco Trench	1400	7.1					6
Lake Nitinat	200	71	1.1	2.0	23000		5
Red Sea-Atlantis *	2050	2.6	23	1.5	104		5
East Flower Garden *	72	122	18500	0.65	6.6	-40	7
Orca Basin *	2300	750	1300	<1	730	-73	8

* Brine areas.   [†] Estimated from other data in reference 1.

1 Deuser, Degens and Harvey (1973)
2 Hunt (1969)
3 Swinnerton and Linnenbom (1969)
4 Linnenbom and Swinnerton (1969)
5 Atkinson and Richards (1967)
6 Wiesenburg (1975)
7 Brooks, Bright, Bernard and Schwab (1979)
8 This study.

its stability (Table 5), the residence time of brine in the Orca

Basin must be longer than in other anoxic basins. Sackett et al.

(1979) found a $\delta^{14}C$ value for the total CO_2 in the brine of

-501 °/$_{oo}$. This figure would imply an age of one half-life of ^{14}C,

or about 5700 years. This residence time is much longer than for

other anoxic basins. There is much uncertainty in the ^{14}C age,

however, due to a lack of knowledge of the ^{14}C content of carbon

compounds that entered the basin with the brine. Addy and Behrens

(1980) used sedimentological data and ^{14}C measurements of the car-

bonate in the sediments to calculate an age for the initial input

of brine into the Orca Basin. They determined that the brine began

flowing in to the basin 7900 years ago, a date even older than the

age from the ^{14}C measurements of Sackett et al. (1979). The age of

Orca Basin water is greater than 800-year deep water residence

time for the Cariaco Trench (Fanning and Pilson 1972) or the 2000-

year residence time for bottom water in the Black Sea (Ostland 1974).

Unlike methane, the concentration of hydrogen sulfide in the

Orca Basin brine (Fig. 36) is much lower than in other anoxic

basins such as the Cariaco Trench or the Black Sea (Fanning and

Pilson 1973; Brewer and Spencer 1974). Except at the brine sea

water interface, sulfide is below the detection limits of the

molybdenum blue technique used in this study (Cline 1969). In the

Black Sea at 2000 m, both methane and hydrogen sulfide are observed

in high concentrations (Degens and Ross 1974). In the hot

Red Sea brine at 2050 m, methane is present (Burke et al. 1980)

but hydrogen sulfide is absent. There is little evidence that

significant sulfate reduction is taking place in the Red Sea brine

(Craig 1969). It can be argued that the rate of sulfide produc-

tion in the Orca Basin is not sufficient to maintain a high dis-

solved sulfide level, due to the presence of iron with which it

precipitates as metastable iron sulfides. Alternately, it has

been suggested (Trabant and Presley 1978) that sulfate reduction

proceeds normally in the Orca brine, and there is simply a large

influx of iron from the sediments which is controlling the sulfide

levels in the brine. This discussion will show that the rate of

sulfate reduction is slow in the Orca Basin, and that reduced

sulfur species are completely removed from solution by reactive

iron. As such, the available sulfur is rapidly depleted from so-

lution before any conversion of FeS to FeS_2 can occur, by the

reaction

$$H_2S \xrightarrow{\text{Fe}} FeS \xrightarrow{S^o} FeS_2 \qquad (25)$$
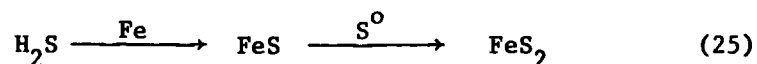
Addy and Behrens (1980) noted that there is no pyrite in the

Orca Basin sediments.

Sulfate reduction is occurring in the Orca Basin. The sul-

fate in the pore waters decreases to zero at a depth of five to

seven meters in the sediment (Sackett et al. 1979). Fig. 37 shows

a plot of the sediment data presented tabularly by Sackett et al.

(1979). The open circles represent the actual sulfate profile that

they observed. Also shown are the chloride gradient and a predic-

ted sulfate profile (SO_4, closed circles) that would be found if

sulfate were diffusing down through the sediment at the same rate

as chloride, with no sulfate reduction. From the differences in

the actual and predicted sulfate profiles, it is obvious that sul-

fate reduction is occurring in the Orca Basin sediments. The

presence of hydrogen sulfide at the interface with the oxygenated

Gulf of Mexico (Fig. 36) water also shows that sulfide is being

produced there. However, the absence of H_2S in the brine itself

may indicate that little sulfide is being produced in the anoxic

waters or if so, it is rapidly removed. The only appreciable sul-

fate reduction is probably occurring at the interfaces, the sites

of highest reactivity.

Although it is difficult to obtain rate data from concentra-

tion profiles alone, enough information is available about sulfate

profiles worldwide to gain some insight into rates in the Orca

Basin. The basis for the following discussion follows the review

of Goldhaber and Kaplan (1974) on worldwide sulfate profiles and

the more recent paper of Berner (1978). Both of these papers dis-

cussed a correlation between the sedimentation rate and the sul-

fate reduction rate, or the initial sulfate gradient in the near

surface sediments.
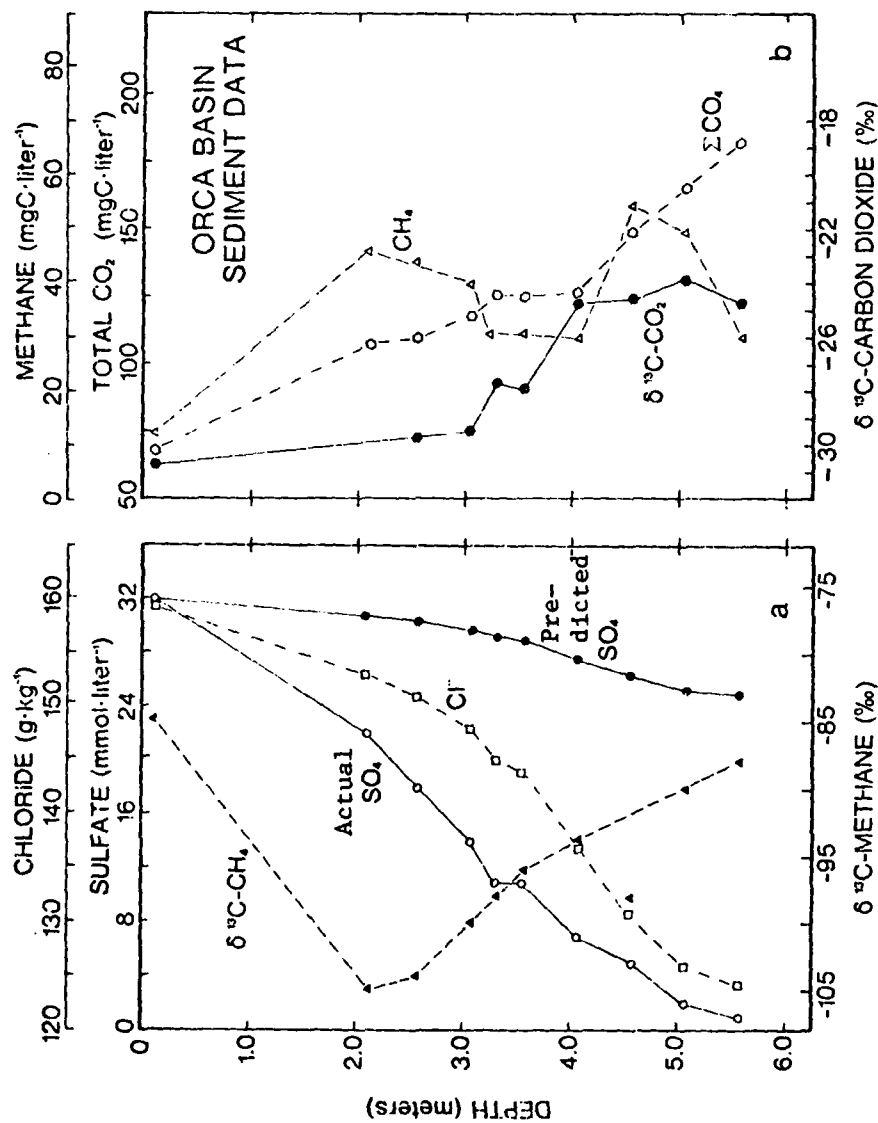
Fig. 37. Sediment geochemistry data from a piston core taken in the Orca Basin (27°01.3'N, 91°16.5'W) at a water depth of 2340 m. Data are plotted from tabulated values given in Sackett et al. (1979). Predicted SO_4 profile is calculated as described in the text.

Berner (1978) has shown that the log of the slope of the sulfate profile in marine sediments is directly correlated with the log of the sedimentation rate. Also the rate constant for sulfate reduction is directly correlated with the rate of sediment deposition. This trend has been shown to apply to diverse environments from nearshore sediments to abyssal Pacific sediments sampled during the Deep-Sea Drilling Project. The actual sulfate sediment profile in Fig. 37 (data from Sackett et al. 1979) has a slope of 0.053 mM $SO_4 \cdot cm^{-1}$. The sedimentation rate in the Orca Basin has been determined by Addy and Behrens (1980) to be 61 $cm \cdot ka^{-1}$. Approximately 21 $cm \cdot ka^{-1}$ of this sedimentation is attributable to the preservation of excess carbonate material, as a result of the anoxic hypersaline conditions which exist in the Orca brine. Tompkins and Shephard (1979) estimated a sedimentation rate of 100 $cm \cdot ka^{-1}$. However, the core that they used for making this estimate was taken in the smaller lobe of the Orca Basin and had evidence of slumping, which would cause their rate to be high.

Taking the rate versus rate hypothesis one step further, Berner (1978) showed that there is a positive correlation, and a very predictable one, between the sedimentation rate and the rate of sulfate reduction. This point was also well illustrated by Goldhaber and Kaplan (1974). Goldhaber and Kaplan (1974) concluded that, besides temperature and pressure (which effect all reactions), the rate of sulfate reduction is dependent upon:

(1)   total organic carbon preserved in the sediment

(2)   the state of complexing of the organic matter

(3)   availability of organic matter for biogenic degradation

(4)   the environment of deposition

(5)   the sedimentation rate.

They noted that factors 1, 2 and 3 are directly influenced by factors 4 and 5, and that there was a direct relationship between the rate sulfate reduction and the rate of sediment accumulation. Considering factor 1, Sackett et al. (1979) noted that the percentages of organic carbon in Orca sediments are higher than for normal shelf and slope sediments. According to Goldhaber and Kaplan (1974) this would result in higher sulfate reduction rates.

From a comparison of the sulfate reduction rates in the Orca Basin with those in the small basin next to Orca, it can be shown that the rate of sulfate reduction is slower in the Orca Basin, relative to the smaller basin and to other areas of similar sedimentation rate. The sulfate profile in the small basin next to the Orca Basin has been measured by Bernard (1978). A comparison of the initial sulfate gradient, $(\partial SO_4 / \partial z)_o$, of the small basin (0.11 mM $SO_4 \cdot cm^{-1}$) with the Orca Basin (0.053 mM $SO_4 \cdot cm^{-1}$) indicates that the gradient is steeper and thus the rate of sulfate reduction in the other basin is greater than the Orca Basin. Yet the sedimentation rate in the Orca Basin is at least 20 $cm \cdot ka^{-1}$ higher. The sulfate reduction rate should be higher, not

lower in the Orca Basin. If the hypothesis of Berner (1978) were applicable to this area, the sedimentation rate in the small basin next to Orca should have a sedimentation rate twice as fast as the Orca Basin. The two basins are separated by only 25 km. Thus it is reasonable to assume that the same material being deposited due to sedimentation is available to each basin.

The major factor causing the differences in the initial sulfate profiles and sulfate reduction rates of the two basins must be the high salinity brine in the Orca Basin. The hypersaline water in the Orca Basin does not completely inhibit sulfate reduction per se, but the rate of sulfate reduction seems to be decreased as a result of the high salt content, creating a smaller sulfate gradient.

The idea that the rate of microbial activity is slower in the Orca Basin than in other anoxic environments is consistent with the effects of salt stress on microbes (Kushner 1978). A reduced microbial activity rate might also explain some seemingly anomalous carbon isotope data that has been reported for the basin sediments (Sackett et al. 1979). It should be remembered that the production of methane from organic material is a two-step process. One suite of bacteria breaks down organic matter into small organic molecules and carbon dioxide. Methanogenic bacteria then reduce these compounds to methane. The sediment methane data taken from Sackett et al. (1979) are shown in Fig. 37. They

explained the data by suggesting that the source material for the carbon in the Orca Basin must be isotopically lighter than could be accounted for by the isotopic ratios of the products (CO_2 and CH_4) they observed. They further suggested that the ultimate source for the isotopically light organic carbon in the basin might be methane migrating upward from a deeper reservoir. This methane would be oxidized to CO_2 and subsequently reduced back to methane, yielding the isotopic balances observed. Several mass balance calculations from mixture models suggested that the source carbon for the source organic material in the basin needed to be $-42\%_{oo}$ to account for values observed.

An alternate argument can be made, if one considers that the rate of sulfate reduction and methane production are lower in this unusual environment than in other areas where methane has been measured and classified isotopically (Bernard 1978). Most of the organic material found in the sediments of the Orca Basin had an isotopic composition essentially the same as other sediments in the region ($\delta^{13}C \cong -22\%_{oo}$). Some depths, however, had isotopically light organic carbon, which may represent slumped sediments, originally deposited in estuarine environments during the Pleistocene (Sackett et al. 1979). For this discussion, I assume that the normal slope organic carbon ($\delta^{13}C = -22\%_{oo}$) is the source carbon for methane and carbon dioxide found in the basin water and sediments. The normal isotopic fractionation for methane produced during this process varies as a function of several factors,

including isotopic content of the source material (Bernard 1978)

and temperature of reaction (Games et al. 1978). A decrease

in temperature increases fractionation, perhaps by decreasing

the reaction rate, thus allowing increased bacterial selectivity

of the source carbon. The idea of enhanced isotopic fractionation

at reduced reaction rates has been suggested in several studies.

Kaplan and Rittenberg (1964) showed that isotopic fractionation

(^{32}S vs. ^{34}S) during sulfate reduction was directly influenced by

the rate of sulfate reduction. The magnitude of the separation

between sulfur isotopes was inversely proportional to the rate

of sulfate reduction. The same effect should be true for methane

carbon fractionations.

In reality, factors other than reaction rate are responsible

for changes in fractionation. Fractionation in microbial systems

occurs along enzymatic pathways, due to the preferences of trans-

port enzymes for carbon-12 atoms. Under slower reaction rates, or

salt stress, the enzymatic pathways may change or the effect of

various back reactions (with different fractionations) may become

important. These complex systems are difficult to investigate.

Thus the simplistic idea of greater fractionation at reduced rates

has been generalized to describe the overall effects of these

processes.

Also important for this discussion is a consideration of the

organic material used during sulfate reduction. It is now well

established that methane can be consumed during sulfate reduction in natural environments (Barnes and Goldberg 1976; Reeburgh 1976; Martens and Berner 1977; Murry et al. 1978). However, methane is not the preferred substrate for sulfate reducing bacteria (Rosenfeld 1947; McKenna and Kalio 1965). Sulfate reducers derive more energy from consuming organic material with a carbon chain length greater than one. In one study where the sulfate reduction rate was low, no methane was consumed (Sorokin 1957). Methanogenesis in the Orca Basin sediments would produce isotopically light methane which would remain unaltered during slow sulfate reduction.

If the rate of methanogenesis is very slow in the Orca Basin sediments, one would expect a greater fractionation than has been observed in other environments. Laboratory fractionation experiments (e.g., Games et al. 1978) are performed under conditions where reaction rates are relatively high, so results can be obtained rapidly. Games et al. (1978) found fractionation factors of 1.044 to 1.061 for methane produced in laboratory cultures. If they had used the carbon dioxide in the Orca Basin as the source material, these fractionations would produce methane in the range -71 $^o/_{oo}$ to -88 $^o/_{oo}$. If their methane production rates had been slower, the fractionation might be even greater. Greater fractionation would produce methane lighter than -88 $^o/_{oo}$, and could produce the -105 $^o/_{oo}$ that was measured by Sackett et al. (1979).

The idea of the salt in the basin being the factor which reduces the rates of methanogenesis and sulfate reduction is paramount to this discussion. In the Red Sea brines, Watson and Waterbury (1969) attempted to culture sulfate reducing bacteria in brine at various sodium chloride concentrations. They found that there was a reduction in the rate of sulfate reduction with the increasing salinity and no sulfate reducers could grow at salinities greater than 125 $^\circ/_{oo}$. Some sulfate reduction is taking place in the Orca Basin sediments, as evidenced from the sulfate profiles shown in Fig. 37. However, the rate of sulfate reduction may not be constant throughout the entire sediment column. Microbial activity may be more rapid in certain areas. One of these areas would be the sediment-water interface zone, where the most labile organic material reside. It has often been noted that very rapid sulfate reduction rates occur in a very thin zone near the sediment-water interface (Berner 1972; Sweeney 1972; Goldhaber and Kaplan 1974). Rapid sulfate reduction at the sediment-brine interface could account for both the decrease in methane and the increase in ^{13}C of the methane in the near surface sediments (Fig. 37). This is the same type of response that is found in coastal sediments in the Gulf of Mexico (Bernard 1978) with methane concentrations decreasing and becoming isotopically heavier near the sediment water interface. Significantly, in the Orca Basin, the heaviest methane is found at the sediment-brine interface.

Methane consumption during more rapid sulfate reduction at the sediment-brine interface would also account for the fact that methane is isotopically heavier in the water column ($\delta^{13}C$ = -73.5 ‰) than in the sediments ($\delta^{13}C$ = -85 to -105‰). The lighter methane would be consumed at the interface leaving the isotopically heavier methane to diffuse out into the water column. Conversely, away from the sediment-brine interface, where microbial populations would be lower (Zobell 1942), rates of sulfate reduction and methanogenesis may increase with depth. This would happen since there is a decreasing chloride gradient with depth. The data in Fig. 37 are consistent with this explanation. $\delta^{13}C$ of the methane would increase with depth in the sediment as the sulfate reduction rates increase or as heavier organic carbon is encountered for use in methane production.

In the water column, there is too much scatter in the methane and $\delta^{13}CH_4$ data (Fig. 30) to determine the processes affecting the methane distribution there. Methane is obviously consumed at the brine-sea water interface by aerobic oxidation, but there are no other noticeable trends in the deeper data. The high salinity brine in the Orca Basin is fairly well mixed, as was discussed in Chapter II. This mixing is obvious in the methane distribution. In summary, the observed methane profile in the high salinity brine results from production and consumption in the sulfate containing sediment and brine, with only limited loss of

methane from the brine, probably by diffusion across the brine-sea water interface.

Mechanisms of H_2S Removal

Having concluded that sulfate reduction is an active process in the Orca Basin, one must ask where the produced sulfide goes. Free sulfide that is produced is rapidly removed to the sediments as iron sulfide. The iron sulfides that are formed, however, are not pyrite (FeS_2) but metastable iron sulfides such as greigite (Fe_3S_4) and machinawite (FeS) among others (Addy and Behrens 1980). Berner et al. (1979) have noted that the formation of pyrite is directly influenced by the presence of available sulfur. The conversion from metastable iron sulfides to pyrite occurs by the addition of sulfur to FeS (Rickard 1975), and not by the removal of iron. A generalized reaction is (Berner et al. 1979):

$$Fe_3S_4 + 2H_2S \rightleftharpoons 3FeS_2 + 4H^+ + 4e^- \qquad (26)$$
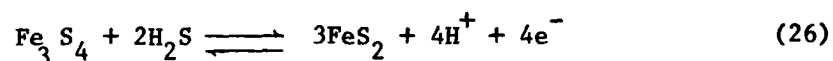
Metastable iron sulfides such as greigite and mackinawite are thermodynamically unstable relative to pyrite, in the presence of H_2S (Berner 1972). Thus the absence of pyrite in the Orca Basin sediments is indicative of the influence of iron in rapidly removing the free sulfide from solution.

The 30-33 $\mu mol \cdot liter^{-1}$ concentrations of iron that were found in the brine (Fig. 36) are two orders of magnitude higher

than the iron values reported for the Black Sea (Brewer and Spencer 1974). In the Black Sea, the hydrogen sulfide concentration is 300–500 $\mu mol \cdot liter^{-1}$ and iron sulfides are known to precipitate, as evidenced by their concentrations in the sediment (Berner 1974). The high iron concentration in the Orca Basin has caused almost complete sulfide removal from the Orca Basin waters. With a slow input of microbial sulfide to the brine, the iron that is entering the brine from sediment reaction or from decomposing plankton precipitates all available sulfide. In the Orca Basin, sulfide is the limiting species in FeS precipitation.

Other Light Hydrocarbons in the
Brine

The production of methane by fermentation shows (Thayer 1931; Stadtman and Barker 1951) that fatty acids are not decarboxylated during methanogenesis and regardless of the length of the carbon chain no hydrocarbons higher than methane should be produced. In spite of this conclusion, C_2 and C_3 hydrocarbons are found in many anoxic environments (Table 17) and are probably produced by bacteria (Bernard 1978). In the Orca Basin, ethane concentrations as high as 1300 $nmol \cdot liter^{-1}$ were observed, over 50,000 times the concentration found in the deep Gulf water. Propane was also observed just above the interface at a level of 0.4 $nmol \cdot liter^{-1}$,

almost 20 times the deep Gulf concentration. This type of increase

in non-methane gaseous hydrocarbons has also been observed in the

Cariaco Trench (Linnenbom and Swinnerton 1969), the Black Sea

(Hunt 1974), the Red Sea brine and Lake Nitinat (Swinnerton and

Linnenbom 1969) and other anoxic waters (Table 17). Bernard (1978)

has shown that these hydrocarbons are also found in anoxic sediments.

He attributed these gases to bacterial production. Biological

production of C_2 and C_3 hydrocarbons has yet to be satisfactorily

explained. The generally accepted mechanisms of anaerobic decompo-

sition (Berner 1971) would preclude microbial production of ethane

and propane. Gaseous hydrocarbons higher in molecular weight than

methane are normally the result of petroleum production. However,

the depth distribution of ethane in the Orca Basin (Fig. 30)

indicates an origin similar to methane: biogenic.

Methane at the Interface

The maximum in methane, ethane, and propane above the brine-

sea water interface was not entirely unexpected. The microbial

biomass distribution (LaRock et al. 1979) exhibits a pattern above

the interface similar to the observed methane distribution. The

two may be associated. The increased density of the brine, rela-

tive to the Gulf water, would cause particles falling to the sea

floor to be temporarily interrupted in their journey. They would

rest at the interface until they reach isotonic balance with the

higher salinity brine. Only after particle densities reach the level of the next brine layer would they settle below the interface. An increased microbial biomass would be expected to correlate with a great number of particles. Degradation of particles at density interfaces has been proposed to account for the near surface methane maxima that have been observed in many areas of the world oceans (Brooks et al. 1980). The main difference here is the depth of maxima above the Orca Basin. This methane maximum is deeper than any previously reported.

The methane depth distribution above the brine interface is also consistent with the concept of methane consumption in oxygenated waters. Rudd et al. (1974) have shown that, in oxygenated waters, methane consumption rates are the highest where the oxygen values are minimal. They made this observation from determinations of methane consumption rates in oxygen minimum layers of several Canadian Shield lakes. As can be seen in Fig. 32, the methane maximum above the interface is in water that has a decreasing oxygen gradient, but where oxygen is still present. This would rule out possible methane consumption during sulfate reduction, since sulfate is not reduced while oxygen is available. Oxygen, from molecular oxygen, must be the oxidizing agent in any microbial methane consumption above the interface.

It must be assumed that interface methane, and presumably ethane and propane, being produced are produced in anaerobic

microenvironments. These microenvironments in the aerobic water
column need not be entirely sulfate depleted as Oremland (1975) has
reported small amounts of methane production (1.81 to 1.86 $\mu mol \cdot m^{-2} \cdot hr^{-1}$) in sulfate-rich marine sediments in the Florida Keys. Methane
may be produced throughout the entire interface region in these
microenvironments, with a constant production rate. This idea,
plus surface venting, has been proposed to account for the methane
maxima in some surface waters (Scranton and Brewer 1977). If this
were the case, the decrease in methane below the maximum would
result from an increased rate of methane consumption in the zone
where the oxygen concentration is the lowest. The increased
consumption at low oxygen concentrations observed by Rudd et al.
(1974) may not have real implications for consumption vs. oxygen
level. Not coincidentally, the largest population of methane
consuming bacteria would also be found in the low oxygen region,
since it is closest to the methane source.

N_2O Consumption During Denitrification

In the sequence of organic decomposition which proceeds from
oxygen consumption to carbon dioxide reduction, oxidized nitrogen,
especially NO_3^- and NO_2^-, is consumed by various denitrifying
bacteria and converted to gaseous nitrogen compounds, mainly
nitrogen gas and ammonia. The geochemistry of molecular nitrogen
gas was discussed in Chapter III. The presence of the 500 $\mu mol \cdot$

liter^{-1} of ammonia can be accounted for based on organic decomposi-

tion, using the Orca brine excess carbon to nitrogen ratio as a

starting point. In measurements of nutrient regeneration in the

anoxic sediments, Martens and Berner (1977) show a large NH_3 pro-

duction, but note very emphatically that there was no production

of molecular nitrogen in the sediments. The same is true for the

high salinity, anoxic brine in the Orca Basin. Yet, Weiss (1969)

has suggested that there is nitrogen production in the Red Sea

brines, presumably from decomposition of organic nitrogen. This

process causes both the high N_2 concentrations and the high N_2/Ar

ratios that he observed there.

Denitrification is nearly complete in the Orca Basin waters.

All NO_3^- and NO_2^- have been reduced and the main repository for

reduced organic nitrogen is ammonia. Nitrous oxide (Fig. 34)

decreases from over 15 nmol·liter^{-1} above the brine to only a

trace amount in the brine. Thus, almost all the N_2O has been con-

sumed during denitrification in the Orca Basin waters. Cohen and

Gordon (1978) have demonstrated that N_2O can be consumed not only

in completely anoxic waters such as Saanich Inlet, but they noted

biochemical N_2O was consumed by marine denitrifying bacteria.

Barbaree and Payne (1967) and Payne et al. (1970) found that cul-

tures of _Pseadomonas_ _perfectomarinus_ can use N_2O as a terminal

oxidant and reduce it to N_2. Matsubara and Mori (1968) also

show that anaerobic cultures of _P._ _denitrificans_ can reduce N_2O to

N_2 with lactate as the terminal hydrogen donor. Although N_2O has been depleted in the Orca brine and increased N_2 concentrations have been measured there (Fig. 26), it seems unlikely that N_2 production from N_2O is significant there. For the organic nitrogen (which is eventually converted to ammonia) to participate in the nitrogen production, it must first be oxidized to NO_3^-. In anaerobic waters, however, there is little reason to believe that this type of reaction would occur, and if so that the NO_3^- would then be converted to N_2. The possibilities of a two step production of N_2 from ammonia in the oxygen step region have been discussed earlier.

In summary, the decomposition processes that produce the reduced gases in the Orca Basin are no different than in other anoxic environments. The rates are just slower. A combination of the slower reaction rates and the high stability of the brine in the Orca Basin makes this environment an ideal laboratory for studying the mechanisms involved in anaerobic decomposition. The isotopic fractionations found there are the greatest reported to date, far greater than could be produced in laboratory experiments over the lifetime of a graduate student. An examination of the degree of sulfur fractionation in this basin would prove valuable for better understanding reduced gas biogeochemistry under hypersaline conditions.

CHAPTER V

CARBON DIOXIDE AND THE CARBONATE SYSTEM IN

THE HYPERSALINE BRINE

The Orca Basin brine is basically a sea water solution that
has been saturated with sodium chloride (Table 3). Besides sodium
chloride, however, the most important compound in higher concen-
tration in the brine than in normal sea water is carbon dioxide.
Some carbon dioxide probably entered the basin with the inflowing
brine, but most excess CO_2 was produced in the basin itself. The
isotopically light carbon dioxide ($\delta^{13}C$ = -16.4%$_{oo}$) in the brine
(Sackett et al. 1979), compared to the source Gulf water ($\delta^{13}C$ =
0.3%$_{oo}$), indicates that the excess carbon dioxide has a biogenic
source. Biogenic reactions which produce carbon dioxide have been
discussed in the previous chapter (see Table 12). The effects of
hypersalinity in the Orca Basin on the interactions controlling
carbon dioxide system in the Orca Basin are considered here. The
previous chapters have been concerned with dissolved gases which
generally do not react with water. Carbon dioxide, on the other
hand, engages in a series of equilibrium reactions when it comes
in contact with water or sea water. These carbonate system re-
actions will determine the disposition of the biogenic CO_2 added
to the brine from the anaerobic decomposition of organic matter.

Ionic interactions are important in defining the carbon dioxide system. The total ionic strength of the Orca Basin brine (4.10) is quite large relative to normal sea water (~0.7). The ionic strength and ionic balance percentages of the ions in the Orca Basin, sea water and several other brines are given in Table 18. Since the ionic strength of brines is so high, one would expect their physical-chemical properties to be strongly influenced by ionic interactions. Any physical-chemical effects would be due both to the total ion concentration, as well as to the nature of the ions which are important in the interactions in question. Different ions participate to varying degrees in ion pairing (Garrels and Thompson 1962). In sea water, there are interactions between Na^+, K^+, Ca^{++}, and Mg^{++} with HCO_3^-, $CO_3^=$, and $SO_4^=$. Johnson and Pytkowicz (1979) have recently calculated that Cl^- can also form ion pairs in sea water to produce an $NaCl^o$ complex. This possibility has interesting potential for the Orca Basin since the ionic balance percentages of Na^+ and Cl^- are significantly higher than sea water (Table 18). Pytkowicz and Atlas (1975) have shown that knowledge of variations in solution composition are sufficient to predict changes in buffer intensity which reflect variations in apparent dissociation constants of the carbonate system. Thus the relative percentages of cations and anions in the Orca Basin, as well as the total ion concentration, play an important role in deciphering carbon dioxide interactions in the brine.

Table 18. Ionic balance percentages and total ionic strength for standard sea water (SSW = 35%oo salinity), Dead Sea brine (DSB = 299%oo), Orca Basin brine (OBB = 258%oo), Red Sea brine (RSB = 256%oo), and East Flower Garden brine (EFG = 218%oo).

Brine	Na^+	K^+	Mg^{++}	Ca^{++}	Cl^-	$SO_4^=$	HCO_3^-	I
SSW	77.7	1.66	17.3	3.3	90.3	9.34	0.36	0.52
DSB	28.2	2.88	55.0	13.9	99.7	0.25	0.06	
OBB	96.2	0.39	2.01	1.32	98.1	1.77	0.12	4.10
RSB	91.9	1.26	1.51	5.36	99.6	0.36	0.05	6.36
EFG	95.1	0.26	2.42	2.22	97.5	2.43	0.06	

Alkalinity Considerations

In describing the geochemistry of carbon dioxide in aquatic systems, three parameters must be considered: pH, total CO_2, and alkalinity. While pH and total CO_2 can be directly measured, alkalinity is a more difficult to estimate. In sea water, the total or titration alkalinity is the result of anions of various weak acids which are not charge balanced with hydrogen ions. The major acids to be considered are carbonic and boric, since their concentrations are normally much larger than the secondary group: phosphoric, silicic, sulfuric, and hydrofluoric acids. Only weak acids with dissociation constants smaller than the first dissociation constant of carbonic acid are included in the titration alkalinity (Edmond 1972). (Throughout this chapter, the dissociation constant will be understood to mean the apparent dissociation, K', which has the activity coefficients included.) For normal sea water, the titration alkalinity is described as:

$$TA = [HCO_3^-] + 2[CO_3^=] + [B(OH)_4^-] + [Si(OH)_3O^-] \qquad (27)$$
$$+ 2[HPO_4^=] + 3[PO_4^=] + [OH^-] - [H^+]$$

In anoxic waters, terms representing the nitrogen and sulfur products of anaerobic decomposition ($[NH_3]$, $[HS^-]$) can also be added to the other weak acids which contribute to the total alkalinity (Knull and Richards 1969; Gaines and Pilson 1972). Since the concentrations of weak acids other than carbonic and

boric are relatively low in sea water, they are generally excluded from the total alkalinity. Boric acid contributes only a few percent to the titration alkalinity of normal sea water. However, it needs to be considered for precise alkalinity determinations of normal oceanic samples.

In the Orca Basin, carbonic acid is by far the major contributor to the titration alkalinity. The dissociation constants for acids other than carbonic acid are poorly known even for normal sea water, and are non-existant for hypersaline solutions. Thus, for my discussions of carbonate systems in the Orca Basin, I have ignored all alkalinity components other than carbonic acid and its dissociation products. This omission causes no concern for borate, silicate, or phosphate. It may, however, be an inappropriate assumption with regard to NH_3. The ammonia level in the Orca Basin is about 500 $\mu mol \cdot liter^{-1}$, or about 10% of the total carbonate concentration. However, it is not the total species concentration which determines the contribution to alkalinity, but rather the weak acid contribution determined from both the dissociation constants and the total concentration. For ammonia, the contribution to alkalinity would be described as:

$$A_{NH_3} = [NH_3] \ \frac{K'_{NH3}}{a_H + K'_{NH_3}} \tag{28}$$

where A_{NH_3} is the ammonia alkalinity, $[NH_3]$ is the total ammonia concentration and K'_{NH_3} is the apparent dissociation constant for

ammonia. One can assume pK'_{NH_3} = 9.2 (Sillen and Martell 1964), which is the dissociation constant for infinite dilution, since no equilibrium values are available even for sea water. Using the pH of the Orca Basin (6.83), it can be calculated that the 500 $\mu mol\cdot$ liter^{-1} of ammonia in the Orca Basin contributes only 2.13 $\mu eq\cdot$ liter^{-1} to the alkalinity. Millero et al. (1979) calculated A_T to be 4750 $\mu eq\cdot liter^{-1}$, thus making the ammonia contribution insignificant - if K'_{NH_3} is correctly assumed. For the anoxic water of the Pettaquamscutt River, Gaines and Pilson (1972) assumed that the total dissolved ammonia was equal to its alkalinity contribution. This assumption would require pK'_{NH_3} to be around 6.9 and may be inappropriate. Yet, the dissociation constant for ammonia is unknown. There is even some confusion as to whether the ammonia contribution should be considered a weak acid (Gieskes 1974) or a weak base (Knull and Richards 1969). Considering the uncertainty as to how to treat the ammonia contribution to the alkalinity, I have chosen to disregard it.

Carbonate System Interactions

Carbon dioxide which enters oceanic waters from the atmosphere, or from decomposition processes, participates in equilibria which may be summarized by a generalized equation:

$$CO_2 + H_2O \rightleftharpoons H_2CO_3 \underset{}{\overset{K'_1}{\rightleftharpoons}} HCO_3^- + H^+ \underset{}{\overset{K'_2}{\rightleftharpoons}} CO_3^= + 2H^+ \quad (29)$$
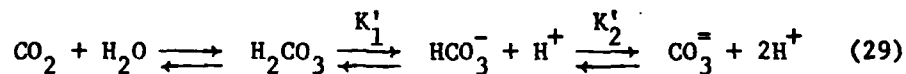
Associated with each step in this series is an equilibrium constant which can be expressed in terms of thermodynamic activities of the participating species. The basic equations necessary for quantifying the interactions of carbon dioxide with its parent solution are (Skirrow 1965):

$$K'_1 = \frac{a_{H^+} [HCO_3^-]}{[H_2CO_3]} \qquad \text{First apparent dissociation constant} \qquad (30)$$

$$K'_2 = \frac{a_{H^+} [CO_3^{2-}]}{[HCO_3^-]} \qquad \text{Second apparent dissociation constant} \qquad (31)$$

$$A_c = [HCO_3^-] + 2[CO_3^{2-}] \qquad \text{Carbonate alkalinity} \qquad (32)$$

$$C = [H_2CO_3] + [HCO_3^-] + [CO_3^{2-}] \qquad \text{Total dissolved carbon (refers to inorganic carbon)} \qquad (33)$$

$$A_B = TB \frac{K'_B}{a_{H^+} + K'_B} \qquad \text{Borate alkalinity} \qquad (34)$$

where primes indicate that the constants are apparent dissociation constants, brackets designate molar concentrations and a_{H^+} is the activity of the hydrogen ion (see Table 19 for complete notations).

A detailed knowledge of the carbonic acid equilibrium system is of considerable practical importance. In principle, it allows the concentrations of various species (e.g. HCO_3^-, $CO_3^=$, H_2CO_3, and total CO_2) to be calculated by measuring any two of the parameters

Table 19. Notation for carbonate calculation.

a_H	activity of hydrogen ions, defined by pH $= -$ log a_H
K_1'	first apparent dissociation constant of carbonic acid and $pK_1' = -$ log K_1'
K_2'	second apparent dissociation constant of carbonic acid and $pK_2' = -$ log K_2'
K_B'	first apparent dissociation constant of boric acid and $pK_B' = -$ log K_B'
C	total dissolved inorganic carbon
A_o	titration alkalinity, initial
A_c	carbonate alkalinity
T_B	Total dissolved boron concentration
A_B	borate alkalinity
γ_{H+}	activity coefficient of the hydrogen ion where $[H+] = \dfrac{a_H}{\gamma}$
N_a	normality of HCl used in titrations
A_t^n	titration alkalinity at the nth step of an HCl titration

pH, pCO_2, total CO_2 or alkalinity (Park 1969). In a brine system, however, the situation is more complicated, since such calculations require the knowledge of the apparent dissociation constants for each reaction. While these dissociation constants have been well established for normal sea water at various temperatures and salinities (Mehrbach et al. 1973), brine values vary depending on both the ionic composition and total ionic strength.

Few brine carbonate systems parameters have been studied in detail. Amit and Bentor (1971) performed a series of fresh water dilutions on the dead Sea brine. They noted that the pH of the brine increased with dilution - a phenomena not found in solutions devoid of HCO_3^- salts. The pH-increase with decreasing salinity was attributed to depression of bicarbonate dissociation in strong brines. Upon dilution, the bicarbonate dissociates, hydroxide ions are formed and the pH increases

$$HCO_3^- + H_2O \longrightarrow H_2CO_3 + OH^- \tag{35}$$
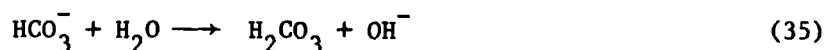
Their dilution curves (given in Fig. 38) provide a good comparison for the Orca Basin. The Dead Sea brine and the Orca Basin brine differ in several ways. The Dead Sea brine is a chloride brine characterized by relatively high concentrations of calcium and magnesium, low sodium and very low sulfate and inorganic carbon concentrations (Table 3). The Orca Basin brine is a sodium chloride saturated sea water with slightly higher sulfate and
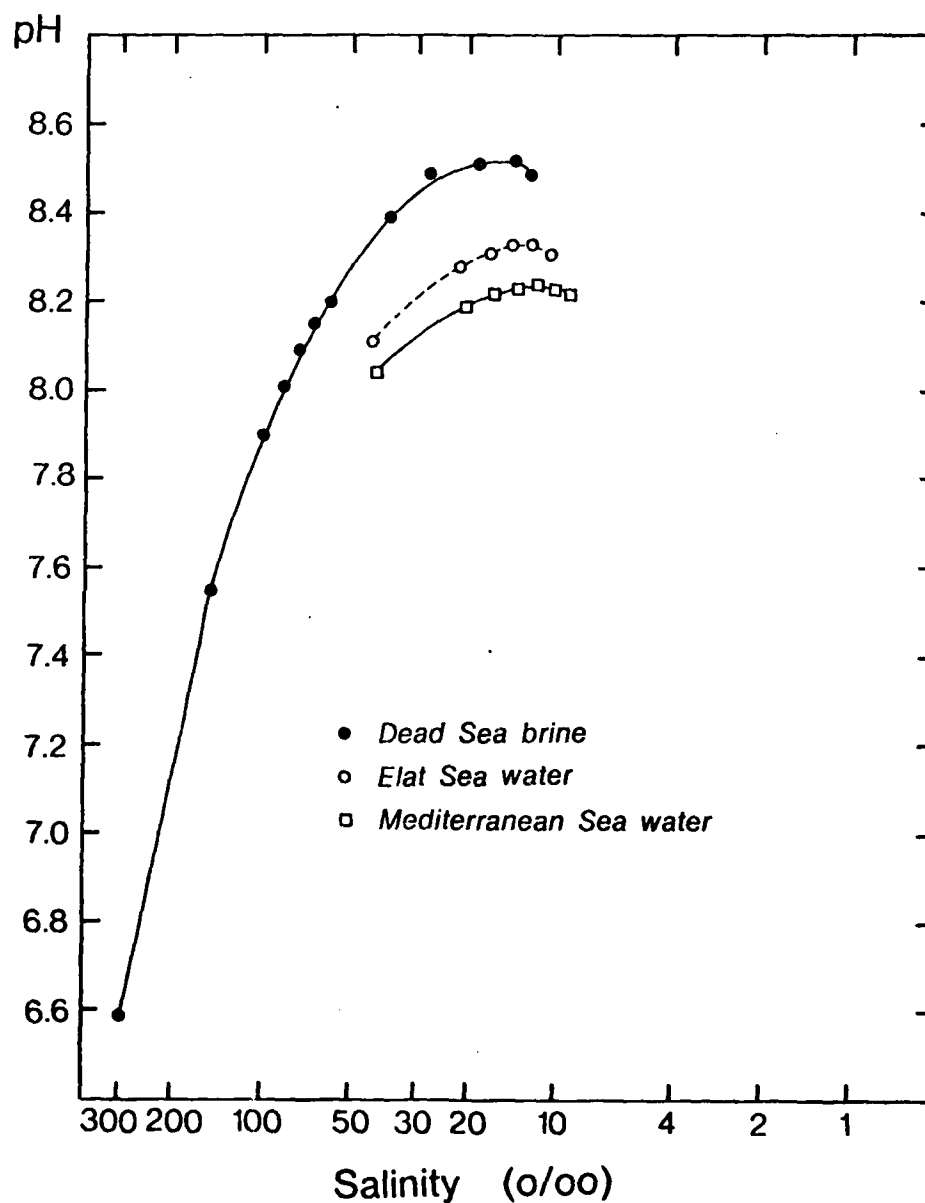
Fig. 38.   pH versus log salinity dilution curves for the
Dead Sea brine and two other waters (after Amit and Bentor
1971).

calcium, a deficiency in magnesium and about twice the total inorganic carbon as sea water. Thus two differences which will cause varying carbonate interactions between these two brines are the differences in ion interactions and in the total CO_2 levels.

Sass and Ben-Yaakov (1977) have done a thorough study of the carbonate system in the Dead Sea brines. They developed a generalized method to determine the alkalinity, total carbonate and dissociation constants of any system. Applying this method to the Dead Sea brines, they observed that as the salt content increases, the dissociation constants also increase, resulting in a consequential pH decrease. Their work confirmed the earlier conclusions of Amit and Bentor (1971) in this regard. More importantly, their results showed that the chemistry of carbonate system in hypersaline waters differ only in degree of interactions and not in nature from the carbonate chemistry in less saline waters. Thus, the carbonate system equations that have been developed to describe sea water carbonate equilibria can also be applied to hypersaline waters such as the Orca Basin brine.

The Orca Basin carbon dioxide system was investigated using both the pH-dilution process of Amit and Bentor (1971) and the titration techniques used by Sass and Ben-Yaakov (1977). Field measurements were made of total carbon dioxide and pH. Laboratory titrations of brine with HCl and $NaHCO_3$ are also used to unravel the carbonate system interactions. Treatment of the data reflects

a desire of the author to make comparisons between the Orca Basin

brine, the Dead Sea brine, and deep Gulf sea water. For this

reason, the calculation methodology involved is parallel to that of

Sass and Ben-Yaakov (1977).

Methods

Sampling

Sampling requirements for total CO_2 are less stringent than

for other Orca Basin gases. This is true since the CO_2 in the

brine is mainly tied up as bicarbonate and carbonate. Less than

one percent of the effervescing gas from the brine was CO_2. Brine

samples were taken on several cruises for pH, total CO_2, and alka-

linity analysis. Both Niskin and Nansen bottles were used with

no obvious systematic variations between bottle types. pH samples

were transferred by gravity flow to 125 ml hard plastic bottles

which were allowed to overflow and then sealed with rubber stoppers.

pH values were measured (by Tonalee Carlson) as soon as the brine

had come to thermal equilibrium at 25°C.

Brine was sampled for total CO_2 analysis using 12 ml

plastic syringes attached to the Nansen or Niskin bottles with

tygon tubing. A three-port Luer-tip stopcock was used to flush

the syringe so an air free sample could be obtained. Some samples

were also taken on cruise EN-32 using the all glass sample con-

tainers shown in Fig. 21. All samples were kept refrigerated

and in the dark until analysis aboard ship – usually within 12 hours.

Alkalinity analyses were performed in the laboratory, rather than aboard ship. Samples for alkalinity titration were collected in 300 ml glass bottles with plastic-on-metal crimp shut tops. Each bottle was filled and about 100 ml of brine was allowed to overflow. 20 ml of brine was decanted and one ml of a saturated NaN_3 solution was added to each bottle to inhibit bacterial removal of CO_2. Samples for alkalinity titration were stored at 4°C and in the dark until analysis in the laboratory at Texas A&M University.

Analytical Techniques

pH. The pH of the Orca brine was measured at 25°C using Beckman glass electrodes in conjunction with a Radiometer Model PHM64 pH-millivolt meter. Millivolt measurements were made and converted to pH by making the same measurements on three different National Bureau of Standards (NBS) buffers of known pH, and calculating the brine pH using linear regression. Pykowicz et al. (1974) have shown that operationally defined hydrogen ion activity measurements (pX, where $X = ka_H$ and k represents the effects of liquid junction and asymmetry potentials) compare well with pH, since k is almost unity.

The problem of electrode junction potential should be briefly mentioned since previous studies (Ben-Yaakov and Sass 1977) had

questioned the validity of pH measurements in hypersaline waters

of the Dead Sea brine (Amit and Bentor 1971). Like this study,

Amit and Bentor (1971) used conventional pH electrodes with in-

herent liquid junction potentials. Ben-Yaakov and Sass (1977) con-

structed a pH electrode without a liquid junction and made inde-

pendent measurements of the pH of synthetic Dead Sea brine. Their

measurements were strikingly similar to the values reported by

Amit and Bentor (1971). Their verification confirmed that the po-

tential problem resulting from the liquid junction in conventional

pH electrodes is not a significant factor in making pH measurements

in hypersaline solutions.

Total carbon dioxide. A gas chromatographic system which

uses the on-line gas stripping techniques of Swinnerton et al.

(1962) was used for total CO_2 analysis. A schematic of the system

is shown in Fig. 39. One ml of concentrated phosphoric acid

was injected via a septum (S) into the glass stripping chamber

(GS). After all air had been stripped from the acid, a 6 to 12 ml

brine sample was injected into the stripper where the bicarbonate

and carbonate are converted to gaseous CO_2. The CO_2 is swept from

the stripper by a helium carrier gas flowing at 20 ml·min^{-1}. The

gas is dried using either a 20 mesh drierite or 40/60 mesh silica

gel drying column (DC) and passed to a 40/60 mesh silica gel sep-

aration column (SiGel, 1.0 m x 0.64 cm O.D. stainless steel) at

50°C for separation of air and CO_2. The gas chromatograph used
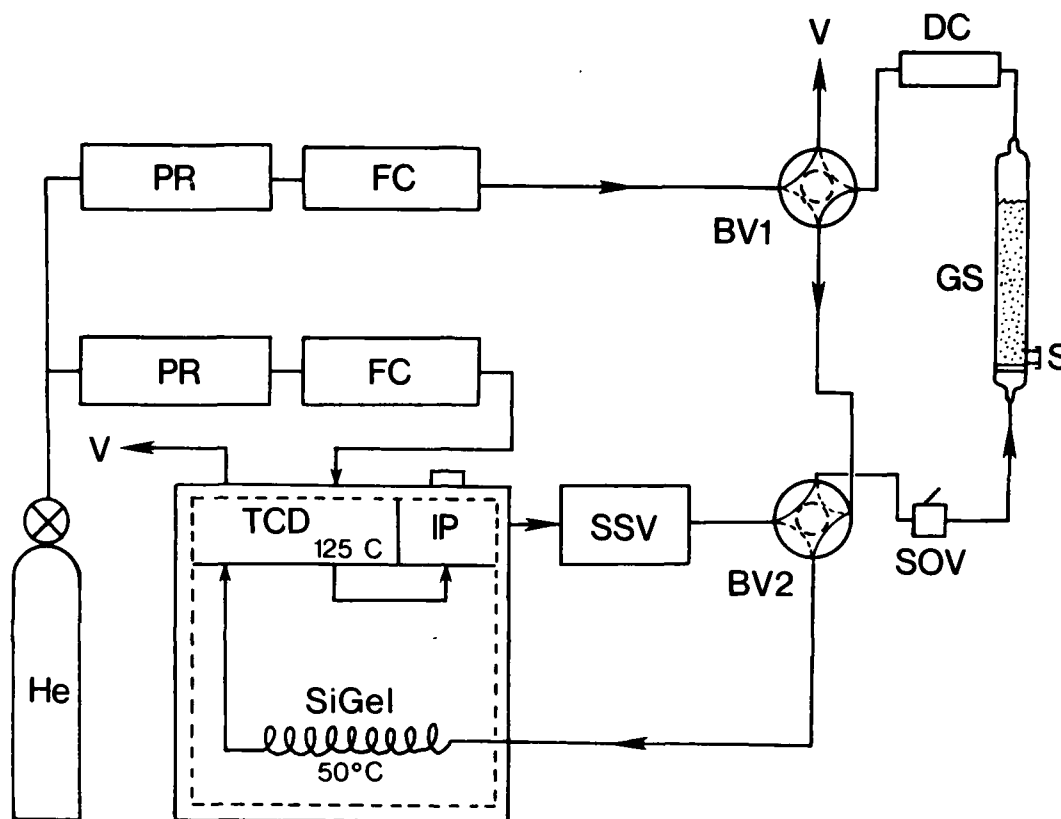
Fig. 39.   Schematic presentation of the gas chromatographic
system used to measure total carbon dioxide in the Orca Basin
brine.   Acid is injected into the gas stripping chamber (GS)
via a rubber septum (S) and followed by injection of the brine
sample.   The helium (He) carrier gas flow forces the carbon
dioxide from the chamber through a drying column (DC) and into
the gas chromatograph.   The carbon dioxide is separated from
air in the sample by a silica gel column (SiGel) thermostated
at 50°C.   The carbon dioxide is measured with a thermal con-
ductivity detector (TCD) operating at 125°C.   Standard gas
(pure carbon dioxide) is introduced into the system via a 6-
port standard sample valve (SSV) and analyzed in the same
manner as the water samples.

was a Hewlett-Packard 5830 instrument equipped with a thermal conductivity detector operated at 125°C. Baseline stability and peak shape were monitored using the printer-plotter associated with the unit, and peak area integration was performed by the microprocessor which controls the gas chromatograph. Matheson bone-dry (99.7%) carbon dioxide gas was used as a standard. Standard loop volumes of the pure CO_2 were injected through the stripper for calibration of the system. Calculations of total CO_2 were made using Eq. 14 and the appropriate data for carbon dioxide.

The sample was injected into the gas stripper in either of two ways. Syringe samples were injected directly into the stripper through a septum using a 20-gauge needle. Brine collected in the glass sample containers (Fig. 21) were flushed into the stripper by diverting the helium stream through the samples using their two 3-port stopcocks (see Fig. 21). Before the stopcocks were turned to divert the helium flow through the sampler, the carrier gas flow was purged through the system for five minutes to remove all contaminating air and carbon dioxide. No significant differences were found between either type of sample (syringe or glass container), thus confirming that little CO_2 is lost during the sample collection or by diffusion through the plastic syringe.

Dilution techniques. The dilution agent in all experiments described in this work was distilled water. The water used was stirred in contact with the atmosphere for 24 hours which was long

enough to reach $CO_3^=$ - HCO_3^- - CO_2 equilibrium with CO_2 in air. All dilutions were weight dilutions and experiments were carried out at room temperature (~23°C) with the brine and distilled water at the same temperature. Two sets of brine samples were diluted. One set contained preserved brine which was opened to the air immediately prior to dilution. These samples had a total CO_2 concentration of 4.41 mmol·liter^{-1}. A second set of samples were opened and equilibrated with the atmosphere with stirring for 24 hours. The total CO_2 of these samples had been reduced to a constant 3.44 mmol· liter^{-1} after 24 hours of equilibration. Total CO_2 analyses were run on several of the dilutions from both sets to examine whether the total CO_2 dilution curve followed the predicted dilution relationship. pH measurements were made on diluted brine samples over the range 262°/$_{oo}$ to 7°/$_{oo}$. For comparison, Gulf of Mexico surface and deep water samples were diluted from 35°/$_{oo}$ down to 4°/$_{oo}$ salinity with concurrent pH measurements at each dilution. pH measurements on the diluted samples were made after the brine and dilution water had been mixed together for three minutes. The instrumentation and techniques used for pH determinations were the same as those described in the earlier section on pH measurements.

Titration with HCl. The sample titration with HCl is performed using techniques similar to Edmond (1970). A 187 ml volume of brine was titrated using 1.0 N HCl in a closed titration flask

with constant stirring. Titrations were carried out in a thermostated water bath at 25°C. Acid was delivered through an immersed capillary tip of a microburette (Guilmont Model S4200A), accurate to 0.001 ml. The pH of the titrated solution was monitored using the techniques described previously (p. 197). All inlets into the sample chamber were air tight and the sample filled all cavities – thus preventing CO_2 loss during the titration. In their study of the Dead Sea brines, Sass and Ben-Yaakov (1977) performed their HCl titration on 50 ml samples open to the atmosphere. They experienced some loss of gaseous CO_2 during their titration and could not accurately calculate the total CO_2 concentrations from their results. Such a problem was avoided here by performing the HCl titrations in a closed vessel.

NaHCO$_3$ titration. Orca Basin brine samples and 50% (w/w) dilutions of brine with distilled water were titrated with 0.5N $NaHCO_3$. Titrations were carried out at room temperature on a 50 ml sample continuously stirred in a 100 ml Pyrex beaker open to the atmosphere. Titrant was added to the beaker using the same burette used for the HCl titration. pH was measured as described above. A total of 5 ml of $NaHCO_3$ was added to the brine in increments of 0.25 ml. pH was measured one minute after the addition of each aliquot, a time sufficient to allow equilibrium to be reached.

Model Calculations

HCl Titration: General Equation

In any chemical system, the total (or titration) alkalinity is equal to the sum of the titratable bases available, minus the available hydronium ion. In oceanic waters, the major components of total alkalinity are the carbonate alkalinity (A_c), borate alkalinity (A_B) and hydioxide ion (OH^-). The most general form of the total alkalinity equation is given as:

$$A_T = A_c + A_B + [OH^-] - [H^+] \tag{36}$$

The $[OH^-]$ concentration of sea water is low (relative to A_c and A_B) and is generally ignored. Thus Eq. 37 reduces to

$$A_T = A_c + A_B - [H^+] \tag{37}$$

During HCl titration of a water sample, the addition of H^+ ions alters the charge balance of the system such that Eq. 32 no longer represents the original carbonate alkalinity. Also, as addition of acid occurs, the original alkalinity (A_o) and total inorganic carbon (C) decreases due to dilution. At any nth step in the titration with HCl, the total alkalinity at that step, A_T^n, can be expressed by an equation which considers both the change in the charge balance as well as the dilution effect (mass balance):

$$A_T^n = \frac{A_o V_o - V_a N_a}{V_o + V_a} \tag{38}$$

where V_o is the initial volume of sample titrated, V_a is the volume of acid added by all the steps up to and including the nth step and N_a is the normality of the HCl. By inspection, when V_a equals zero (before titration begins), $A_t^n = A_o$.

Expanding Eq. 38, we can write a two term equation

$$A_t^n = \frac{A_o V_o}{V_a + V_o} - \frac{V_a N_a}{V_o + V_a} \tag{39}$$

such that the separate effects of dilution and titration on the alkalinity during HCl addition can be observed. The first term on the right hand side of Eq. 39 describes dilution, while the second term represents the lowering of the alkalinity by the titration with HCl. Using Eq. 39 and the carbonate system equations given as Eq. 30-34, one can derive a general equation for an acid titration which can be used to determine the alkalinity and the magnitude of dissociation constants involved. In this process, we are ignoring the contributions to alkalinity from species other than carbonate components. Even in normal oceanic waters, borate and hydroxide play only a minor role in determining the total alkalinity. In the Orca Basin, where total carbonate levels are twice that of sea water, the borate and hydroxide would have even a more diminished effect. With these assumptions, Eq. 36 reduces to

$$A_T = A_c - [H^+] \tag{40}$$

and is considered to be the total alkalinity in the following discussion. Effects on Orca Basin alkalinity by other species (e.g. H_2S, NH_4^+) are also ignored since the dissociation constants for other than carbonate species are not known in hypersaline systems. Secondly, the titrations performed on laboratory samples were devoid of any H_2S (and probably NH_4) since the samples were stored for several months. During initial degassing, most gases - but not total CO_2 - were lost from the brine due to stripping by the effervescing nitrogen and methane (see Chapter III).

One final identity is needed, before Eq. 39 is transformed into a relationship from which alkalinity and the dissociation constants can be calculated. That identity is the relationship between carbonate alkalinity (A_c) and total carbonate (C). By simple algebraic manipulation of Eqs. 30-33, we arrive at the relationship

$$A_c = C \left(\frac{a_H K_1' + 2K_1'K_2'}{a_H^2 + a_H K_1' + K_2'} \right) = C(Q) \tag{41}$$

If we now equate Eq. 39 and 40,

$$A_c - [H^+] = \frac{A_o V_o}{V_a + V_o} - \frac{V_a N_a}{V_o + V_a} \tag{42}$$

and multiplying by ($V_a + V_o$) we have

$$A_o V_o - (V_a + V_o)A_c + (V_a + V_o)[H^+] = V_a N_a \tag{43}$$

Now, remembering that at any point n on a titration curve, the total carbonate is going to be diluted such that

$$C_n = C \, \frac{V_o}{V_a + V_o} \tag{44}$$

Substituting Eq. 44 for C in Eq. 41, and the combined term into Eq. 43 gives

$$A_o V_o - (V_a + V_o) \frac{V_o}{V_a + V_o} \, C \cdot Q \tag{45}$$

$$+ (V_a + V_o)[H^+] = N_a V_a$$

where

$$Q = \frac{a_H K_1' + 2K_1' K_2'}{a_H^2 + a_H K_1' + 2K_1' K_2'} \quad .$$

Substituting $\frac{a_H^+}{\gamma}$ for $[H^+]$ and dividing through by V_o gives a complete generalized titration equation

$$A_o - C \cdot Q + \frac{a_H^+}{\gamma} \left(\frac{V_a + V_o}{V_o} \right) = \frac{N_a V_a}{V_o} \tag{46}$$

which can be used to calculate the alkalinity of a sample. Sass and Ben-Yaakov (1977) arrived independently at the same equation which they used in a different form:

$$\frac{1}{V_o} \left[A_o V_o + \frac{a_H}{\gamma_{H^+}} (V_o + V_a) - N_a V_a \right]$$

$$= C \, \frac{a_H K_1' + 2K_1' K_2'}{a_H 2 + a_H K_1' + K_1' K_2'} \tag{47}$$

They have used a two step process to solve Eq. 47 for A_o, C, K_1', K_2', and γ_{H^+}. The first step involves setting the right hand side equal to zero, and then solving the left hand side for A_o and γ_{H^+} by linear regression. A_o and γ_{H^+} are then used as constants to solve all of Eq. 47 using a series of guesses for K_2' and linear regressions techniques to determine the best fit values of K_1', K_2', and C. Their solution technique was applied to the Orca Basin brine titrations. The mathematics of their solution are outlined for completeness in Table 20.

NaHCO$_3$ Titration

Additional knowledge of the carbonate system can also be gained by addition of one individual component to a solution and examining the resultant perturbations. The parameters that can easily be monitored are carbonate alkalinity, total CO_2 and pH. The interdependence of carbonate alkalinity, total CO_2 and pH is described by a Deffeyes (1965) diagram showing the variations of alkalinity with input of carbon dioxide at various pH values. Fig. 40 gives an example of a typical Deffeyes diagram for normal salinity sea water. The pH is uniquely determined for each value of total CO_2 and alkalinity. Also shown on this figure are the relative changes in carbonate alkalinity and total CO_2 due to the addition of bases or acids, carbon dioxide, bicarbonate, ions, carbonate ions or distilled water. By adding NaHCO$_3$ to a solution, both the alkalinity and the total inorganic carbon are increased

Table 20.   Sass and Ben-Yaakov (1977) mathematical solution to the general titration formula. Primes on constants are omitted for simplicity.

General equation, LHS = RHS

$$\frac{1}{V_o} \left[AV_o + \frac{a_H}{\gamma H+} (V_o + V_a) - N_a V_a \right] = C \ \frac{a_H K_1 + 2K_1 K_2}{a_H^2 + a_H K_1 + K_1 K_2} \tag{47}$$

STEP 1: At low pH, RHS is negligibly small and can be neglected, thus

$$a_{H+} (V_o + V_a) = -AV_o \gamma_{H+} + N_a \gamma_{H+} \cdot V_a \tag{48}$$

This equation has the linear   form y = m + Kx, where

$$y = a_{H+} (V_o + V_a) \qquad m = AV_o \gamma_{H+}$$

$$x = V_a \qquad\qquad K = N_a \gamma_{H+}$$

γ_{H+} and A can be determined by linear regression since a_{H+} and

$(V_o + V_a)$ change for each titration step.

STEP 2: Define Z as the LHS of the general equation and rearrange

$$\frac{Z(a_H)^2}{2K_2 + a_{H+}} = CK_1 - K_1 \ Z \ \left(\frac{K_2 + a_{H+}}{2K_2 + a_{H+}} \right) \tag{49}$$

Using A and γ_{H+} from Step 1, Z becomes a known quantity. By guessing K_2, Eq. 49 has a linear form with

$$y = \frac{Z(a_{H+})^2}{2K_2 + a_{H+}} \qquad m = CK_1$$

$$x = Z \left(\frac{K_2 + a_{H+}}{2K_2 + a_{H+}} \right) \qquad K = -K_1$$

Using linear regression techniques, C, K_1 and r^2 (coefficient of determination) are determined for each guess of K_2. By iteration techniques, successive values of K_2 are used until the r^2 value closest to 1.0 is obtained. The calculated K_1 and C at that value of K_2 thus provide the best fit of the titration points to the model.
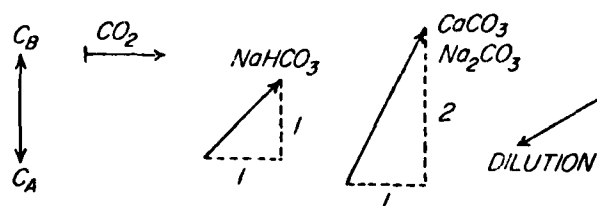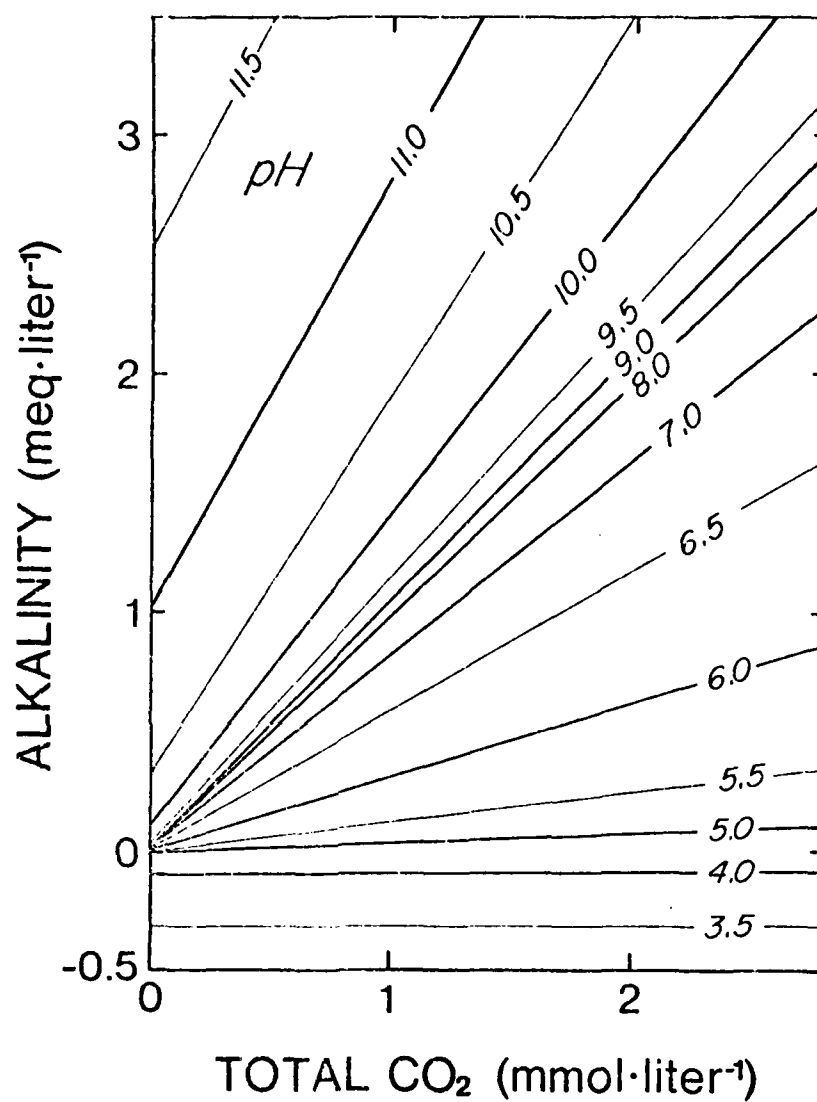
Fig. 40. Typical Deffeyes diagram for sea water (after Deffeyes 1965).

by the same amount. Such a titration thus leaves the ratio of A_c/C unchanged during the $NaHCO_3$ addition. The pH, however, will change during the titration. It will either increase or decrease, depending upon whether the A_c/C of the sample is greater or less than one. This pH change interpretation can be shown schematically, for any sea water or brine system by a simplified, general A_c versus C diagram. The diagram (Fig. 41) is derived from Eq. 41 and contains straight pH locus lines for fixed values of A_c/C. For A/C equal to one, Eq. 41 reduces to

$$(a_{H+})^2 = K_1'K_2' \tag{50}$$

or

$$pH_{12} = 0.5(pK_1' + pK_2') \tag{51}$$

where pH_{12} is the mean of pK_1' and pK_2'. As $NaHCO_3$ is added to a brine (or sea water) solution, the pH increase or decrease to a constant saturation pH which approaches the limiting value of pH_{12} (Weyl 1961). Thus, $NaHCO_3$ titration of a sample will give an independent estimate of $K_1'K_2'$. This titration will also allow one to determine whether alkalinity is greater or less than total inorganic carbon. This determination can be visualized by examining dashed lines 1 and 2 in Fig. 41. These lines represent a $NaHCO_3$ titration curve of a sample. pH lines (solid) increase from lower right to upper left. As the sample is titrated, A_c and C increase
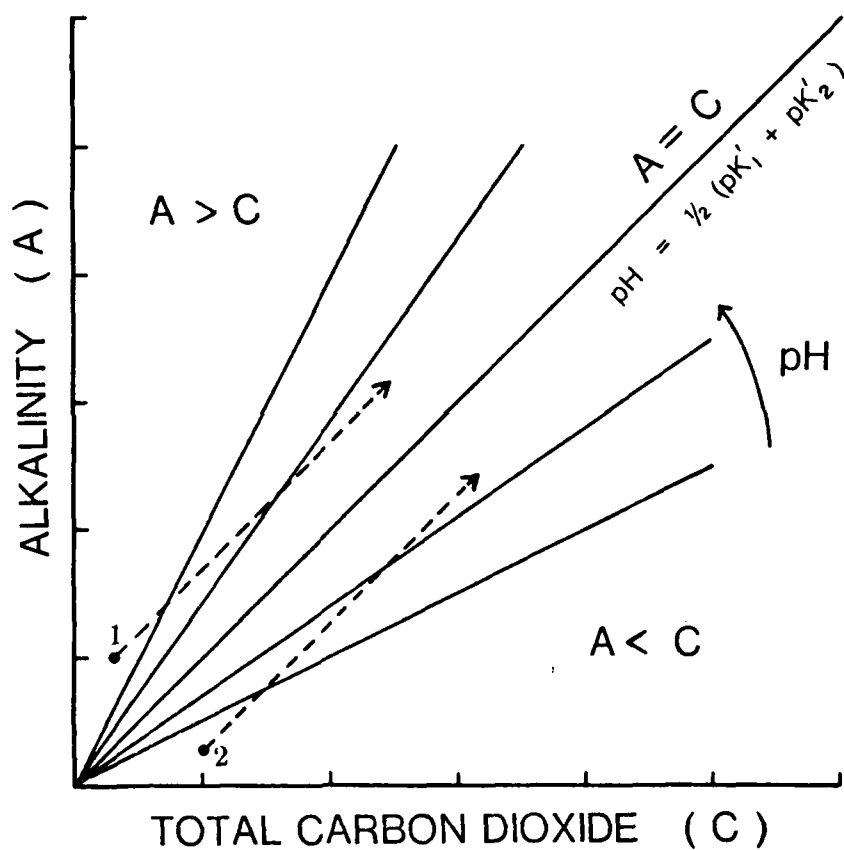
Fig. 41.   Theoretical alkalinity (A) versus total CO_2 (C) plot showing lines of constant pH.   Lines 1 and 2 represent the results of a $NaHCO_3$ titration with A > C (1) or A < C (2).

at the same rate. If A = C, no pH change is observed. For A<C (line 1), pH increases and if A>C (line 2), pH decreases during the titration, at least up to bicarbonate saturation. Thus, a $NaHCO_3$ titration of a sample yields independent information as to whether the alkalinity of a sample is greater than or less than the total CO_2.

Buffer Intensity

The buffer intensity or buffer capacity, B, of a solution is the amount of acid or base required to change the pH by one unit. Since Eq. 41 represents the carbonate alkalinity-total CO_2-pH relationship of a solution, it is the starting point for determining the buffer intensity. By taking the derivative of Eq. 41 w'th respect to a_{H^+}, one arrives at an expression for the buffer intensity of a solution (Pytkowicz and Atlas 1975)

$$B = 2.303 \cdot C \cdot K_1' \, a_H \, \frac{a_H^2 + 4K_1'a_H + K_1'K_2'}{(a_H^2 + K_1'a_H + K_1'K_2')^2} \qquad (52)$$

The plus signs on the hydrogen activity are omitted here for simplicity. Thus for two systems, the buffer intensity (capacity) of each system can be compared for any pH values, if the total CO_2 and equilibrium constants are known.

Results and Discussion

pH and Total CO_2 Relationships

In the aerobic Gulf of Mexico waters, in the region of the
Orca Basin, profiles of pH and total carbon dioxide (Fig. 42) are
typical of the oceanic environment. Surface pH is about 8.2 ± 0.1
and decreases with depth to slightly less than 7.8 at 500 meters,
before increasing to 7.9 in the deeper water. The total CO_2 depth
profile is almost a mirror image of the pH distribution. Total
CO_2 increases with depth are a major cause of the decreasing pH.
These increases in Gulf CO_2 levels result from the aerobic res-
piration of marine organisms (see Table 12), which causes an
oxygen minimum where total CO_2 is highest and pH is lowest.

Below 2100 m in the Orca Basin, the total CO_2 again increases
and pH decreases as oxygen levels begin to decrease. Fig. 43
shows the pH and total CO_2 profiles through the Orca Basin inter-
face into the brine. pH decreases to 6.83 in the high salinity
brine, while total CO_2 increases to an average of about 4.45 mmol·
liter^{-1}. Sackett et al. (1979) have shown that the excess CO_2 in
the brine (relative to deep Gulf values) results from introduction
of isotopically light, biogenic CO_2 into the Orca Basin water.
The pH decrease reflects this increase in CO_2, but the change in
pH may also be affected by the total ion composition of the brine.
This possibility will be discussed in the next section.
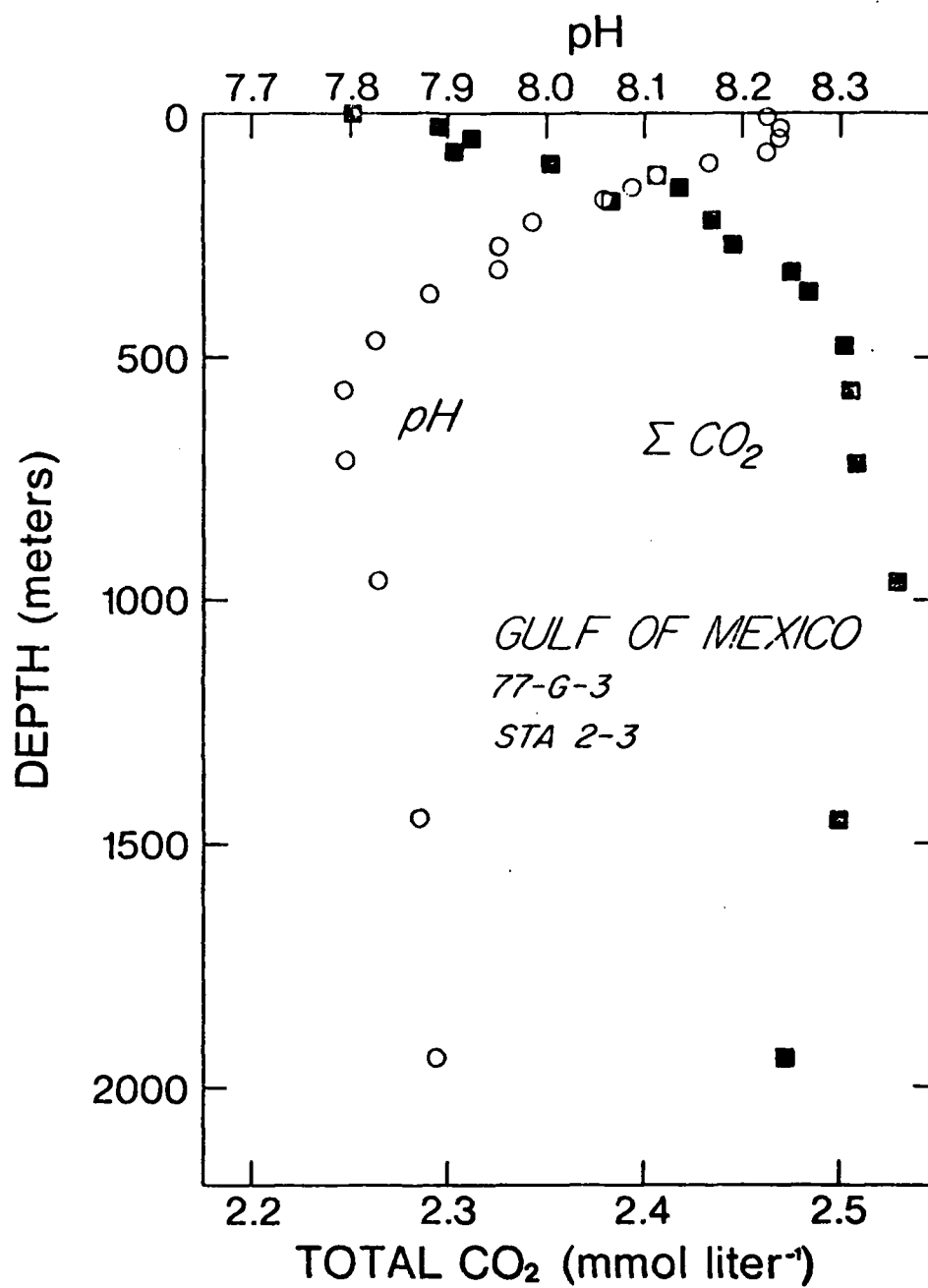
Fig. 42. pH and total carbon dioxide depth distribution in the northwestern Gulf of Mexico.
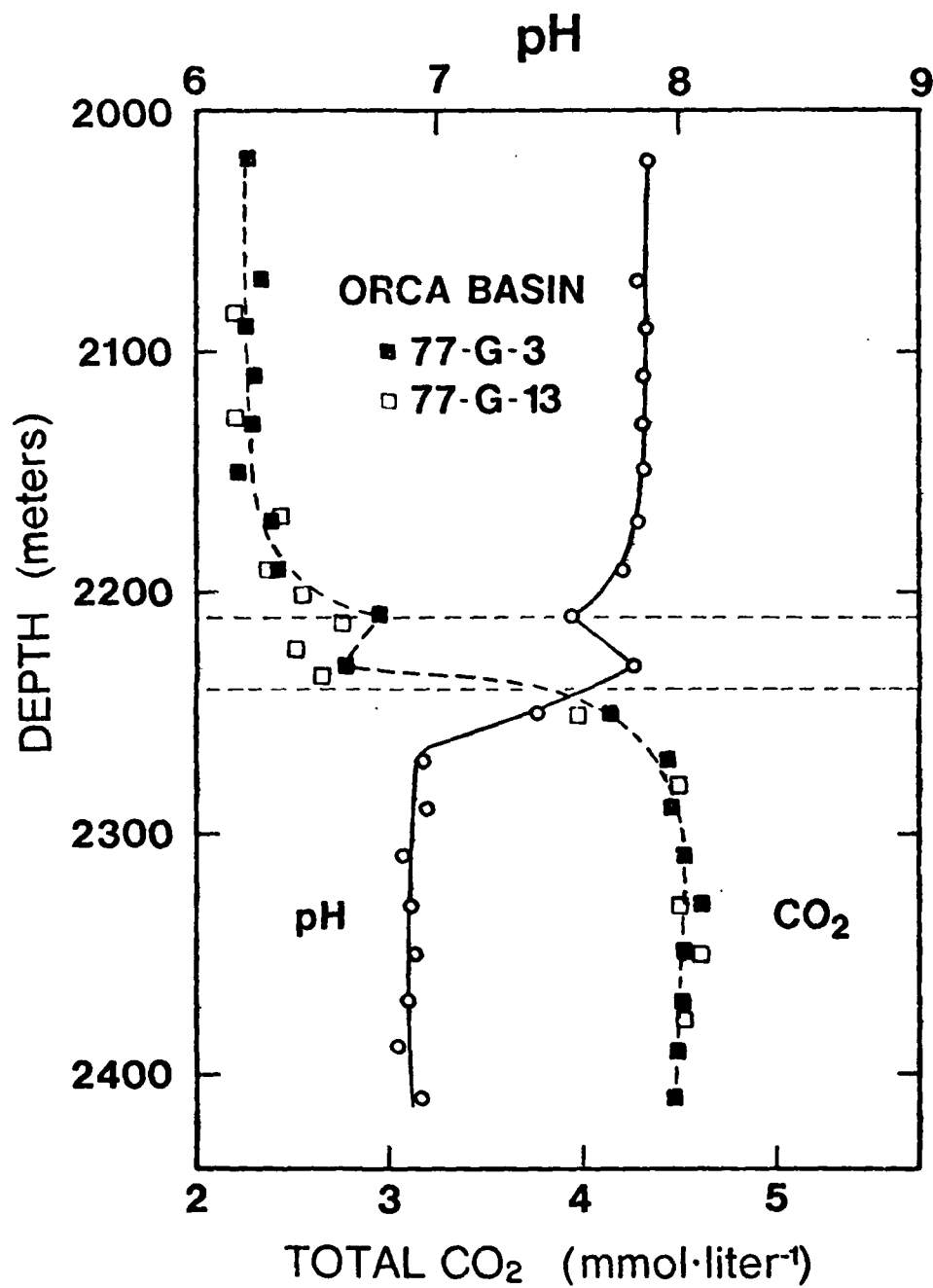
Fig. 43.   pH and total carbon dioxide profiles through the
Orca Basin brine interface and into the high salinity brine.

In the interface region, there is an obvious discontinuity in both the pH and total CO_2 depth distribution. Both parameters follow a predictable pattern (based on O_2 consumption and CO_2 production) down to about 2210 m, then change sharply, before continuing their expected increase (CO_2) or decrease (pH) into the high salinity brine (see Fig. 43). The total CO_2 profile shows only a one point maximum on cruise 77-G-3, but the inverse relationship with pH contributes to the reliability of this data point. Sackett et al. (1979) also observed the same discontinuity in their total CO_2 data at this level. However, they chose to ignore the single point maximum and they drew a smooth curve through the other data points in this region. Data from cruise 77-G-13 is more detailed in this zone (open squares in Fig. 43). These data confirm the CO_2 discontinuity that was observed along with pH and oxygen anomalies in this zone.

A detailed plot of pH and oxygen with depth through the interface region is shown in Fig. 44. Data from two different years are plotted for pH. It is apparent that the discontinuity in the pH-depth profile occurs in transition zone T3, the zone where salinity increases from 50-70°/₀₀ and oxygen concentration is low, but present. Thus, the unusual oxygen step-region has a characteristic pH profile change associated with it, along with the large temperature gradient shown in Fig. 10. The decreasing pH down to 2210 m reflects increasing production of CO_2 through the
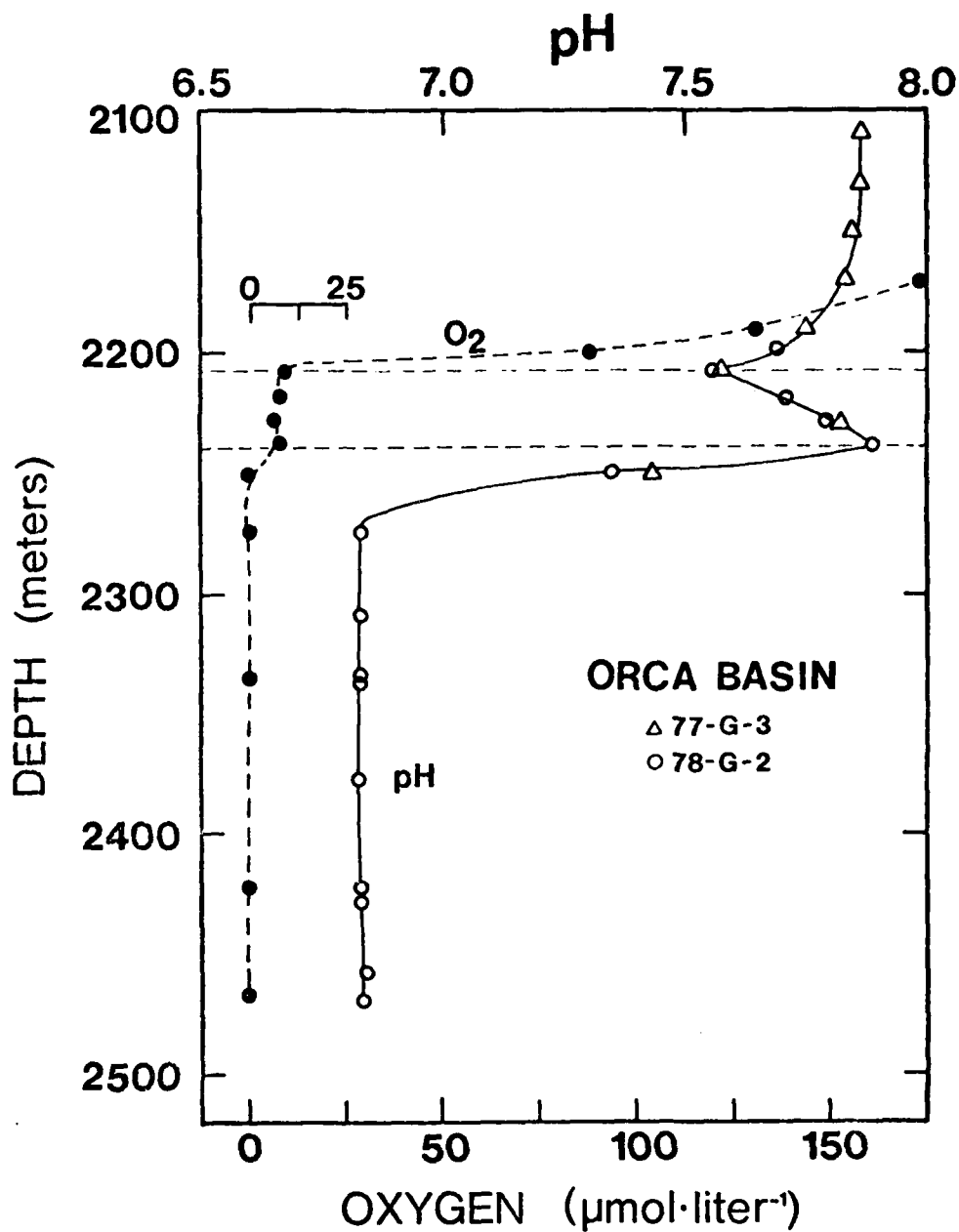
Fig. 44. Detailed plot of pH and dissolved oxygen through the interface region of the Orca Basin.

increasing density region. The $\delta^{13}CO_2$ data of Sackett et al. (1979) support this concept, with increasingly lighter (isotopically) CO_2 found as the interface is traversed.

The increase in pH and decrease in total CO_2 through the oxygen step region (transition zone T3) are not completely understood. The factors acting to cause this discontinuity must be a complex of mixing and biological processes. Both temperature and salinity change rapidly in this region. Physical mixing processes may be important, but significant transport of carbon dioxide from the brine is questionable, since transport through the interface probably occurs only by molecular diffusion. Another, probably more significant process would be degradation of organic material at the top of this low oxygen region. Particles settling on to the interface would undergo decay, mediated by microbial populations which are as high as this interface (LaRock et al. 1979) as at some sediment-sea water interfaces (Zobell 1942). Degradation of organic matter would produce more CO_2 where the bacteria biomass was highest, at the top of this zone. Decreasing pH would result from this CO_2 increase. The pH increase might also be affected by ammonia production there, or by some slight diffusion of ammonia into this region from the brine below. Addition of ammonia to the water would cause the pH to increase. However, the magnitude of this effect is unknown. A detailed survey of physical and biological parameters in this low oxygen zone is needed to explain the pH and CO_2 distributions.

In the high salinity brine, there are no obvious trends in either pH or total CO_2. Sackett et al. (1979) also found

relatively constant values for all other carbon budget components
in the high salinity brine. They reported a $\delta^{13}C$ of the inorganic
carbon of $-6.4 \pm 1.0\%_{oo}$. This negative $\delta^{13}C$ value is indicative
of biogenic input of carbon dioxide into the brine. They esti-
mated that the biogenic CO_2 input must have a $\delta^{13}C$ of $-33\%_{oo}$ to
produce the net $\delta^{13}C$ value observed. Average total CO_2, pH and
$\delta^{13}CO_2$ values for several brines are compared in Table 21. With
no change in the dissociation constants, Eq. 41 predicts that pH
will decrease as total CO_2 increases. This is indeed the case for
the Orca Basin. There is a two-fold increase in CO_2 levels due to
CO_2 production in the brine. However, with the highest total CO_2
of all the brines listed in Table 21, the Orca Basin brine also
has the highest pH. All three brines have evidence of biogenic
CO_2 input, based on the $\delta^{13}C$ data. The higher Orca Basin pH must
result from the Orca Basin brine having a higher buffer capacity
than either the Dead Sea or Red Sea brines.

If one assumes that the origin of the excess CO_2 is biogenic,
then the major concern becomes the species distribution and effect
of this excess CO_2 in the brine. Kennett and Penrose (1978) have
noted that the calcite microfossils in the Orca Basin sediments
are well preserved. This effect must result from a change in the
carbonate system distribution in the brine. Other (non-brine)
Gulf sediments with high CO_2 levels show no exceptional calcium
carbonate preservation. The following sections describe the

Table 21. Total carbon dioxide, $\delta^{13}C-CO_2$ and pH from several brine areas.

Brine	Total CO_2 (mmol·liter^{-1})	$\delta^{13}C$ (‰)[*]	pH
Orca Basin	4.57	−16.4	6.83
Red Sea [*]			
Discovery Deep	0.60	−16.8	6.5
Atlantis II Deep	2.80	−5.6	5.61
Dead Sea [†]	2.55	−	6.3

[*] Data from Weiss (1969).

[†] Data from Sass and Ben-Yaakov (1977).

experimental data used explain why the pteropod shells are well preserved in the Orca Basin.

Brine Dilution Experiment

The results of the pH-dilution experiment for the Orca brine and Gulf of Mexico sea water are shown in Fig. 45. Four dilution experiments were undertaken, two with brine and two with Gulf of Mexico sea water. In all of the dilutions, the pH increased initially and then decreased after going through a maximum. Amit and Bentor (1971) described this type of pH response with dilution as being due to the "hidden alkalinity" effect. Sass and Ben-Yaakov (1977) noted however, that this response is actually due to the change in the ionic strength of the solution, which in turn causes an increase in the dissociation constants of the carbonate system, thus removing hydrogen ions from solution.

Upon dilution with distilled water, the pH of both Orca Basin brine samples increased progressively. The two brines were prepared differently before the experiment. One sample was stirred for 24 hours before the dilution was begun, while the other was fresh, preserved brine right out of the bottle. The effect of the stirring was to reduce the total carbon dioxide of the brine down from 4.41 mmol·liter^{-1} to 3.44 mmol·liter^{-1}. The brine with the higher total carbonate (closed diamonds in Fig. 45) has an initial pH of about 7.3 and increases only to a pH of about 7.8 at a
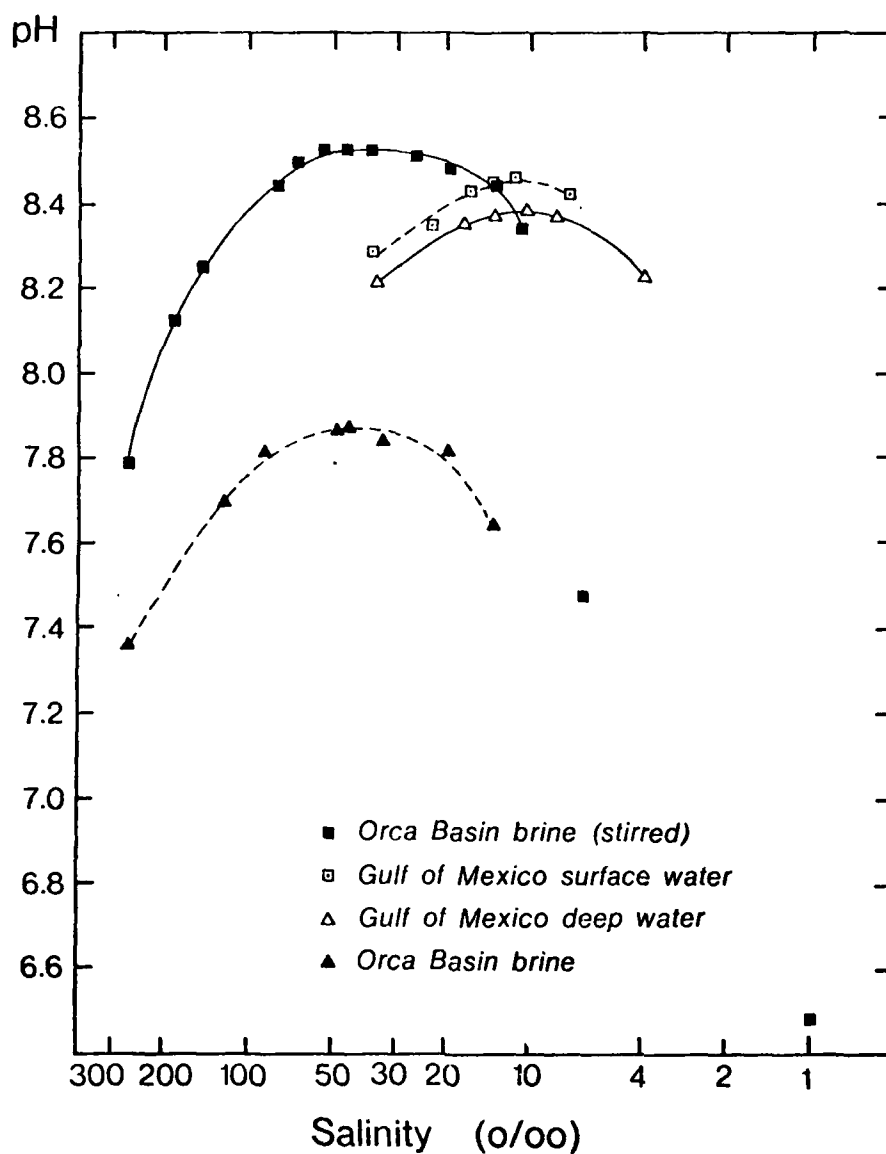
Fig. 45. pH versus log salinity dilution curves for two
samples of Orca Basin brine and for surface and deep water
from the Gulf of Mexico.

salinity of 35 °/ₒₒ. The carbonate depleted brine (initial pH = 7.8) reached a pH of 8.5 at 35 °/ₒₒ salinity. The differences between the two brine dilution curves are a direct result of one sample having more carbon dioxide.

Fig. 46 shows that relatively little, if any, carbon dioxide was lost during the dilution experiment. The carbon dioxide in the two experiments both show a regular dilution curve, with only the slopes different, due to different initial amounts of carbon dioxide in the brines. Yet the initial carbon dioxide difference makes all the difference in the pH-dilution curves. The brine with the higher total CO_2 never approximates the pH of the Gulf sea water. The brine with the lower CO_2 constant has the upper part of its dilution curve in the sea water pH range. The Dead Sea dilution curves of Amit and Bentor (1971), presented in Fig. 38, show a relationship similar to the low CO_2 curve for the Orca Basin.

The importance of biogenic carbon dioxide to the carbonate system in the Orca Basin is obvious from the pH-dilution results. In the Dead Sea, the surrounding area is fairly desolate and little organic carbon enters the Dead Sea brine. With the absence of biogenic carbon dioxide in the Dead Sea, the total carbonate measures only 2.5 mmol·kg^{-1}, a value close to the levels found in the nearby Elat Sea water (Amit and Bentor 1971). Thus when the Dead Sea brine is diluted down to sea water salinities, the carbonate content is much reduced, and the pH of the diluted brine
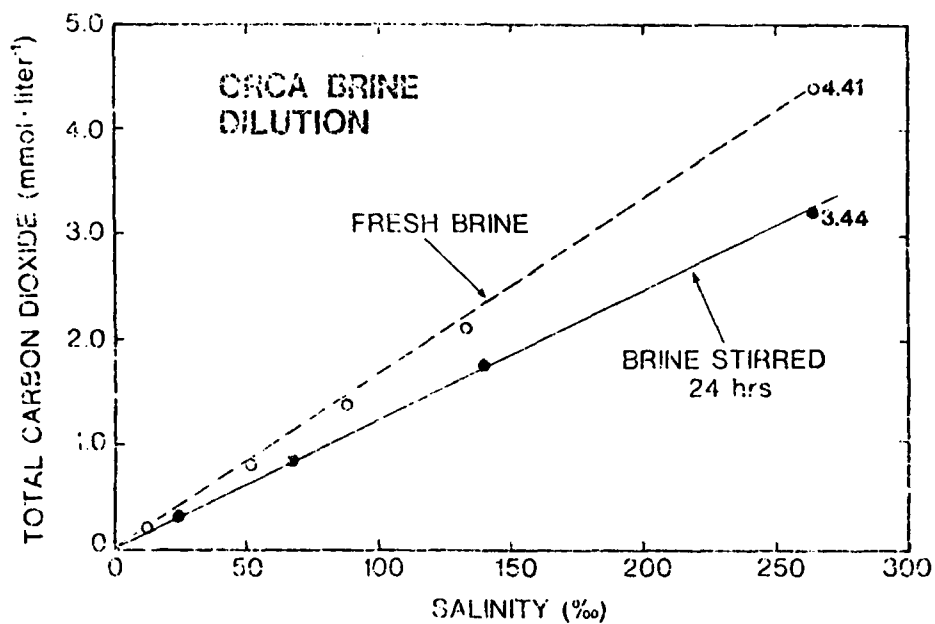
Fig. 46.   Change in total carbon dioxide with dilution of
Orca Basin brine.   These CO_2 measurements were made on the same
samples analyzed for pH and shown in Fig. 45.   Total CO_2 values
for each brine sample are shown in units of mmol·liter^{-1}.

exceeds the pH of the Elat Sea water. In the Orca Basin with the high total carbonate, the dilution pH values are lower than the sea water pH values. This effect must result from the higher total CO_2 of the Orca brine, as well as the fact that the salt did not originate from present Gulf of Mexico sea water.

The pH-dilution curve of the Orca brine is also shifted to the left, compared to the dilution curve for the Gulf of Mexico water. This effect was not observed by Amit and Bentor (1971) who compared the Dead Sea brines to the Elat and Mediterranean Sea waters. This shift means that a higher pH was reached at a higher salinity in the Orca brine, as compared to the Dead Sea brine. This response may be due to the difference in ionic nature of the two brines (see Table 3). The Dead Sea brine is higher in calcium and magnesium and relatively depleted in sulfate. In contrast to the Orca Basin, and in contrast to almost all other known surface water bodies (Nissembaum 1975), magnesium is the dominant cation in the Dead Sea brine.

The pH-dilution curve is controlled predominately by a relaxation of the dissociation constants as more water is added to the brine. The two brines would be expected to respond differently if changes in the dissociation constants were due to the different ionic compositions of the brines. Ben-Yaakov and Gold-haber (1973) noted that sea water dissociation constants of the carbonate system vary in sensitivity to changes in different ions.

They defined a sensitivity parameter for the change in each con-
stant with respect to the major ions. They showed that the
apparent constants are especially sensitive to a variation in the
concentration of magnesium in solution. Ionic composition, as well
as the total ionic concentration, are important in determining the
carbonate system dissociation constants. The differences in the
ionic balances between the Dead Sea and Orca Basin can be dramati-
cally seen when referenced to the chloride content of each brine.
Relative to chloride, and compared with average Gulf of Mexico sea
water, Mg and Ca are enriched by a factor of about three in the
Dead Sea, but they are depleted by a factor of one-third and one-
tenth, respectively, in the Orca Basin (Table 22). Ion complexa-
tions due to the higher magnesium and calcium levels in the Dead
Sea brine would thus allow the pH levels to increase more slowly
with dilution, than in the Orca Basin brine where the concentra-
tions of those important ions is lower.

Alkalinity Versus Total CO_2

As was discussed earlier, titration of a bicarbonate solution
with one of the carbonate system components can yield useful
information as to the species distribution, when the data is in-
terpreted on a Deffeyes diagram. The results of a titration of
the Orca brine with 1.0 N sodium bicarbonate solution is shown in
Fig. 47. With reference to Fig. 41, the initial increase in brine

Table 22.   Ion enrichment factors relative to sea water for calcium and magnesium (referenced to chloride).

Brine	Ca Enrichment	Mg Enrichment
Orca Basin [*]	0.346	0.105
Red Sea [†]	1.436	0.078
Dead Sea [‡]	3.716	2.828

[*] Shokes et al. (1977).

[†] Brewer et al. (1969).

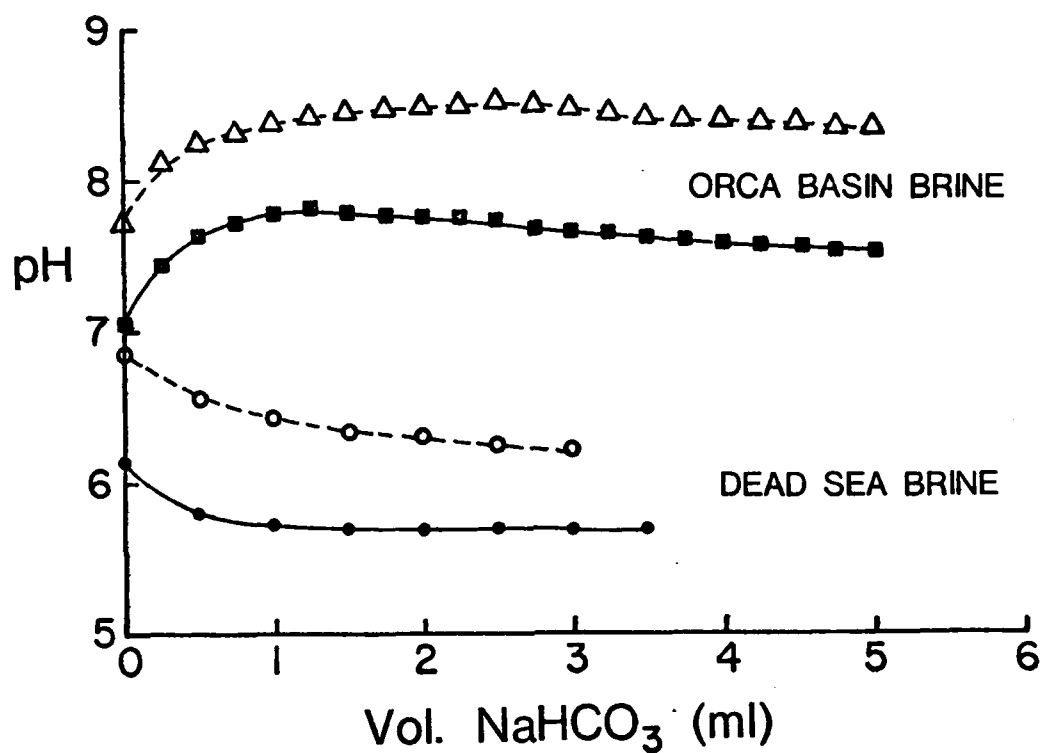[‡] Amit and Bentor (1971).

Fig. 47.   Change in pH of the Orca Basin brine and Dead Sea brines with addition of 0.5 N NaHCO3.   Solid symbols are pure brine and open symbols are 50% dilutions   (Dead Sea brine data from Sass and Ben-Yaakov 1977).

pH with the addition of the $NaHCO_3$ indicates that the total carbonate level in the Orca Basin is higher than the alkalinity. The Dead Sea data of Sass and Ben-Yaakov (1977) are shown for comparison. In the Dead Sea brine, the alkalinity was greater than the total carbon dioxide, as seen by the reduction of pH with the addition of bicarbonate (see Fig. 47).

It should be pointed out here, that the brine that was used for titration with sodium bicarbonate was stored (with sodium azide poisoning) for several months before titration. It is possible that there was some change in the carbonate composition before titration. I make this comment since Millero et al. (1979) have reported that the total alkalinity of the brine is 4.015 ± 0.008 $meq \cdot kg^{-1}$ for Orca Basin brine. This value translates to 4.75 $meq \cdot liter^{-1}$ using a value of 1.185 for the density of the brine at room temperature. This alkalinity value is greater than the 4.57 $mmol \cdot liter^{-1}$ total inorganic carbon value reported by Sackett et al. (1979) and also higher than the 4.50 $mmol \cdot liter^{-1}$ determined in this study. It is possible that the ammonia in the water is causing the higher alkalinity that was measured by Millero et al. (1979). Thus the influence of other factors may affect the alkalinity in the Orca Basin, as they do for other anoxic hypersaline waters (Gaines and Pilson 1972).

To confirm the conclusion that A/C was less than unity, several brine samples were left open to the air and stirred for 24

hr to remove CO_2. Titration of these samples with 0.5 N $NaHCO_3$ produced a titration curve in which the pH decreased with addition of titrant. The lower CO_2 sample had an alkalinity greater than the total CO_2 concentration. This titration also showed that the observed pH changes were not due to the brine dilution, since dilution alone, at either high or low total CO_2 levels, would increase the pH of the brine.

Alkalinity in the High Salinity Brine

As discussed in the carbonate model section, using the calculation methods of Sass and Ben-Yaakov (1977) with an acid titration of a solution allows calculation of the dissociation constants as well as alkalinity and total carbonate. A typical titration with HCl of Orca Basin brine is depicted in Fig. 48. Also shown is an HCl titration of deep Pacific Ocean sea water (salinity=34.8%₀). The following observations can be made from this titration:

(1) The pH of the inflection point of the HCl titration is a function of the salinity of the solution.

(2) The shape of the HCl titration curve for the Orca brine is similar to the sea water curve, but shifted downward (to lower pH) due to the high carbonate content of the brine and the difference in dissociation constants resulting from the high salinity.
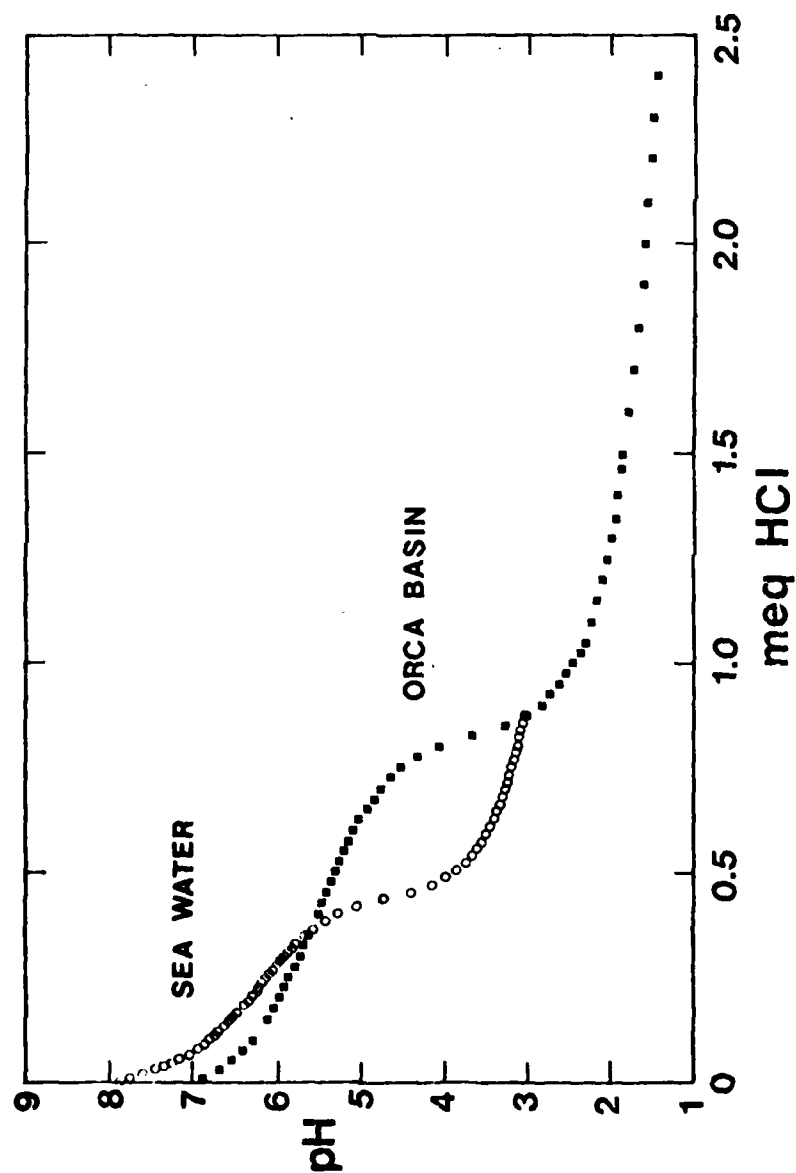
Fig. 48. Representative HCl titration curves of sea water and Orca Basin brine. Volume of sample was 180 ml for each.

For interpretation of the data in Fig. 48, the buffer capacity (the incremental change in pH for a given volume of HCl added) was calculated and plotted for each series of data points. The results of this calculation are presented in Fig. 49. The buffer capacity versus pH curve is also plotted for the sea water HCl titration as a comparison. Maxima and minima in these curves correspond to the pK' values of the dissociation constants of the carbonate system in each solution. For example, the pK_2' value for sea water would correspond to the minimum at a buffer capacity of about 0.25. The pK_1' value for sea water corresponds to the buffer capacity maximum at a pH of about 6.1. Since the pH of the Orca Basin is so low, there is no upper minimum to use in graphically determining the pK_2'. The pK_1' corresponds to the maximum in buffer capacity which occurs at a pH of 5.5. A pK_1' of 5.5 for the brine represents a factor of three increase in the K_1' dissociation constant, compared to sea water.

Application of the iterative solution technique of Sass and Ben-Yaakov to this titration allows more accurate calculation of the dissociation constant. Using the titration data plotted in Fig. 48 and the mathematical sequence given in Table 20, the alkalinity, the total carbon dioxide, and the carbonate dissociation constants were calculated for the Orca Basin and for sea water, for comparison. The results of this calculation are presented in Table 23. Analysis of other samples gave lower carbon dioxide

233
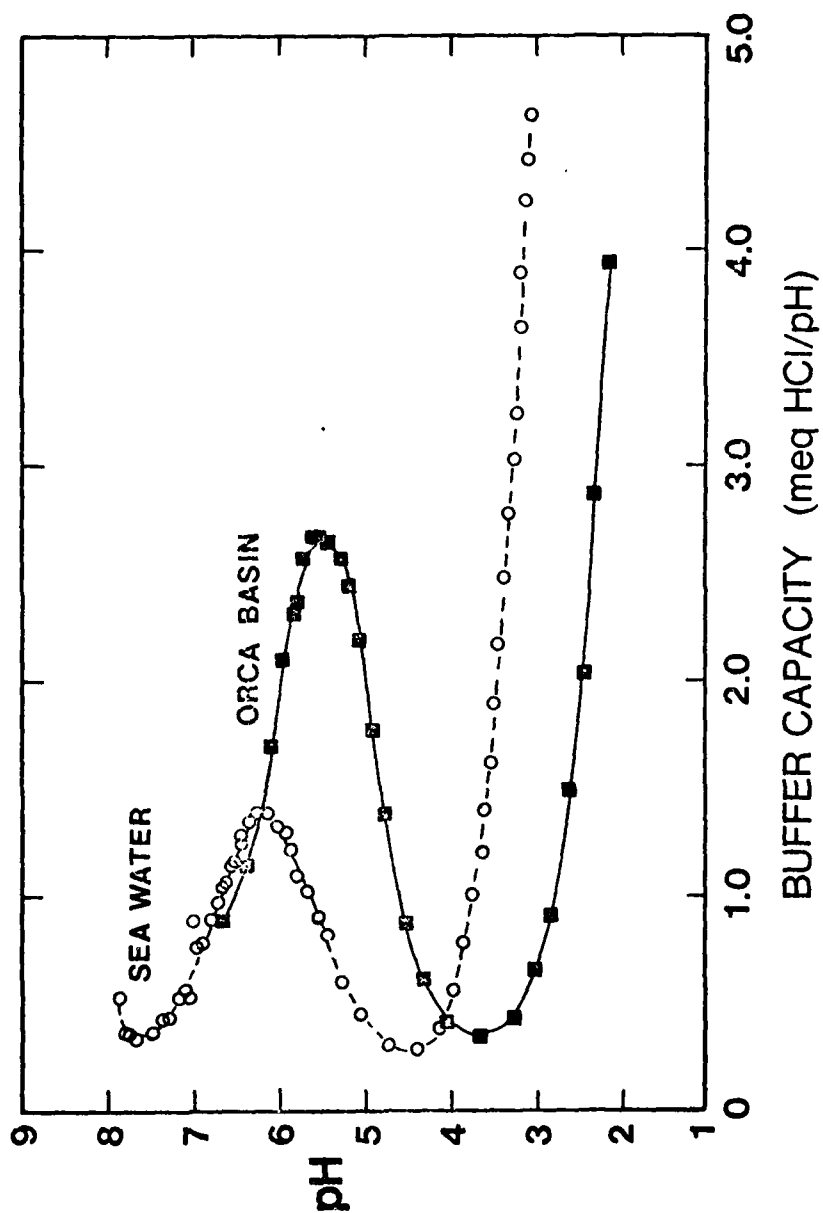
Fig. 49. Buffer capacity (the incremental change in pH for a given addition of HCl) plotted as a function of pH. This type of plot can be used to estimate the dissociation constants, as described in the text. Titration data and samples are the same as for Fig. 48.

Table 23. Calculated alkalinity and carbonate dissociation
constants for seawater and Orca Basin brine.

Brine	Alkalinity (meq·liter^{-1})	Total CO_2 (mmol·liter^{-1})	pK_1	pK_2
Sea water	2.20	2.13	5.80	9.14
Orca Basin brine	4.701	4.750	5.49	8.34
Dead Sea brine *	3.86	4.41	5.09	6.23

* From Sass and Ben-Yaakov (1977).

concentrations, but also lower alkalinity concentrations, indicative of some CO_2 loss.

The dissociation constants increase with increasing salinity in the Orca Basin. In the Dead Sea brine, Sass and Ben-Yaakov (1977) also noted this increase in the dissociation constants. Their values are given in Table 23 for comparison. It is immediately obvious that the dissociation constants of the Dead Sea brine are altered more (relatively to sea water) due to the increasing salt content, than are the constants for the Orca Basin. This magnitude of difference can be seen more dramatically when the distribution of carbonate system species is calculated for the Orca Basin and the Dead Sea brines. The results of the species distributions as a function of pH are given in Fig. 50. The results are presented as relative percentages of each species as a function of pH. Presented in this manner, the relative distributions in each solution can be directly compared without considering the total carbonate concentration.

The distribution of the carbonate species in the Dead Sea brine is very different from either sea water or Orca Basin brine. At the natural pH of the Dead Sea, the concentrations of carbonate and bicarbonate ions are approximately equal. This is atypical for the other systems, where bicarbonate is by far the dominant inorganic carbon ion in solution at _in situ_ pH values.

The shape of the distribution in the Orca Basin is very much like that of sea water, but all distribution curves are shifted
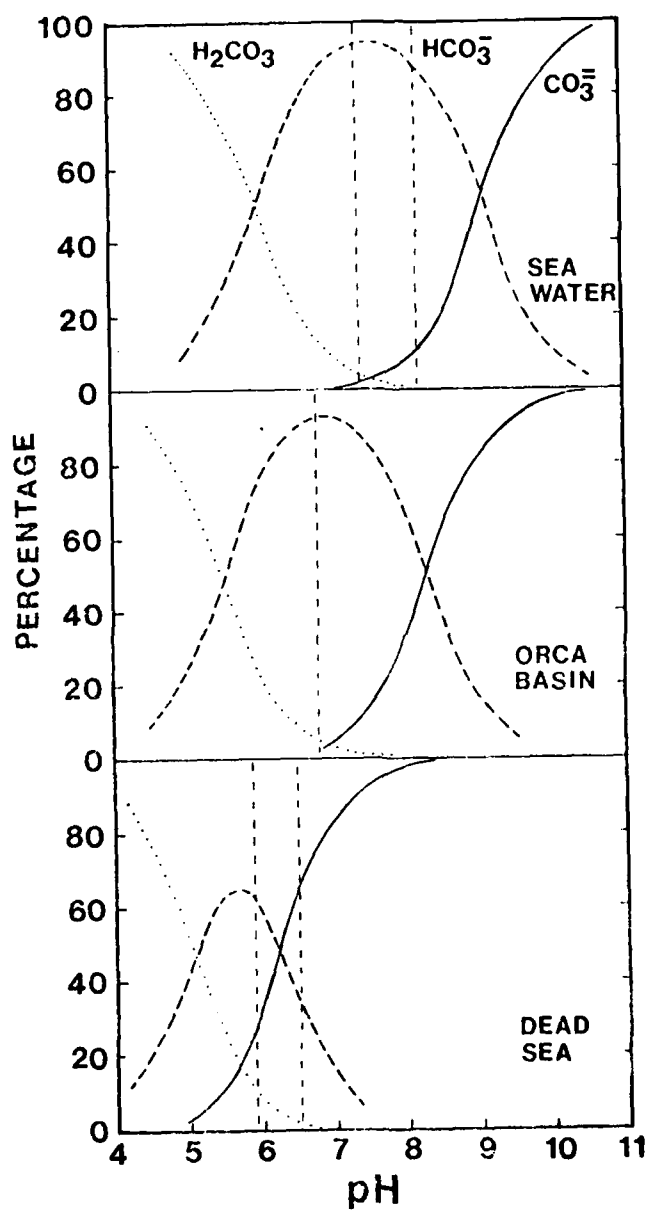
Fig. 50.   Carbonate system species distributions for sea water, the Orca Basin brine and the Dead Sea brines. The vertical dashed lines indicate the pH ranges of the natural systems.

toward lower pH values. Orca Basin brine has a pH of 6.83. This

small difference in the species profiles underscores the chemical

nature of the Orca Basin brine. The Orca Basin brine is like sea

water that has been saturated with sodium chloride. On the other

hand, the major ionic differences between the Dead Sea brine and

sea water play havoc with the carbonate species distribution there.

Sass and Ben-Yaakov (1977) have attributed most of the disparity

in the Dead Sea carbonate system to the concentration of magnesium

in the Dead Sea brine. The bicarbonate to carbonate dissociation

constant is about threefold more sensitive to variations in mag-

nesium concentration than is the K_1' (Ben-Yaakov and Goldhaber

1977). This effect is attributed to the relatively high stability

of $MgCO_3^o$ complex as compared to that of $MgHCO_3^-$ (Garrels and

Thompson 1962). The high K_2' dissociation constant for the Dead

Sea brine causes the observed distributions. Since both K_1' and

K_2' are greater, but only two or three times sea water values, the

Orca Basin brine distributions are similar to sea water.

Pteropod Preservation in the Sediments

The consequences of salinity causing an increase in the

dissociation constants, combined with the biogenic total CO_2 in

the brine has resulted in such a high concentration of carbonate

ion in the sediments, that there is rather striking preservation

of carbonaceous material in the Orca Basin sediments. Even ptero-
pod tests, which are made of the more soluble aragonite, are
preserved in the sediment. Fig. 51 shows several electron micro-
scope photographs (taken by L. A. Barnard) of some of the ptero-
pods found in the Orca Basin sediments. As noted by Kennett and
Penrose (1978), the preservation is striking. There is no
evidence of even the tiny etch marks often observed on
calcium carbonate tests undergoing slow dissolution in typical
marine sediments (Alexandersson 1975). Fig. 52 shows one of the
pteropods found in the basin, and two additional magnifications
of one portion of the pteropod. These micrographs show that there
is absolutely no dissolution of this soluble aragonitic species
(Cavolinia longirostris).

The observation of the well-preserved microfossils in the
sediment, with no evidence of $CaCO_3$ precipitation, implies
the Orca Basin sediments are in equilibrium with respect to cal-
cium carbonate. Since the concentration of carbonate ion in the
brine is no higher than in normal sea water, one must consider
the solubility coefficient of calcium carbonate in the brine sedi-
ments to be different than in normal marine environments. Also
there is an excess of 17 mmol·Ca·kg^{-1} brine in the Orca Basin.
This excess calcium would contribute to the preservation of the
calcite and aragonite tests in the brine. But, where did this
excess calcium come from? Could it be from past dissolution of
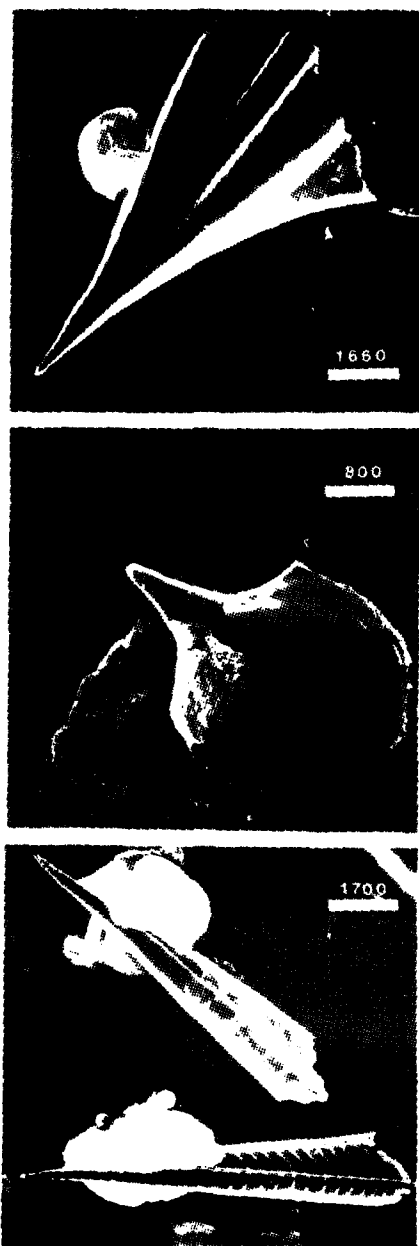
Fig. 51. Scanning electron photographs of three pteropod
species preserved in the Orca Basin sediments. The number above
the length scale on each micrograph gives the scale length in
micrometers.
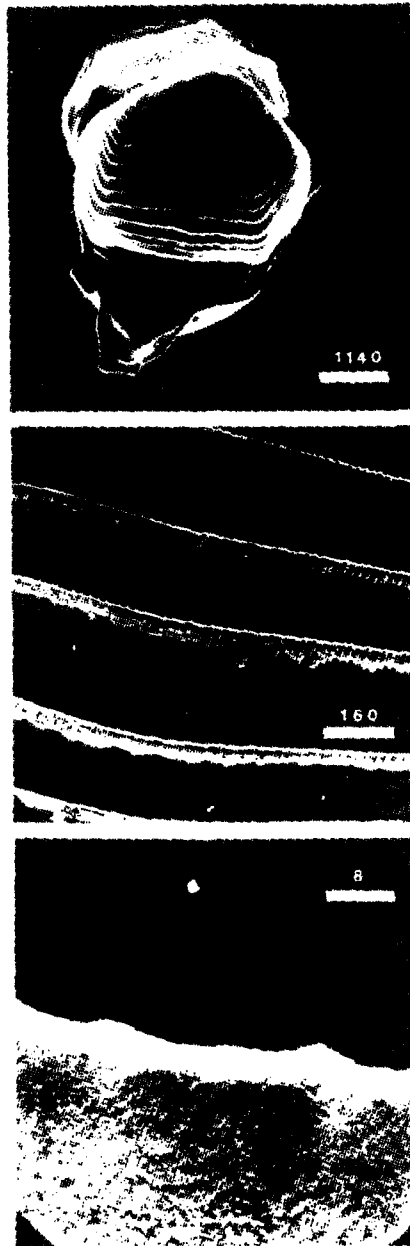
Fig. 52. Three scanning electron photographs of a *Cavolinia longirostris* pteropod found in the Orca Basin sediments. The number above each length scale on each micrograph gives the scale length in micrometers. Even at high magnification, there is no evidence of aragonite dissolution in the Orca Basin sediments.

calcium carbonate in the brine? This seems improbable since the

pteropods in the brine are preserved throughout the sediment

column (Addy and Behrens 1980). In one core section at a depth of

689 cm, Addy and Behrens (1980) found that the percentage of sand

increased significantly, to 21%. The increase in sand was entirely

skeletal, calcium carbonate tests. In fact, they noted that

the preservation of calcium carbonate in the sediments increased

the sedimentation rate by as much as 21 $cm \cdot ka^{-1}$. Thus, the excess

calcium must have an alternate source.

Excess Calcium and K_{sp}' of Brine

It will be shown here that this excess calcium originated

with the inflowing brine and not from calcium carbonate dissolu-

tion in the basin. $CaCO_3$ can decompose to form

$$CaCO_3 \longrightarrow Ca^{++} + CO_3^= \tag{53}$$

With this dissolution, Ca^{++} increases (1 mole) along with alka-

linity (2 equivalents) and total CO_2 (1 mole). At the same time,

organic material is decomposing in the brine producing CO_2, HNO_3

(or NH_3) and H_3PO_4 (Table 12). In sea water CO_2, HNO_3 and H_3PO_4

react with $CO_3^=$ (Brewer et al. 1975). Thus, the combined decom-

position equation (aerobic) which includes $CO_3^=$ reaction can be

written as

$$(CH_2O)_{106}(NH_3)_{16}H_3PO_4 + 138O_2 + 124CO_3^= \qquad (54)$$

$$= 16NO_3^- + HPO_4^= + 230\ HCO_3^- + 16H_2O\ .$$
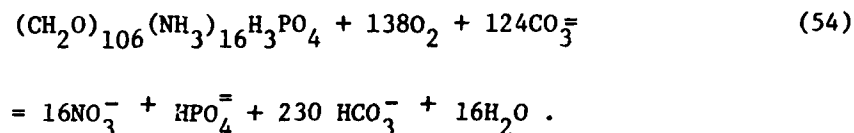
This combined reaction scheme (Eq. 54) results in an increase of 106 moles in ΣCO_2 and a decrease in 17 equivalents in alkalinity. Chen (1978) has discussed this combined effect of $CaCO_3$ dissolution and decomposition of organic matter in the ocean. He represents the decomposing of x μmol of $CaCO_3$ and y μmol of organic matter in sea water by the expressions:

$$\Delta TA = 2x - 17y \qquad (55)$$

$$\Delta \Sigma CO_2 = x + 106y \qquad (56)$$

$$\Delta NO_3 = 16y \qquad (57)$$

where TA is in microequivalents and ΣCO_2 and NO_3 are in micromoles. The same equations are applicable to anaerobic decomposition since the same ratios are involved, only NH_3 is produced as the terminal nitrogen product. In examining the Orca Basin, Eq. 57 becomes

$$\Delta NO_3 + \Delta NH_3 = 16y \qquad (58)$$

since both aerobic (initially) and anaerobic processes have been active in bringing the brine to its present state. Eqs. (55) and (56) and Eqs. (56) and (57) were solved by Chen (1978) for x, the $CO_3^=$ concentration which is equivalent to ΔCa, the change in

calcium concentration (see Eq. 54). The results are

$$\Delta Ca = x = 0.46288 \ \Delta TA + 0.074236 \ \Delta\Sigma CO_3 \qquad (59)$$

$$\Delta Ca = x = 0.5 \ \Delta TA + 0.53125 \ \Delta NO_3 \qquad (60)$$

Since alkalinity, total CO_2, nitrate and ammonia have all been measured for the Orca Basin, the predicted ΔCa^{++} can be calculated showing the increase in Ca^{++} from possible dissolution of $CaCO_3$ and decomposition of organic matter. These calculations are shown in Table 24. Eq. 59 predicts a ΔCa^{++} of a 0.96 $mmol \cdot kg^{-1}$ while Eq. 60 predicts 1.12 $mmol \cdot kg^{-1}$ for an average of 1.04 $mmol \cdot kg^{-1}$. This increase is far below the measured ΔCa^{++} (compared to deep Gulf water) of 17.0 $mmol \cdot kg^{-1}$ (Table 3). It can also be calculated (Table 24) that if enough Ca^{++} were put into Gulf sea water to reach the Orca Basin levels, the resultant alkalinity would be approximately 35 $meq \cdot kg^{-1}$. Thus the excess Ca^{++} in the Orca Basin must have entered with the original brine, probably from the dissolution of calcium sulfate along with NaCl.

The complete preservation of the aragonitic pteropod shells in the Orca Basin is unusual. While some other anoxic environments have partial preservation of pteropod tests (see, for example, Berger and Soutar 1970), preservation is complete in the Orca Basin sediments. Since no $CaCO_3$ precipitation occurs in the Orca Basin, one can assume that Orca brine is in equilibrium with respect

Table 24. Calculations showing the possible changes in total calcium content resulting from the increases in alkalinity, total CO_2, and ammonia in the Orca Basin.

Date for Calculations

ΔCa^{++} = 17.0 mmol·kg^{-1} (Shokes et al. 1977)

ΔTA = 4.015 meq·kg^{-1} (Millero et al. 1979 and this study)

$\Delta \Sigma CO_2$ = 1.913 mmol·kg^{-1} (Sackett et al. 1979 and this study)

$\Delta NO_3^- + NH_3$ = 441 μmol·kg^{-1} (this study)

Basic Equations

a. ΔCa^{++} = 0.46288 ΔTA + 0.074236 $\Delta \Sigma CO_2$

b. ΔCa^{++} = 0.5 ΔTA + 0.53125 $(\Delta NO_3 + NH_3)$

Ca^{++} Predicted Changes

a. ΔCa^{++} = 0.46288 (1765 μeq·kg^{-1}) + 0.074236 (1.913 μmol·kg)

ΔCa^{++} = 958 μmol·kg

b. ΔCa^{++} = 0.5(1765 μeq·kg^{-1}) + 0.53125(441 μmol·kg^{-1})

ΔCa^{++} = 1117 μmol·kg^{-1}

Average = 1037 μmol·kg^{-1}

Alkalinity Required to Produce Orca ΔTA

a. $\Delta TA = \dfrac{Ca^{++} - 0.074236\ CO_2}{0.46288}$

ΔTA = 36.4 μeq·kg^{-1}

b. $\Delta TA = \dfrac{Ca^{++} - 0.53125\ (NO_3^- + NH_3)}{0.5}$

ΔTA = 34.5 μeq·kg^{-1}

Average TA = 35.5 μeq·kg^{-1}

to aragonite, and the apparent solubility product (K_{sp}') for

aragonite can be calculated. This constant is defined in terms

of total concentration, i.e. the product of the total calcium

(Ca^{++}) and total carbonate $(CO_3^=)$ ions. Total calcium is given in

Table 3. Carbonate ion concentration is obtained from the

relationship:

$$[CO_3^=] = \frac{A_c K_2'}{(a_H^+ + 2K_2')} \tag{61}$$

Using the pH of the brine as 6.83 and a pK_2' of 8.34, one obtains

a value of 3.2×10^{-6} $mol^2 \cdot kg^{-2}$ for K_{sp}' at 25°C. This value

is about six times larger than the corresponding value for sea

water (Ben-Yaakov and Goldhaber 1973). If the Orca brine had normal

sea water calcium concentration (see Table 3), the ion product for

$[Ca^{++}][CO_3^=]$ would be 1.2×10^{-6} $mol^2 \cdot kg^{-2}$. This would make the

brine undersaturated with respect to aragonite by a factor of

three. Thus, it is the high calcium content of the brine which

causes the complete preservation of the aragonitic pteropod shells

in the Orca Basin sediments.

CHAPTER VI

SUMMARY AND CONCLUSIONS

The advective, diffusive, and reactive processes acting upon the dissolved gases in the hypersaline waters of the Orca Basin are no different than in other marine, anoxic environments. Only the magnitude of the constants and the rates of reaction are affected by the increased concentrations of dissolved salts in the Orca Basin water. The processes differ from other less saline areas only in degree of interaction. This study has shown the potential of dissolved gas studies in understanding those processes.

This investigation confirmed that the Orca Basin brine is the result of the low temperature dissolution of a sea floor salt deposit by Gulf of Mexico sea water, with the resultant brine flowing into the depths of the basin. The similarity of the nitrogen to argon ratio in the Orca Basin water (exclusive of salt), to that of deep Gulf of Mexico water (also corrected for the salt content) supports the hypothesis of low temperature solution of a sill salt. This first postulate was based on the ion content of the brine, relative to evaporite and solution deposit systems. The dissolved nitrogen and argon data provided an independent confirmation of that mechanism of brine formation, and furthermore, gave a temperature maximum for the dilution water of less than 5°C. The bottom water temperature in the Gulf of Mexico is 4.2°C.

The step-like feature in the oxygen concentration was perhaps the most interesting of the observations involving dissolved gases. A simple consideration of the possible mixing processes which occur at the brine-sea water interface revealed that it would be possible to account for this step-like feature from mixing processes alone. More work is needed to prove this conclusively. Detailed, continuous, simultaneous measurements of temperature, salinity, dissolved oxygen, and pH across the brine-sea water transition regions should be made with great precision in order to indicate accurately the nature of the mixing processes at the Orca Basin interface.

Measurements of other parameters indicated that the brine-sea water interface in the Orca Basin is physically active, chemically reactive, and behaves much like the sediment-sea water interface in other anoxic regions. This fact was most apparent from the dissolved molecular nitrogen and ammonia distributions in the interface and transition zones. The observed distributions of dissolved molecular nitrogen in the low oxygen region were strikingly similar to the near surface sediment distributions that were reported by Barnes et al. (1975) for the southern California borderland basin sediments. This similarity illustrates the important laboratory potential of the Orca Basin system. The interface there is like a sediment-sea water interface, except that it can be sampled over a length scale of meters, rather than the

centimeters and millimeters required for sediment work. In
reviewing the other constituents, such as nitrous oxide and
ammonia, these parameters also change, going from the Gulf water
into the brine, in the same manner that sea water-sediment inter-
stitial water transitions are made in many environments. Thus, the
Orca Basin interface region could be useful in examining the
transition processes of consumption and production by which con-
centration gradients change rapidly across interface boundaries.

The dissolved reduced gases in the high salinity brine are
produced by the same decomposition processes that are operative
in other anoxic basins. The high concentrations of methane and
ethane in the brine result from the great stability of the brine
in the basin, which has a residence time of over 6000 years. Both
methane and ethane are produced in the basin. However, in spite
of the high concentrations observed, empirical evidence from
isotopic composition of the carbon compounds (methane and carbon
dioxide), along with the unusual depth distributions of iron and
hydrogen sulfide (when compared with other anoxic areas),
indicated that the rates of microbial decomposition are slower in
the Orca Basin. The presence of preserved _Sargassum_ seaweed deep
in the sediments is further evidence for reduced decomposition
rates in the Orca Basin. Reduced microbial activity produces
little free sulfide to react with the iron in the brine. High
concentrations of iron have accumulated in the water column.

The carbonate system in the high salinity brine is similar to sea water which has simply been saturated with sodium chloride. The relative distributions of the carbonate species are the same as those found in normal salinity sea water. The low pH in the brine results from the input of 2.2 $mmol \cdot liter^{-1}$ of biogenic carbon dioxide. The carbonate dissociation constants differ only because of the different degree of interaction caused by the higher salt content. The apparent solubility product constant of aragonite in the brine is about six times larger than the corresponding value for sea water at 25°C. Thus it must be the high concentrations of calcium in the brine which has caused the preservation of pteropod shells in the basin sediments.

This investigation has shown the utility of dissolved gas in examining the active physical and biological processes in unusual environments. Such an examination should also answer questions about the Orca Basin that had been posed during previous studies. An examination of both reactive and unreactive gases has yielded significant information about the formation of the brine, as well as about the rates of reaction in the brine. The objectives of this work have been met with solutions that are internally consistent. Dissolved gases can be powerful geochemical tracers for oceanic processes.

REFERENCES

Adams, D.D. 1973. A laboratory model for plankton decomposition in anaerobic and aerobic sea water. Ph.D. Thesis, Dalhousie University, Halifax, Nova Scotia, Canada. 228 p.

Addy, S.K. and E.W. Behrens. 1980. Time accumulation of hyper-saline anoxic brine in Orca basin (Gulf of Mexico). Mar. Geol. 37: 241-252.

Alexandersson, E.J. 1975. Etch patterns on calcareous sediment grains: peterographic evidence of marine dissolution of car-bonate minerals. Science 189: 47-48.

Amit, O. and Y.K. Bentor. 1971. pH-dilution curves of saline waters. Chem. Geol. 7: 307-313.

Antoine, J.W. and W.R. Bryant. 1969. Distribution of salt and salt structures in the Gulf of Mexico. Amer. Assoc. Pet. Geol. Bull. 53: 2543-2550.

Armstrong, F.A.J., C.R. Stearns, and J.D.H. Strickland. 1967. The measurement of upwelling and subsequent biological processes by means of the Technicon AutoAnalyzer and associated equipment. Deep-Sea Res. 14: 381-389.

Atkinson, L.P. and F.A. Richards. 1967. The occurrence and distri-bution of methane in the marine environment. Deep-Sea Res. 14: 673-684.

Atlas, E.L., S.W. Hager, L.I. Gordon, and P.K. Park. 1971. A practical manual for use of the Technicon AutoAnalyzer in sea-water nutrient analyses; revised. Oregon State University, Department of Oceanography, Technical Report 215. 49 p.

Barabee, J.M. and W.J. Payne. 1967. Products of denitrification by a marine bacterium as revealed by gas chromatography. Mar. Biol. 1: 136-139.

Barnes, R.O., K.K. Bertine, and E.D. Goldberg. 1975. N_2:Ar, nitrification and denitrification in southern California borderland basin sediments. Limnol. Oceanogr. 20: 962-970.

Barnes, R.O. and E.D. Goldberg. 1976. Methane production and consumption in anoxic marine sediments. Geology 4: 297-300.

Benard, H. 1901. Les tourbillons cellulaires dans un nappe liquide transportant de la chaleur par convection en regime permanent. Ann. Chim. Phys. 23: 62-144.

Ben-Yaakov, S. 1970. A method for calculating the in situ pH of seawater. Limnol. Oceanogr. 15: 326-328.

Ben-Yaakov, S. and M.B. Goldhaber. 1973. The influence of sea water composition on the apparent constants of the carbonate system. Deep-Sea Res. 20: 87-99.

Ben-Yaakov, S. and E. Sass. 1977. Independent estimate of pH of Dead Sea brine. Limnol. Oceanogr. 22: 374-376.

Berger, W.H. and A. Soutar. 1970. Preservation of plankton shells in an anaerobic basin off California. Geol. Soc. Amer. Bull. 81: 275-282.

Bernard, B.B. 1978. Light hydrocarbons in marine sediments. Ph.D. Thesis, Texas A&M University, College Station, Tx. 144 p.

Bernard, B.B. 1979. Methane in marine sediments. Deep-Sea Res. 26A: 429-443.

Bernard, B.B., J.M. Brooks, and W.M. Sackett. 1976. Natural gas seepage in the Gulf of Mexico. Earth Planet. Sci. Lett. 31: 48-54.

Berner, R.A. 1971. Principles of chemical sedimentology. McGraw-Hill Book Co., 240 p.

Berner, R.A. 1972. Sulfate reduction, pyrite formation and the oceanic sulfur budget, p. 347-361. In D. Dryssen and D. Jagner [eds.], The changing chemistry of the oceans. Almquist & Wiksell.

Berner, R.A. 1974. Iron sulfides in Pleistocene deep Black Sea sediments and their paleo-oceanographic significance, p. 524-531. In E.T. Degens and D.A. Ross [eds.],The Black Sea - geology, chemistry and biology, Mem. 20. Amer. Assoc. Pet. Geol. George Banta Company.

Berner, R.A. 1978. Sulfate reduction and the rate of deposition of marine sediment. Earth Planet. Sci. Lett. 37: 492-498.

Berner, R.A., T. Baldwin,and G.R. Holdren, Jr. 1979. Authigenic iron sulfide as paleosalinity indicators. J. Sed. Petrol. 49: 1345-1350.

Borchert, H. and R.O. Muir. 1964. Salt deposits; the origin, metamorphisis and deformation of evaporites. Van Nostrand. 338 p.

Bouma, A.H., L.B. Smith, B.R. Sidner, and T.R. McKee. 1975.
Submarine geomorphology and sedimentation patterns of the Gyre
intraslope basin, northwest Gulf of Mexico. Technical Report
75-9-T, Department of Oceanography, Texas A&M University,
College Station, Tx. 163 p.

Braitsch, O. and A.G. Herrmann. 1963. Zur Geochemie des Broms in
Salinaren Sedimenten, Teil I. Experimentelle Bestimmung der
Br-Verteilung in verschiendenen naturlichen Salzsystemen.
Geochim. Cosmochim. Acta 27: 361-391.

Breed, R.S., E.G.D. Murray, and N.R. Smith. 1957. Bergley's manual
of determative microbiology, 7th ed. The Williams and Wilkins
Co. 1094 p.

Brewer, P.G., C.D. Densmore, R. Munns, and R.J. Stanley. 1969.
Hydrography of the Red Sea brines, p. 138-147. In E.T. Degens
and D.A. Ross [eds.], Hot brines and recent heavy metal deposits
in the Red Sea. Springer-Verlag.

Brewer, P.G. and D.W. Spencer. 1974. Distribution of some trace
elements in Black Sea and their flux between dissolved and
particulate phases, p. 137-143. In E.T. Degens and D.A. Ross
[eds.], The Black Sea - geology, chemistry, and biology, Mem. 20.
Amer. Assoc. Pet. Geol. George Banta Company.

Brewer, P.G., G.T.F. Wong, M.P. Bacon, and D.W. Spencer. 1975.
An oceanic calcium problem. Earth Planet. Sci. Lett. 26-81-87.

Brisou, J. and N. Vargues. 1961. Proteolysis and nitrate reduction
in sea water, p. 410-414. In C.H. Oppenheimer [ed.], Symposium
on marine micribiology, Charles C. Thomas.

Broenkow, W.W. 1969. The distribution of nonconservative solutes
related to the decomposition of organic matter in anoxic basins.
Ph.D. Thesis, University of Washington, Seattle, Wash. 207 p.

Broenkow, W.W. and J.D. Cline. 1969. Colorimetric determination of
dissolved oxygen at low concentrations. Limnol. Oceanogr.
14: 450-454.

Brooks, J.M., T.J. Bright, B.B. Bernard, and C.R. Schwab. 1979.
Chemical aspects of a brine pool at the East Flower Garden Bank,
northwestern Gulf of Mexico. Limnol. Oceanogr. 24: 735-745.

Brooks, J.M., D.F. Reid, and B.B. Bernard. 1980. Methane in the
upper water column of the Gulf of Mexico. Deep-Sea Res.
In press.

Burke, Jr., R.A., J.M. Brooks, and W.M. Sackett. 1980. Light hydro-
carbons in Red Sea brines and sediments. Geochim. Cosmochim.
Acta (submitted).

Carlucci, A.F. and P.M. McNally. 1969. Nitrification by marine
bacteria in low concentrations of substrate and oxygen. Limnol.
Oceanogr. 14: 736-739.

Carpenter, J.H. 1965. The accuracy of the Winkler method for
dissolved oxygen analysis. Limnol. Oceanogr. 10: 135-140.

Chen, C.A. 1978. Decomposition of calcium carbonate and organic
carbon in the deep oceans. Science 201: 735-736.

Claypool, G.E. and I.R. Kaplan. 1974. The origin and distribution
of methane in marine sediments, p. 99-139. In I.R. Kaplan
[ed.], Natural gases in marine sediments. Plenum Press.

Cline, J.D. 1969. Spectrophotometric determination of hydrogen
sulfide in natural waters. Limnol. Oceanogr. 14: 454-458.

Cline, J.D. and F.A. Richards. 1972. Oxygen deficient conditions
and nitrogen reduction in the eastern tropical North Pacific
Ocean. Limnol. Oceanogr. 17: 885-900.

Cohen, Y. 1978. Consumption of dissolved nitrous oxide in an anoxic
basin, Saanich Inlet, British Columbia. Nature 272: 235-237.

Cohen, Y. and L.I. Gordon. 1978. Nitrous oxide in the oxygen minimum
of the eastern tropical North Pacific: evidence for its con-
sumption during denitrification and possible mechanisms for its
production. Deep-Sea Res. 25: 509-524.

Collins, A.G. 1975. Geochemistry of oilfield waters. Elsevier
Scientific Publishing Company. 496 p.

Cooke, R.C. 1973. The use of activated charcoal for the removal
of oxygen from gas systems. Limnol. Oceanogr. 18: 150-152.

Craig, H.C. 1969. Geochemistry and origin of the Red Sea brines,
p. 208-242. In E.T. Degens and D.A. Ross [eds.], Hot brines
and recent heavy metal deposits in the Red Sea. Springer-
Verlag.

Crank, J. 1975. The mathematics of diffusion. 2nd edition. Clarendon
Press. 414 p.

Crozier, T.E. and S. Yamamoto. 1974. Solubility of hydrogen in water,
sea water, and sodium chloride solutions. J. Chem. Eng. Data
19: 242-244.

Davis, J.B. and H.F. Yarbrough. 1966. Anaerobic oxidation of hydro-
carbons by Desulfovibrio desulfuricans. Chem. Geol. 1: 137-144.

Deffeyes, K.S. 1965. Carbonate equilibria: a graphic and algebraic
approach. Limnol. Oceanogr. 10: 412-426.

Degens, F T. and D.A. Ross [eds.]. 1974. Hot brines and recent
heav metal deposits in the Red Sea. Springer-Verlag. 632 p.

Deuser, W.G., E.T. Degens, and G.R. Harvey. 1973. Methane in Lake
Kivu: New data bearing on its origin. Science 181: 51-54.

Douglas, E. 1964. Solubilities of oxygen, argon, and nitrogen in
distilled water. J. Phys. Chem. 68: 169-174.

Edmond, J.M. 1970. High precision determination of titration alka-
linity and total carbon dioxide content of sea water by
potentiometric titration. Deep-Sea Res. 17: 737-750.

Edmond, J.M. 1972. The thermodynamic description of the CO_2
system in seawater: development and current status.
Proc. Roy. Soc. Edinburgh 72: 371-387.

Emery, K.O. and D. Hogan. 1958. Gases in marine sediments. Bull.
Amer. Assoc. Petrol. Geol. 42: 2174-2188.

Fanning, K.A. and M.E.Q. Pilson. 1972. A model for the anoxic zone
of the Cariaco Trench. Deep-Sea Res. 19: 847-863.

Fleming, R.H. 1940. Composition of plankton and units for reporting
population and production. Proc. Sixth Pac. Sci. Assoc.
3: 535-540.

Fredericks, A.D. 1972. Distribution of organic carbon, p. 6-7.
In Vivian C. Bushnell [ed.], Serial atlas of the marine environ-
ment. Folio 22, Chemistry, primary productivity, and benthic
algae of the Gulf of Mexico. Amer. Geograph. Soc.

Froelich, P.N., G.P. Klinkhammer, M.L. Bender, N.A. Luedtke, G.R.
Heath, D. Cullen, and P. Dauphin. 1979. Early oxidation of
organic matter in pelagic sediments of the eastern equatorial
Atlantic: suboxic diagenesis. Geochim. Cosmochem. Acta.
43: 1075-1090.

Fuhs, G.S. 1961. Der mikrobielle Abbau von Koklenwasserstoffen.
Arch. Mikrobiol. 39: 374-422.

Gaines, A.G. and M.E.Q. Pilson. 1972. Anoxic water in the Petta-
quamscutt River. Limnol. Oceanogr. 17: 42-49.

Games, L.M., J.M. Hayes, and R.P. Gunsalus. 1978. Methane-producing bacteria: natural fractionation of the stable carbon isotopes. Geochim. Cosmochim. Acta. 42: 1295-1297.

Garrels, R.M. and M.E. Thompson. 1962. A chemical model for sea water at 25°C and one atmosphere total pressure. Amer. J. Sci. 260: 57-66.

Garrison, L.E. and R.G. Martin, Jr. 1973. Geologic structures in the Gulf of Mexico basin. U.S. Geological Survey, Prof. Paper 773. 85 p.

Gieskes, J.M. 1974. The alkalinity-total carbon dioxide system in sea water, p. 123-151. In E.D. Goldberg [ed.], The Sea, v. 5: Marine Chemistry. Wiley Interscience.

Gille, J. 1967. Interferometric measurement of temperature gradient reversal in a layer of convecting air. J. Fluid Mech. 30: 371-384.

Glueckauf, E. 1951. The composition of atmospheric air, p. 3-10. In T.F. Malone [ed.], Compendium of meteorology, Amer. Meteor. Sci.

Goering, J.J. 1968. Denitrification in the oxygen minimum layer of the eastern tropical Pacific Ocean. Deep-Sea Res. 15: 157-164.

Goldhaber, M.B. and I.R. Kaplan. 1974. Controls and consequences of sulfate reduction rates in recent marine sediments. Soil Sci. 119: 42-55.

Gordon, K.I., Y. Cohen, and D.R. Standley. 1977. The solubility of molecular hydrogen in seawater. Deep-Sea Res. 24: 937-941.

Guinasso, N.L., Jr. 1977. Continuous temperature profile in the Orca Basin. EOS, Trans., Amer. Geophys. Union. 58: 1175.

Hammond, D.E. 1974. Dissolved gases in Cariaco Trench sediments: Anaerobic diagenesis, p. 71-89. In I.R. Kaplan [ed.], Natural gases in marine sediments. Plenum Press.

Harned, H.S. and B.B. Owen. 1950. Physical chemistry of electro-lytic solutions. Reinhold Publishing Co. 645 p.

Holser, W.T. 1966. Bromide geochemistry of salt rocks, p. 248-275. In J.L. Rau [ed.], Second Symposium on Salt, v. 1, Northern Ohio Geological Soc.

Hunt, J.M. 1974. Hydrocarbon geochemistry of the Black Sea, p. 599-604. In E.T. Degens and D.A. Ross [eds.], The Black Sea - geology, chemistry, and biology, Mem. 20, Amer. Assoc. Pet. Geol., George Banta Company.

Johnson, K.S. and R.M. Pytkowicz. 1979. Ion association of chloride and sulphate with sodium, potassium, magnesium, and calcium in seawater at 25°C. Mar. Chem. 8: 87-94.

Kaplan, I.R. and S.C. Rittenberg. 1964. Microbiological fractionation of sulfur isotopes. J. Gen. Microbiol. 34: 195-212.

Karl, D.M., P.A. LaRock, and D.J. Schultz. 1977. Adenosine triphosphate and organic carbon in the Cariaco Trench. Deep-Sea Res. 24: 105-113.

Kennett, J.P. and N.L. Penrose. 1978. The occurrence of fossil holocene seaweed and attached calcareous polychaetes in an anoxic basin, Gulf of Mexico. Nature 276: 172-173.

Kester, D.R. 1975. Dissolved gases other than CO_2, p. 498-556. In J.P. Riley and G. Skirrow [eds.], Chemical Oceanography, v. 2, 2nd ed., Academic Press.

Knull, J.R. and F.A. Richards. 1969. A note on the sources of excess alkalinity in anoxic waters. Deep-Sea Res. 16: 205-212.

Kushner, D.J. 1968. Halophilic bacteria, v. 10, p. 73-99. In W.W. Umbreit and D. Perlman [eds.], Advances in applied microbiology. Academic Press.

Kushner, D.J. 1978. Microbial life in extreme environments. Academic Press. 465 p.

Laking, P.N. 1974. The Black Sea, its geology, chemistry, biology: a bibliography. Woods Hole Oceanographic Institution. 368 p.

Lamb, H. 1945. Hydrodynamics. Dover Publications, 371 p.

LaRock, P.A., R.D. Lauer, J.R. Schwartz, K.K. Watanabe, and D.A. Wiesenburg. 1979. Microbial biomass and activity distribution in an anoxic, hypersaline basin. Appl. Environ. Microbiol. 37: 466-470.

Larsen, H. 1967. Biochemical aspects of extreme halophilism, p. 97-132. In A.H. Rose and J.F. Wilkinson [eds.], Advances in microbial physiology. Academic Press.

Lingane, J.J. and R.L. Pecsok. 1948. Preparation of standard chromous sulfate or chromous chloride solution of determinate concentration. Anal. Chem. 20: 425-428.

Linnenbom, V.J. and J.W. Swinnerton. 1969. Distribution of low molecular weight hydrocarbons and excess molecular nitrogen in the Cariaco Trench, p. 125-130. In Symposium on investigation and resources of the Caribbean Sea and adjacent regions. Rep. 71.1, FAO Fisheries, Willemstad, Curacao.

McAuliffe, C. 1971. GC determination of solutes by multiple phase
equilibration. Chem. Tech. 1: 46-51.

McKee, T.R., L.M. Jeffrey, B.J. Presley, and U.G. Whitehouse. 1978.
Holocene sediment geochemistry of continental slope and intra-
slope basin areas, northwest Gulf of Mexico, p. 313-326. In
A.H. Bouma, G.T. Moore, and J.M. Coleman [eds.], Framework,
facies, and oil-trapping characteristics of the upper continental
margin. Amer. Assoc. Pet. Geol.

McKee, T.R. and B.R. Sidner. 1976. An anoxic high salinity intra-
slope basin in the northwest Gulf of Mexico, p. 125-131.
In A.H. Bouma [ed.], Beyond the Shelf Break. AAPG Marine Geology
Communications Short Course, Amer. Assoc. Pet. Geol.

McKenna, E.J. and R.E. Kallio. 1965. The biology of hydrocarbons.
Annu. Rev. Microbiol. 19: 183-208.

McKinney, R.E. and R.A. Conway. 1957. Chemical oxygen in biological
waste treatment. Sewage Ind. Waste 29: 1097-1106.

Manheim, F.T. and J.L. Bischoff. 1969. Geochemistry of pore waters
from Shell Oil Company drill holes on the continental slope
of the northern Gulf of Mexico. Chem. Geol. 4: 63-82.

Martens, C.S. and R.A. Berner. 1977. Interstitial water chemistry
of anoxic Long Island Sound sediments. I. Dissolved gases.
Limnol. Oceanogr. 22: 10-25.

Martens, C.S., R.A. Berner, and J.K. Rosenfeld. 1978. Interstitial
water chemistry of anoxic Long Island Sound sediments. 2.
Nutrient regeneration and phosphate removal. Limnol. Oceanogr.
23: 605-617.

Matsubara, T. and T. Mori. 1968. Studies on denitrification:
IX. Nitrous oxide, its production and reduction to nitrogen.
J. Biochem. 64: 863-871.

Mehrbach, C., C.H. Culberson, J.E. Hawley, and R.M. Pytkowicz. 1973.
Measurement of the apparent dissociation constants of carbonic
acid in seawater at atmospheric pressure. Limnol. Oceanogr.
18: 897-907.

Merrell, W.J., Jr. 1971. Wind-induced inertial oscillations in a
linearly stratified sea. Ph.D. Dissertation, Texas A&M
University, College Station, Texas. 97 p.

Millero, F.J., A.L. Surdo, P. Chetirkin, and N.L. Guinasso. 1979.
The density and speed of sound of Orca basin waters. Limnol.
Oceanogr. 24(2): 218-225.

Munk, W.H. 1966. Abyssal recipes. Deep-Sea Res. 13: 707-730.

Murphy, J. and J.P. Riley. 1962. A modified single solution method
    for determination of phosphate in natural waters. Anal. Chim.
    Acta. 27: 31-36.

Murray, J.W., V. Grundmanis, and W.M. Smithie, Jr. 1978. Inter-
    stitial water chemistry in the sediments of Saanich Inlet.
    Geochim. Cosmochim. Acta. 42: 1011-1026.

Murray, R.G.E. and S.W. Watson. 1963. An organelle confined within
    the cell wall of Nitrosocystics oceanus (Watson). Nature
    197: 211-212.

Neumann, G. and W.J. Pierson, Jr. 1966. Principles of physical
    oceanography. Prentice-Hall, Inc. 545 p.

Newman, F.C. 1976. Temperature steps in Lake Kivu: a bottom heated
    saline lake. J. Phys. Oceanogr. 6: 157-163.

Nissenbaum, A. 1975. The microbiology and biogeochemistry of the
    Dead Sea. Microb. Ecol. 2: 139-161.

Novelli, G.D. and C.E. Zobell. 1947. Assimilation of petroleum
    hydrocarbons by sulfate-reducing bacteria. J. Bacteriol. 47:
    447-448 (abstract).

Nowlin, W.D. Jr. 1972. Winter circulation patterns and property
    distributions, p. 3-51. In L.R.A. Capurro and J.L. Reid
    [eds.], Contributions on the physical oceanography of the Gulf
    of Mexico, v. 2, Gulf Publishing Co.

Oremland, R.S. 1975. Methane production in shallow water, tropical
    marine sediments. Appl. Microbiol. 30: 602-608.

Ostland, H.G. 1974. Expedition "Odysseus 65": radiocarbon age of
    Black Sea deep water, p. 127-132. In E.T. Degens and D.A.
    Ross [eds.], The Black Sea - geology, chemistry, and biology.
    Mem. 20, Amer. Assoc. Pet. Geol. George Banta Company.

Park, K. 1969. Oceanographic CO_2 system: An evaluation of ten
    methods of investigation. Limnol. Oceanog. 14: 179-186.

Payne, W.P., P.S. Riley, and C.P. Cox, Jr. 1970. Separate nitrite,
    nitric oxide, and nitrous oxide reducing fractions from
    Pseudomonas perfectomarinus. J. Bacteriol. 106: 356-36.

Prabhakara, C., G. Dalu, and V.G. Kunde. 1974. A search for global
    and seasonal variation of methane from Nimbus 4 Iris measurements.
    J. Geophys. Res. 79: 1744-1749.

Pytkowicz, R.M. and E. Atlas. 1975. Buffer intensity of seawater. Limnol. Oceanogr. 20: 222-229.

Pytkowicz, R.M., S.E. Ingle, and C. Merbach. 1974. Invariance of apparent equilibrium constants with pH. Limnol. Oceanogra. 19: 665-669.

Quayle, J.R. 1972. The metabolism of one-carbon compounds by microorganisms, p. 119-203. In A.H. Rose and D.W. Tempest [eds.], Advances in microbial physiology, v. 7, Academic Press.

Ramm, A.E. and D.A. Bella. 1974. Sulfide production in anaerobic microcosms. Limnol. Oceanogr. 19: 110-118.

Redfield, A.C. 1934. On the proportions of organic derivatives in sea water and their relation to the composition of plankton, p. 176-192. In James Johnstone Memorial Volume. University of Liverpool Press.

Reeburgh, W.S. 1969. Observations of gases in Chesapeake Bay sediments. Limnol. Oceanogr. 14: 368-375.

Reeburgh, W.S. 1976. Methane consumption in Cariaco Trench waters and sediments. Earth Planet. Sci. Lett. 28: 337-344.

Richards, F.A. 1955. The Cariaco Trench. Oceanus 3: 9-10.

Richards, F.A. 1957. Oxygen in the ocean, p. 185-238. In J.W. Hedgpeth [ed.], Treatise on marine ecology and paleoecology, v. 1, Mem. 67, Geol. Soc. Amer.

Richards, F.A. 1965. Anoxic basins and fjords, p. 611-645. In J.P. Riley and G. Skirrow [eds.], Chemical oceanography, v. 1. Academic Press.

Richards, F.A. 1975. The Cariaco Basin (Trench). Oceanogr. Mar. Biol. Annu. Rev. 13: 11-67.

Richards, F.A. and B.B. Benson. 1961. Nitrogen/argon and nitrogen isotope ratios in two anaerobic environments, the Cariaco Trench in the Caribbean Sea and Dramsfjord, Norway. Deep-Sea Res. 7: 254-264.

Richards, F.A., J.D. Cline, W.W. Broenkow, and L.P. Atkinson. 1965. Some consequences of the decomposition of organic matter in Lake Nitinat, an anoxic fjord. Limnol. Oceanogr. 10 (Suppl.): R185-R201.

Rosenfeld, W.D. and S.R. Silverman. 1959. Carbon isotope fractionation in bacterial production of methane. Science 130: 1658-1659.

Rosenfeld, W.S. 1947. Anaerobic oxidation of hydrocarbons by sulfate-reducing bacteria. J. Bacteriol. 54: 664-665.

Rudd, J.W.M., R.D. Hamilton, and N.E.R. Campbell. 1974. Measurement of microbial oxidation of methane in lake water. Limnol. Oceanogr. 19: 519-524.

Sackett, W.M., J.M. Brooks, B.B. Bernard, C.R. Schwab, H. Chung, and R.A. Parker. 1979. A carbon inventory for Orca Basin brines and sediments. Earth Planet. Sci. Lett. 44: 73-81.

Sackett, W.M., S. Nakaparshin, and D. Dalrymple. 1970. Carbon isotope effects in methane production by thermal cracking, p. 37-53. In G.D. Hobson and G.C. Spears [eds.],Advances in organic geochemistry. 1966. Pergamon Press.

Sass, E. and S. Ben-Yaakov. 1977. The carbonate system in hyper-saline solutions: Dead Sea brines. Mar. Chem. 5: 183-199.

Schmidt, U. 1978. The latitudinal and vertical distribution of molecular hydrogen in the troposphere. J. Geophys. Res. 83: 941-946.

Schmidt, U. 1979. The solubility of carbon monoxide and hydrogen in water and sea-water at partial pressures of about 10^{-5} atmospheres. Tellus 31: 68-74.

Schoener, A. and G.T. Rowe. 1970. Pelagic Sargassum and its presence among the deep-sea benthos. Deep-Sea Res. 17: 923-925.

Scranton, M.I. and P.G. Brewer. 1977. Occurrence of methane in the near-surface waters of the western subtropical North Atlantic. Deep-Sea Res. 24: 127-138.

Shokes, R.F., P.K. Trabant, B.J. Presley, and D.F. Reid. 1977. Anoxic, hypersaline basin in the Northern Gulf of Mexico. Science 196: 1443-1446.

Sillen, L.G. and A.E. Martell. 1964. Stability constants of metal-ion complexes. The Chemical Society (London). 754 p.

Skirrow, G. 1965. The dissolved gases — carbon dioxide, p. 227-322. In J.P. Riley and G. Skirrow [eds.], Chemical Oceanography, v. 1, Academic Press.

Solorzano, L. 1969. Determination of ammonia in natural waters by the phenolhypochlorite method. Limnol. Oceanogr. 14: 799-801.

Sorokin, Y.I. 1957. On the ability of sulfate-reducing bacteria to utilize methane for the reduction of sulfates to hydrogen sulfide. Dokl. Akad. Nauk. SSSR 115: 816-818.

Stadtman, T.C. and H.A. Barker. 1951. Studies on methane fermentation. IX. The origin of methane in acetate and methanol fermentation by Methanosarcina. J. Bacteriol. 61: 81-86.

Stookey, L.L. 1970. Ferrozine - a new spectrophotometric reagent for iron. Anal. Chem. 42: 779-781.

Sverdrup, H.U., M.W. Johnson, and R.H. Fleming. 1942. The oceans — their physics, chemistry, and general biology. Prentice-Hall. 1087 p.

Sweeney, R.E. 1972. Pyritization during diagenesis of marine sediments. Ph.D. Thesis, University of California, Los Angeles. 194 p.

Swinnerton, J.W. and V.J. Linnenbom. 1967. Determination of C_1 to C_4 hydrocarbons in sea water by gas chromatography. J. Gas Chrom. 5: 570-573.

Swinnerton, J.W. and V.J. Linnenbom. 1969. Low molecular weight hydrocarbon analyses of Atlantis II waters, p. 251-253. In E.T. Degens and D.A. Ross [eds.], Hot brines and recent heavy metal deposits in the Red Sea. Springer-Verlag.

Swinnerton, J.W., V.J. Linnenbom, and C.H. Cheek. 1962. Determination of dissolved gases in aqueous solutions by gas chromotography. Anal. Chem. 34: 483-485.

Technicon. 1976. Ammonia in water and sea water. Technicon Industrial Systems, Industrial Methods No. 154-71W, 2 p.

Thayer, L.A. 1931. Bacterial genesis of hydrocarbons from fatty acids. Bull. Amer. Assoc. Pet. Geol. 15: 441-453.

Thorstenson, D.C. and F.T. MacKenzie. 1974. Time variability of pore water chemistry in recent carbonate sediments, Devil's Hole, Harrington Sound, Bermuda. Geochim. Cosmochim. Acta. 38: 1-19.

Tompkins, R.E. and L.E. Shephard. 1979. Orca Basin: Depositional processes, geotechnical properties, and clay mineralogy of holocene sediments within an anoxic hypersaline basin, northwest Gulf of Mexico. Mar. Geol. 33: 221-238.

Trabant, P.K. and B.J. Presley. 1978. Orca Basin, an anoxic pool on the continental slope, Northwest Gulf of Mexico, p. 303-311. In A.H. Bouma, G.T. Moore, and J.M. Coleman [eds.], Framework, facies, and oil-trapping characteristics of the upper continental margin. AAPG Studies in Geology No. 7.

Trüper, H.G. 1969. Bacterial sulfate reduction in the Red Sea hot brines, p. 263-271. In E.T. Degens and D.A. Ross [eds.], Hot brines and recent heavy metal deposits in the Red Sea. Springer-Verlag.

Turner, J.S. 1965. The coupled turbulent transport of salt and heat across a sharp density interface. Inter. J. Heat Mass Trans. 8: 759-767.

Turner, J.S. 1968. The behaviour of a stable salinity gradient heated from below. J. Fluid Mech. 33: 183-200.

Turner, J.S. 1973. Buoyancy effects in fluids. University Press, Cambridge. 367 p.

Turner, J.S. and H. Stommel. 1964. A new case of convection in the presence of combined vertical salinity and temperature gradients. Proc. U.S. Nat. Acad. Sci. 52: 49-53.

Vaccaro, R.F. 1965. Inorganic nitrogen in sea water, p. 365-408. In J.P. Riley and G. Skirrow [eds.], Chemical Oceanography, v. 1, Academic Press.

Valley, S.L. 1965. Handbook of geophysics and space environments. McGraw-Hill. 683 p.

Valyashko, M.G. 1956. Geochemistry of bromine in processes of halogenesis and use of bromine content as a genetic and prospecting criterion. Geochemistry 6: 33-49.

Vary, P.S. and M.J. Johnson. 1967. Cell yields of bacteria grown on methane. Appl. Microbiol. 15: 1473-1478.

Vogel, A.I. 1968. Quantitative inorganic analysis. John Wiley & Sons. 446 p.

Watson, S.W. and J.B. Waterbury. 1969. The sterile hot brines of the Red Sea, p. 272-281. In E.T. Degens and D.A. Ross [eds.], Hot brines and recent heavy metal deposits in the Red Sea. Springer-Verlag.

Weast, R.C. 1969. Handbook of chemistry and physics, 50th ed., Chemical Rubber Co., Cleveland, Ohio. 2356 p.

Weatherburn, M.W. 1967. Phenol-hypochlorite reaction for determination of ammonia. Anal. Chem. 39: 971-974.

Weiss, R.F. 1968. Piggyback samples for dissolved gas studies on sealed water samples. Deep-Sea Res. 15: 695-699.

Weiss, R.F. 1969. Dissolved nitrogen, argon, and total carbonate in the Red Sea brines, p. 254-262. In E.T. Degens and D.A. Ross [eds.], Hot brines and recent heavy metal deposits in the Red Sea. Springer-Verlag.

Weiss, R.F. 1970. The solubility of nitrogen, oxygen, and argon in water and seawater. Deep-Sea Res. 17: 721-735.

Weiss, R.F. 1971. Solubility of helium and neon in water and seawater. J. Chem. Eng. Data 16: 235-241.

Weiss, R.F. 1974. Carbon dioxide in water and seawater: the solubility of a non-ideal gas. Mar. Chem. 2: 203-215.

Weiss, M.F. and H. Craig. 1973. Precise shipboard determination of dissolved nitrogen, oxygen, argon, and total inorganic carbon by gas chromatography. Deep-Sea Res. 20: 291-303.

Weiss, R.F. and T.K. Kyser. 1978. Solubility of krypton in water and seawater. J. Chem. Eng. Data 23: 69-72.

Weiss, R.F. and B.A. Price. 1980. Nitrous oxide solubility in water and seawater. Mar. Chem. 8: 347-359.

Wertlieb, D. and W. Vishniac. 1967. Methane utilization by a strain of Rhodopseudomonas gelatinosa. J. Bacteriol. 93: 1772-1724.

Weyl, P.K. 1961. The carbonate saturometer. J. Geol. 69: 32-44.

Wiesenburg, D.A. 1975. Processes controlling the distribution of methane in the Cariaco Trench, Venezuela. M.S. Thesis, Old Dominion University, Norfolk, Va. 106 p.

Wiesenburg, D.A., L.A. Barnard, and D.R. Schink. 1977. Nitrogen in the Orca Basin: effects of denitrification at the brine-sea water interface. EOS, Transactions, Amer. Geophys. Union. 58: 1175.

Wiesenburg, D.A. and N.L. Guinasso, Jr. 1979. Equilibrium solubilities of methane, carbon monoxide, and hydrogen in water and sea water. J. Chem. Eng. Data 24: 356-360.

Wilson, T.R.S. 1978. Evidence for denitrification in aerobic pelagic sediments. Nature 274: 354-356.

Winkler, L.W. 1888. Dei Bestimmung des im Wasser gelosten Sauerstoffes. Chem. Ber. 21: 2843-2855.

Yamamoto, S., J.B. Alcauskas, and T.E. Crozier. 1976. Solubility of methane in distilled water and seawater. J. Chem. Eng. Data 21: 78-80.

Zobell, C.E. 1942. Changes produced by microorganisms in sediments after deposition. J. Sed. Petrol. 12: 127-136.

Zobell, C.E. 1946. Marine microbiology. Chronica Botanica Co. 240 p.

VITA

Denis Alan Wiesenburg was born to Otto Karl Wiesenburg and Denise Higginbotham in Pascagoula, Mississippi on November 4, 1948. He attended parochial and public schools in Pascagoula, Mississippi, and graduated from Pascagoula High School in May, 1966.

He attended Duke University in Durham, North Carolina and received a Bachelor of Arts degree in Chemistry in June, 1970. He attended Old Dominion University in Norfolk, Virginia, from 1970 to 1974 and received a Masters of Science degree in Oceanography in August, 1975. From September, 1974, to June, 1975, he was enrolled at Dalhousie University in Halifax, Nova Scotia, Canada, where he studied chemical oceanography.

In 1975, he came to Texas A&M University as a graduate student in the Oceanography Department. He currently resides with his wife, Jean Herbert, and his son, Heath Karlton, at 1005 Milner Drive, College Station, Texas.

The typist for this dissertation was Bee Gee Hart.